

✓ F-88  
SIN

# STABILITY ANALYSIS AND OPTIMIZATION OF A MULTIBED QUENCH REACTOR FOR AMMONIA SYNTHESIS

A THESIS

Submitted in fulfilment of the requirements  
for the award of the degree  
of  
DOCTOR OF PHILOSOPHY  
in  
CHEMICAL ENGINEERING



By

**SUDHINDRA NATH SINHA**



DEPARTMENT OF CHEMICAL ENGINEERING  
UNIVERSITY OF ROORKEE  
ROORKEE-247 667 (INDIA)

JULY, 1988

CANDIDATE'S DECLARATION

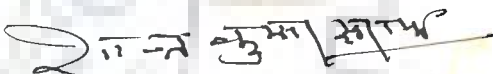
I hereby certify that the work which is being presented in the thesis entitled "STABILITY ANALYSIS AND OPTIMIZATION OF A MULTIBED QUENCH REACTOR FOR AMMONIA SYNTHESIS" in fulfilment of the requirement for the award of the Degree of Doctor of Philosophy submitted in the Department of Chemical Engineering of the University is an authentic record of my own work carried out during a period from August, 1984 to July, 1988 under the supervision of Dr.S.K.Saraf.

The matter embodied in this thesis has not been submitted by me for the award of any other Degree.

Dated: July 7, 1988

  
( SUDHINDRA NATH SINHA )

This is to certify that the above statement made by the candidate is correct to the best of my knowledge.

  
( SHANT KUMAR SARAF )

Professor of Chemical Engineering  
University of Roorkee, Roorkee  
(U.P.) 247667-India

The candidate has passed the Viva-Voce examination held on  
at . The thesis is recommended for award of the  
Ph.D. Degree.

(S.K.SARAF)

Guide

External Examiner

## ABSTRACT

(1)

The stability analysis and optimization of an axial flow three bed quench type ammonia synthesis reactor was carried out to optimize its performance. The reactor operation at optimal cold shot fractions for a given set of the operating and design parameter values will result in the maximization of the rate of production of ammonia and stable operation. This will result in low bed temperatures and reduced total pressure drop. The low bed temperatures will result in increase in catalyst life whereas reduced pressure drop will reduce the operating cost.

Modern large capacity reactors are used for production of ammonia used as a feedstock in the production of urea. Urea is essential to boost agricultural production in India. A realistic and accurate mathematical model of a large capacity multibed autothermic quench-type ammonia synthesis reactor was formulated and solved by modified Milne-Predictor-Corrector numerical integration technique using an appropriate convergence strategy. The optimization of the cold shot distribution was achieved by taking maximization of the rate of ammonia production as an objective function. The Box complex direct search optimization technique was used for sixteen set of conditions over a wide range of values of six operating and design parameters. These parameters were feed gas flow rate,  $H_2/N_2$  ratio in feed, inerts concentration in feed, catalyst activity factor, total volume of catalyst and operating pressure of the reactor.

In order to estimate the model parameters for an industrial reactor for simulation study, data from plant were extracted for the period of steady-state operation over several months. The data had a serious limitation that no measured value of cold shot fractions were available except for the first bed inlet where its value was always kept at zero. Validation of simulation model from the plant data was carried out by obtaining best values of model parameters and cold shot fractions. The estimated model parameters are: frequency factor and activation energy in the reverse reaction rate constant correlation for the catalyst used; correction for fugacity coefficient term; and heat exchange capacity of external heat exchanger. Their best values are found to be  $4.11482 * 10^{16} \text{ mol NH}_3 / \text{s/m}^3$ ;  $97622.4 \text{ kJ/kmol}$ ;  $1.379$ ; and  $316000 \text{ W/K}$  at feed flow rate of  $0.74 * 10^6 \text{ Nm}^3 / \text{h}$ , (where N indicates N.T.P. conditions), respectively. The simulated cold shot values as fractions of total feed gas for the average plant conditions (base case) are found to be  $0.245$  and  $0.100$  for the second and the third bed inlet, respectively. Cold shot to the first bed was taken to be zero as per plant practice.

The optimization computations for one set of conditions required generally 5 to 8 minutes of CPU time on DEC 20 computer system. The optimization results indicate that the conversion and the bed temperatures are quite sensitive to the values of the operating and design parameters. Cold shot fractions at optimal conditions are strongly dependent on these parameters. An indiscriminate use of cold shot fractions resulted in either quenching of the reactor or a non optimal performance resulting

(iii)

in significant loss of production, higher bed temperatures and increased pressure drops. The use of optimal cold shot fractions increased the rate of production of ammonia by 20 to 110 t/d (where 1 t = 1000 kg and 1 d = 86.4 ks) compared to actual plant production of 1286.9 t/d, even if the operating and design parameters changed in adverse direction by about 10 to 30 percent from the base value. The rate of ammonia production shows an increase with an increase in flow rate, catalyst activity, operating pressure or total catalyst volume; or and a decrease in inerts concentration. It was found that the region near optimal is not sharp with constraints on upper values of cold shot fractions resulting in the extinction of the reactor. It is further observed that optimal cold shot fractions do show a trend, to an extent linear with respect to change in parameters, namely, feed gas flow rate, catalyst activity factor, total catalyst volume and the reactor operating pressure.

An increase in the rate of ammonia production of 10.3 percent (132 t/d) is observed if the operation is carried out at optimal cold shot fractions to first, second and third bed of 0.110, 0.233 and 0.232, respectively, for the base case. It is observed that the effect of change in  $H_2/N_2$  ratio in the feed gas from 3.0 is not significant on reactor performance and rate of ammonia production. It is observed that the reactor stability near its optimal operation is quite sensitive to increase in cold shot fractions and an increase beyond a critical value may result in its extinction or blow-out. The use of simulation model is, therefore, highly desirable to operate the reactor near

(iv)

optimal values of cold shot fractions for any set of parameter values in order to achieve maximum ammonia production rate. Simulation model can also be used for developing a suitable control strategy for cold shot distribution for ensuring optimal reactor operation.



## ACKNOWLEDGEMENT

(v)

I am thankful to Dr.S.K.Saraf, Professor, for his guidance and keen interest shown in my thesis work from time to time inspite of his preoccupation with other works.

I am thankful to Dr.B.S.Varshney, Professor and Head, Department of Chemical Engineering for providing necessary facilities.

I owe a lot to my father, Late Shri Thakur Lakshmi Shankar Sinha who was very keen to see my doctorate complete. I could not give him due attention during his ailment as I became busy in my doctorate work along with teaching work. It was to my bad luck that he could not see my work complete and went to heavenly abode within six months of my registering for doctorate work. Further, I owe a lot to my mother, Shrimati Prabha Sinha who very much needs my attention now. I owe a lot to the patience and co-operation of my wife, Shrimati Neeta Sinha and two sons Ashish and Mohit to whom I could not give proper attention during the course of my research work.

I am thankful to the co-operation extended by my colleagues Mr. Ravindra Bhargava, Dr. I.M.Mishra, Dr. Surendra Kumar and Dr. Bikas Mohanty in completion of my work.

Finally I am thankful to all my friends who have contributed in one way or other towards completion of my work.

**S.N.SINHA**

# C O N T E N T S

(vi)

CANDIDATE'S DECLARATION

ABSTRACT

(i)

ACKNOWLEDGEMENT

(v)

CONTENTS

(vi)

LIST OF FIGURES

(ix)

LIST OF TABLES

(xi)

NOMENCLATURE

(xii)

## CHAPTER-I

1. INTRODUCTION

1

## CHAPTER-II

2. LITERATURE REVIEW

5

2.1. Literature review on ammonia synthesis  
reactor modelling and simulation

5

2.2. Literature review on Kinetic,  
thermodynamic and Physical properties

15

## CHAPTER-III

3. REACTOR MODELLING AND DESIGN RELATIONSHIPS

19

3.1. Reactor modelling and design relations

19

3.2. Effectiveness factor relation

35

3.3. Equilibrium conversion relation

37

3.4. Conversion corresponding to maximum rate

38



## CHAPTER-IV

(vii)

- |      |  |    |
|------|--|----|
| 4.   | TECHNIQUE FOR OPTIMIZATION OF AMMONIA<br>SYNTHESIS REACTOR | 42 |
| 4.1. | Description of the complex search method                   | 44 |

## CHAPTER-V

- |      |  |    |
|------|--|----|
| 5.   | COMPUTATION TECHNIQUE                  | 49 |
| 5.1. | Computation technique for optimization | 49 |
| 5.2. | Convergence policy                     | 52 |
| 5.3. | Numerical integration procedure        | 53 |
| 5.4. | Computer program features              | 57 |

## CHAPTER-VI

- |      |  |    |
|------|--|----|
| 6.   | ESTIMATION OF SIMULATION MODEL PARAMETERS<br>FROM PLANT DATA                   | 60 |
| 6.1. | Purpose of estimation of Parameters and<br>parameters description              | 60 |
| 6.2. | Parameters estimation technique  | 61 |
| 6.3. | Selection of Physical properties,<br>thermodynamic and kinetic correlations    | 63 |
| 6.4. | Description of procedure for kinetic and<br>thermodynamic parameter estimation | 65 |
| 6.5. | Procedure for the estimation of external<br>heat exchanger capacity            | 67 |
| 6.6. | Reliability and accuracy of the validated<br>simulation model                  | 68 |

## CHAPTER-VII

(viii)

7.	RESULTS AND DISCUSSION	70
7.1.	Parameter estimation for reactor simulation model	70
7.2.	Choice of variables and their ranges for simulation studies	87
7.3.	Simulation results for the base conditions	90
7.4.	Effect of variations in design and operating parameters on reactor performance	120
7.5.	Considerations for optimal design and operation	132

## CHAPTER-VIII

8.	CONCLUSIONS AND RECOMMENDATIONS	134
8.1.	Conclusions	134
8.2.	Recommendations	137
	REFERENCES	138
APPENDIX-A	TABLES OF OPTIMIZATION RESULTS	144
APPENDIX-B	COMPUTER PROGRAM FOR SIMULATION AND OPTIMIZATION OF A MULTIBED QUENCH TYPE REACTOR FOR AMMONIA SYNTHESIS	151

LIST OF FIGURES

(ix)

<u>DESCRIPTION</u>	<u>FIGURE</u>	<u>PAGE</u>
Simplified Flow Diagram of Three Bed Quench Type Ammonia Synthesis Reactor with Internal and External Heat Exchange Capacity.	3.1	21
Ammonia Concentration and Temperature Profiles in Catalyst Beds (See Table 7.2.1 for base conditions).	7.1	94
Ammonia Concentration Versus Temperature in Catalyst Beds (See Table 7.2.1 for base conditions).	7.2	95
Reactor Operating Points and Their Stability (See Table 7.2.1 for base conditions).	7.3	96
Effect of Feed Gas Flow Rate on Ammonia Concentration-Temperature Profile in Catalyst Beds for Optimal Cold Shot Distribution (Base conditions, set No. 1, are given in Table 7.2.1).	7.4	97
Effect of Feed Gas Flow Rate on Reactor Operating Points and Their Stability (Base conditions, set No. 1, are given in Table 7.2.1).	7.5	98
Effect of $H_2/N_2$ Ratio in Feed on Ammonia Concentration-Temperature Profile in Catalyst Beds for Optimal Cold Shot Distribution (Base conditions, set No. 1, are given in Table 7.2.1).	7.6	99
Effect of $H_2/N_2$ Ratio in Feed on Reactor Operating Points and Their Stability (Base conditions, set No. 1, are given in Table 7.2.1).	7.7	100
Effect of Inerts Concentration in Feed on Ammonia Concentration-Temperature Profile in Catalyst Beds for Optimal Cold Shot Distribution (Base conditions, set No. 1, are given in Table 7.2.1).	7.8	101
Effect of Inerts Concentration in Feed on Reactor Operating Points and Their	7.9	102

Stability (Base conditions, set No. 1, are given in Table 7.2.1).		(x)
Effect of Catalyst Activity Factor on Ammonia Concentration-Temperature Profile in Catalyst Beds for Optimal Cold Shot Distribution (Base conditions, set No. 1, are given in Table 7.2.1).	7.10	103
Effect of Catalyst Activity Factor on Reactor Operating Points and Their Stability (Base conditions, set No. 1, are given in Table 7.2.1).	7.11	104
Effect of Total Catalyst Volume on Ammonia Concentration-Temperature Profile in Catalyst Beds for Optimal Cold Shot Distribution (Base conditions, set No. 1, are given in Table 7.2.1).	7.12	105
Effect of Total Catalyst Volume on Reactor Operating Points and Their Stability (Base conditions, set No. 1, are given in Table 7.2.1).	7.13	106
Effect of Operating Pressure on Ammonia Concentration-Temperature Profile in Catalyst Beds for Optimal Cold Shot Distribution (Base conditions, set No. 1, are given in Table 7.2.1).	7.14	107
Effect of Operating Pressure on Reactor Operating Points and Their Stability (Base conditions, set No. 1, are given in Table 7.2.1).	7.15	108

LIST OF TABLES

(xi)

<u>TABLE</u>	<u>DESCRIPTION</u>	<u>PAGE</u>
3.2.1	Constants for Equation (3.2.1).	36
6.2.1	Selected Plant Data Extracted from a Typical Ammonia Plant Log Sheets.	62
7.1.2.1	Comparison of Frequency Factor and Activation Energy Values in the Reverse Reaction Rate Constant, $k_r$ .	72
7.1.2.2	Comparison of Equilibrium Constant, $K_r$ .	75
7.1.2.3	Comparison of Fugacity Coefficient Term, $K_\phi$ .	76
7.1.2.4	Comparison of Values of Heat of Reaction, ( $-\Delta H$ )	78
7.1.2.5	Comparison of Heat Capacities of $\text{NH}_3$ , $\text{H}_2$ , $\text{N}_2$ and $\text{CH}_4$ .	80
7.1.3.1	Summary of Results for Parameter Estimation.	82
7.1.5.1	Comparison of Simulation Results with Plant Data at Average Value of Estimated Parameters.	85
7.2.1	Operating and Design Parameters Average Value and Range Investigated.	89
7.3.1.1	Summary of Computed Results.	91
7.3.1.2	Temperature and Ammonia Concentration Values at Bed Inlet and Outlet for Different Conditions.	92
7.4.7	Comparison of Parameter Sensitivity.	130

## NOMENCLATURE

(xii)

$b_0, b_1, b_2,$ $b_3, b_4, b_5$ and $b_6$	coefficients of effectiveness factor correlation that are dependent on gas pressure
$C_1, C_2$ and $C_3$	various terms in the reaction rate equation that are independent of gas temperature
$C_p$	heat capacity of gas, kJ/kmol/K
$C_{pj}$	heat capacity of component j, kJ/kmol/K
$f$	catalyst activity factor, dimensionless
$F_2$	molal flow rate of hydrogen in feed to reactor, mol/s
$F_{DH}$	fraction of total feed entering through preheating section, dimensionless
$F_{Di}$	cold shot to bed 'i' as a fraction of total feed to reactor, dimensionless
$F_j$	molal flow rate of component j in feed to reactor, mol/s
$(-\Delta H_{R2})$	heat of reaction, kJ/kmol of hydrogen converted
$k_r$	reverse reaction velocity constant, mol/s/m of catalyst
$K$	equilibrium constant of the reaction $3/2 H_2 + 1/2 N_2 = NH_3$ , dimensionless
$K_{c1}, K_{c2}$ and $K_{c3}$	coefficients at a given temperature and pressure, dimensional
$K_f$	fugacity coefficient term, dimensionless

N	gas flow rate at any point in the reactor, mol/s
N	total molal flow rate in a bed, mol/s
$N_j$	molal flow rate of component j, mol/s
$N_{0j}$	molal flow rate of component j leaving external and internal preheating sections (hypothetical bed 0 exit), mol/s
P	partial pressure of gas constituent, atm (where 1 atm = 101.325 kPa)
P	gas pressure at any point in the reactor, atm
Para1, Para2	parameters for correction of frequency factor and activation energy in the reverse reaction rate constant correlation, respectively; dimensionless
Para3	parameter to account for inadequacy of $K_p$ correlation
$(-r)_2$	rate of reaction without mass transfer limitation in catalyst given as moles of hydrogen converted per unit time per unit catalyst volume, mol/s/cm <sup>3</sup>
T	gas temperature in catalyst bed, K
$T_H$	gas temperature on tube side of external heat exchanger, K
T	gas temperature in internal preheating section, K
$T_{SH}$	gas temperature on shell side of external heat exchanger, K
$T_{SHE}$	gas temperature at the exit of internal preheating section, K

(UA)	heat exchange capacity of bed, $\text{W/K/cm}^3$
(UA) <sub>H</sub>	heat exchange capacity of external heat exchanger, $\text{W/K/cm}^3$
$v_1$	volume of the reactor in bed 'i', $\text{cm}^3$
$v_H$	volume of the external heat exchanger on tube side, $\text{cm}^3$
$x_{12}$	fractional conversion of hydrogen in bed 'i' based on total hydrogen in feed to reactor, dimensionless
$y$	mole fraction of gas constituents
<b>Greek Symbols</b>	
$\alpha_j$	coefficient proportional to stoichiometric coefficient for component j ( $\alpha_1 = -1/3, \alpha_2 = -1, \alpha_3 = -2/3, \alpha_4 = \alpha_5 = 0$ ), dimensionless
$\gamma$	activity coefficient of gas constituents, dimensionless
$\xi$	effectiveness factor to account for mass transfer resistance in the catalyst pellet, dimensionless
$\eta$	conversion of nitrogen, dimensionless
$\omega_N$	coefficient for pressure drop based on unit bed volume, $\text{atm/cm}^3$
$\omega_{HN}$	coefficient for pressure drop based on unit tube side volume of external heat exchanger, $\text{atm/cm}^3$
$\phi$	fugacity of gas constituent, atm



**Subscript**

eq	corresponds to equilibrium
F	corresponds to feed
H	corresponds to external heat exchanger on tube side
i	designates the catalyst bed number
j	designates components (1-nitrogen, 2-hydrogen, 3-ammonia, 4-methane, and 5-argon)
m	corresponds to maximum reaction rate
N	corresponds to base conditions
S	corresponds to internal preheating section shell side
SH	corresponds to external heat exchanger shell side
T	corresponds to total

## CHAPTER I

### 1. INTRODUCTION

Simulation, optimization and stability analysis of the modern large capacity multibed quench-type (cold-feed cooling) ammonia synthesis reactors is essential for their proper and accurate control and optimal performance.

Ammonia is an essential feedstock for the manufacture of urea which is required in large tonnage for boosting agricultural production. Agriculture contributes to about fifty percent of the national income (Pachaiyapan, 1984) and provides livelihoods for about seventy-five percent of Indian population. Nitrogenous fertiliser production is estimated at about six million tons in 1987-88 and is expected to rise further. In order to meet the anticipated requirements, many new plants are coming up mainly based on natural gas as a feedstock requiring huge investments of the order of six billion rupees (1983 price).

The ammonia technology and engineering for its manufacture has rapidly advanced in the last decade and the plants of 1350 t/d (where 1 t = 1000 kg and 1 d = 86.4 ks) capacity and over are common now-a-days. The latest policy of the Indian Government is to standardise the ammonia technology and build new plants on either of the two technologies, namely, Haldor-Topsoe and Kellogg of axial or radial flow designs. In view of the large ammonia production and high capital investment requirements, even a few percent improvement in production from existing plants is worth hundreds of million rupees every year.

Ammonia is produced by catalytic exothermic reversible reaction of hydrogen and nitrogen in the mol. ratio of approximately 3:1 at elevated pressures (100 to 1000 atm, where 1 atm = 101.325 kPa) and temperatures (675 to 925 K) using doubly promoted iron catalyst. The current trend is towards low pressure (150 to 200 atm) and low temperature (650 to 770 K) operation using highly active catalyst. It is essential to carry out the reaction in an autothermal reactor with axial or radial flow and quench cooling in between catalyst beds and /or internal heat exchange and external heat exchange. Quench type reactors are more common for ammonia synthesis because of high pressure operation. In these reactors intermediate cooling of reaction mixture is achieved by the addition of cold-feed to the reaction mixture at the inlet of a catalyst bed. The description of reactors of various designs are given by Walas (1959), Vancini (1971), Zardi (1982) and others. Due to the opposing requirements of temperature for high reaction rate and high equilibrium conversions, the intermediate cooling between catalyst beds of an ammonia synthesis reactor is essential. Autothermal reactor operation involving feed-back of reaction heat to the incoming cold reactor feed are generally found to possess multiplicity of steady-state operating points. This behaviour of autothermal reactor was first explained by van Heerden (1953). The reactor steady-state point corresponding to highest conversion is the desirable operating point. Beside this, in general, there are two other operating points, the intermediate one is unstable and the one corresponding to the lowest conversion is a trivial operating

point. The stability limit is observed when both the unstable and stable points (of high conversion) coincide with each other due to relative shifting of heat generation and heat removal curves because of changes in plant operating parameters. Reactor blow-out or extinction is a well known problem experienced in autothermal operation with certain changes in plant operating parameters (Froment and Bischoff, 1979a).

Since van Heerden, several other workers (Shah, 1967; Shipman and Hickman, 1968; Vek, 1977; Gaines, 1977; Rase, 1977; Ramkumar, 1978; Lutschutenkow et al., 1978; Reddy and Husain, 1978; Singh and Saraf, 1979; Sinha et al., 1981; Khayan and Pironti, 1982; Mansson and Andresen, 1986) have presented their work on simulation of ammonia synthesis reactor that have contributed significantly to a better understanding of the behaviour of ammonia synthesis reactor performance. However, the extensive literature survey as presented in Chapter-II shows that no published work is available regarding optimization of an existing industrial reactor for ammonia synthesis of multibed quench-type with internal and/or external heat exchanger taking cold shot distribution as decision variables. Also there is lack of information regarding steady-state stability analysis of such reactors operating at optimum conditions.

Therefore, the objectives of the present study can be summarized as follows:

1. Development of a realistic and accurate simulation model for a three-bed autothermic quench reactor for ammonia synthesis for carrying out simulated performance studies under different design

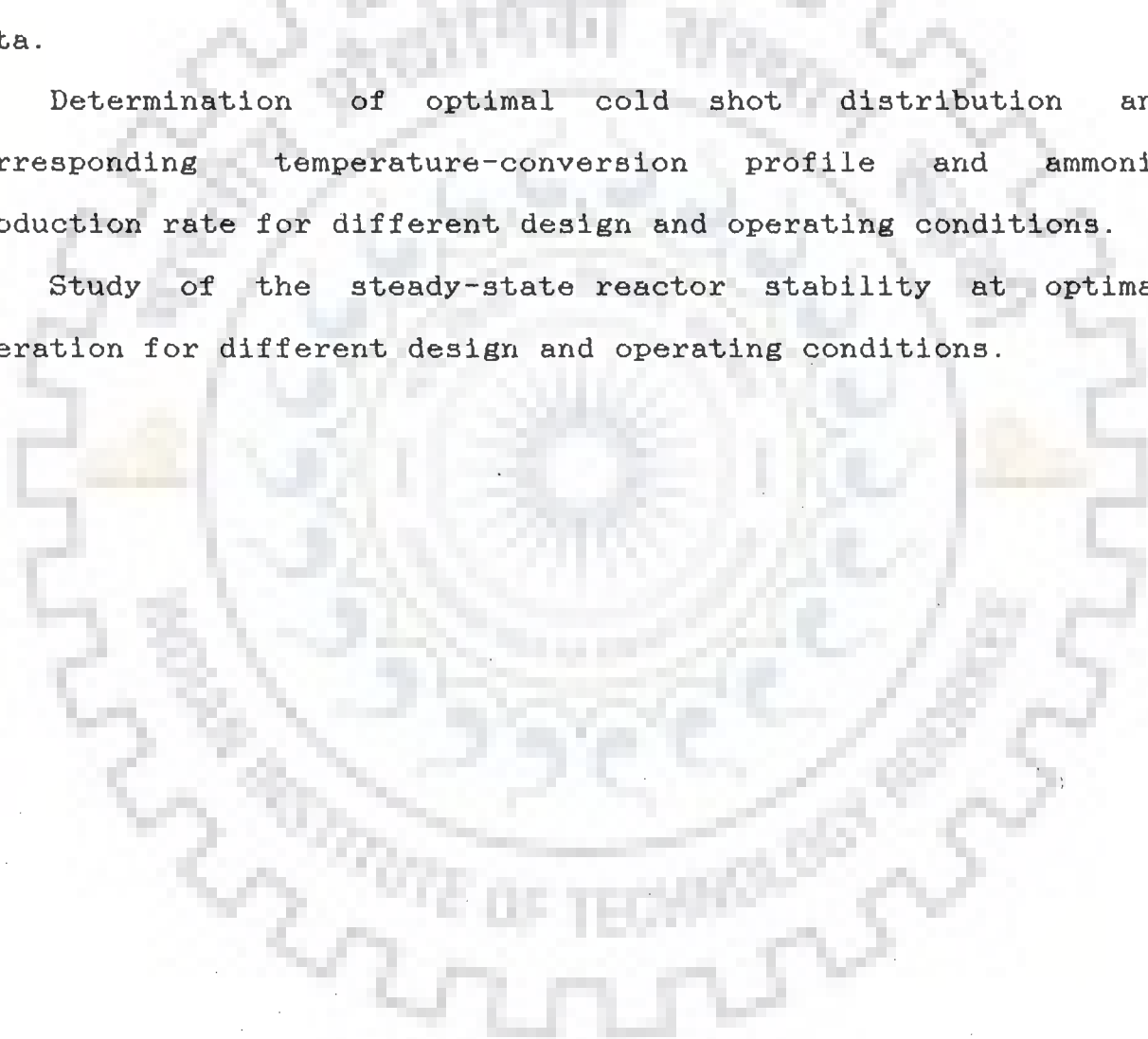
and operating conditions.

2. Development of reliable and efficient optimization strategies for the maximization of ammonia production rate using cold shot distribution as decision variables.

3. Validation of simulation model and the determination of the kinetic and external heat exchange rate parameters using plant data.

4. Determination of optimal cold shot distribution and corresponding temperature-conversion profile and ammonia production rate for different design and operating conditions.

5. Study of the steady-state reactor stability at optimal operation for different design and operating conditions.



CHAPTER II2. LITERATURE REVIEW2.1 Literature review on ammonia synthesis reactor modelling and simulation.

Modelling and analysis of autothermic processes, in particular ammonia synthesis reactor, have attracted considerable attention of research workers after the first reported study of van Heerden (1953). Van Heerden formulated a simplified one dimensional mathematical model for his packed bed catalytic reactor having a large number of tubes placed axially in the bed. The cold feed passes through the tubes countercurrent to the flow of gases in the catalyst bed and gets heated to desired temperature before entering the catalyst bed where exothermic reversible ammonia synthesis reaction occurs.

Van Heerden solved the three coupled differential equations, namely, material and energy balance equations for the reacting gases in the catalyst bed, and energy balance equation for the feed preheating inside the tubes for his simplified mathematical model of the reactor by using a stepwise numerical integration procedure. The solutions so obtained were in quantitative agreement with the actual data obtained for a commercial reactor of the same type.

Van Heerden observed from his analysis that due to reversible and exothermic nature of ammonia formation reaction a plot of heat generation rate due to reaction as a function of catalyst bed inlet temperature has a sigmoid shape but at very

high bed inlet temperatures the heat generation rate falls rapidly due to equilibrium limitations at high temperatures. He observed that the catalyst bed temperature first rises, passes through a maximum value and then decreases towards reactor exit. He also observed that a definite range of operating parameters exists for stable operation of an autothermic ammonia synthesis reactor at high conversion conditions in the vicinity of the quenching or blow-out point.

Van Heerden further observed from his theoretical analysis that as catalyst activity or the heat transfer capacity decreases the stability of the reactor decreases, whereas if the feed rate decreases the stability of reactor increases.

Annable (1952) derived a one-dimensional single-bed model of Haber-Bosch type ammonia synthesis reactor using a Temkin-Pyzhev (1940) rate equation. He found that the simulation model results were in close agreement with plant observations. But he did not investigate the effect of change in operating and design variables on the performance of the reactor and its stability using his simulation model.

Kjaer (1958) formulated his mathematical model for a single bed by considering the two-dimensional variation in temperature, axial and radial, and solved the resulting model equations consisting of three partial differential equations using double-step numerical integration technique by hand computation. His results of production rate and average bed temperature were in very good agreement with the plant data. However, the model developed by Kjaer could not explain the radial temperature

gradients reported by Slack et al. (1953). The results of Kjaer indicated that the radial temperature gradients may not be significant.

Baddour et al. (1965) studied the behaviour of a TVA ammonia synthesis reactor (Tennessee Valley Authority reactor) using a simplified one-dimensional model to account for axial variation of bed temperature and conversion. They used Temkin and Pyzhev reaction rate equation. The results of the simulation model were found to be within 15 to 20 percent of the plant data for the production rate and bed temperature profile. Their study indicated an improvement in ammonia production rate at higher space velocity of feed gas when reactor is operated at high first bed inlet temperature. However, an increase in space velocity is found to lower the reactor stability. Use of higher ammonia or inerts content in the feed was found to be detrimental, both, to reactor production rate and its stability, even though average bed temperature was not affected significantly. Any decrease in catalyst activity resulted in a decline in both, the reactor stability and its production rate and necessitated an increase in the first bed inlet temperature. The effect of increase in the heat transfer capacity was to increase the reactor stability with increased local overheating of catalyst. However, no significant effect on reactor production rate and average bed temperature was observed. They also observed that bed temperature profile at the optimum conditions was not sensitive to changes in operating conditions.



Shah (1967) developed a one-dimensional model to analyse the behaviour of a two-bed ammonia synthesis reactor with cold shot cooling. Shah made certain assumptions to simplify his model equations while accounting for the non-ideal behaviour of the gases in the reaction rate equation, heat of reaction and specific heat values. He found that these nonidealities have a significant effect on the reactor performance. Realising the inadequacy of the Temkin and Pyzhev rate equation, Shah used the modified Temkin and Pyzhev reaction rate equation in his simulation model. Shah also assumed a linear decrease in pressure with distance in the direction of flow of gas. His results of simulation agreed well with the plant data.

Shah solved his mathematical model consisting of coupled non-linear differential equations using a numerical integration technique known as the Milne Predictor-Corrector (Milne, 1953) and observed that the method of solution was stable and converged rapidly.

Shah observed from his simulation model studies that increase in cold shot fraction decreased the reactor stability; increase in inerts decreased the stability without significantly affecting the production rate; and increase in ammonia content of feed decreased both production rate and stability. He also observed that the increase in the first bed inlet temperature resulted in an increase in production rate till equilibrium inhibition was obtained. Shah further observed that the increase in pressure resulted in higher production rate but any change in H /N ratio did not affect the production rate significantly. The

effect of change in space velocity and catalyst activity on production was found to be the same as that reported by Baddour et al. (1965).

Shipman and Hickman (1968) carried out simulation and optimization of a five-bed ammonia reactor with external heat exchanger and cold shot quenching. They carried out optimization using independent variables consisting of operating variables of cold shot distributions and design variables of cold shot location, catalyst bed length and heat exchanger length. Search for optimization was carried out for minimising the converter cost using a modified gradient search method.

Shipman and Hickman observed that increase in the number of catalyst beds beyond three is not of much consequence for minimizing reactor cost. Further, cold shot distributions have a significant effect and there exists an optimal distribution. However, near the optimum the small variations in cold shot do not affect the optimal solution significantly.

Gaines (1977) simulated and optimized a four-bed ammonia converter with cold shot cooling and preheating. He used a modified Temkin and Pyzhev reaction rate equation and used the findings of Nielsen (1968) and Dyson and Simon (1968) for making it more realistic. He also considered the effect of catalyst pellet mass transfer resistance by incorporating in the rate equation the effectiveness factor as given by Dyson and Simon (1968). He optimized the bed temperature profile to maximise conversion at the reactor exit and recommended a declining outlet temperature profile from the first to the fourth bed. He found

that the last bed outlet temperature is most critical for improving reactor conversion. He concluded that there is an optimal ratio of actual ammonia mol percent to equilibrium ammonia mol percent at the catalyst bed outlet for achieving maximum conversion. The effect of important parameters, such as space velocity, feed temperature, pressure, inerts and ammonia concentration,  $H_2/N_2$  ratio and catalyst activity were found to be similar as reported by earlier workers. His results were in good agreement with plant data.

Vek (1977) considered two types of radial flow four-bed ammonia converters for modelling and optimization. The first type consisted of two heat exchangers -one internal heat exchanger placed between the first and the second bed and another external heat exchanger at the end of the last bed. The second type consisted of an external heat exchanger only, but with gas recirculation in the first bed. He accounted for variation of overall heat transfer coefficient in reactor. He found his simulation results in agreement with the plant data. From his analysis he observed that first type had better operational stability and a higher ammonia production rate. Typical outputs were between 100 to 130  $t/d/m^3$  of catalyst as compared to 35 to 50  $t/d/m^3$  of catalyst volume obtained normally.

Rase (1977) also presented a case study of multibed ammonia synthesis reactor with cold shot cooling. His range of operating variables include pressure at three values of 150, 225, and 300 atm and inerts in feed at 12 percent. For safe operation of the catalyst the allowable bed temperature was limited to 803

K. Rase observed that operation at lower pressure of 150 atm was more desirable for saving energy costs, and increasing the life and activity of catalyst.

Sinha (1977, 1981) modelled and analysed the behaviour of one-dimensional three-bed ammonia synthesis reactor with cold shot cooling and internal and external heat exchange. The results suggested that ammonia production rate is quite sensitive to operating parameters, such as, first bed inlet temperature, cold shot temperature and its distributions, ammonia and inerts content in the feed, feed pressure and design parameters such as cold shot location. It was observed that ammonia production rate increases with a decrease in ammonia and inerts contents in the feed, increase in space velocity, and increase in the first bed inlet temperature with proper cold shot distributions and location. However, the indiscriminate use of cold shot at a low first bed inlet temperature was found to be disastrous for ammonia production.

Reddy and Husain (1978) modelled a single-bed ammonia synthesis reactor of Casale type with cold shot quenching at the bed inlet using a one-dimensional model. They considered the actual flow route of gases in the reactor and the axial variation of heat transfer capacity. Model parameters were validated using plant data. Reddy and Husain studied the effect of operating parameters on the performance of the reactor. They found that the increase in feed flow rate reduces the ammonia conversion markedly at higher flow rate;  $H_2/N_2$  ratio has an optimum value around 2.5 for maximum conversion; and a decrease in inerts

and/or ammonia concentration increases ammonia conversion.

Ramkumar (1978) studied the behaviour of a one-dimensional three-bed ammonia synthesis reactor with cold shot cooling, internal and external heat exchange. He also accounted for the mass transfer resistance in the catalyst pellet by incorporating the effectiveness factor correlation of Dyson and Simon (1968) in the reaction rate equation. He observed that for increasing production rate, the space velocity and first bed inlet temperature should be higher, inerts content in the feed should be lower, and the cold shot distribution and location must be optimal.

Lutschutenkow et al. (1978) also presented the behaviour of a one-dimensional four-bed model of an ammonia synthesis reactor with external heat exchange. They observed maximum ammonia productivity near the autothermal limit. They also observed the bed outlet temperature to be independent of the cold shot at the bed inlet, and the ammonia productivity to depend on the  $H_2/N_2$  ratio in the feed and bed outlet temperature but not the reactor inlet temperature.

Singh and Saraf (1979) modelled and analysed the behaviour of one-dimensional ammonia synthesis reactors of two types. The first type was a three-bed reactor with external heat exchange and inter-bed heat exchanger for cooling without any cold shot. The second type was a single-bed reactor with external heat exchanger and cold shot cooling at the bed inlet. The effect of mass transfer resistances in the catalyst pellet was considered by incorporating effectiveness factor in the reaction rate

equation by partially solving the intrapellet diffusion equation at each axial location. They used different rate equations for two types of catalysts. Their simulation results were found to be in good agreement with plant data.

Khayan and Pironti (1982) studied the behaviour of an ammonia converter with heat exchanger using a two-dimensional model to account for axial as well as radial gradients of temperature and concentration. They solved the resulting non-linear coupled partial differential equations using the Crank-Nicolson numerical technique. Their results matched the plant data within 2 percent. They observed that radial gradients are insignificant.

Mansson et al. (1986) carried out optimization study of an ammonia synthesis reactor to maximize exit ammonia mole percent. Performance of the reactor was found by optimizing the bed temperature profile for a given mass flow rate and inlet conditions. Performance was compared with conventional operation. They observed that considerable improvement in performance may be achieved.

The literature review presented above clearly indicates that these simulation and optimization studies have significantly contributed to the understanding of the effect of operational and design parameters on the performance of ammonia synthesis reactors. However no published information is available regarding optimization of an existing industrial multibed quench reactor with internal and/or external heat exchanger for ammonia synthesis taking cold shot distribution as a decision variable

for wide range of variation of all important design and operating parameters. Very little published information exists on the steady-state stability analysis of such optimally operating reactors.

It may also be noted that no attempt has been made to review the simulation and optimization literature not specifically related to ammonia synthesis reactor.



## 2.2. Literature Review on Kinetic, Thermodynamic and Physical Properties:

Shah (1967) reported the kinetic, thermodynamic and thermochemical properties correlations using the data reported by Annable, Hougen and others. Shah gave correlations for reverse reaction rate constant,  $k_r$ , taking the Arrhenius form of dependence on temperature and also used a multiplying factor to correct for pressure deviations from 300 atm. His equilibrium constant correlation is a six-constant equation, an exponential function of temperature terms only.  $K_p$ , fugacity coefficient term, is correlated as a five-constant polynomial in temperature and pressure. His heat of reaction correlation is a ten-constant polynomial and heat capacity of ammonia correlation is a seven-constant equation, both equation involving pressure and temperature terms only. For nitrogen hydrogen and methane heat capacity correlations, Shah used four-constant polynomials in temperature with the coefficients of polynomial found for the mean pressure. For argon, the heat capacity was taken at a fixed value as it was independent of temperature and pressure. Shah observed that the more elaborate correlations used by him resulted in predictions by simulation model close to the plant performance.

Dyson and Simon (1968) gave  $k_r$  correlation by fitting the data of Nielsen in an Arrhenius form. However unlike shah's approach, there is no pressure correction term in their correlation. They used an equilibrium constant correlation proposed by Gillespie and Beattie, a five-constant equation



involving functions of temperature in an exponential form. Dyson et al. also used published correlations for the activity coefficients of  $H_2$ ,  $N_2$  and  $NH_3$  as four- or five-constant equations involving complex functions of temperature and pressure in an exponential form. They concluded that their correlations are quite precise to give fugacity values comparable to those obtained by more elaborate calculation of fugacity from an equation of state using both Beattie-Bridgman and Redlich-Kwong equations.

Gaines (1977) reported an Arrhenius form of correlation for  $k_r$  based on the data of Nielsen, similar to that of Dyson and Simon. The activity coefficients of  $H_2$ ,  $N_2$  and  $NH_3$  were correlated using equations involving three independent constants and showing temperature pressure and composition dependence. Gaines used a six-constant polynomial for heat of reaction involving pressure and temperature terms with correction for heat of mixing. He used an eight-constant BWR equation of state to compute directly the gas mixture heat capacities by first computing the constants for the mixture by appropriate relations.

Reddy and Husain (1978) have used the same correlations as reported by Shah (1967) for  $K$ ,  $K_p$ , heat of reaction and heat capacities of individual component.

Singh and Saraf (1979) took the usual Arrhenius form of correlation for  $k_r$  with appropriate values of the order of reaction parameter, frequency factor and activation energy for two types of catalysts based on data reported by Guacci et al. Correlations for  $K$  and heat capacities used by them are similar

to those reported by Dyson and Simon (1968).

Mansson and Andresen (1986) used the usual Arrhenius form of correlation for the rate constants in his reaction rate equation using three empirically determined sets of interdependent values of activation energy and frequency factor. The equilibrium constant correlation was obtained from Gillespie and Beattie as cited by Mansson et al. The activity coefficient correlations for  $H_2$ ,  $N_2$  and  $NH_3$  is taken based on Beattie and Bridgman, and Beattie work, as cited by Mansson et al., as a complex function of temperature, pressure and mole fractions in a way similar to that of Gaines but incorporating additional terms dependent on mole fractions to make it more accurate.

The heat of reaction correlation was that given by Nielsen, a seven-constant equation in temperature and pressure. Heat capacity correlations were those reported by Gillespie and Beattie as cited by Mansson et al. and heat of mixing was neglected in computing the mixture heat capacity as per the justification given by Nielsen and Strelzoff as cited by Mansson et al.

Hay and Honti (1976a) have presented correlations for thermodynamic properties. Of particular interest is that reported for the equilibrium constant, an exponential function of temperature giving a minimum percentage deviation from the theoretical values of Harrison and Kobe and comparing well with the experimental values reported by Haber, Larson and Dodge, Stephenson and McMahon as cited by Hay and Honti.

Perry's Chemical Engineers Handbook (1950) reports correlations for heat capacities of  $H_2$ ,  $N_2$  and  $NH_3$ , as three-constant polynomials in temperature. A correlation for heat of reaction is also given as a polynomial in temperature. Various other correlations for thermochemical properties are reported in the International Critical Tables (1928), Kirk and Othmer (1978) and by many other authors which vary in their degree of complexity, accuracy and range of application.



CHAPTER III3. REACTOR MODELLING AND DESIGN RELATIONSHIPS**3.1. Reactor modelling and design relations.**

Mathematical modelling of the multibed reactor consists in writing mass, energy and momentum balance equations for each of the reactor sections along with equations defining the boundary conditions imposed by cold shot addition at the bed inlet. The rigorous model precisely defining the heterogeneous ammonia synthesis reaction may be written in the form of partial differential equations for momentum, mass and energy balances in three-dimensional space and time. However such a system of highly non-linear and coupled partial differential equations will be very difficult to solve. This will require excessive computation time and very large memory on the large new generation computers. Convergence problems enhance these difficulties further that are inherent in the solution of autothermal reactor with external and/or internal heat exchange between the reaction mixture and the feed gas. Therefore, a rigorous approach is impractical and recourse must be made to more approximate engineering approach for simulation purpose that simplifies the modelling of converter significantly without sacrificing the accuracy to predict reactor performance and stability of operation keeping in view the extent of uncertainty inherent in the basic data used in the simulation model.

For this study, only the steady-state behaviour is taken into consideration and the change in operating parameters is

assumed to be slow enough that reactor operation is regarded as a succession of pseudo-steady states. It is further assumed that there are no gross perturbations that deliberately push the steady operation to another steady state. The validity of the steady-state assumption is discussed by Shah (1967). Yet another argument for considering the operation to be at steady-state is given by Reddy and Husain (1978) by pointing out that since the gas mixture velocity is always high, its residence time is likely to be very small, probably, of the order of a few seconds. Therefore, for the design and performance predictions of commercial reactor, the additional information obtained by considering the unsteady state simulation model is not commensurate with the phenomenal increase in modelling effort and computer time required for its solution.

A simplified flow diagram of a typical three-bed quench type high capacity ammonia synthesis axial flow reactor with internal and external heat exchange capacities is shown in Fig.3.1. The feed gas is divided into four parts; the largest fraction goes to bottom heat exchanger and the remaining gas is distributed into three cold shots for mixing with the gases entering different catalyst beds. The fraction of feed entering the bottom heat exchanger on its shell side gets preheated as a result of heat exchange from the reaction product leaving the third bed and flowing countercurrently on the tube side. This preheated fraction of feed is heated further by exchanging heat from the hot reaction mixture flowing countercurrently in the catalyst bed depending on the amount of heat transfer area available for the

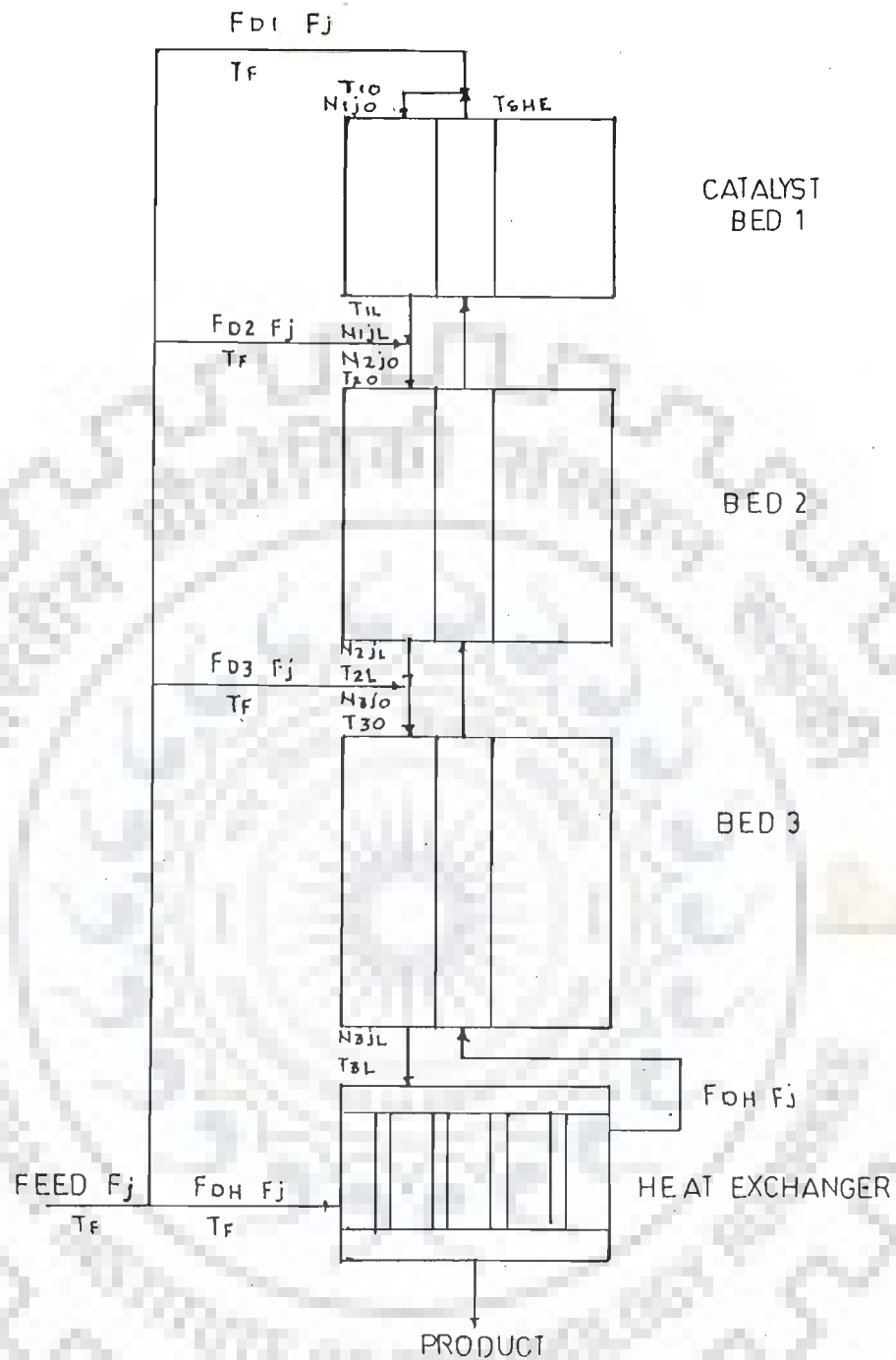


FIG. 3.1. SIMPLIFIED FLOW DIAGRAM OF THREE BED QUENCH TYPE AMMONIA SYNTHESIS REACTOR WITH INTERNAL AND EXTERNAL HEAT EXCHANGE CAPACITY

internal heat exchange. This heated fraction of feed enters the first catalyst bed inlet after mixing with cold shot fraction to the first bed.

### Assumptions.

For obtaining mass, energy and momentum balance equations in manageable form, following simplifying assumptions are made:

1. Reactor operation is at steady state.
2. Radial velocity, temperature, pressure and concentration gradients are absent. There is complete mixing in the radial direction in the bed.
3. There is no back mixing in axial direction.
4. Pressure drop variation is linear in the direction of flow. The effect of cold shot is accounted for by assuming that the coefficient of pressure drop varies with 1.8 power of the superficial mass velocity,  $G$ , at the inlet of a catalyst bed (Froment and Bischoff, 1979b). This dependence is based on Leva equation for packed beds indicating that the pressure drop is proportional to  $(fG)^2$  where  $f$  is the friction factor. Hicks has observed that this  $f$  is proportional to  $(G)^{-0.2}$ . Therefore, pressure drop is proportional to  $(G)^{1.8}$ .
5. Cold shot enters the reactor at the temperature of feed gas and at a pressure equal to the pressure in the reactor at the point of its entry.
6. Heat exchange capacity, that is the product of heat transfer coefficient and heat transfer area per unit catalyst bed volume remains constant throughout the reactor. Similarly, heat exchange

capacity per unit tube side volume in the external heat exchanger is also constant.

7. For gas-solid reaction, the interphase heat and mass transfer and the intraparticle heat transfer resistances are neglected.

8. Intraparticle mass transfer resistance in catalyst pellet is significant and is accounted for by considering the effectiveness factor. A polynomial relationship for the effectiveness factor with gas temperature and composition using pressure as a parameter is used to simplify the simulation model.

#### **Validity of assumptions.**

Except during start up and shut down of the reactor, the operation of a continuous process remains at a steady-state. Unsteady-state analysis becomes essential only for predicting the reactor behaviour during the start up and shut down periods.

The radial gradients of velocity, temperature, pressure and concentration across the cross-section of the catalyst bed are insignificant as compared to the axial gradients. This is supported by the findings of Kjaer (1958) and Khayan et al. (1982). These investigators considered the two-dimensional reactor model and found that the radial gradients are negligible.

Axial diffusion of enthalpy is ignored in view of the findings of Eymery (1964) as reported by Reddy and Husain (1982).

The pressure drop across the length of the bed is very small as compared to the pressure of gas at any point in the bed. In industrial converters the total pressure drop is found to be well within five percent of the gas pressure. Therefore, the assumption of linear variation of pressure along the reactor bed



is justified. However, a correction has been made in pressure drop correlation from one bed to another to account for the substantial increase in the gas flow rate in a particular bed because of the cold shot additions. The effect of increase in flow rate is taken into account by assuming that the coefficient of pressure drop varies with 1.8 power of superficial mass velocity,  $G$ . For a catalyst bed of uniform cross sectional area, it is quite evident that at the inlet of a bed  $G$  is proportional to the total feed fraction entering the bed.

In an ammonia synthesis reactor, the overall heat transfer coefficient varies along the bed length because of the changes in flow rate and the variation in physical properties of the gas mixture along the bed length. However, this variation in heat transfer coefficient is small and for all practical purposes, it may be assumed to be constant throughout the bed length. In any case, if considered essential, this variation can be accounted for as the calculations in numerical integration proceed from point to point at which all conditions are known, computing the value of heat transfer coefficient at any point using appropriate correlations.

The mass, momentum and heat balance equations can be written, keeping in view the foregoing assumptions and their justifications, for the ammonia synthesis reaction



over a differential reactor section of catalyst volume  $dv_i$  (in bed  $i$ ).

**Mass balance.**

The mass balance for hydrogen (subscript 2) is given by,

$$F_2 \frac{dx_{i2}}{dv} = (-r_2 \xi) \quad (3.1.2)$$

where,

$F_2$  = molal flow rate of hydrogen in feed to the reactor, mol/s,

$x_{i2}$  = fractional conversion of hydrogen in bed 'i' based on total hydrogen in feed to reactor, dimensionless;

$(-r_2)$  = rate of reaction without mass transfer limitations in catalyst given as moles of hydrogen converted per unit time per unit of catalyst volume, mol/s/cm<sup>3</sup>

$\xi$  = catalyst effectiveness factor to account for mass transfer resistance in the pellet, dimensionless.

**Energy balance.**

The energy balance equation is obtained by equating the heat of reaction to the summation of the sensible heat gain of the reaction gas mixture and the amount of heat transferred to the synthesis gas (cold feed) in the internal preheating section. This will give,

$$(-\Delta H_{R2}) (-r_2 \xi) dv = \left( \sum_{j=1}^5 N_{ij} C_{pj} \right) dT_i + (UA) (T_i - T_{si}) dv \quad (3.1.3)$$

where,

$(-\Delta H_{R2})$  = heat of reaction, kJ/kmol of hydrogen converted

$N_j$  = molal flow rate of component j, mol/s

$C_{pj}$  = heat capacity of component j, kJ/kmol/K

$T$  = gas temperature in the catalyst bed, K

$(UA)$  = heat exchange capacity of bed per unit catalyst bed volume,  $W/K/cm^3$

$T_s$  = gas temperature in the internal preheating section, K.

For  $(UA)$ , area of heat transfer,  $A$ , is defined per unit volume of catalyst bed. For a given reactor of certain design and configuration, area of heat transfer per unit volume of catalyst bed is likely to be constant throughout the bed length so that  $(UA)$  remains constant throughout the bed length as  $U$  is assumed constant.

Subscript  $j$  designates components (1- nitrogen, 2-hydrogen, 3- ammonia, 4-methane, and 5-argon) and subscript  $i$  denotes the catalyst bed number.

The energy balance equation for the feed gas in internal preheating section is:

$$F_{DH} \left( \sum_{j=1}^5 F_j C_{Pj} \right) dT_{Si} = -(UA)_i (T_i - T_{Si}) dv_i \quad (3.1.4)$$

Where  $F_{DH}$  is the fraction of total feed entering through preheating section and negative sign on right hand side takes into account the fact that in internal preheating section the direction of flow of feed gases is opposite to the direction of increase of catalyst bed volume.

For all the three beds the above set of equations (3.1.2), (3.1.3) and (3.1.4) are applicable and subscript  $i$  will be replaced by subscripts 1, 2 and 3 as computations are carried out for bed 1, 2 and 3, respectively.

It may be noted that the energy balances assume that heat of mixing for reaction mixture is negligible. Only Gaines (1977) appears to have considered heat of mixing terms in the

energy balance, but it is believed that at the reactor operating conditions (temperature 600 to 900 K, pressure 170 to 200 atm, and ammonia mole percent 1.5 to 16.0) the heat of mixing due to the non-ideality of reaction gas mixture may really be insignificant. Further more, appropriate correlations are used to account for variations in specific heat values with temperature and for ammonia with pressure also.

It is worthwhile to mention here that the fractional conversion of hydrogen,  $x_2$ , is based on total moles of hydrogen fed to reactor inclusive of all cold shots. Such a choice of  $X_2$  ensures that it increases monotonically as reaction mixture reacts while passing through the catalyst beds.

Additional mass and energy balance equations are needed to obtain the boundary conditions for the solution of reactor balance equations for each catalyst bed. The boundary conditions at each catalyst bed inlet are introduced due to the discontinuities resulting from the addition of cold shots at each bed inlet.

Mass balance equations for catalyst bed 1.

At the inlet (Subscript 0).

$$N_{i0} = F_j \left( F_{DH} + \sum_{i=1}^1 F_{Di} \right) + \alpha_j F_2 x_{210} \quad (3.1.5)$$

Where,

$$i = 1, 2, 3; \text{ and } j = 1, 2, 3, 4, 5$$

$F_j$  = molal flow rate of component j in feed to reactor,  
mol/s

$F_{Di}$  = cold shot to bed i as a fraction of total feed to reactor, dimensionless

At the exit (subscript 1).

$$N_{1j1} = F_j \left( F_{DH} + \sum_{i=1}^1 F_{Di} \right) + \alpha_j F_{21} X_{2,i-1,1} \quad (3.1.6)$$

where,

$$i = 1, 2, 3 \text{ and } j = 1, 2, 3, 4, 5$$

During cold shot addition at the inlet of any bed it may be noted that since reaction is not occurring, therefore, the value of  $x$  at the exit of the previous bed ( $i-1$ ) is the same as at the inlet of the next bed  $i$

$$X_{2,i-1,1} = X_{2,i,1}$$

Energy balance equations.

At the entry of bed  $i$  (after mixing of coldshot).

$$\left( \sum_{j=1}^5 N_{1j0} C_{pj} \right) T_{i0} = \left( \sum_{j=1}^5 N_{(i-1)j1} C_{pj} \right) T_{(i-1)1} + F_{Di} \left( \sum_{j=1}^5 F_j C_{pj} \right) T_{F_i} \quad (3.1.7)$$

where,

$$i = 1, 2, 3$$

$$N_{0j1} = F_{DH} F_j$$

$$T_{01} = T_{SHE}$$

$N_{0j1}$  is the molal flow rate of component  $j$  leaving external and internal preheating sections (hypothetical bed 0 exit), mol/s

$T_{SHE}$  = temperature of the preheated feed gases after passing through the external and internal preheating sections, K

Subscript 0 and 1 designate inlet and exit of the bed, respectively

Coefficient  $\alpha_j$  is proportional to stoichiometric coefficient for component  $j$  and have values  $\alpha_1 = -1/3$ ,  $\alpha_2 = -1$ ,  $\alpha_3 = 2/3$  and  $\alpha_4 = \alpha_5 = 0$

Here again equations (3.1.5), (3.1.6), and (3.1.7) are applicable to each bed by putting proper values of  $i$  as 1, 2 and 3.

### External heat exchanger balances.

In the external heat exchanger (subscript H) no chemical reaction occurs and it is simply a countercurrent heat exchanger to preheat only  $F_{DH}$  fraction of the total cold feed gases flowing through the external heat exchanger by all the product gases leaving the last reactor bed.

The energy balance for the feed gas gives, on shell side of heat exchanger

$$F_{DH} \left( \sum_{j=1}^5 F_{j,pj} C_{pj} \right) dT_{SH} = -(UA)_H (T_H - T_{SH}) dv_H$$

Where,

$T_{SH}$  = feed gas temperature on shell side of external heat exchanger, K

$(UA)_H$  = heat exchange capacity of external heat exchanger per unit tube side volume, W/K/cm<sup>3</sup>

$T_H$  = gas temperature on tube side, K

$V_H$  = tube side volume of external heat exchanger, cm<sup>3</sup>.

The negative sign on right hand side again accounts for the fact that the direction of flow of feed gases is opposite to the direction of increase of external heat exchanger volume.

Similarly for product gases, on tube side of heat exchanger:

$$\left( \sum_{j=1}^5 N_{3jl} C_{pj} \right) dT_H = -(UA)_H (T_H - T_{SH}) dV_H \quad (3.1.9)$$

For  $(UA)_H$ , the same argument also holds as in the case of the heat exchange capacity in catalyst bed side.  $N_{3jl}$  is the flow rate, moles of component  $j$  leaving third catalyst bed and

entering the external heat exchanger on tube side.

The flow rate of moles of component  $j$  at any point in bed  $i$ ,  $N_{ij}$  is obtained from the following equation,

$$N_{ij} = F_j \left( F_{DH} + \sum_{i=1}^1 F_{Di} \right) + \alpha_j F_2 X_{2i} \quad (3.1.10)$$

The above equation is valid for any of the three catalyst beds, only bed number 1, 2 or 3 will be written in place of subscript  $i$ .

The total molal flow rate in a bed,  $N_{iT}$  is given by,

$$N_{iT} = \sum_{j=1}^5 N_{ij} \quad (3.1.11)$$

which is valid for any of the three beds, only  $i$  needs to be replaced by appropriate bed number 1, 2 or 3.

Due to the pressure drop inside the heat exchanger and in the catalyst beds, the pressure of synthesis gas decreases from point to point in the direction of its flow. A suitable expression to estimate the pressure drop and, therefore, the pressure within the reactor is essential. Correlations are available in literature to find the pressure drop of flow of gases through the heat exchanger and the packed beds. For precise calculations these may be used. However, since the pressure drop through the convertor rarely exceeds 3 percent of the convertor pressure and also because changes in molal flow rates due to conversion in any bed is also small, no purpose will be served by using more complicated pressure drop correlations as the accuracy so achieved may be insignificant as compared to the extra complexity added in the simulation model and resultant increase in computer time. In view of this fact, the simulation model assumes that pressure,  $p$ , in atm varies linearly along the flow

path in any bed  $i$ . To account for the changes in the flow rate at any bed inlet due to cold shot addition, the pressure drop,  $dP_i$  is corrected for increase in flow of gases at the inlet of bed  $i$ , using 1.8 power of molal flow rates.

$$-dP_i = \omega_N \left\{ \frac{\sum_{j=1}^5 N_{j0}}{\sum_{j=1}^5 F_{jN}} \right\}^{1.8} dv_i \quad (3.1.12)$$

Where  $\omega_N$  is a coefficient, that is, pressure drop based on unit bed volume,  $\text{atm/cm}^3$ ; and subscript  $N$  corresponds to a reference or normal value of feed gas flow rate for which  $\omega_N$  is preassigned, an estimated value obtained from the normally observed pressure drops in the reactor. The above equation can be applied to any bed by assigning  $i = 1, 2$  or  $3$ .

Similarly, pressure drop expression is written for tube side, that is, product gases side of external heat exchanger as below

$$-dp_H = \omega_{HN} \left\{ \frac{\sum_{j=1}^5 N_{3j1}}{\sum_{j=1}^5 F_{jN}} \right\}^{1.8} dv_H \quad (3.1.13)$$

$\omega_{HN}$  is coefficient for pressure drop based on unit tube side volume of external heat exchanger,  $\text{atm/cm}^3$ .

A reasonable value for the total pressure drop based on commercial plant data is assumed and the total pressure drop is distributed in a realistic manner for external and internal preheating sections, catalyst beds and product gas side in heat exchanger. For catalyst beds linear pressure drop is assumed in each bed to account for the effect of pressure change on reaction rate, heat of reaction and activity coefficient as indicated earlier in equation 3.1.12. A linear pressure variation is assumed for product gases on tube side of heat exchanger also. However, for preheating sections, an average pressure value,



average of inlet and outlet pressures is used because the pressure drop in this section is generally quite small. The foregoing equations require the relationships for reaction rate, heat of reaction and heat capacities as a function of temperature, pressure and composition of gas.

### Reaction rate.

The modified Temkin and Pyzhev rate expression as given by Shah (1967) is used in the simulation model. The rate equation used is as follows :

$$-r = 29.4204 f k_r \left\{ \frac{P_1^{1.5} N_2^{1.5}}{(P_2^{0.5} N_2^{1.5})} \left[ \frac{P_1^{1.5} N_2^{1.5}}{(N_3^{1.5} N_T^{0.5})} \right] - \frac{N_3^{0.5} N_T^{0.5}}{N_3^{1.5} N_T^{0.5}} \right\} \quad (3.1.14)$$

Where,

$(-r)$  = reaction rate, mol of  $H_2$  reacted/s/m<sup>3</sup> of catalyst

$f$  = catalyst activity factor, dimensionless

Catalyst activity factor,  $f$ , may depend on many factors: For a given catalyst, the values of  $f$  may change with catalyst life. The fresh catalyst may be assumed to have a limiting value of  $f$  as unity and the same may decrease with catalyst age slowly. The catalyst is normally discarded after few years when the  $f$  value decreases to about 0.6 to 0.8 depending on the plant practice. In the simulation model  $f$  value is given a preassigned value as input data and the same can be made to vary if considered necessary.

$k_r$  = reverse reaction velocity constant, mol/s/m<sup>3</sup> of catalyst

$K$  = equilibrium constant of the reaction  $3/2 H_2 + 1/2 N_2 = NH_3$

$K_y$  = fugacity coefficient term

$N$  = gaseous constituent flow rate at any point in the reactor bed, mol/s

Subscripts indicate the gas component (1, 2, 3 and T refers to N<sub>2</sub>, H<sub>2</sub>, NH<sub>3</sub> and total components, respectively).

The correlation used for reverse reaction velocity constant is similar to that given by Shah (1967). The parameters specific to the catalyst used are frequency factor or preexponential factor and the activation energy. Adjustment was made in their values given in Shah's correlation through the use of multiplying factors Para1 and Para2 for the modification to the values used by Shah. The best values of Para1 and Para2 and, therefore, the frequency factor and activation energy suited for the catalyst used in the plant were found by validation of the simulation model using plant data as discussed subsequently in chapter-VI. The modified form of the equation used for  $k_r$  is as follows.

$$k_r = (300/p)^{0.63} \exp[(33.5566) (\text{Para1}) - (24092.2) (\text{Para2})/T] \quad (3.1.15)$$

The correlation used for equilibrium constant,  $K$ , is that reported by Hay and Honti (1976) that gives an average deviation of 0.00055 in logK and a maximum deviation of 0.0016 in logK over the temperature range of interest.

The equation is as follows:

$$\log_{10} K = (2250.322/T) - 0.8534 - 0.656 * \ln T - 2.58987 * 10^{-4} * T + 1.48961 * 10^{-7} * T^2 \quad (3.1.16)$$

The fugacity coefficient term,  $K_y$ , is also similar to Shah (1967). However, it was found necessary to adjust the value of  $K_y$

through the use of another multiplying factor, Para3, to the values given by Shah correlation. Values of  $K_p$  calculated from the correlation used by Shah were found to be lower than the values computed from correlations reported by many other workers. Further, only through this adjustment the model validation using plant data could be achieved more satisfactorily. This aspect is discussed in greater details in chapter VII. The equation used for  $K_p$  is as follows :

$$K_p = (\text{Para3}) * (1.7343 - 8.143 * 10^{-4} * P + 5.714 * 10^{-7} * P * T - 2.6714 * 10^{-3} * T + 2 * 10^{-6} * T^2) \quad (3.1.17)$$

The correlation used for heat of reaction is that given by Gillespie and Beattie as cited by Hay and Honti (1976).

Since the correlation reported by Shah (1967) for heat of reaction was found to be unsatisfactory. The equation used in simulation model is as follows :

$$\begin{aligned} -\Delta H_{R2} &= (2/3) * (0.54528 * P + (840.609 * P / T) \\ &+ (459.734 * 10^6 * P/T^3) + 5.34685 * T \\ &+ 0.2525 * 10^{-3} * T^2 - 1.69167 * 10^{-6} * T^3 \\ &+ 9157.09) * 4.1868 \end{aligned} \quad (3.1.18)$$

The correlations used for heat capacities, kJ/kmol/K, of  $N_2$ ,  $H_2$  and  $NH_3$  are those reported by Perry (1950) and the heat capacity correlation for  $CH_4$  is that given in International Critical Tables (1928). Heat capacity of argon is taken at 20.798 as reported by Shah (1967). The equations used in the model are as follows :

$$C_{p1} = (6.822 + 1.631 * 10^{-3} * t - 0.345 * 10^{-6} * t^2) * 4.1868 \quad (3.1.19)$$

$$C_{p2} = (6.919 + 0.218 * 10^{-3} * t + 0.279 * 10^{-6} * t^2) * 4.1868 \quad (3.1.20)$$

$$C_{p3} = (8.497 + 8.001 * 10^{-3} * t - 1.764 * 10^{-6} * t^2) * 4.1868 \quad (3.1.21)$$

$$C_{p4} = (3.00 + 0.0228 * T - 4.8 * 10^{-6} * T^2) * 4.1868 \quad (3.1.22)$$

$$C_{p5} = 20.798 \quad (3.1.23)$$

where,

$$t = T - 273$$

T = absolute temperature, K

Subscripts 1, 2, 3, 4 and 5 designate nitrogen, hydrogen, ammonia, methane and argon, respectively, as indicated earlier.

### 3.2. Effectiveness factor relation.

The effectiveness factor,  $\xi$ , correlation as a function of temperature, pressure and gas composition given by Dyson and Simon (1968) is used in the simulation model to account for the mass transfer limitations in rate equation for ammonia synthesis heterogeneous catalytic reaction. The equation used is given below :

$$\xi = b_0 + b_1 * T + b_2 * \eta + b_3 * T^2 + b_4 * \eta^2 + b_5 * T^3 + b_6 * \eta^3 \quad (3.2.1)$$

Where,

$\eta$  = dimensionless conversion of nitrogen and given by,

$$\eta = y_3 / (y_3 + 2 * y_1)$$

$$\text{or } \eta = [(1 + ((2 * y_{2F}) / (3 * y_{3F})) * x_2) / (1 + 2 * (y_{1F} / y_{3F}))] \quad (3.2.2)$$

Where  $y_1$ ,  $y_2$ ,  $y_3$  are mole fractions of nitrogen, hydrogen and ammonia, respectively, at any point in the bed and subscript F indicates mole fractions in the inlet feed. Therefore at a point in the reactor  $\eta$  is known for a known feed gas composition and actual hydrogen fractional conversion,  $X$ .

In equation (3.2.1)  $b_0$ ,  $b_1$ ,  $b_2$ ,  $b_3$ ,  $b_4$ ,  $b_5$  and  $b_6$  are constants with pressure as parameter as given in Table 3.2.1

Table 3.2.1

Constants for equation (3.2.1)

	<u>Pressure, atm</u>		
	<u>150</u>	<u>225</u>	<u>300</u>
$b_0$	-17.539096	-8.2125534	-4.6757259
$b_1$	0.07697849	0.03774149	0.02354872
$b_2$	6.900548	6.190112	4.687353
$b_3$	-1.082790 *10 <sup>-4</sup>	-5.354571 *10 <sup>-5</sup>	-3.463308 * 10 <sup>-5</sup>
$b_4$	-26.42469	-20.86963	-11.28031
$b_5$	4.927648 *10 <sup>-8</sup>	2.379142 *10 <sup>-8</sup>	1.540881 * 10 <sup>-8</sup>
$b_6$	38.93727	27.88403	10.46627

The correlation was developed for the case of  $H_2/N_2$  ratio of 3 and inerts concentration of 12.7 mol percent. However, in the present study the same correlation as given above is also used in view of only slight variations in the conditions used for simulation study. Dyson and Simon (1968) observed that the calculated values of effectiveness factors for the conditions other than those specified above had shown variations from those computed by using equation (3.2.1), but the overall effect on the design and performance of industrial ammonia synthesis reactors was negligible. Furthermore, if transport equations

(Dyson and Simon, 1968; Singh and Saraf, 1979) inside the catalyst are used for finding effectiveness factor additional complexities will be added without increasing accuracy significantly.

### 3.3. Equilibrium conversion relation.

The details of equilibrium conversion relation are given by Ramkumar (1978) for  $H_2/N_2$  ratio of 3 and summarised below along with relation for  $H_2/N_2$  ratio other than 3.

Equilibrium constant for reaction (3.1.1) is given by ,

$$K = \frac{\phi_3}{\phi_1^{1/2} \phi_2^{3/2}} = \frac{p_3}{p_1^{1/2} p_2^{3/2}} \frac{\gamma_3}{\gamma_1^{1/2} \gamma_2^{3/2}}$$

or  $K = K_p \cdot K_\gamma$  (3.3.1)

where  $\phi$ ,  $p$  and  $\gamma$  represent fugacity, partial pressure and fugacity coefficient, respectively.

$K$  is given as,

$$K_p = \frac{P \cdot y_{3eq}}{(P \cdot y_{1eq})^{1/2} (P \cdot y_{2eq})^{3/2}}$$

or  $K_p = (1/P) \cdot (y_{3eq} / (y_{1eq}^{1/2} \cdot y_{2eq}^{3/2}))$  (3.3.2)

Where  $P$  is the total gas pressure, and subscript eq refers to mole fractions at equilibrium.

The equilibrium mole fraction of  $H_2$ ,  $N_2$  and  $NH_3$  may be represented as,

$$y_{1eq} = (y_{1F} - y_{2F} \cdot x_{2eq} / 3) / (1 - 2 \cdot y_{2F} \cdot x_{2eq} / 3) \quad (3.3.3)$$

$$y_{2eq} = (y_{2F} - y_{2F} \cdot x_{2eq}) / (1 - 2 \cdot y_{2F} \cdot x_{2eq} / 3) \quad (3.3.4)$$

$$y_{3eq} = (y_{3F} + 2 \cdot y_{2F} \cdot x_{2eq} / 3) / (1 - 2 \cdot y_{2F} \cdot x_{2eq} / 3) \quad (3.3.5)$$

After substituting values of  $K$  and  $y_{1eq}$ ,  $y_{2eq}$ ,  $y_{3eq}$  from equations (3.3.2) to (3.3.5) in equation (3.3.1), we get after manipulation

$$K * P/K_p = \left\{ (y_{3F} + 2 * y_{2F} * x_{2eq} / 3) * (1 - (2/3) * y_{2F} * x_{2eq}) \right\} / \left\{ (y_{1F} - y_{2F} * x_{2eq} / 3)^{1/2} * (y_{2F} - y_{2F} * x_{2eq})^{3/2} \right\} \quad (3.3.6)$$

Where  $K$  and  $K_p$  are given by equations (3.1.16) and (3.1.17), respectively, and are functions of pressure and temperature of gas at any position in reactor bed. So for known temperature and pressure at any point and known feed composition, the equilibrium conversion in terms of fraction of hydrogen in feed,  $x_{2eq}$ , can be calculated using equation (3.3.6). This requires trial and error procedure or a single variable search method can be used for achieving quick solution within a desired tolerance. Generally, the  $H_2/N_2$  ratio is kept at 3. So for this case equation (3.3.6) can be simplified further to result in a quadratic equation as given below :

$$(1 + K_{c1}) * x_{2eq}^2 - [2 * K_{c1} + 3 * (1 - y_{3F}) / 2 * y_{2F}] * x_{2eq} + [K_{c1} - 9 * y_{3F} / 4 * y_{2F}^2] = 0 \quad (3.3.7)$$

$$\text{where } K_{c1} = 3 * K * P / (4 * K_p) \\ = 1.29904 * K * P / K_p$$

Therefore, with values of  $K$ ,  $K_p$  found at any axial position in the bed and with feed gas composition known, the above quadratic equation can be solved without any trial and error to determine the  $x_{2eq}$  values, which lies between 0 and 1.

#### 3.4. Conversion corresponding to maximum rate.

From equation (3.1.14) the reaction rate equation can be written as

$$-r_2 = C_1 * k_r * \left[ \frac{K}{K_p} \right]^2 * C_2 - C_3 \quad (3.4.1)$$

$$\text{where } C_1 = 29.4204 * f \quad (3.4.2)$$

$$C_2 = P^{1.5} * y_1^{1.5} * y_2^{1.5} / y_3 \quad (3.4.3)$$

$$\text{and } C_3 = y_1 / (P^{0.5} * y_1^{1.5} * y_2^{1.5}) \quad (3.4.4)$$

$C_1$ ,  $C_2$  and  $C_3$  are independent of gas temperature, dimensional.

The maximum of reaction rate as a function of temperature at otherwise constant conditions can be obtained by:

$$\left[ \frac{\partial(-r_2)}{\partial T} \right] = 0$$

It may be noted that the reaction rate shows a maxima with respect to temperature of gas in the bed only for an exothermic reversible reaction corresponding to any gas composition, that is, for any specified value of  $x_2$ . For a known value of catalyst activity factor,  $f$  all  $C_1$ ,  $C_2$  and  $C_3$  are independent of temperature, and only  $k_r$ ,  $K$  and  $K_p$  depend on temperature. Since  $k_r$ ,  $K$  and  $K_p$  have complex temperature dependence, the normal procedure is to choose a temperature and find the value of  $x_2$  at which the above equation is satisfied. The value of  $x_2$  so obtained is designated as  $x_{2m}$ , where subscript  $m$  refers to maximum rate conditions.

It is important to note that at any specified temperature, pressure and composition in the bed, the effectiveness factor is uniquely determined and actual reaction rate is reduced by that factor. Thus, for conditions corresponding to maximum reaction rate, the effectiveness factor can again be uniquely determined and the actual rate will again be reduced by that factor and the same will still remain the maximum possible rate for those conditions. Therefore, on differentiating equation (3.4.1) at



constant  $C_1$ ,  $C_2$  and  $C_3$  and equating it to zero, we get after simplification:

$$\frac{C_3}{C_2} = \frac{(K/K_p)^2 + 2 * k_r * K * [(\partial K / \partial T) - (K/K_p) (\partial K_p / \partial T)]}{(K_p (\partial k_r / \partial T))} \quad (3.4.5)$$

$$\text{or } \frac{C_3}{C_2} = K \quad (3.4.6)$$

where  $K$  is equal to right hand side of equation (3.4.5) and is only a function of temperature at a given pressure and can be calculated for known temperature and pressure at any position in the reactor bed.  $(\partial K / \partial T)$ ,  $(\partial K_p / \partial T)$  and  $(\partial k_r / \partial T)$  are all known from equations (3.1.15) to (3.1.17) by partially differentiating with respect to temperature and substituting the values of temperature and pressure. But the defining equations (3.4.3) and (3.4.4) show that,

$$\frac{C_3}{C_2} \equiv \frac{y_{3m}^2}{(P * y_{1m} * y_{2m})} = K \quad (3.4.7)$$

where subscript m refers to mole fractions at maximum rate condition. Using the procedure as presented in section 3.3, we get

$$K_{C2} = \frac{(y_{3F}^2 + 2 * y_{2F} * x_{2m} / 3) * (1 - 2 * y_{2F} * x_{2m} / 3)}{(y_{1F} - y_{2F} * x_{2m} / 3) * (y_{2F} - y_{2F} * x_{2m})^3} \quad (3.4.8)$$

Therefore,  $x_{2m}$  can be uniquely determined at any position of reactor bed from the above equation for the known temperature, pressure and feed gas composition. Equation (3.4.8) can also be solved either by trial and error technique or univariate search technique for finding the value of  $x_{2m}$ . For the case when  $H/N$  ratio is 3 equation (3.4.8) can be further simplified to result in a quadratic equation in  $x_{2m}$  as given below,

## CHAPTER IV

### TECHNIQUE FOR OPTIMIZATION OF AMMONIA SYNTHESIS REACTOR

In the design and operation of ammonia synthesis reactor a number of decision variables exist that are free to be adjusted for achieving optimization. In an existing plant with fixed design parameters and for a given feed flow rate, composition, temperature and pressure, cold shots to various beds can be allocated in such a manner as to give maximum ammonia production rates. At the design stage, catalyst distribution in different beds can also be adjusted in addition to the cold shot distribution to maximize ammonia production rates.

In this study the production rate of ammonia is taken as the objective function to be optimized subject to the implicit constraints given by design relations presented earlier and several explicit constraints for example, sum of cold shot fraction should be between 0 and 1, conversion should be lower than its equilibrium value, etc. In an existing reactor, the objective function, that is, ammonia production rate, is a function of many independent operating variables; for example, feed gas flow rate, feed pressure, bed inlet temperatures,  $H_2/N_2$  mole ratio in feed, ammonia and inerts mole fractions in feed, and cold shot distributions to various catalyst bed inlets. The objective function is also a function of many design parameters; for example, total volume of catalyst, catalyst distribution in different beds, heat exchange capacity in the catalyst bed and

external heat exchanger.

The objective function for this study is highly nonlinear and coupled, implicit, constrained, multivariable and discontinuous in nature. It also involves internal loop optimization with severe convergence problem of a multimodal function that is also highly nonlinear, constrained, implicit and coupled in nature.

With the help of high speed digital computers with large memory, sophisticated optimization techniques could be used to solve such problems. Therefore, now it is realistic to attempt to establish an optimization procedure for obtaining the optimum results.

In general the gradient or indirect search methods (Beveridge and Schechter, 1970; Gangiah, 1980) have faster convergence in comparison to direct search methods. The gradient methods are based on evaluation of derivatives whereas the direct search methods are based on evaluation of objective functions without calculating the derivatives. However in practice, as in the present study, it is either extremely difficult or impossible to provide analytical functions for calculating derivatives needed in gradient methods. The function may not be differentiable or the derivatives may be difficult to compute numerically, as in this case where it may lead to magnification of errors and large computation time.

Among direct search methods the complex search method as given by Adelman and Stevens (1972), based on the method of Box (1965), Nelder and Mead (1965) and a similar constrained

polyhedron search method presented by Gangiah (1980) is selected for use as an optimization technique.

Other methods of direct search are also available based on "evolutionary operation" and "Monte Carlo techniques" (Luus and Jaakola, 1973; Campbell and Gaddy, 1976; Heuckroth et al., 1976). However, as observed by Gangiah (1978, 1980), they are found less efficient in several cases.

#### 4.1. Description of the complex search method (Adelman and Stevens, 1972; Gangiah, 1980; Nelder and Mead, 1965).

This method consists of finding an original feasible "Complex (constrained simplex)" of solutions, eliminating the "worst" of these by reflection through the centroid of the remaining points, and repeating until an optimum has been reached. Worst point is defined as the point at which the objective function is found to have a minimum value. So the direction of search is from the worst through the centroid and step length is obtained by reflection through the centroid on the opposite of worst point. The acceleration in step size is provided by reflection coefficient,  $\alpha_r$ , say 1.3 (Adelman and Stevens, 1972; Box, 1965), for mapping the entire feasible region by enlargement of complex so that the convergence at global optima in the constrained feasible region is obtained.

The problem statement in general, can be written as

$$\text{maximize } Y(X) = f(x_1, x_2, \dots, x_n)$$

Subject to the implicit constraints

$$g_i(x) < 0, \quad i = 1, 2, \dots, r$$

$$h_j(x) > 0, \quad j = 1, 2, \dots, s$$

$$e_k(x) = 0, \quad k = 1, 2, \dots, m$$

here  $m < n$

and the bounds or explicit constraints

$$x_{\min} < x_i < x_{\max}$$

$$i = 1, 2, \dots, (n-m)$$

Let  $x_{ij}$ ,  $j = 1, 2, \dots, (n-m+1)$  is the  $j$ th vertex point and  $i$  is the coordinate or number of decision variable.

The centroid of all  $x_{ij}$  excluding the worst point  $x_{ij}$  (worst),

$$\bar{x}_i = \{1/(2(n-m))\} \sum_{\substack{j=1 \\ j \neq w}}^{(2(n-m)+1)} x_{ij} \quad (4.1)$$

here  $i = 1, 2, \dots, (n-m)$

### Algorithm

1. Select the  $\{2(n-m) + 1\}$  vertices.
2. Test for explicit constraints at a vertex, if constraints are violated the decision variables are set to the bounds.
3. Solve implicit equality constraints numerically. Test for implicit inequality constraints. If any inequality constraint is violated, the corresponding variable is set to the constraint value. If all implicit inequalities are satisfied go to next step

or else proceed to step 5 by assigning the vertex as worst-valued.

4. Evaluate the objective function. If only the worst vertex has been replaced, go to step 8 or else proceed to next step.

5. Repeat steps 2 to 4 for all vertices if it is a newly formed complex or else go to step 6.

6. Compute the centroid of the complex as given in equation (4.1) by finding the worst valued vertex.

7. Find the new vertex to replace the worst valued vertex. This is done by formula

$$x_{ij}^{(new)} = \bar{x}_i + \alpha_r [\bar{x}_i - x_{ij}^{(worst)}] \quad (4.2)$$

where  $\bar{x}_i$  is the  $i$ th coordinate of centroid,  $x_{ij}^{(new)}$  is the  $i$ th coordinate of the new  $j$ th point to form a new complex and  $x_{ij}^{(worst)}$  is the  $i$ th coordinate of the worst  $j$ th point in the complex.

8. Repeat steps 2 to 4. If this new trial point replacing the worst is again worst, the point is moved half-way towards the centroid of the remaining points. If this trial also results in the worst valued point, the point is further moved half-way towards the remaining distance from centroid. If this also fails to improve due to special nature of an objective function, the reflection is seen to get new trial vertex.

The procedure terminates when the complex collapses within a certain preassigned tolerance of objective function values or up to a certain number of iterations, whichever is reached first. Otherwise, go to step 6.

In the present case, it is observed that for certain cold

shot distributions (several vertices) that are not true optima, the ammonia production rates are nearly the same, and therefore, it is impractical to assign any tolerance other than zero. The search was then terminated by preassigning the number of iterations so that the true constrained optima could be obtained.

The Box complex search has the following advantages over the other optimization techniques (Adelman and Stevens, 1972; Gangiah, 1980).

1. The method is stable, versatile, and the solution is very fast due to fast convergence.
2. Programming is easy.
3. It yields other valuable information about the system apart from the optimum solution. The response of the system is well mapped over a wide range of values of the independent variables. The sensitivity of the optimum, that is response to small changes in independent variables is obtained as the method converges to the optimum and evaluates the response to small perturbations in the variables. This additional information is of great value in both design, operation and optimum control of chemical plants.
4. It is superior to other sequential direct search methods (pattern search, parallel tangents, etc.) and can find the true optimum rather than local optima nearest to the starting point because of the fact that the points in the initial complex are scattered throughout the feasible region, with a good chance that at least one will lie in the vicinity of the true constrained optima.

5. The use of reflection factor greater than 1.0 causes an initial enlargement of the complex due to acceleration in step length, thus assuring a good initial scan of the entire feasible region.





## CHAPTER V

### 5. COMPUTATION TECHNIQUE

#### 5.1 Computation technique for optimization.

The material and energy balance equations written for a differential section of a bed of ammonia synthesis reactor are presented in chapter -III. For such a system of highly non-linear and coupled equations, numerical integration is essential because analytical integration is not possible. A suitable numerical integration technique based on modified Milne-Predictor-Corrector method is used by choosing small step size. Computation accuracy will depend upon the magnitude of step size chosen. Tolerance limits at each step for conversion and temperature are checked against the preassigned limits, chosen in this study as  $5 \times 10^{-5}$  for fractional conversion of hydrogen and  $5 \times 10^{-3}$  K for temperature. The tolerance limits can be externally changed, if required, as input data. The stepwise procedure is given below:

Step 1. Read data set for reactor conditions and parameters

Step 2. Test the range of search based on the lower and upper limits on  $T_{SHE}$ , the temperature of the feed gas at the exit of the internal preheating section. If the program works, go to the next step or alter the bounds until the program works and set the region of search for  $T_{SHE}$ .

Step 3. In the region of search assume  $T_{SHE}$  with an interval, say 20 K, in  $T_{SHE}$  values. The computation starts from the lower limit of the search region and proceeds with 20 K (say)

increments until the upper limit of  $T$  is reached. Go to the next step if cold shot is added; otherwise, go to step 5.

Step 4. Determine the temperature of resultant stream by the regula falsi interpolation technique since the heat capacity of the mixture is not known. Molal flow rate is calculated by material balance.

Step 5. Carry out the numerical integration, step by step in the forward direction, up to the end of the first bed to establish the exit conditions.

If a cold shot is added to second bed, go to next step or else go to step 7.

Step 6. Determine the temperature and molal flow rate of resultant stream as given in step 4.

Step 7. Carry out the numerical integration, step by step in forward direction, up to the end of the second bed to establish the exit conditions.

If a cold shot is added, go to next step; otherwise, go to step 9.

Step 8. Determine the molar flow rate and temperature of the resultant stream.

Step 9. Carry out numerical integration, step by step in forward direction, up to the end of the third bed to establish exit conditions.

Step 10. Carry out numerical integration for external heat exchanger up to its exit.

Step 11. At the end of last step 10, value of  $T$ , the computed temperature of feed entering the external heat exchanger



on shell side, is obtained.  $T_{SHI}$  is compared with  $T_F$ , the actual feed temperature and if difference,  $DELTA = [(T_{SHI} - T_F)]$  lies outside the tolerance limit of  $\pm 2K$  (fed externally as an input data and may be varied, if desired) then convergence is not achieved. The next  $T_{SHE}$  is chosen for carrying out a pattern search. If  $DELTA$  value for the next  $T_{SHE}$  value is of the same sign as that for the preceding  $T_{SHE}$  value, repeat step 4 onward for the case of cold shot addition at the first bed inlet or steps 5 onward without cold shot addition.

Step 12. In case convergence is not achieved but the  $DELTA$  calculated is of the opposite sign to that of the  $DELTA$  obtained for the preceding  $T_{SHE}$  value, then the value of  $T_{SHE}$  that results in converged  $DELTA$  is searched in the interval of the present  $T_{SHE}$  and preceding  $T_{SHE}$  values according to the convergence criteria of the regula falsi interpolation technique.

Step 13. In case convergence is achieved and  $T_{SHE}$  is less than the upper bound of the region of search for  $T_{SHE}$ , then steps 3 onwards are repeated with an increment of 20 K (say) in  $T_{SHE}$ .

Step 14. The highest converged value of  $T_{SHE}$  is taken as the stable and desirable operating point and corresponding ammonia conversion and production rate are taken as the value of objective function for the given data set and the chosen values of decision variables (cold shot and/or catalyst distribution) for which the calculations were carried out.

Step 15. Steps 2 onwards are repeated for optimization over the decision variables (cold shot and/or catalyst distribution) using the Box complex optimization technique discussed earlier

in chapter IV.

Step 16. Repeat steps 1 to 15 for the new input data set until the computations for all the input data sets are completed.

## 5.2. Convergence policy.

During the course of computation as given in section 5.1 convergence is desired in the value of DELT within a prespecified tolerance for getting the value of  $T_{SHE}$  that is a solution to the system of equation of ammonia synthesis reactor. In majority of cases it is found that some where in the region of search for  $T_{SHE}$  the DELT value will change sign, if any solution, other than trivial solution corresponding to negligible conversion and  $T_{SHE}$  value close to  $T_F$  value, exists at all. When such a region is isolated or detected then the convergence in DELT is achieved by applying regula falsi technique in the selected region. Another approach is to use golden section search or fibonacci search by taking absolute value of DELT i.e.  $|DEL T|$  as an objective function. However, in this study the Regula falsi technique has been applied with great success to achieve very fast convergence in almost all cases. In the Regula falsi technique the next trial for  $T_{SHE}$  is made in the interval of sign changes of DELT by using the following relationship:

For  $(n + 2)$ th iteration,

$$T_{SHE, (n + 2)} = T_{SHE, (n+1)} + \frac{(T_{SHE, n} - T_{SHE, (n+1)}) * ABS(DEL T(N+1))}{ABS(DEL T(n+1)) + ABS(DEL T(n))} \quad (5.1)$$

Where  $n$  can take any integer value 1, 2, 3 -----.

For this new point  $T_{SHE,(n+2)}$  DELT is calculated based on the steps discussed in section 5.1 and if convergence is not achieved, for further search the point that has the same sign as DELT among  $T_{SHE,n}$  and  $T_{SHE,(n+1)}$  is discarded and the next interpolation is made according to equation 5.1.

### 5.3. Numerical integration procedure.

Modified Milne-Predictor-Corrector method (Milne, 1953; Shah, 1967) is used for numerical integration of nonlinear and coupled differential equations. This method is found to be stable with a fast speed of convergence at each step of numerical integration. The error in computation is less as compared to fourth-order Runge-Kutta method (Lambert, 1974).

This method requires generating first four points by following predictor and corrector steps (Ivo Babuska, 1966):

#### First point:

This point is the inlet to first bed where on the assumption of temperature  $T_{SHE}$ , all the information becomes available. Using relations presented in chapter-III the differential equations in the design relations take the following functional form:

$$\frac{dx}{dv} = f_1(X, T, P)$$

$$\frac{dT}{dV} = f_2(X, T, P)$$

$$\frac{dT_s}{dv} = f_3(T, T_s)$$

**Second point:**

With the first point known, the derivatives at the first point are calculated. The derivatives are used to predict the first guess of the second point, the predictor step. The derivatives are then calculated at this first guess of the second point and using the corrector step the second point estimate is refined till the last guess and its preceding guess value match within a preassigned tolerance limit. This method is stable and in a few iterations convergence is achieved. In symbolic form:

Predictor step.

$$y_2 = y_1 + y_1' \Delta h, \quad y_1' = \frac{dy_1}{dh}$$

Corrector step.

$$y_2 = y_1 + (y_2' + y_1') \frac{\Delta h}{2}, \quad y_2' = \frac{dy_2}{dh}$$

where  $y$  is a dependent variable such as  $x$ ,  $T$  and  $T$ ;  $h$  is an independent variable such as  $v$ ;  $\Delta h$  is small but finite increment in  $h$ ; superscript prime refers to first derivative and subscript 1, 2, 3 etc. refer to variable values at first point, second point, third point etc.

**Third Point:**

Predictor and Corrector steps for the third point are given below. The third point estimates are refined using the corrector step till convergence is achieved.

Predictor step.

$$y_3 = y_2 + (3y_2' - y_1') \frac{\Delta h}{2}$$

Corrector step.

$$y_3 = y_2 + (5y'_3 + 8y'_2 - y'_1) \frac{\Delta h}{12}, \quad y'_3 = \frac{dy_3}{dh}$$

Fourth point:

The fourth-point predictor and corrector steps are given below. The fourth-point estimates are refined till convergence is obtained.

Predictor step.

$$y_4 = y_3 + \frac{\Delta h}{12} (23y'_3 - 16y'_2 + 5y'_1)$$

Corrector step.

$$y_4 = y_3 + \frac{\Delta h}{24} (9y'_4 + 19y'_3 - 5y'_2 + y'_1),$$

After the first four points have been generated, the Milne-Predictor-Corrector step is applied to generate remaining points. As Milne-Predictor-Corrector technique is more stable and very fast in convergence, only single application of corrector step may, in general, give accurate values for the new point within the tolerance limit.

Fifth point:

Predictor step.

$$y_5 = y_4 + \frac{4\Delta h}{3} (2y'_2 - y'_3 + 2y'_4)$$

Corrector step.

$$y_5 = y_4 + \frac{\Delta h}{3} (y'_3 + 4y'_4 + y'_5)$$

For the sixth point onwards a modified step is taken between

predictor and corrector steps is also used that further accelerates convergence by making use of the magnitude of error at previous point between values from predictor and corrector. This error is added in the value obtained from predictor step to guess in advance values that are used for finding the derivative in the corrector step.

Modifier step at  $i$ th point:

$$\Delta_{(i-1)} = y_{(i-1)} - y_{(i-1)} \text{ (converged corrector step value) - } y_{(i-1)} \text{ (predictor step value)}$$

Sixth point onward for  $i$ th point:

Predictor step.

$$y_i = y_{i-4} + \frac{4\Delta h}{3} (2y'_{(i-3)} - y'_{(i-2)} + 2y'_{(i-1)})$$

Corrector step.

Using a  $y_i$  (modified), that is,  $y_i + \Delta_{(i-1)}$ , the  $y'_i$  for corrector step is found.

$$y_i = y_{(i-2)} + \frac{\Delta h}{3} (y'_{(i-2)} + 4y'_{(i-1)} + y'_i)$$

(corrector step)

where  $i = 6, 7, \dots$



#### 5.4. Computer program features.

A computer program to simulate and optimize ammonia synthesis reactor performance has been written in FORTRAN - 77 and executed on DEC 2025 system of Roorkee University Regional Computer Centre. It consists of a main program and 24 subroutines having over 2500 statements. The program is efficient and requires minimum possible computation time and memory requirements. It takes about 25 seconds CPU time to compile, about 4 seconds of CPU time for loading and linking the program, and about 6 to 8 seconds of CPU time to run a single data set of operating and design conditions after carrying out the search over the entire feasible operating region of  $T$ . Complete SHE solution of the system of equations is obtained for both high conversion and thermally unstable and stable operating points, if such points exist, while ignoring the trivial low conversion and low temperature point. It could be located in 10 to 15 iterations. Further, it took about 5 to 8 minutes of CPU time for optimization of cold shot distribution to maximize ammonia production depending on the initial points of complex search (fed as a part of the input data), the degree of difficulty experienced by the system equations in arriving at the optimum and the precision to which the maximization of objective function (ammonia production rate) is desired.

The main program is arranged in three sections, namely, READ DATA, policy of convergence and optimization section, and PRINT RESULTS. Numerous comment statements have been used in the main program and the subroutines to make them more understandable. The

computer program listing is given in Appendix-B. The program has following additional features:

1. The optimization could be done with an option of feeding a single data set and the self-generation of the remaining vertices of complex or feeding all the data sets of the vertices. It can further start the optimization search with known values of data sets and their corresponding objective function values without recalculating the objective function again. This would be advantageous when one wants to further test an optimum result based on the earlier searches by using the best possible Box complex for which objective function values are already available. This can help in establishing the optimum beyond any shadow of doubt.
2. The program has an option to carry out optimization or just to carry out a single search for a single data set or multiple data sets.
3. The program has an option to consider the particle effectiveness factor either as unity corresponding to the absence of mass transfer limitation or to compute the effectiveness factor at each point using the Dyson and Simon (1968) relationship.
4. The program has an option to print detailed results at each point in the bed or at some interval or to print only the summary of results at the inlet and outlet of each bed.
5. The program has an option to make searches at new vertices either by taking the actual values generated or at values rounded to a certain preassigned decimal point or only to search at

certain preassigned levels of the variables by shifting the actual value of the variable to its nearest preassigned level. This feature is important in order to search the cold shot distributions only at values that can be readily adjusted in plant.



## CHAPTER-VI

### 6. ESTIMATION OF SIMULATION MODEL PARAMETERS FROM PLANT DATA

6.1 Purpose of estimation of Parameters and parameters description.

For any mathematical model that is developed on theoretical consideration of mass and energy balances it is always necessary to adjust and tune certain parameters that are dependent on the specific process conditions so as to make the simulation model predictions closer to plant performance. In the case of ammonia synthesis reactor simulation, the parameters that are specific to the catalyst used are the preexponential or frequency factor and the activation energy in the reverse reaction rate constant. Adjustment was made through the use of Para1 and Para2, respectively, as the multiplying factors to the base values for the frequency factor and activation energy values reported by Shah (1967), see equation 3.1.15. It was also found necessary to adjust the value of the fugacity coefficient,  $K_f$ , through the use of Para3, multiplying factor to the correlation for  $K_f$  reported by Shah (1967), see equation 3.1.17.

The heat exchange capacity of the external heat exchanger, which depends on the heat exchanger design, was also estimated after making corrections for changes in the flow rates by the parameter estimation technique.

## 6.2. Parameter estimation technique.

The objective function for estimation of optimal value of the parameter is taken as the minimization of the sum of squares, that is found to be multimodal, constrained, multivariable and nonlinear in nature. Therefore the complex search technique (discussed in chapter-V) is used along with external adjustment of the direction and step size in between searches to reach the minimum of sum of squares. Actual plant data for an axial flow multibed quench type ammonia synthesis reactor of a modern Indian plant has been chosen to simulate its performance using the simulation package developed during this investigation. In the plant only temperatures at the end of each bed, ammonia concentration at the end of last bed, first bed inlet temperature and the tube side external heat exchanger exit temperature are monitored. Inlet feed composition, temperature, pressure and pressure drop across the reactor are also measured. Table 6.2.1 gives selected data for different conditions as obtained from the plant log sheets for several months. The data was selected for a period during which plant operation was found to be steady.

It was found that the cold shot distribution, the most important variable for reactor operation, is not measured at the plant. It was necessary to consider cold shot distribution also as a variable while estimating model parameters. For more accurate prediction of the model parameters, it is desirable to know the bed temperatures at the inlet and also at several intermediate points in the catalyst bed as well as the ammonia concentration at least at the end and the beginning of each

Table 6.2.1

## Selected Plant Data Extracted from a Typical Ammonia Plant Log Sheets

Catalyst: Volume = 67.6 m<sup>3</sup>, Distribution Bed1: Bed2: Bed3 = 1:1.4:2.0

Data Set	Feed Pressure (atm)	Feed Flow Rate Nm <sup>3</sup> /h	Feed Temp. K	Feed Composition:				Total Press Drop, Inlet atm	Reactor Temperature			Exit NH <sub>3</sub> mol % 3rd Bed	
				H <sub>2</sub> /N <sub>2</sub> Ratio	NH <sub>3</sub> mol %	CH <sub>4</sub> mol %	A <sub>r</sub> mol %		1st Bed Exit	2nd Bed Exit	3rd Bed Exit		
1.	190.0	0.740*10 <sup>6</sup>	414.0	3.00	1.61	8.80	4.04	2.7	652	783	752	749	13.42
2.	192.0	0.800*10 <sup>6</sup>	415.0	3.11	1.89	9.30	3.97	2.6	654	778	759	759	13.40
3.	173.0	0.740*10 <sup>6</sup>	414.0	2.82	1.70	7.00	4.25	2.8	655	784	765	756	13.12
4.	185.0	0.785*10 <sup>6</sup>	413.0	3.04	1.84	8.52	3.84	2.7	653	781	761	757	13.60
5.	184.0	0.775*10 <sup>6</sup>	417.0	2.96	1.71	8.59	4.65	2.8	651	775	763	757	13.47
6.	186.0	0.760*10 <sup>6</sup>	414.0	3.28	1.70	6.88	4.27	2.8	656	792	765	758	13.14
7.	183.0	0.770*10 <sup>6</sup>	417.0	3.08	1.70	7.74	4.06	2.7	655	782	768	761	13.45
8.	183.0	0.780*10 <sup>6</sup>	417.0	3.03	1.72	8.25	3.80	2.8	652	778	763	758	13.20

Note: Units of feed flow rate are given as Nm<sup>3</sup>/hr. The prefix N before m<sup>3</sup> merely indicates m<sup>3</sup> at the N.T.P. conditions.

bed. In view of the limitations of data as discussed above, the model parameter values estimated from the plant data have some inherent accuracy limitations.

The objective function for minimization is chosen as the sum of the squares of the difference in the computed and observed values of bed exit temperature for each of the three beds and the ammonia mole percent at the exit of last bed. Since the difference in the values of ammonia mole percent at the exit of last bed is an order of magnitude smaller than the difference in the values for each of the bed exit temperature, a suitable weighting function was used. This is used as a multiplier to the square of the difference in the computed and observed values of ammonia mole percent in order to make the objective function more sensitive to small mismatch in the ammonia concentration. The value of weighting function chosen for the present study is 200.

### 6.3. Selection of physical properties, thermodynamic and kinetic correlations.

Several correlations (Perry, 1950; Shah, 1967; Dyson and Simon, 1968; Hay and Honti, 1976; Gaines, 1977; Reddy and Husain, 1978; Singh and Saraf, 1979; Mansson and Andresen, 1986) are reported in literature that vary in their degree of complexity, accuracy and range of application for the physical, thermodynamic and kinetic properties required for ammonia synthesis reactor simulation. The physical and thermodynamic properties required are the specific heat, heat of reaction, equilibrium constant and activity coefficient for the pressure,

temperature and composition of the reaction mixture at the different axial positions in the reactor. Computation of specific heats of the reaction mixture requires the specific heat correlation for individual constituents of the reaction mixture, namely, nitrogen, hydrogen, ammonia, methane and argon. Specific heat of the mixture is evaluated by summing up the individual molal contributions by neglecting heat of mixing. This assumption is quite realistic because all constituents, except ammonia, behave close to ideally at the temperature and pressure condition existing in the bed. The effect of non-ideality of ammonia is not likely to be important because of high temperature and relatively low concentration, two to fifteen mole percent in the reaction mixture.

The kinetic parameters needed in simulation model are the reverse reaction rate constant for the ammonia synthesis reaction catalyst and the order of reaction parameter,  $\alpha$ . It may be noted here that in the present study the order of reaction parameter is assumed to have a constant value of 0.5. The validity of this assumption has been discussed by many workers (Shah, 1967; Dyson and Simon, 1968; Gaines, 1977; Reddy and Husain, 1978). However, Singh and Saraf (1979) have preferred to use values of 0.55 and 0.69 for the two catalysts considered in their study. The usual Arrhenius form of expression is used for the temperature dependence of the reverse reaction rate constant with the proviso to determine the most appropriate value of the frequency factor and activation energy using plant data as pointed out in section 3.1.



The correlations selected for this study are presented in chapter-V, see equations 3.1.15 to 3.1.22. These correlations are simple, widely used and predicts reasonably accurate values of the thermochemical properties at the reactor conditions. More accurate and elaborate correlations could have been used but that may not be of much use in view of the small improvements in computed results and large increase in computation time. The conclusions of Mansson and Andresen (1986) with reference to the effect of non-ideal behaviour of reaction mixture support the above observation. It may also be noted that the plant data may never be quite accurate and elaborate due to the inherent limitations in the measurement of parameters by the instruments that are used. So searching for a very accurate correlation may not be worthwhile. However, more accurate correlations can always be substituted in the simulation model, if considered necessary.

The main aim of present investigation is not to find the best correlation for the properties but only to use reasonably accurate correlations for developing a reliable and efficient simulation model, validated from the plant data, and to use this simulation model for establishing the optimal operating and design conditions for maximizing ammonia production rate.

#### 6.4. Description of procedure for kinetic and thermodynamic parameter estimation.

The most optimal values of kinetic and thermodynamic parameters namely, Para1, Para2 and Para3 are determined from the plant data using the simulation program developed for an axial

flow multibed quench type ammonia synthesis reactor. This is done by first delinking the external heat exchanger from the reactor as the heat exchanger performance will not effect the computations of temperature and concentration profile in the bed since the first bed inlet temperature is known from the plant data. The computation will then only depend on kinetics of the catalyst and the conditions in the bed. For model validation computations the simulation program had to be modified to some extent to take care of the special computation algorithm requirements for the model validation. For the model validation, computations start with the known value of the first bed inlet temperature for the plant and computes the bed exit temperature up to the third bed with first set of guessed values of the five variables, namely, Para1, Para2, Para3 and cold shots fractions at the inlet of second and third beds. It is to be noted that no cold shot fraction is added at the inlet to first bed as per the present plant practice and the plant supplier's recommendations.

From the actual (plant) and computed bed exit temperatures for all three beds and the exit ammonia concentration from the last bed, the objective function, that is, the sum of squares of the errors is then computed as discussed in the section 6.2. The objective function so generated is found to be highly nonlinear, constrained and multimodal. Therefore, a direct search technique, the Box complex search, is used to find the most optimal values of the five variables. The parameter estimation by this optimization procedure also required

external intervention for changing the direction and step size of the search for the above referred five parameters in order to jump one region of local minima to another region of local minima. In this way the true minima of objective function was established. Without external intervention, the search terminated sometimes at a local minima. Similar computations were carried out for three sets of plant operating conditions.

#### 6.5. Procedure for the estimation of external heat exchanger heat exchange capacity:

For a given plant operating condition data set, after establishing the optimal values of Para1, Para2 and Para3 and second and third bed inlet cold shot fractions the heat exchange capacity  $(UA)_H$  of the external heat exchanger was found by computing the heat exchanger tube and shell side temperature profile. It was carried out by making a guessed value of heat exchange capacity, preferably taken on higher side than that calculated approximately by estimating the total amounts of heat transfer and average temperature difference for heat exchange. The heat exchange capacity is based on per unit heat exchanger tube side volume. From the computed temperature profile, it was then possible to locate a position at which the temperature on the shell side matched closely with the actual feed temperature. From this, the guess for the  $(UA)_H$  value was improved to obtain an accurate value of heat exchange capacity  $(UA)_H$  within 2 to 3 iterations. In this way, the heat exchange capacity values were found for the three data sets of plant operating conditions. It was observed that heat exchange capacity at high flow rate was

significantly higher showing its dependence on the flow rate. Therefore a 0.8 power dependence of heat transfer coefficient on flow rate was assumed based on the well known Dittus-Boelter heat transfer coefficient correlation (McAdams, 1954) for heating and cooling inside tubes. It may be noted that Kramer and Westerterp (1963b) have also reported that the overall heat transfer coefficient  $U$  is approximately proportional to (flow rate)<sup>3/4</sup>. On this basis the best average value of heat exchange capacity was obtained for the base condition flow rate of  $0.74 \times 10^6 \text{ Nm}^3/\text{h}$  from the three heat exchange capacity values. It may be noted that the units of feed flow rate are given as  $\text{Nm}^3/\text{h}$  in this study. The letter N before m merely indicates m<sup>3</sup> of the feed gas at the N.T.P. conditions. Eventhough such use of N in S.I. units is not permissible, but for ease of comparison of gas flow rates with varying temperature and pressure, the use of N to refer N.T.P. conditions is frequently found in engineering practice.

#### 6.6. Reliability and accuracy of the validated simulation model:

After determining the best values of parameters Para1, Para2, Para3, (UA)<sub>H</sub> and the cold shot fractions at the inlet of second and third bed by the optimization and averaging procedure as discussed above, it was considered desirable to find the sum of squares for the selected data sets using the best parameter values. This was carried out to see how best the model validation had been achieved and to establish the reliability and accuracy of simulation model for using it for reactor performance analysis and optimization. Two strategies for

testing the accuracy were tried. The first was to consider the first bed inlet temperature as obtained from the plant data as the starting point and test the model validation. This resulted in some mismatch in calculated and actual feed temperatures. The second strategy was to make iterations to obtain calculated and actual feed temperatures within a certain tolerance. The latter strategy resulted in some mismatch in the calculated and actual temperatures at the first bed inlet. It may be noted here that the observed values of feed temperatures in the plant are likely to be much more accurate than the observed values of first bed inlet temperature. This may be attributed to some variations in the actual axial location of the temperature sensing probe at the inlet of a catalyst bed. Exact location of the temperature sensing probe will significantly influence the recorded value of the first bed inlet temperature. A difference of 5 to 10 K between measured and computed first bed inlet temperatures due to above mentioned reason may not be unusual. It may, however, be noted that slight variations in the physical location of the feed temperature-sensing probe will not affect the temperature measurement at all.

## CHAPTER-VII

### 7. RESULTS AND DISCUSSION

#### 7.1. Parameter estimation for reactor simulation model.

Adopting the procedure for parameter estimation as discussed in section 6.1, the simulation package is made quite accurate for a modern ammonia synthesis reactor selected for the present optimization study. An accurate model is essential for applying the results of the simulation and optimization in the plant with confidence and also for developing a reliable and accurate on-line control.

##### 7.1.1. Plant performance data for an axial flow multibed quench-type ammonia synthesis reactor.

The plant data is shown in detail in Table 6.2.1 and discussed in section 6.2. In all, eight data sets were extracted from the log sheets of the plant for the period during which the plant conditions were steady that also coincided with the time at which feed and product gas samples were drawn for composition analysis. The time of data ensured compatibility of composition analysis and the operating parameters. The bed temperatures shown are the average of two temperature observations from probes located opposite each other at any axial position. The two temperatures were found to be within 3K, indicating negligible radial dispersion. The base set of operating conditions was selected on the basis of average values of parameters existing in the plant and is reported as data set 1 in Table 6.2.1.

It is observed from Table 6.2.1 that some operating parameters that include operating pressure (173.0 atm in data set 3) and feed gas flow rate ( $0.80 * 10^6 \text{ Nm}^3/\text{h}$  in data set 2) deviate from the base value by about 10 percent. It was, therefore, considered desirable to use data sets no. 1, 2 and 3 for independent parameter estimation, that is, to find three sets of optimum values of model parameters as discussed in section 6.1. Based on these three set of values, the best estimates of parameter values were made as discussed in sections 7.1.3 and 7.1.4.

#### 7.1.2. Selection of kinetic, thermodynamic and physical property correlations.

The reasons for the selection of the various correlations that are used in mathematical model are discussed in section 6.3.

##### Reverse reaction rate constant correlation, $k_r$ .

The kinetic parameter,  $k_r$  (for an arbitrary condition of 200 atm and 773 K) and the corresponding values of frequency factor and activation energy are presented for the various correlations that are reported by Shah (1967), Gaines (1977), Singh and Saraf (1979) and Dyson and Simon (1968) in Table 7.1.2.1 for comparison. The correlation used in the present investigation is a modification of Shah's correlation as given by Equation 3.1.15. The corresponding values of parameters obtained by parameter estimation technique and used in the present work are also given in Table 7.1.2.1.

All the parameter values have been converted to the same

Table 7.1.2.1

## Comparison of Frequency Factor and Activation Energy

Values in the Reverse Reaction Rate Constant,  $k_r$ .

Correlation/ Reference	Frequency Factor mol/s/m <sup>3</sup>	Activation Energy kJ/kmol	$k_r$ , mol NH <sub>3</sub> /s/m <sup>3</sup> at 200 atm and 773 K	Remark
Shah (1967)	$0.94829 \times 10^{16}$	100869.2	276.2	
Present work	$4.11482 \times 10^{16}$	97622.4	3268.3	*
Gaines (1977)	$0.12968 \times 10^{16}$	94700.8	254.0	
Singh and Saraf (1979)	$0.01434 \times 10^{16}$	82297.0	1297.4	**
	$0.04491 \times 10^{16}$	90379.6	334.4	***
Dyson and Simon (1968)	$0.04916 \times 10^{16}$	85896.0	1462.9	

Note: \* Modification of Shah's correlation obtained by data validation.

\*\* Montecatini Edison catalyst

\*\*\* Haldor-Topsoe catalyst



units and per mol ammonia formed for ease in comparison. Units for reverse reaction rate constant, frequency factor and activation energy are  $\text{mol NH}_3/\text{s/m}^3$ ,  $\text{mol NH}_3/\text{s/m}^3$ , and  $\text{kJ/kmol}$ , respectively. It can be observed from the table that  $k_r$  values at 200 atm and 773 K range between 254.0 (correlation of Gaines, 1977) to 3268.3 (present work). The value of reaction rate constant obviously depends on the inherent activity of the catalyst and it appears that the catalyst used in the reactor for the plant under consideration is quite active. The current trend in ammonia synthesis is to use relatively low-pressure (150-200 atm) and high-activity catalyst.

It may be pointed out that when Shah's (1967) correlations were used for data validation with the plant values of first bed inlet temperatures the conversion was found to be significantly lower as compared to the plant values due to low reaction rates predicted by the rate equation of Shah. It may be observed from Table 7.1.2.1 that the frequency factor and the activation energy values obtained by validation of model from the plant data and used in the present work are also comparable to values reported by Shah, Gaines, Singh and Saraf, and Dyson and Simon. Data in the Table 7.1.2.1 show that the activation energy values range from 82297.0 to 100869.2  $\text{kJ/kmol}$ . The value of the activation energy obtained from model validation in the present study is 97622.4  $\text{kJ/kmol}$  which appears to be very reasonable.

#### K. Equilibrium Constant Correlation.

For the reaction  $3/2 \text{H}_2 + 1/2 \text{N}_2 = \text{NH}_3$  the values of K are computed at two arbitrary temperatures of 723 and 773 K for the

correlations reported by Hay and Honti (1976), Shah (1967), Gaines (1977), and Dyson and Simon (1968). Gaines used the same correlation used by Dyson and Simon.

As observed from the Table 7.1.2.2. the K values at 723 and 773 K range between 0.00662 to 0.00769 and 0.00376 to 0.00437, respectively. In the present investigation, the correlation of Hay and Honti has been used and an average deviation from reported experimental data is reported as 0.00055 in log K with a maximum deviation of 0.0016 in log K over the temperature range of interest. It may be observed that the K values obtained from the correlation of Shah are always on the high side while that of Dyson and Simon are slightly on the low side. The K values decrease with increase in temperature which is consistent thermodynamically for an exothermic reversible reaction.

#### Fugacity Coefficient Term, $K_p$ .

The values of  $K_p$  are computed from the correlations of Shah (1967), Dyson and Simon (1968), and Gaines (1977) and obtained from the data reported by Dodge (1944) and Denbigh (1981) for a comparison with those used in the present work, a modification of Shah's correlation (equation 3.1.17).

It may be noted that all correlations depend on gas temperature and pressure except that of Gaines which is also dependent on gas composition. The  $K_p$  values have been calculated at conditions of 100 atm and 723 K, 300 atm and 723 K, and 300 atm and 773 K for comparison since the data reported by Dodge and Denbigh are available at these conditions. The Dyson and Simon values are very close to those reported by Denbigh and Dodge

Table 7.1.2.2

Comparison of Equilibrium Constant, K.(Reaction Equation:  $3/2 \text{ H}_2 + 1/2 \text{ N}_2 = \text{NH}_3$ )

Correlation/ Reference	K Values at Gas Condition		Remarks
	723K	773 K	
Hay and Honti (1976a)	0.00678	0.00384	*
Shah (1967)	0.00769	0.00437	
Gaines (1977)	0.00662	0.00376	**
Dyson and Simon (1968)	0.00662	0.00376	**

Note: \* Used in present investigation.

\*\* Gillespie and Beattie Correlation as cited by Dyson and Simon (1968).

Table 7.1.2.3

Comparison of Fugacity Coefficient Term, K(for reaction  $3/2 \text{H}_2 + 1/2 \text{N}_2 = \text{NH}_3$ )

Correlation/ Reference	K Values at Gas Condition			Remarks
	100 atm	300 atm	300 atm	
	723 K	723 K	773 K	
Denbigh, K.G. (1981)	0.910	0.747	--	*
Dodge, B.F. (1944)	0.929	0.757	0.773	*
Shah (1967)	0.808	0.728	0.753	
Present Work	1.114	1.004	1.038	**
Dyson and Simon (1968)	0.909	0.746	0.767	
Gaines (1977)	1.526	3.551	3.329	***

Note: \* Experimental data.

\*\* Modification of Shah values by a multiplying factor obtained by model validation with the use of plant data.

\*\*\* For gas composition (mol %):

$\text{H}_2 = 53.0$ ,  $\text{N}_2 = 17.7$ ,  $\text{NH}_3 = 14.8$ ,  $\text{CH}_4 = 9.9$ ,  $\text{Ar} = 4.0$

while Shah's values are on the low side and those of Gaines are quite high for all conditions.

It may be noted that the values of  $K_p$  used in the present investigation appear to be reasonable, slightly higher than those of Denbigh and Dodge but considerably lower than those of Gaines.

Heat of Reaction,  $(-\Delta H)$    
 r  $\text{NH}_3$

The values of heat of reaction were obtained from reported data and computed from the correlations given by Gillespie and Beattie as cited by Hay and Honti (1976), Perry (1950), Shah (1967), Gaines (1977), Nielsen (1968), Kirk and Othmer (1978) and (1929) for comparison. Table 7.1.2.4 shows the values at different conditions.

It may be observed that the heat of reaction increases with increase in the pressure and/or temperature. The Perry and Nielsen correlations are independent of pressure while those of Gillespie and Beattie, Shah and Gaines are also dependent on pressure for accounting the nonideality introduced due to pressure. It may be observed that the values obtained from the correlation of Shah are nearly fifty percent higher and those obtained from the correlation of Gaines are nearly ten percent lower than those obtained from other sources, namely, Gillespie and Beattie, Perry, Nielsen, Kirk and Othmer and the International Critical Tables.

Table 7.1.2.4

Comparison of Values of Heat of Reaction,  $(-\Delta H_r)_{NH_3}$ .

(for reaction  $3/2 H_2 + 1/2 N_2 = NH_3$ )

Correlation/ Reference	$(-\Delta H_r)_{NH_3}$ at Gas Condition,				
	kJ/kmol $NH_3$ formed				
	100 atm 723 K	300 atm 723 K	300 atm 773 K	200 atm 833 K	1 atm 291 K
Gillespie and Beattie *	53624.5	56073.8	56304.1	55592.3	44861.6
Perry (1950)	53494.7	53494.7	54206.5	55048.1	46054.8
Shah (1967)	76199.8	<del>76823.8</del>	79867.4	83602.0	61797.2
Gaines (1977) **	47658.3	<del>48462.2</del>	48985.6	49291.2	41270.1
Nielsen (1968)	53348.2	<del>53348.2</del>	53972.0	54625.2	45837.1
Kirk Othmer (1978) ***	--	--	--	--	46276.7
ICI (1930a) ***	--	--	--	--	45853.8

Note: \* As cited by Hay and Honti (1976b) and also used in present investigation.

\*\* Correlation from Kazarnovskii data as cited by Gaines (1977).

\*\*\* Reported data.

## Heat Capacities of Ammonia, Hydrogen, Nitrogen, Methane and Argon.

The values of heat capacities were computed from the correlations given by Shah (1967), Perry (1950) and the International Critical Tables (1930a, 1930b, 1930c, and 1930d) for comparison at four conditions of 100 atm and 723 K; 300 atm and 723 K; 300 atm and 773 K; and 200 atm and 833 K. It is observed from Table 7.1.2.5 that with increase in gas temperature at constant pressure the heat capacity increases except for ammonia heat capacity computed from Shah's correlation. This is thermodynamically consistent. The values of heat capacity of ammonia calculated from Shah's correlation are higher while those obtained from correlations in the International Critical Tables are lower. Therefore, in the present investigations, the correlations given in Perry's Handbook are considered more suitable and are used in the present work. Similarly, the correlations given in Perry's Handbook are considered more satisfactory for hydrogen and nitrogen and are used in the present work. For methane, the correlation given in the International Critical Tables is used. For argon the constant value reported by Shah is used.

### 7.1.3. Estimation of Kinetic and Thermodynamic Parameters.

The procedure for estimation of kinetic and thermodynamic parameters have been discussed in detail in section 6.4. After selecting the appropriate correlations based on the reasons analyzed in section 7.1.2, the parameter estimation was carried out for the three data sets (set nos. 1, 2 and 3 in Table 6.2.1).

Table 7.1.2.5

Comparison of Heat Capacities of NH<sub>3</sub>, H<sub>2</sub>, N<sub>2</sub> and CH<sub>4</sub>.

Correlation/ Reference	Gas	C <sub>p</sub> , kJ/kmol/K				Remarks
		Constituent 100 atm 723 K	300 atm 723 K	300 atm 773 K	200 atm 833 K	
Shah (1967)	NH <sub>3</sub>	60.58	61.84	58.15	55.35	
	H <sub>2</sub>	29.48	29.48	29.60	29.77	
	N <sub>2</sub>	30.90	30.90	31.19	31.53	
	CH <sub>4</sub>	58.70	58.70	61.21	64.18	
Perry (1950)	NH <sub>3</sub>	49.15	49.15	50.49	52.00	‡
	H <sub>2</sub>	29.60	29.60	29.73	29.85	‡
	N <sub>2</sub>	31.36	31.36	31.61	31.95	‡
ICT (1929)	NH <sub>3</sub>	39.86	39.86	40.28	40.78	
ICT (1930b)	H <sub>2</sub>	28.93	28.93	29.10	29.31	
ICT (1930c)	N <sub>2</sub>	88.34	88.34	95.04	102.91	
ICT (1930d)	CH <sub>4</sub>	71.09	71.09	74.36	78.13	‡

Note: ‡ Used in present investigation.



The results of the computations for minimization of sum of squares of errors are summarised in Table 7.1.3.1. It is observed that for the first data set (base condition) the match in actual bed temperature and computed ones has been brought down to within about 2K. The match in ammonia concentration is also very good and the difference is only 0.264 mol %. These resulted in a sum of squares of error value of 9.1. The optimal parameter values are computed to be 1.076634, 0.967812 and 1.450 for Para1, Para2 and Para3, respectively. Using the computed values of Para1 and Para2, the frequency factor and activation energy values are found to be  $12.40973 \times 10^{16}$  mol/s/m<sup>3</sup> and 97622.4 kJ/kmol, respectively. In the case of increased flow rate of  $0.80 \times 10^3$  Nm<sup>3</sup>/h the optimal Para1, Para2 and Para3 values are found to be 1.01867, 0.967812 and 1.357, respectively, to result in a sum of squares of errors of 17.9 with the absolute maximum difference in bed outlet temperature and ammonia concentration of 3.7 K and 0.053 mol percent.

Using the computed values of Para1 and Para2, the frequency factor and the activation energy values are found to be  $1.77430 \times 10^{16}$  and 97622.4, respectively. Similarly from the table it is observed that at decreased pressure of 173 atm, the optimal Para1, Para2 and Para3 values are obtained to be 1.03757, 0.967812 and 1.330, respectively. The match in temperature and ammonia concentration is again very good with absolute maximum difference in temperature and concentration is found to be 3.2 K and 0.021 mol percent, respectively, and the sum of squares of errors of only 18.7. Using the computed values of Para1 and

Table 7.1.3.1

## Summary of Results for Parameter Estimation.

S. NO.	Operating Pressure (atm)	Feed Gas Flow Rate (Nm <sup>3</sup> /h.)	Feed Temp. (K)	Bed Outlet Temp., K			External Heat Exchanger Exit Temp. (K)	Ammonia Conc. at Outlet of 3rd Bed mol %	Sum of (UA) <sub>H</sub> Squares of Error W/K	Para1	Para2	Para3	Remarks		
1.	190	0.74 * 10 <sup>6</sup>	414	783	752	749	588	13.42	--	--	--	--	*		
				780.7	753.6	750.0		13.684	9.1	294165	1.07664	0.967812	1.450	**	
				- 2.3	1.6	1.0		0.264						***	
2.	192	0.80 * 10 <sup>6</sup>	415	778	759	759	588	13.40	--	--	--	--	*		
				417.4	781.7	760.8	757.9	592.4	13.453	17.9	354600	1.01867	0.967812	1.357	**
				2.4	3.7	1.8	- 1.1	4.4	0.053					***	
3.	173	0.74 * 10 <sup>6</sup>	414	784	765	756	587	13.12	--	--	--	--	*		
				412.1	786.3	768.2	757.8	590.4	13.141	18.7	320645	1.03757	0.967812	1.330	**
				- 1.9	2.3	3.2	1.8	3.4	0.021					***	

Note: \* Plant data.

\*\* Computed results.

\*\*\* Difference of computed value and corresponding plant data.

Units of feed flow rate are given as Nm<sup>3</sup>/h, cubic meter per hour at N.T.P. condition.

Para2, the frequency factor and activation energy are found to be  $3.34553 \times 10^{16}$  and 97622.4. It may be observed that the three sets of optimal values of Para1, Para2 and Para3 obtained by validation of the model by comparing with the plant data for the same catalyst, differ to some extent from each other. The difference in values may be attributed to not so accurate plant data. Therefore, an average of the three values is used in the simulation model. The average values for the three parameters are:

Para 1 = 1.04429,      Frequency factor =  $4.11482 \times 10^{16}$   
 Para 2 = 0.967812,      Activation energy = 97622.4  
 Para 3 = 1.379

The average values are reported in Table 7.1.2.1 and are discussed in section 7.1.2. It may be noted here that the corresponding validated optimal values of cold shots obtained during parameter estimation for the three data sets are (0.245, 0.100), (0.254, 0.090) and (0.176, 0.160) at the inlet of the second and third beds, respectively. The cold shot at the inlet of the first bed is taken to be zero as per the present practice in the plant.

#### 7.1.4. Estimation of Heat Exchange Capacity of the External Heat Exchanger, $(UA)_H$ .

The procedure for estimation of  $(UA)_H$ , W/K as given in section 6.5 was used to obtain the best values for the three data sets as shown in Table 7.1.3.1. The three values corresponding to the data sets 1, 2 and 3 are 294165, 354600 and 320645 W/K. As discussed in section 6.5, it is reasonable to account for the

effect of flow rate on  $(UA)_H$  by assuming a 0.8 power dependence on flow rate of overall heat transfer coefficient,  $U$  (McAdams, 1954; Kramer and Westerterp, 1963b). For comparison the  $(UA)_H$  value obtained for data set 2 at a flow rate of  $0.80 \times 10^6 \text{ Nm}^3/\text{h}$  when converted to the base value flow rate of  $0.74 \times 10^6 \text{ Nm}^3/\text{h}$  becomes 333165. Again the three values are different although the difference in maximum and minimum values at base value of flow rate of  $0.74 \times 10^6 \text{ Nm}^3/\text{h}$  is about 13%. This may be attributed to a large extent to the temperature measurement errors in the plant data. Therefore, an average value is used and  $(UA)_H$  is computed in simulation model by:

$$(UA)_H = 316000 \left( \frac{\text{feed gas flow rate, Nm}^3/\text{h}}{0.74 \times 10^6} \right)^{0.8} \text{ W/K}$$

#### 7.1.5. Comparison of Reactor Simulation Model Predictions with Actual Plant Performance.

As discussed in section 6.6 the reliability of the model is tested at the average value of Para1, Para2, Para3,  $(UA)_H$  and the cold shot values obtained by model validation. The results of computations for sum of squares of errors for all eight data sets (given in Table 6.2.1) are shown in Table 7.1.5.1.

It is observed that by using strategy 1, the sum of squares of errors values range from 20 to 180 and by using iterative strategy 2, the sum of squares of errors values range from 33.9 to 253.0. The value of sum of squares of errors and the computed value of temperature and concentration all along show a very good match. The match in ammonia concentration is also quite good. It,

Table 7.1.5.1

Comparison of Simulation Results With Plant Data At Average Value Of Estimated Parameters.  
 Para1 = 1.04429, Para2 = 0.967812, Para3 = 1.379

Data Set No.	Operating Pressure, (atm)	Feed Gas Flow Rate, (10 <sup>6</sup> Nm <sup>3</sup> /h)	Simulated Cold Shot Fraction		Feed Temp., (K)	First Bed Inlet Temp., (K)	Bed Outlet Temp. (K)			External Heat Exchanger Exit Temp., (K)	Ammonia Prod., t/d	Mol %	Sum Of Squares Of Error	(UA) <sub>M</sub> W/K	Remark
			2nd Bed	3rd Bed			1st	2nd	3rd						
1.	190	0.740	0.245	0.100	414	652	783	752	749	588	1313	13.42	-	316000	†
					395.2	652.0	784.9	759.5	754.6	586.6	13.68	106.8	††		
					414.3	658.3	788.5	761.9	756.2	596.5	1287.2	13.50	253.0	†††	
2.	192	0.800	0.254	0.090	415	654	778	759	759	588	1393.8	13.40	-	336370	†
					414.8	654.0	781.3	754.0	752.9	596.3	1394.0	13.83	180.0	††	
					415.1	654.1	781.4	754.1	752.9	596.5	1393.6	13.83	182.0	†††	
3.	173	0.740	0.176	0.160	414	655	784	765	756	587		13.12	-	316000	†
					410.1	655.0	784.3	765.2	753.9	590.6	1251.4	13.23	20.1	††	
					414.2	656.4	785.0	765.7	754.2	592.8	1247.5	13.19	38.9	†††	
4.	185	0.785	0.223	0.120	413	653	781	761	757	588	1370.4	13.60	-	331280	†
					409.0	653.0	781.6	759.3	752.7	592.5	1364.1	13.74	45.1	††	
					413.1	654.4	782.8	759.9	753.1	594.6	1359.9	13.70	64.8	†††	
5.	184	0.775	0.215	0.129	417	651	775	763	757	587		13.47	-	327890	†
					401.8	651.0	779.5	759.2	751.7	588.4	1339.3	13.52	65.1	††	
					417.2	656.1	783.7	761.2	753.1	596.4	1324.1	13.38	184.0	†††	
6.	186	0.760	0.215	0.091	414	656	792	765	758	589		13.14	-	322800	†
					418.0	656.0	788.8	767.3	761.3	595.5	1280.1	13.17	69.7	††	
					414.1	654.6	787.9	766.8	761.0	593.5	1284.3	13.22	49.9	†††	
7.	183	0.770	0.206	0.110	417	655	782	768	761	589		13.45	-	326190	†
					419.1	655.0	785.3	765.1	757.9	596.3	1301.0	13.22	93.2	††	
					417.1	654.3	784.8	764.9	757.7	595.3	1303.2	13.24	76.5	†††	
8.	183	0.780	0.215	0.110	417	652	778	763	758	588		13.20	-	329580	†
					411.0	652.0	781.5	761.8	755.3	592.6	1337.3	13.43	53.4	††	
					417.1	654.1	783.3	762.6	755.8	595.8	1330.7	13.37	100.0	†††	

NOTE: † Plant data.

†† Strategy 1. First bed inlet temperature is taken as plant data (actual), a noniterative procedure.

††† Strategy 2. First bed inlet temperature is searched to match calculated and actual feed temperatures, an iterative procedure.

therefore, establishes that the values of model parameters found from plant data are indeed good for further analysis and optimization of the plant performance.



## 7.2. Choice of Variables and Their Ranges for Simulation Studies.

Operation of an ammonia reactor is generally associated with changes in the values of operating variables. Important operating variables for a multibed reactor are: cold shot distribution, feed gas flow rate, concentration of inerts (methane and argon) in the feed gas, hydrogen to nitrogen ratio in the feed gas, catalyst activity, operating pressure, and feed gas temperature. At the design stage, a designer can also vary total catalyst volume and catalyst distribution.

Performance of a multibed ammonia synthesis reactor is greatly affected by cold shot distribution. Low cold shot rates as well as high cold shot rates have a pronounced effect on the reduction of ammonia production. Injudicious increases in the cold shot rates result in the quenching of the reactor. In order to study the effect of changes in the operating and/or design variables on the ammonia production rate, it was considered vital to have the optimal cold shot distributions for each of the condition. Otherwise, non-optimal cold shot distribution will totally mask the true effect of the changes in other variables. Accordingly, cold shot distributions are not treated as operating variables, but instead the cold shot distribution is optimized for each set of operating and or design conditions.

Surprisingly, the data obtained from a modern commercial multibed axial flow ammonia reactor did not have any measured values for cold shot flow rates/distribution because of lack of facilities for such measurements. In the present study, the cold

shot distribution for the base case was obtained by validating the plant data. This aspect has been discussed in detail in the preceding section (section 7.1). The base value for each of the operating variable was chosen as the most probable value at which the plant is operating. The changes in operating variables were, in general, restricted to ten percent on either side of the base value (as observed from the plant data for few months), except for catalyst activity factor. The base value of catalyst activity factor was chosen as unity and the effect of deterioration in catalyst activity was investigated at the catalyst activity factor of 0.9, 0.8 and 0.7. Changes in the feed gas temperature as well as catalyst distribution in different beds were not investigated because of their irrelevance in the present context. The catalyst volume was changed only to compare the effect of such changes from those obtained from the corresponding changes in the feed gas flow rate. The base values of operating and/or design variables and their ranges of variations are given in Table 7.2.1. The values of some of the operating and/or design variables kept unchanged of their base values are also given in Table 7.2.1. The base values for these variables were also obtained either from the actual plant data or obtained from the validation of the model by use of plant data (section 7.1).



Table 7.2.1Operating and Design Parameters Average Value and Range Investigated.

S.No.	Description of the Variable	Unit	Selected Values for Simulation Study	
			Base Condition	Range of Variations
<u>Parameter Varied</u>				
1.	Feed Gas Pressure	atm	190	170 to 210
2.	Flow Rate	$\text{Nm}^3/\text{h}$	$0.740 \times 10^6$	$0.667 \times 10^6$ to $0.820 \times 10^6$
3.	H <sub>2</sub> /N <sub>2</sub> Ratio	--	3.0	2.5 to 3.2
4.	Inerts in Feed:			
	CH <sub>4</sub>	mol %	12.84	10.68 to 13.95
	Ar	mol %	8.80	6.88 to 9.30
		mol %	4.04	3.80 to 4.65
5.	Catalyst Activity Factor	--	1.0	0.7 to 1.0
6.	Catalyst Total Volume	$\text{m}^3$	67.6	61.0 to 75.0
<u>Parameters Kept Unchanged</u>				
1.	Catalyst Distribution	--	1.0:1.4:2.0	--
2.	External Heat Exchange Capacity	W/K	316000	--
3.	Internal Preheating Section Heat Exchange Capacity (Catalyst Bed Side)	W/K	0.0	--
4.	Feed Gas Temperature	K	414	--
5.	NH <sub>3</sub> in Feed Gas	mol %	1.61	--

Note: Here prefix N before m stands for N.T.P. conditions.

### 7.3. Simulation Results for Base Conditions.

The simulation program was run on Roorkee University Regional Computer Centre main frame Computer System, DEC 20. Optimization of cold shot fractions for a single set of conditions took nearly 5 to 8 minutes of CPU time. The results of optimization are summarised in Tables 7.3.1.1 and 7.3.1.2. The detailed computed profiles of bed temperature (K) and ammonia concentration (mol percent) are presented in Appendix A, Tables A.1 through A.7, for the sixteen sets of conditions investigated. The detailed results are tabulated at shorter intervals towards the end of each bed to clearly understand the contribution of each additional increment of catalyst volume. It may be noted that for numerical integration each bed was divided into 100 equal increments. Figures 7.1 through 7.15 show the effect of changes in operating and design parameters on the optimal performance and the stability of the reactor. Except for set no. 0, all other sets represent the performance of reactor at the optimal cold shot distributions. Set No. 0 designates the base condition with simulated value of cold shot fractions (since actual cold shot fractions at the first and second bed inlets are not known due to lack of measuring facilities in the plant) obtained by validation of the model by comparison with plant data. Set No. 1 also represents the base conditions except that the cold shot fractions added at the inlet of each of the three beds are at the optimal values obtained from the optimization studies.

TABLE NO. 7.3.1.1  
SUMMARY OF COMPUTED RESULTS

Run No.	Parameter Varied	Value Of Parameter	Cold Shot Distribution				Mol % NH <sub>3</sub> At Outlet Of 3rd Bed	Production Rate OF NH <sub>3</sub> , t/d	Total Pressure Drop, atm
			1st Bed	2nd Bed	3rd Bed	Total			
1	2	3	4	5	6	7	8	9	10
0*	-	-	0.000	0.245	0.100	0.345	13.502	1287.2	2.77
1	-	-	0.110	0.233	0.232	0.575	14.880	1419.2	2.26
2(A)	Flow rate, Nm <sup>3</sup> /h	0.667*10 <sup>6</sup>	0.123	0.253	0.234	0.610	15.188	1306.4	1.83
2(B)	Flow rate	0.820*10 <sup>6</sup>	0.098	0.230	0.219	0.547	14.631	1547.3	2.78
3(A)	H/N ratio	2.5	0.109	0.237	0.236	0.582	14.914	1421.7	2.25
3(B)	-do-	2.8	0.108	0.240	0.234	0.582	14.918	1422.4	2.25
3(C)	-do-	3.2	0.108	0.237	0.226	0.571	14.845	1416.3	2.27
4(A)	Inerts Conc. mol %	10.68	0.145	0.250	0.234	0.629	15.387	1467.0	2.19
4(B)	-do-	13.95	0.089	0.249	0.220	0.558	14.647	1397.1	2.29
5(A)	Catalyst Activity factor	0.7	0.030	0.193	0.192	0.415	13.764	1312.5	2.56
5(B)	-do-	0.8	0.080	0.232	0.203	0.515	14.322	1366.2	2.38
5(C)	-do-	0.9	0.096	0.237	0.220	0.553	14.631	1395.6	2.30
6(A)	Catalyst Volume, m <sup>3</sup>	61.0	0.076	0.239	0.214	0.549	14.646	1397.1	2.17
6(B)	-do-	75.0	0.120	0.253	0.235	0.608	15.184	1447.8	2.37
7(A)	Operating pressure, atm	170.0	0.089	0.235	0.199	0.523	14.167	1351.3	2.34
7(B)	-do-	210.0	0.146	0.253	0.231	0.630	15.691	1495.4	2.21

Note: See Table 7.2.1 for base conditions

TABLE NO. 7.3.1.2

TEMPERATURE AND AMMONIA CONCENTRATION VALUES AT BED INLET AND OUTLET  
FOR DIFFERENT CONDITIONS

Set No.	Temperature And Conversion In The Bed												
	Internal Preheating	1st Bed				2nd Bed				3rd Bed			
	Section	Inlet		Outlet		Inlet		Outlet		Inlet		Outlet	
	Outlet Temp., K	Temp. (K)	Mol% NH <sub>3</sub>	Temp. (K)	Mol% NH <sub>3</sub>	Temp. (K)	Mol% NH <sub>3</sub>	Temp. (K)	Mol% NH <sub>3</sub>	Temp. (K)	Mol% NH <sub>3</sub>	Temp. (K)	Mol% NH <sub>3</sub>
1	2	3	4	5	6	7	8	9	10	11	12	13	14
0	658.3	658.3	1.61	788.5	10.32	692.9	7.81	761.9	12.74	729.6	11.52	756.2	13.50
1	695.1	640.1	1.61	779.8	10.98	675.4	7.96	751.9	13.47	678.3	10.48	737.8	14.88
2(A)	702.3	636.4	1.60	779.0	11.18	665.4	7.83	746.8	13.68	673.7	10.60	735.4	15.19
2(B)	687.8	641.4	1.61	777.5	10.72	676.8	7.87	750.9	13.18	681.7	10.43	738.6	14.63
3(A)	695.4	640.0	1.61	779.5	10.99	672.8	7.90	750.5	13.50	676.0	10.45	736.2	14.91
3(B)	695.7	640.6	1.61	780.3	10.99	672.3	7.87	750.3	13.49	676.5	10.47	736.6	14.92
3(C)	694.7	640.9	1.61	780.1	10.95	674.6	7.91	751.1	13.40	679.6	10.50	738.3	14.85

1	2	3	4	5	6	7	8	9	10	11	12	13	14
4(A)	709.6	629.9	1.61	773.3	11.37	665.7	7.98	749.0	13.85	675.1	10.73	739.1	15.39
4(B)	689.5	645.6	1.61	780.9	10.72	670.7	7.64	747.1	13.13	678.4	10.38	736.0	14.65
5(A)	668.3	656.5	1.61	779.9	9.83	698.1	7.75	762.8	12.37	700.2	10.13	749.7	13.76
5(B)	683.5	647.2	1.61	778.3	10.37	678.6	7.67	749.9	12.76	686.0	10.31	740.5	14.32
5(C)	690.4	643.9	1.61	780.4	10.76	675.6	7.81	750.3	13.16	680.9	10.40	738.2	14.63
6(A)	690.6	644.3	1.61	780.7	10.75	675.8	7.80	750.4	13.14	682.9	10.46	739.5	14.65
6(B)	700.1	636.1	1.61	778.8	11.20	665.0	7.83	746.4	13.68	673.1	10.60	734.9	15.18
7(A)	665	639.7	1.61	769.3	10.29	671.1	7.60	741.4	12.63	680.3	10.25	733.3	14.17
7(B)	709.6	629.8	1.61	773.9	11.61	665.7	8.11	748.9	14.09	676.3	10.95	740.1	15.69

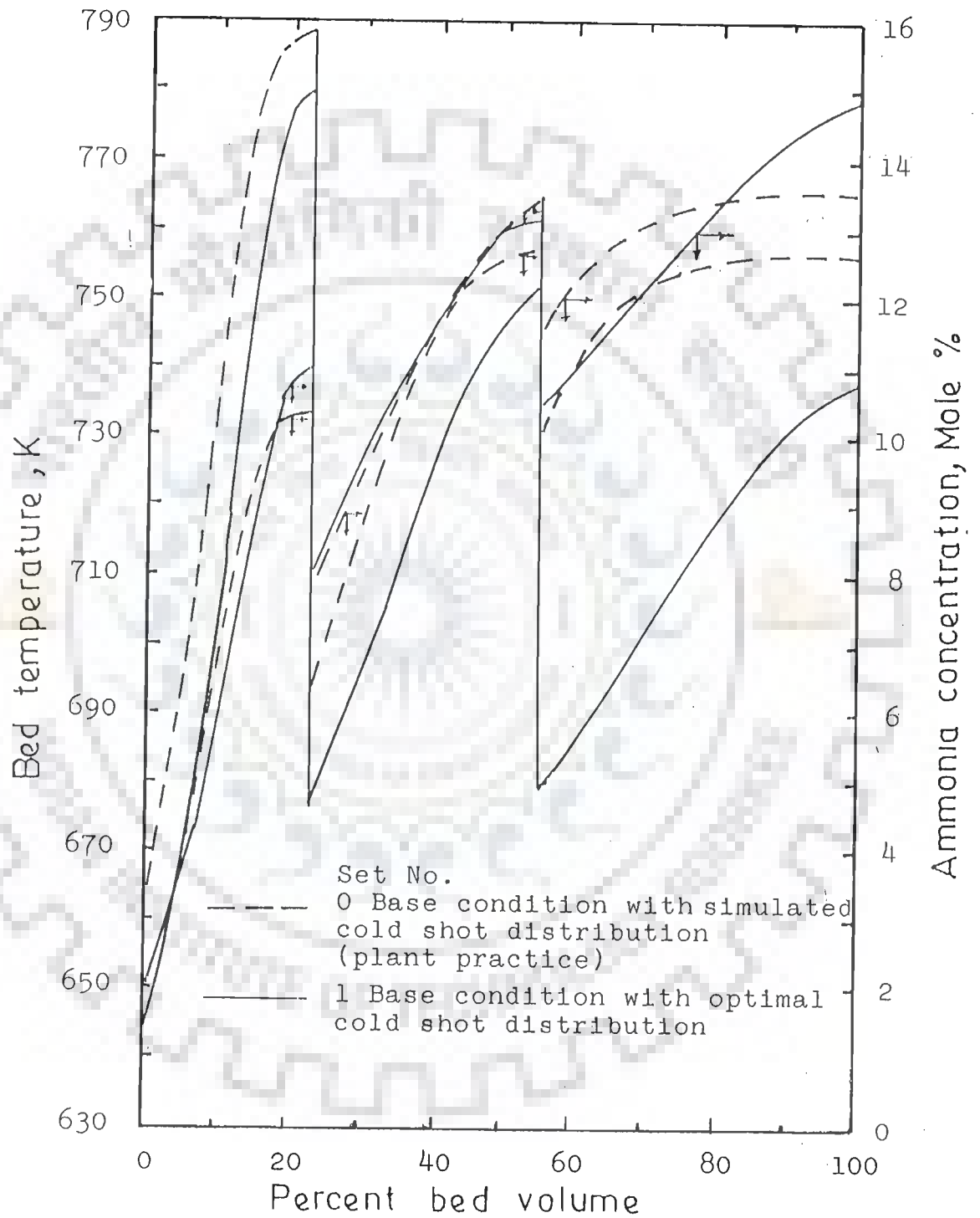


FIG. 7.1 AMMONIA CONCENTRATION AND TEMPERATURE PROFILES IN CATALYST BEDS (See Table 7.2.1 for Base Conditions)

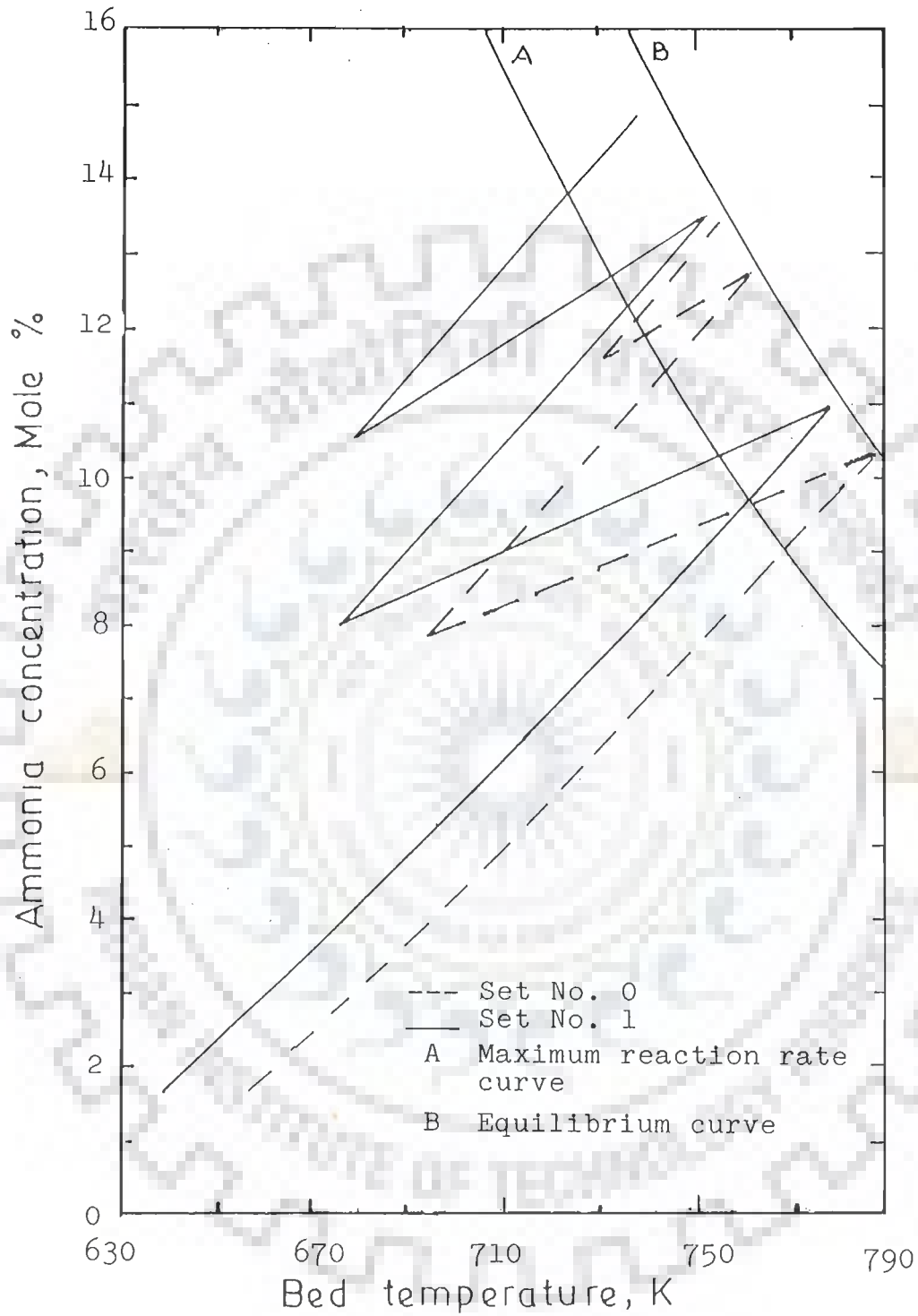


FIG. 7.2 AMMONIA CONCENTRATION VERSUS TEMPERATURE IN CATALYST BEDS (See Table 7.2.1 for Base Conditions)

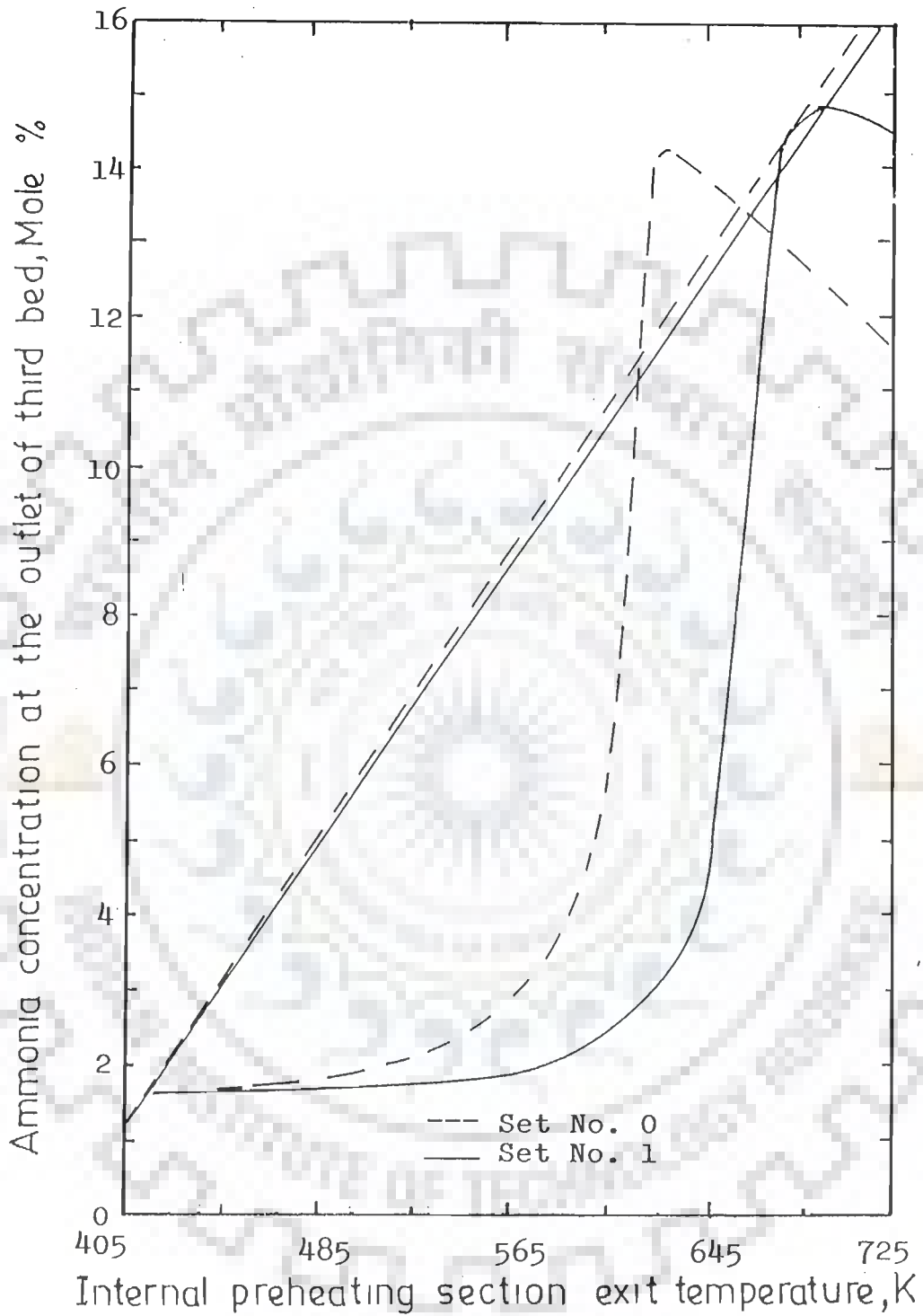


FIG. 7.3 REACTOR OPERATING POINTS AND THEIR STABILITY  
(See Table 7.2.1 for Base Conditions)



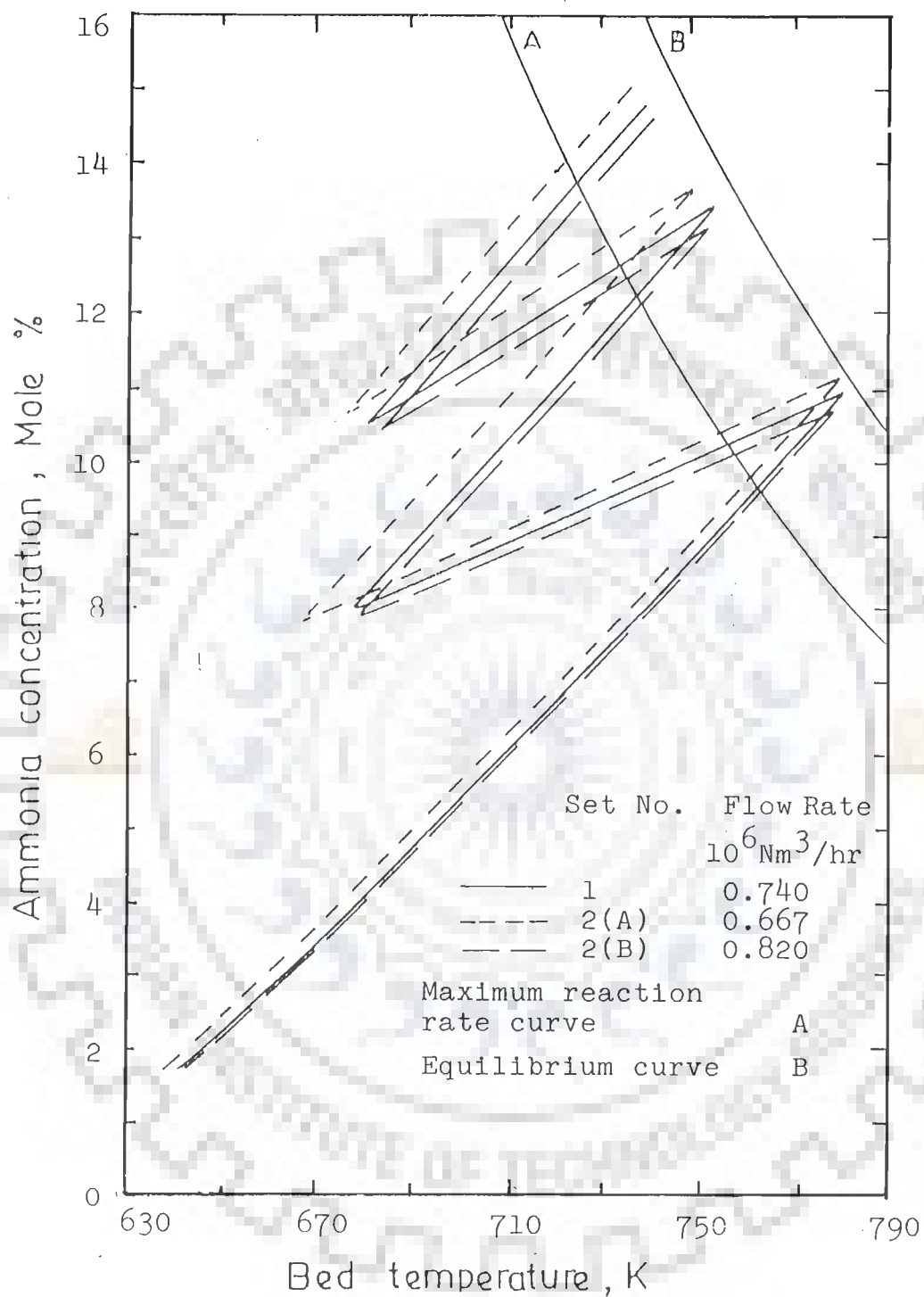


FIG. 7.4 EFFECT OF FEED FLOW RATE ON AMMONIA CONCENTRATION-TEMPERATURE PROFILE IN CATALYST BEDS FOR OPTIMAL COLD SHOT DISTRIBUTION (Base conditions, set No.1, are given in Table 7.2.1)

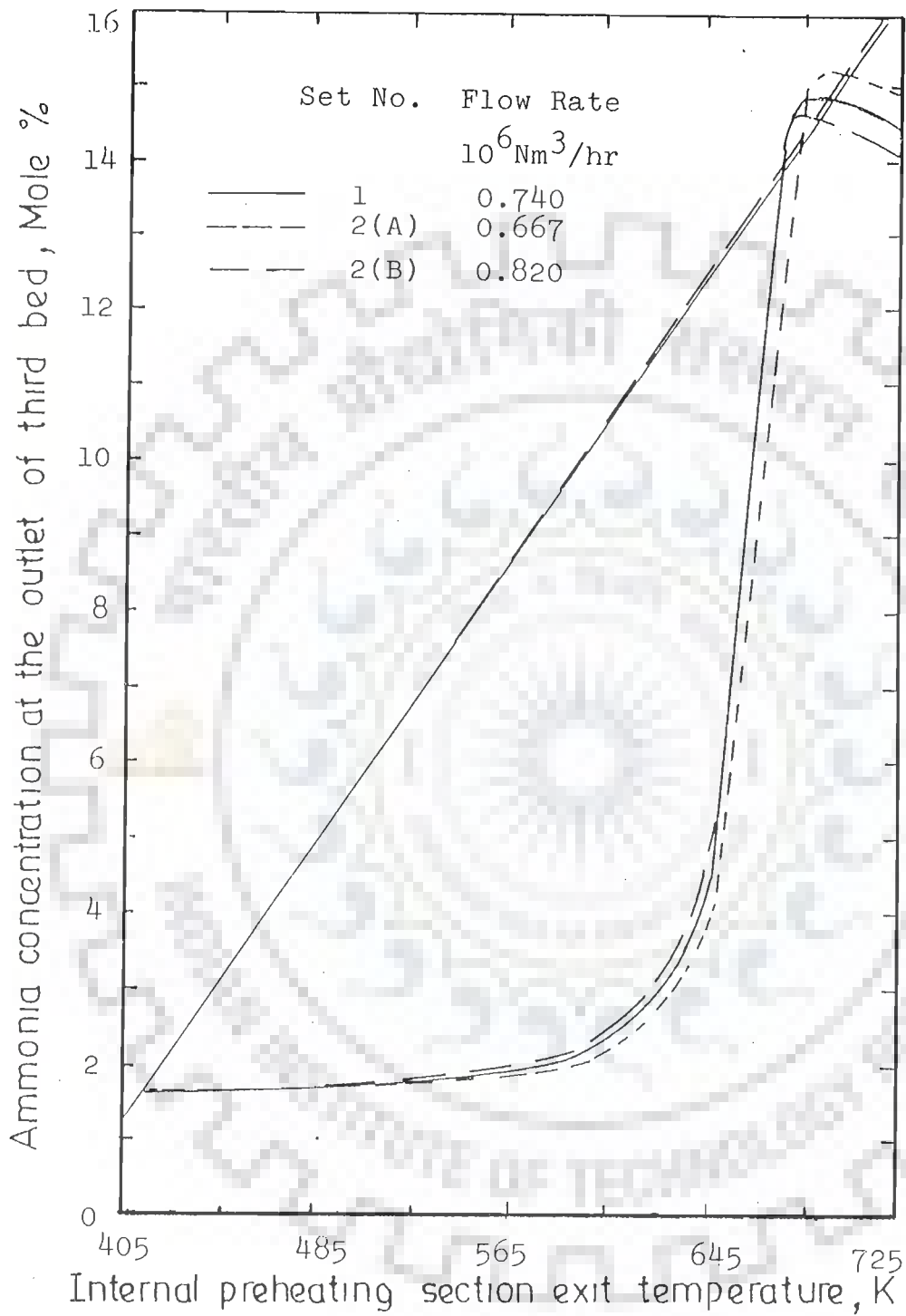


FIG. 7.5 EFFECT OF FEED FLOW RATE ON REACTOR OPERATING POINTS AND THEIR STABILITY (Base conditions, set No.1, are given in Table 7.2.1)

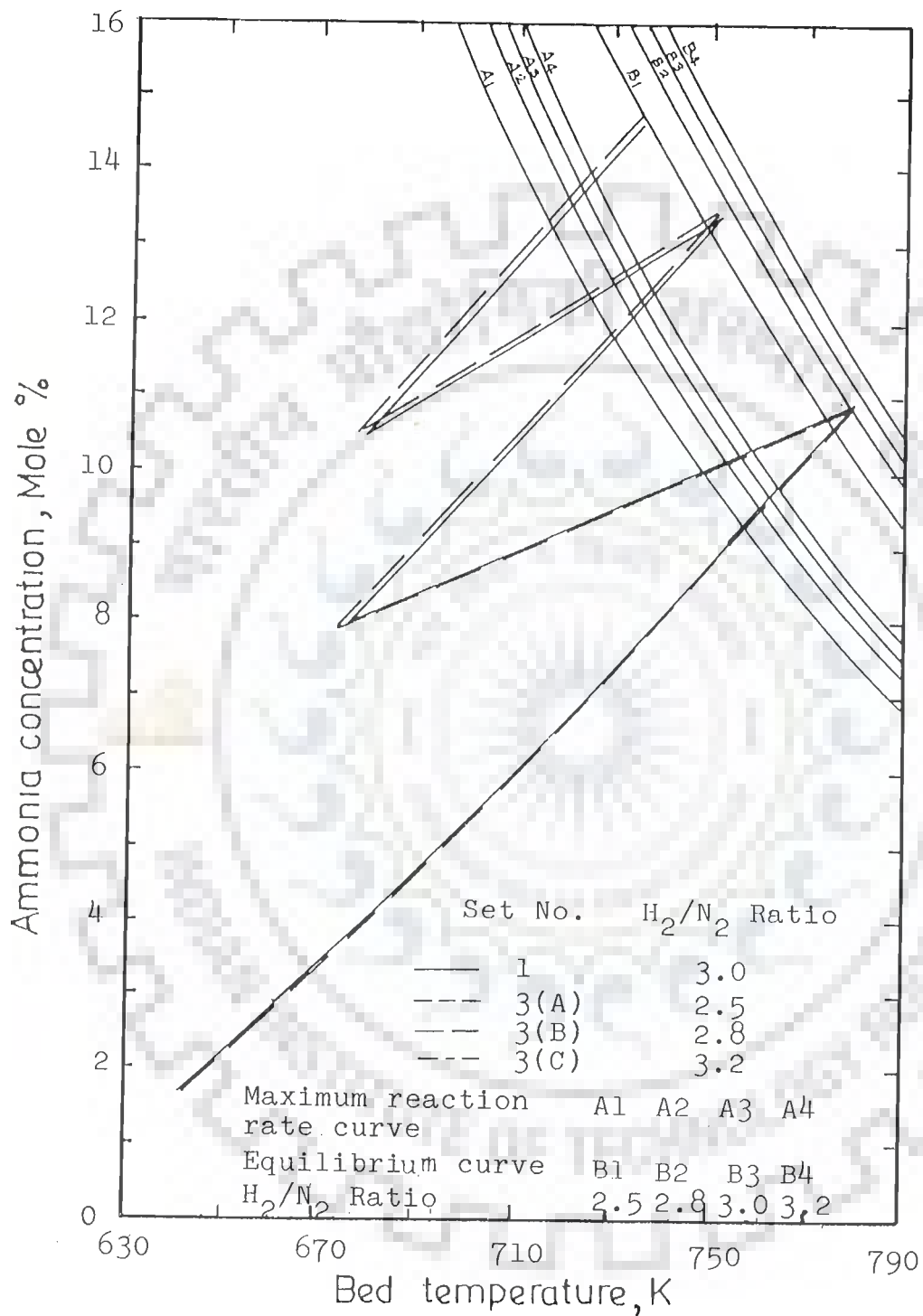


FIG. 7.6 EFFECT OF H<sub>2</sub>/N<sub>2</sub> MOLE RATIO ON AMMONIA CONCENTRATION-TEMPERATURE PROFILE IN CATALYST BEDS FOR OPTIMAL COLD SHOT DISTRIBUTION (Base conditions, set No.1, are given in Table 7.2.1)

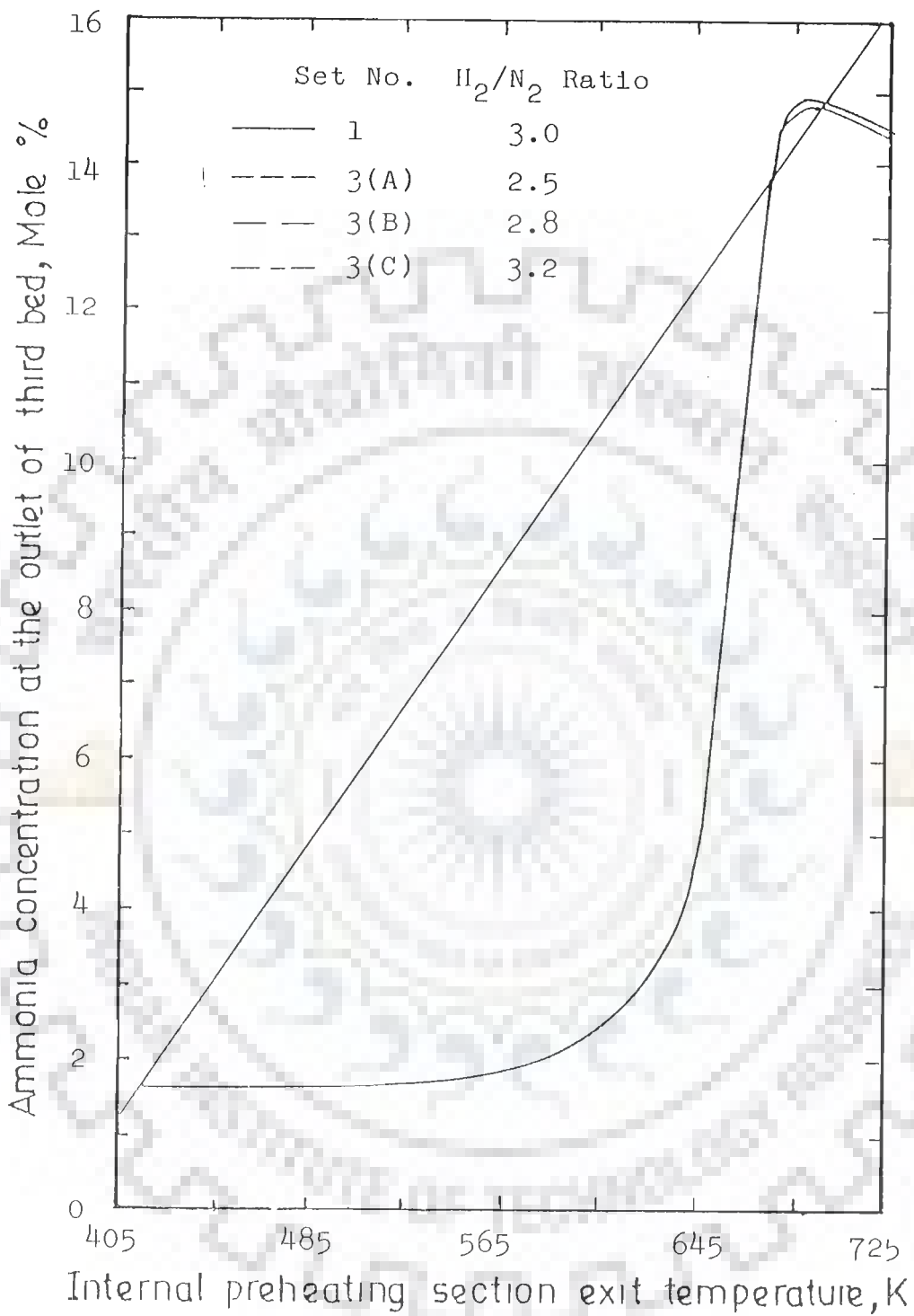


FIG. 7.7 EFFECT OF H<sub>2</sub>/N<sub>2</sub> RATIO ON REACTOR OPERATING POINTS AND THEIR STABILITY (Base conditions, set No.1, are given in Table 7.2.1)

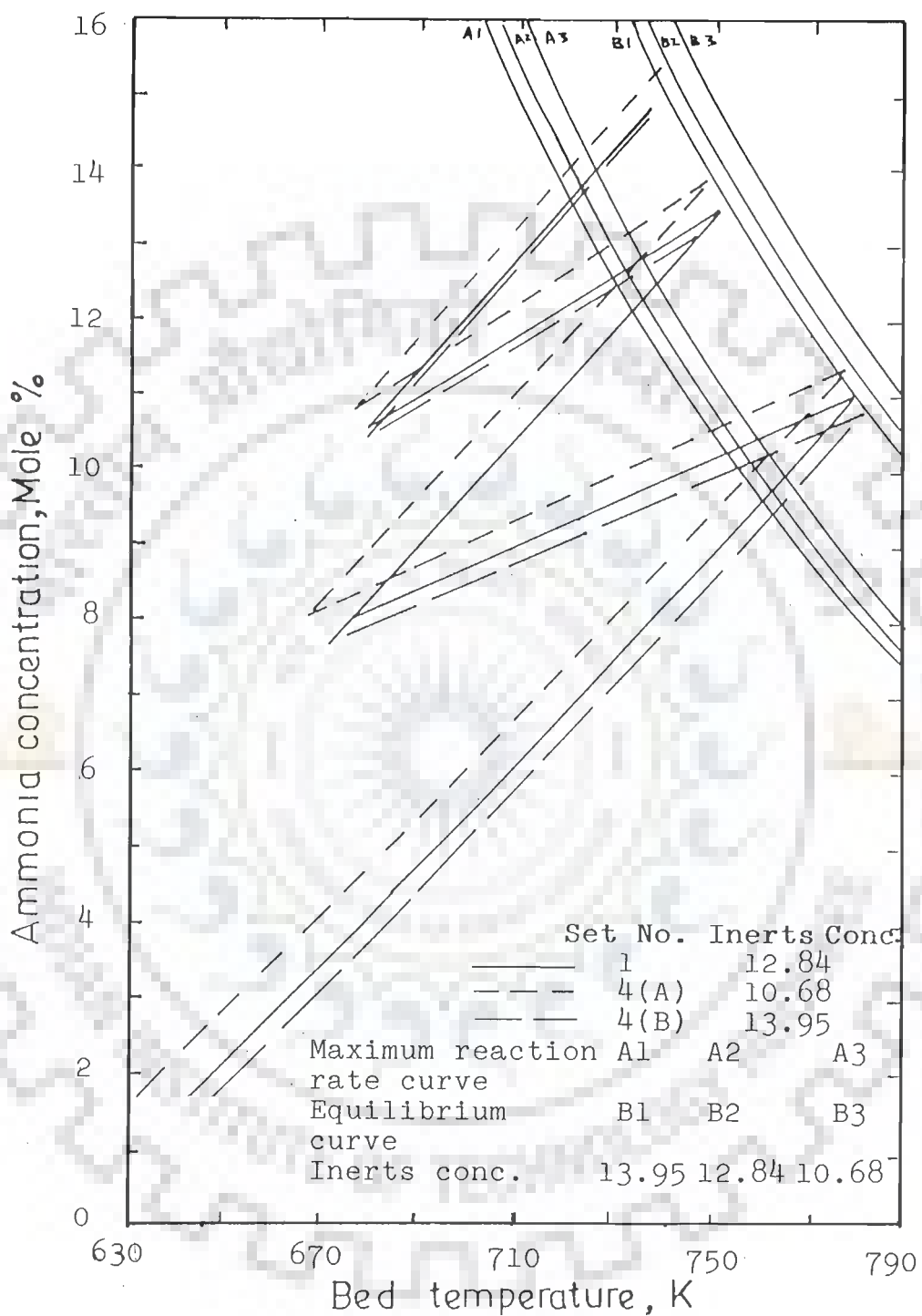


FIG. 7.8 EFFECT OF INERTS CONCENTRATION ON AMMONIA CONCENTRATION-TEMPERATURE PROFILE IN CATALYST BEDS FOR OPTIMAL COLD DISTRIBUTION (Base conditions, set No.1, are given in Table 7.2.1)

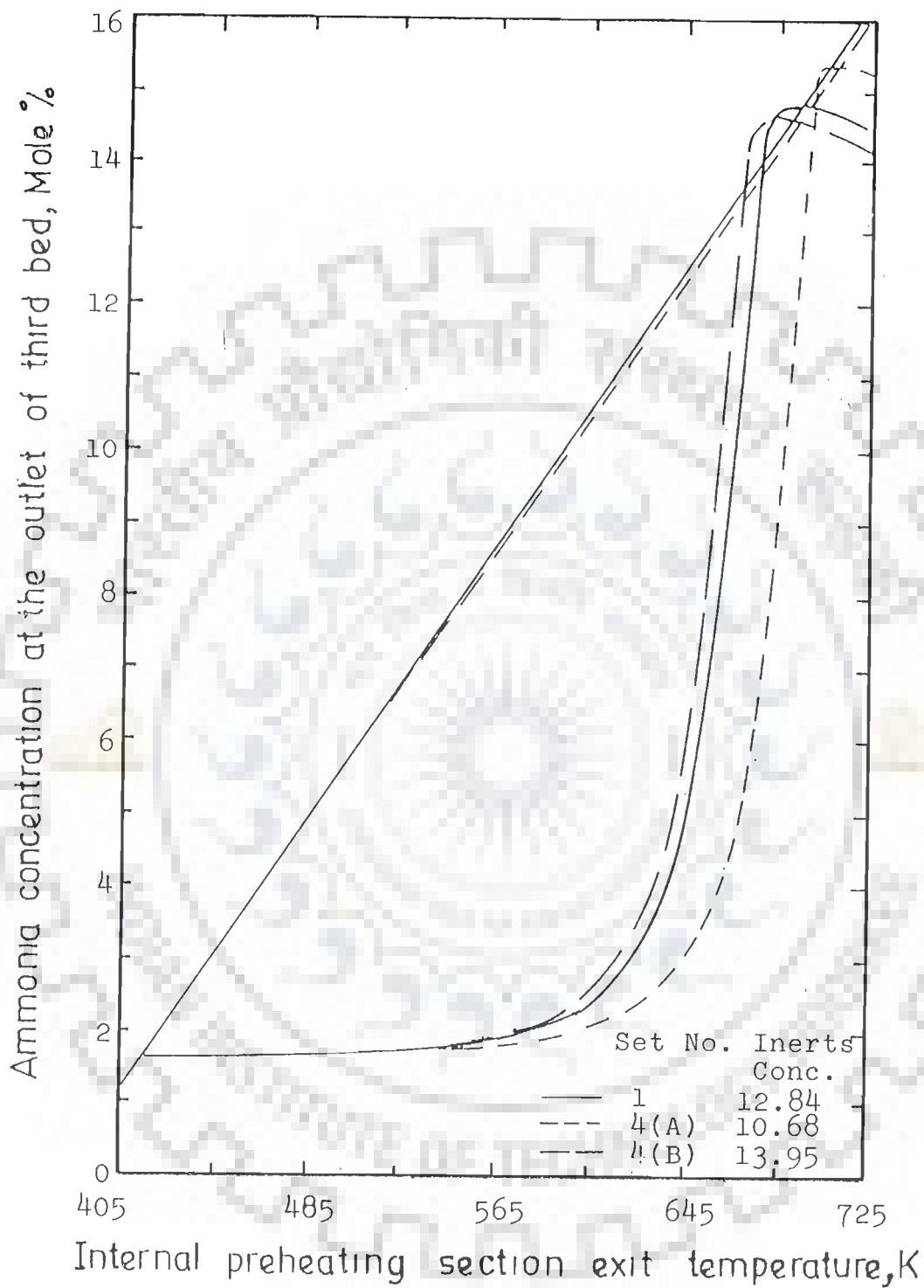


FIG. 7.9 EFFECT OF INERTS CONCENTRATION ON REACTOR OPERATING POINTS AND THEIR STABILITY (Base conditions, set No.1, are given in Table 7.2.1)

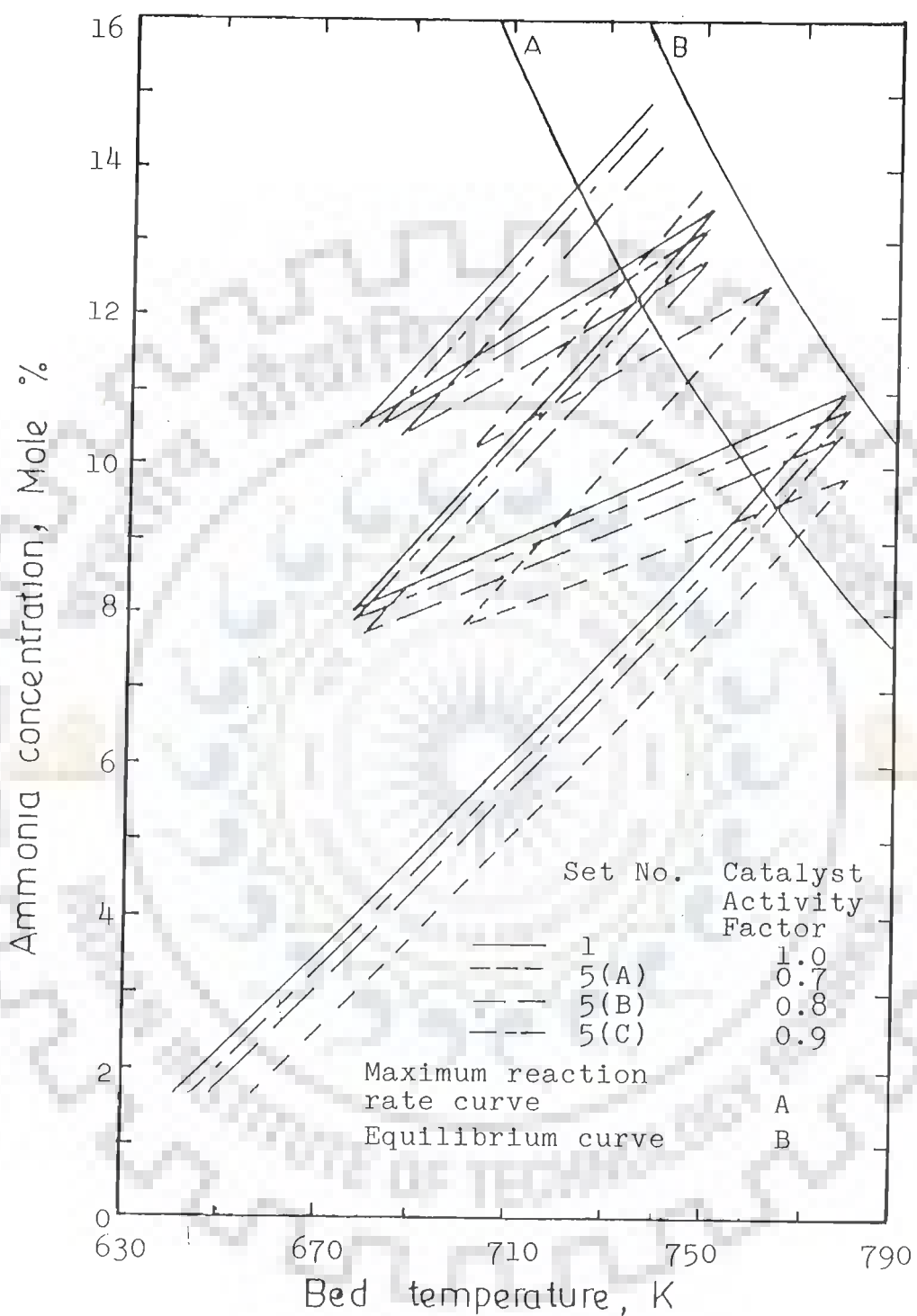


FIG. 7.10 EFFECT OF CATALYST ACTIVITY FACTOR ON AMMONIA CONCENTRATION-TEMPERATURE PROFILE IN CATALYST BEDS FOR OPTIMAL COLD SHOT DISTRIBUTION (Base conditions, set No.1, are given in Table 7.2.1)

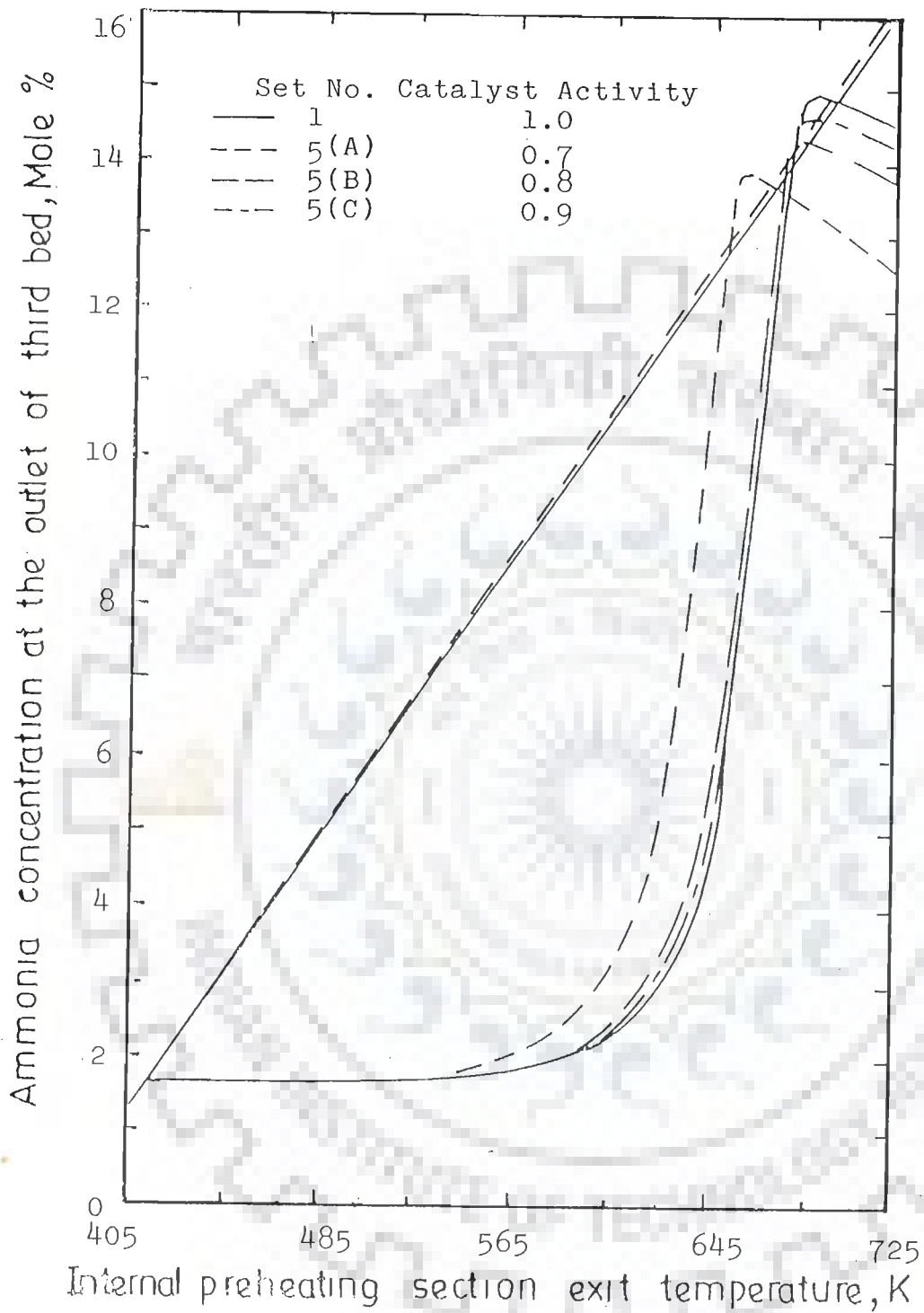


FIG. 7.11 EFFECT OF CATALYST ACTIVITY FACTOR ON REACTOR OPERATING POINTS AND THEIR STABILITY (Base conditions, set No.1, are given in Table 7.2.1)



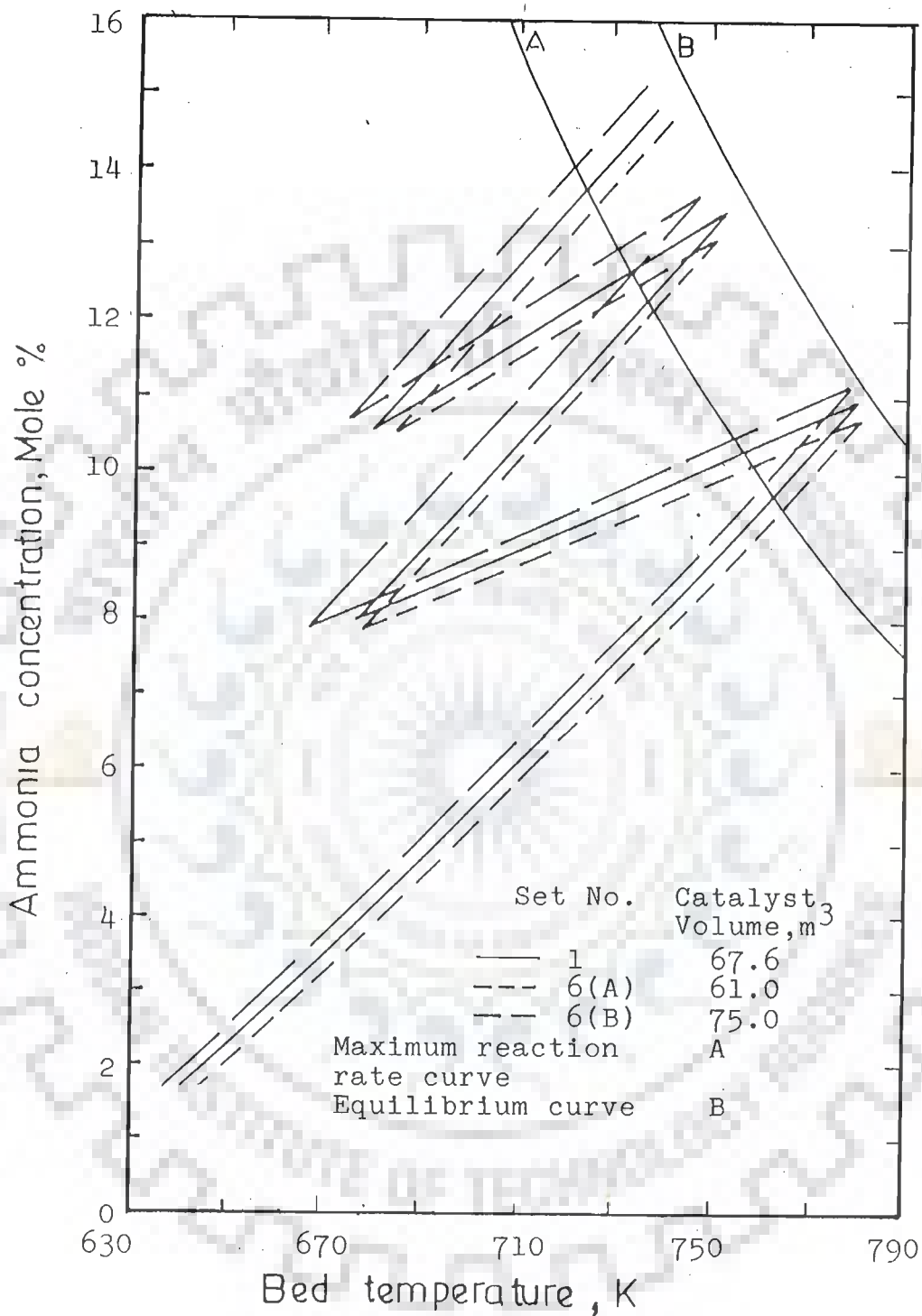


FIG. 7.12 EFFECT OF CATALYST VOLUME ON AMMONIA CONCENTRATION-TEMPERATURE PROFILE IN CATALYST BEDS FOR OPTIMAL COLD SHOT DISTRIBUTION (Base conditions, set No.1, are given in Table 7.2.1)

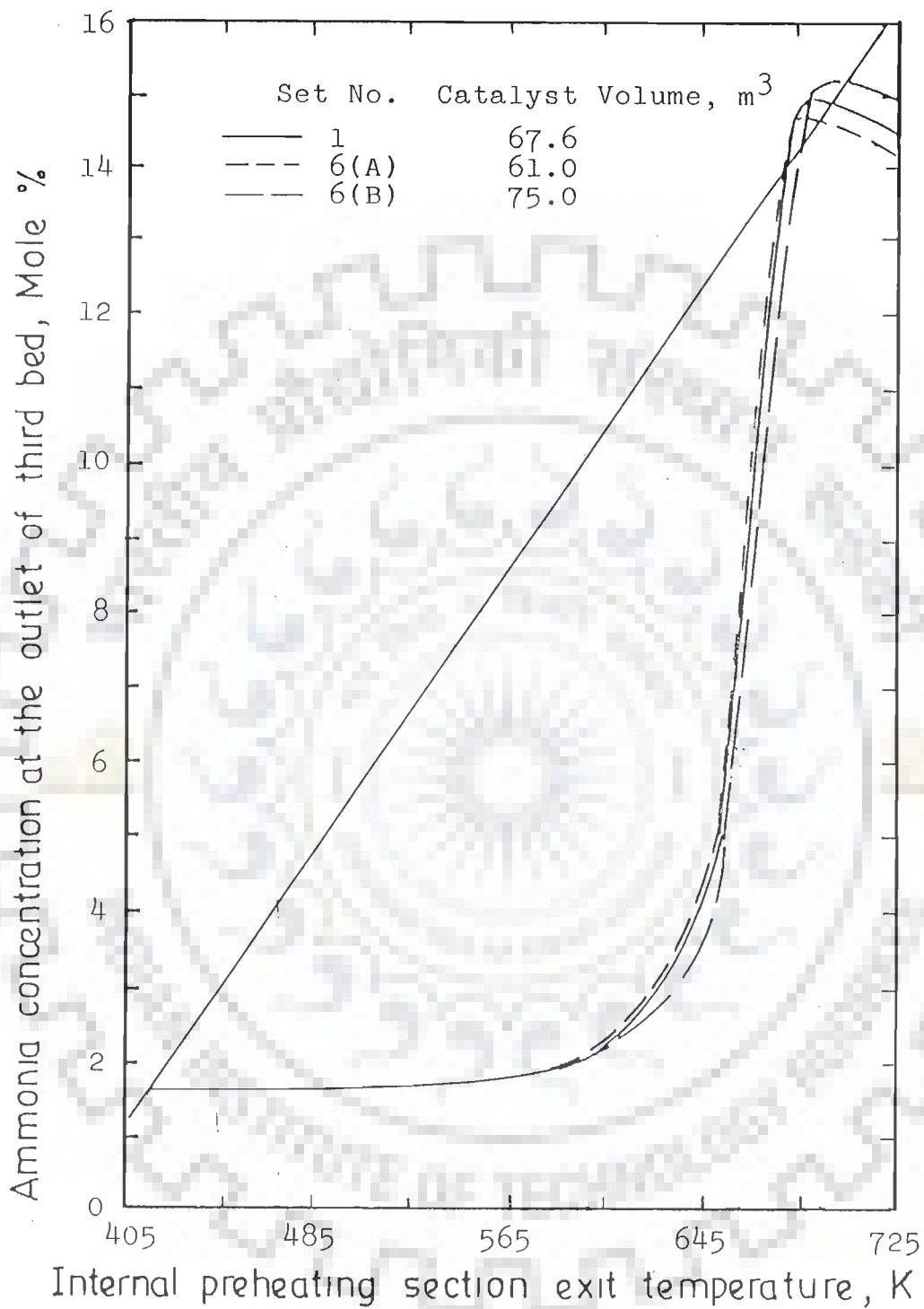


FIG. 7.13 EFFECT OF CATALYST VOLUME ON REACTOR OPERATING POINTS AND THEIR STABILITY (Base conditions, set No.1, are given in Table 7.2.1)

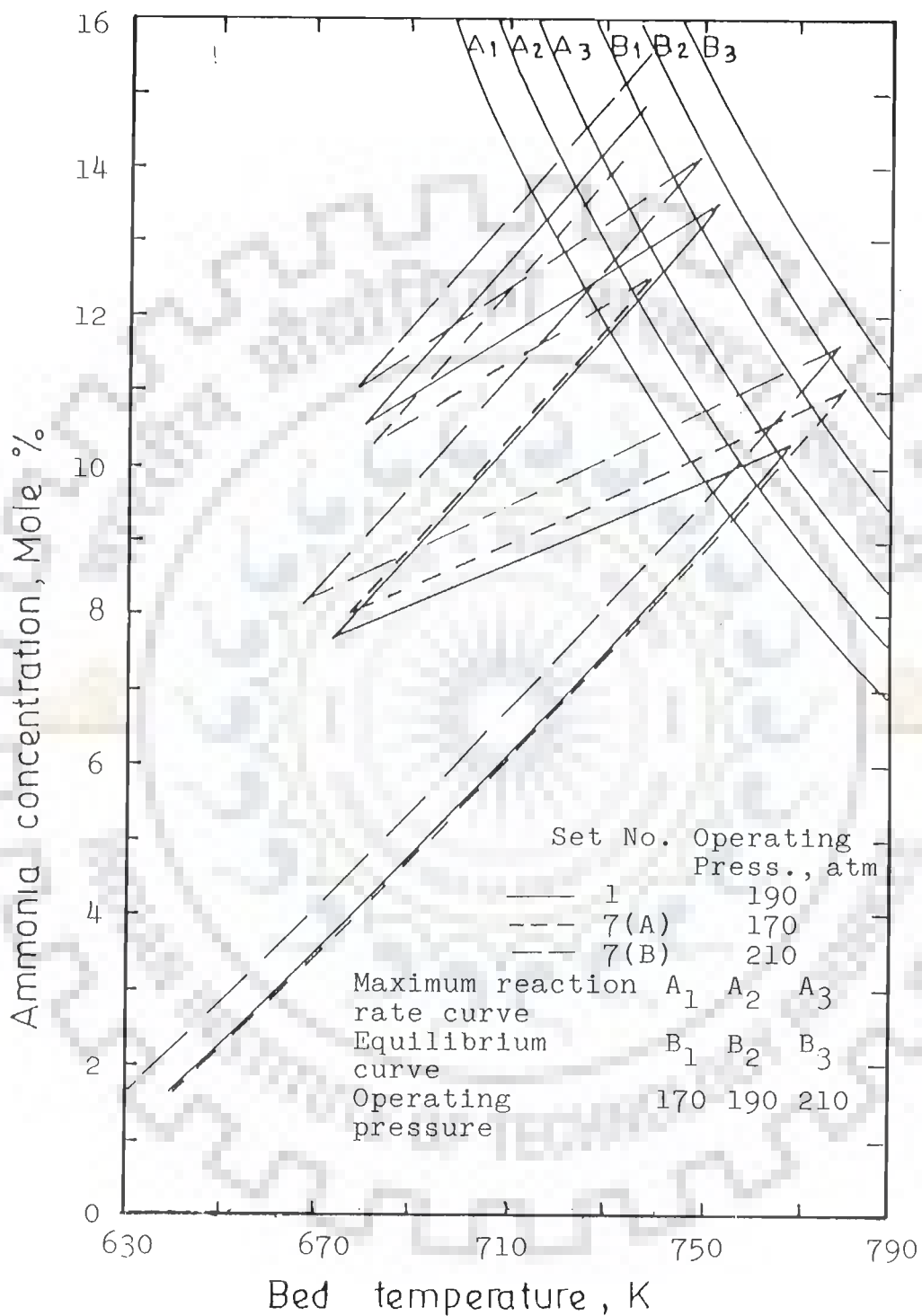


FIG. 7.14 EFFECT OF OPERATING PRESSURE ON AMMONIA CONCENTRATION-TEMPERATURE PROFILE IN CATALYST BEDS FOR OPTIMAL COLD SHOT DISTRIBUTION (Base conditions, set No.1, are given in Table 7.2.1)

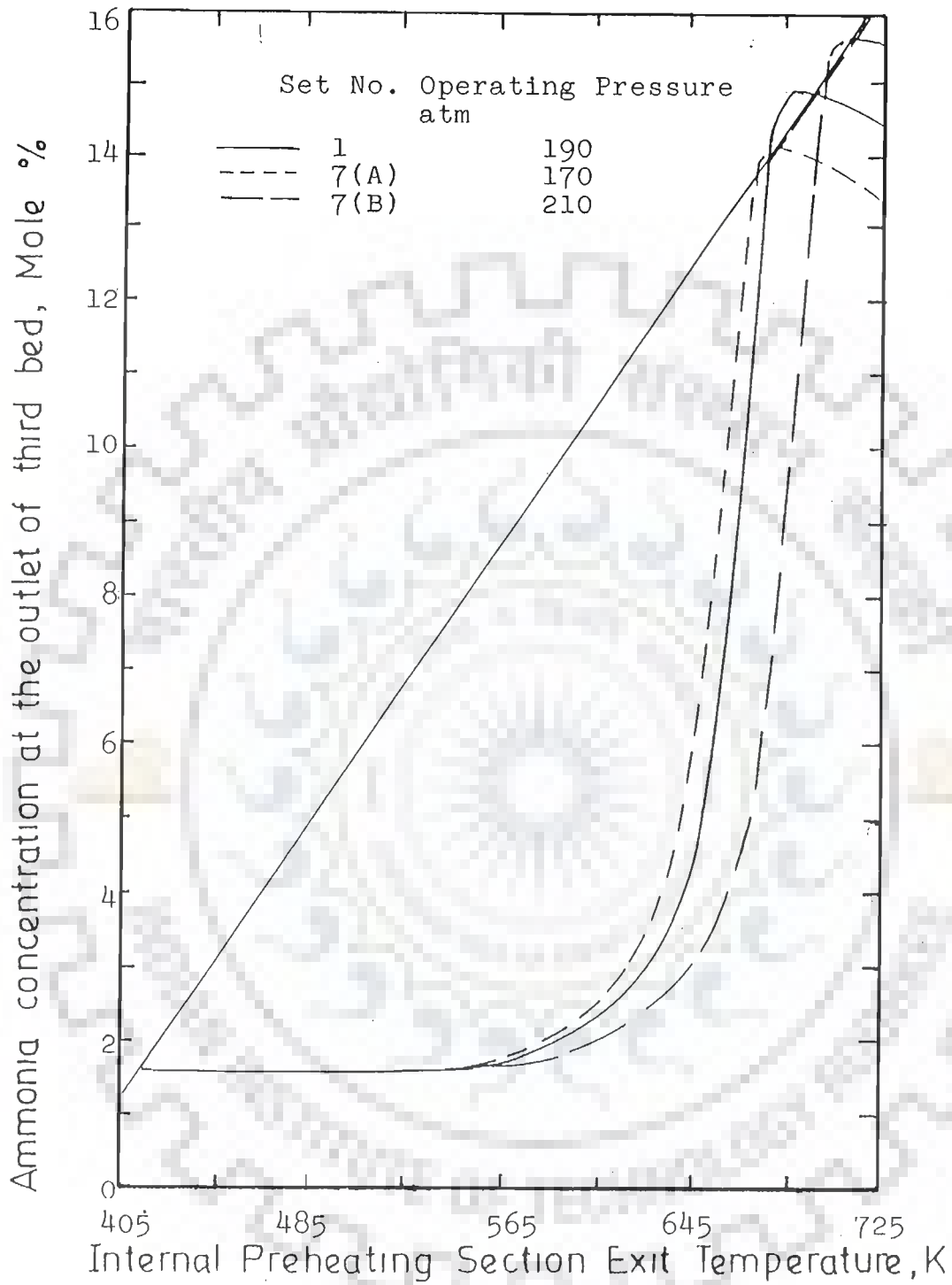


FIG. 7.15 EFFECT OF OPERATING PRESSURE ON REACTOR OPERATING POINTS AND THEIR STABILITY (Base conditions, set No.1, are given in Table 7.2.1)

For set No. 0 and 1 Table A.1 and Figures 7.1 give the detailed temperature and ammonia concentration profiles for each of the three beds in the reactor. Figure 7.2 shows the changes in the ammonia concentration as a function of the temperature in each of the three beds in the reactor along with the changes in ammonia concentration at the equilibrium conditions and also at the maximum reaction rate conditions at different bed temperatures. Further from Fig. 7.2 the variations in the actual temperature and ammonia concentration conditions in the bed can be clearly seen vis-a-vis equilibrium and maximum rate conditions. Figure 7.2 also helps in identifying the directional changes required for the cold shot distributions for maximizing the ammonia production. Figure 7.3 shows the three steady-state operating points (points of intersection) of the reactor for set No. 0 and 1 on typical heat removal and generation curves used commonly to explain the stability behaviour of the reactor operation. More detailed discussions are given in subsequent subsections.

### 7.3.1. Strategy of Optimization by Cold Shot Distribution.

As already discussed in chapter IV, in an operating plant with fixed design parameters and pre-specified feed conditions, the variables that are free to be adjusted for maximizing rate of production of ammonia are the cold shot fraction at the inlet to various beds. In particular, for the type of reactor investigated, these are the three cold shot fractions at the inlet of first, second and third bed, respectively. Therefore, in the present study the cold shot fractions were taken as

independent variables for the optimization in order to maximize the rate of production of ammonia.

During the course of optimization computations experience was gained to evolve a two-step procedure to locate optimal cold shot fractions quickly. In the first step, computations were made for, say, 12 iterations. The cold shot values so obtained corresponding to the maximum rate of ammonia production for 12 iterations were readjusted to make the total cold shots about 10 to 20 percent higher. The adjustment of cold shot was done based on the approach of actual ammonia concentration at the outlet of a particular bed to its corresponding equilibrium value (shown in Table A.1 under column 6 and 10 for set No.0 and 1 respectively). In case the ratio of actual to equilibrium ammonia concentration at the outlet of a particular bed is found to be between 0.95 to 1.00, the cold shot to that bed inlet was correspondingly increased. This was done considering the presence of equilibrium inhibition due to low cold shot value. On the other hand if the actual to equilibrium concentration ratio is below 0.95, the cold shot fraction is correspondingly decreased. The value of the ratio of actual to equilibrium ammonia concentration at the outlet of a bed around 0.95 for optimal is also supported by the observations of Gaines (1977).

With the new adjusted value of cold shot fractions as starting point it was possible to locate optima within 12 to 17 iterations. This strategy proved to be very efficient and the CPU time required for locating the true optima was considerably reduced. The number of iterations obviously depended on the

closeness of starting point to the optima. The optimal cold shot fractions at the inlet of the first, second and the third bed are found to be 0.110, 0.233 and 0.232, respectively, for the base conditions as given in Table A.1 set No.1.

### 7.3.2. Temperature Profile

For the base conditions, set No. 0 and 1, Figure 7.1 shows the profiles for the bed temperature (in K) and ammonia concentration (in mol percent) of the three bed quench-type ammonia synthesis reactor considered for this investigation.

The cold shot fractions to the first, second and the third beds for set 0 are 0.000, 0.245, 0.100, respectively. As can be seen from Fig. 7.1, the bed temperature has initially a high and linear rate of increase. However, later the rate of increase in bed temperature decreases successively from the first bed to the third bed. The observed initial rates of increase in bed temperature (in K per unit total percent bed volume) for the first, second and the third bed are 7.7, 3.0 and 1.6 for set No. 0 and 7.1, 2.9 and 1.5 for set 1, respectively. The initial linear rise in temperature is due to the fact that rate of reaction is not being inhibited by equilibrium, as equilibrium concentration is much higher compared to actual concentration, as is evident from Table A.1 under column 6 and 10. It is well known that the addition of cold shot at the point where reaction is equilibrium inhibited results in increasing the conversion as observed in case of set 0 and set 1 from Figure 7.1 and Table A.1. Addition of cold shot at the first, second and the

third bed results in an increase in ammonia conversion. The optimal cold shot distribution for set 1 resulted in somewhat lower rate of temperature rise as a result of lower bed inlet temperatures. The decrease in the rate of temperature rise from the first to the third bed was due to the fact that ammonia concentrations of the gas become higher as one moves from the first to the third bed inlet.

In case of set No. 0, base condition with non-optimal cold shot, it is observed from Figure 7.1 that toward the end of first and second bed the temperature profile flattened out earlier than what was observed with set No. 1. This is because inadequate cold shot additions at the inlet of each bed result in a higher bed temperature for set 0 as compared to set 1. The higher bed temperature in set 0 resulted in an early equilibrium inhibition. This effect is much more pronounced in third bed for set 0 where nearly fifty percent of third bed volume is ineffective due to equilibrium inhibition compared to a total absence of equilibrium inhibition conditions in set No. 1.

Based on the above discussion, it is evident that non-optimal cold shot distribution results in higher bed temperature and quicker equilibrium inhibition whereas optimal cold shot lowers the bed temperature and removes equilibrium inhibition. The lower bed temperatures are also good for catalyst life. The maximum temperature was found to be 788.5 K in case of set 0 compared to set 1 value of 779.8 K.

### 7.3.3. Conversion profile.

The conversion profile for set Nos. 0 and 1 are shown in



Figure 7.1 and the detailed results are given in Table A.1. Columns 4 and 8 of this Table give actual ammonia concentrations while columns 5 and 9 give concentration at maximum rate for set Nos. 0 and 1, respectively. Whereas columns 6 and 10 give concentrations at equilibrium for set Nos. 0 and 1, respectively. Figure 7.2 shows the concentration as a function of the bed temperature as the reaction progresses along the bed. Figure 7.2 also shows maximum reaction rate and equilibrium curves.

As observed for bed temperature profiles, it is also clear from Figure 7.1 that rate of increase in ammonia concentration is initially high and linear. However for set 1, unlike temperature profile, the ammonia concentration increase is more than that for set 0 which resulted in higher conversions in each bed. The concentration of ammonia, in mol percent, for set 1 increases from 1.61 to 10.98, 7.96 to 13.47 and 10.48 to 14.88 in the first, second and the third bed respectively. Whereas the corresponding increase in ammonia concentration for set 0 are 1.61 to 10.32, 7.81 to 12.74 and 11.52 to 13.50, respectively. The use of non-optimal cold shot distributions for set 0 results in higher bed temperatures which in turn lowers the equilibrium concentration causing equilibrium inhibition at the end of the first and the second bed and from the middle of the third bed in the reactor. This further emphasises the need for optimal cold shot distribution to achieve not only maximum ammonia conversion but also lower bed temperatures. The increase in exit ammonia concentration and corresponding rate of ammonia production at optimal cold shot distribution is quite substantial, about 10.3

percent (132.3 t/d) of the simulated base value.

Further, it may be observed from Figure 7.2 and Table A.1 that the ratio of the actual conversion to the equilibrium conversion at the outlet of first, second and third bed are 0.983, 0.957 and 0.947 respectively for set 1 and corresponding values for set 0 are 0.995, 0.985 and 1.00 respectively. It may be noted that when actual conversion becomes extremely close to equilibrium conversion value (ratios of actual to equilibrium conversion values of 0.999 to 1), the tolerance limit chosen for  $H_2$  conversion ( $5 * 10^{-5}$ ) for Milne-Predictor-Corrector method is too large to give precise conversion value for next step. Therefore, if actual  $H_2$  conversion at any bed point is  $5 * 10^{-5}$  (approximately 0.002 ammonia mol %) or less than the equilibrium conversion, then it is safe to assume that equilibrium conversion value has been achieved. This situation can be observed for last three bed points in the third bed for set 0 in Table A-1.

The set 0 values obviously indicate the need for readjustment of cold shot to establish the optimal, as obtained in set 1, by adopting the strategy given in section 7.3.1. because only 0.083 increase in ammonia mol percent is observed in the last 50 percent of catalyst volume in the third bed.

#### 7.3.4. Performance Analysis at Optimal Operation and General Considerations.

Based on computations for optimization, it was quite significant to observe that the optimal condition is not sharp but instead the region around it is flat. Many more combination

✓  
should  
in table  
of set

??

✓

of cold shot fractions were possible at which the rate of ammonia production (or the corresponding exit ammonia concentration) was within 0.3 percent of the optimal value. Some such sets of cold shot fractions at the inlet of the first, second and the third beds are (0.092, 0.275, 0.205), (0.110, 0.233, 0.224), (0.085, 0.275, 0.205), (0.085, 0.275, 0.212), (0.110, 0.225, 0.232), and (0.110, 0.233, 0.216) and the corresponding rates of ammonia production are 1417.4, 1417.8, 1415.9, 1415.9, 1415.4 and 1415.0 t/d, respectively.

However, the increase in any of the cold shot fractions above optimal resulted in quenching of the reaction. In the base case (set 1) it was observed that an increase in magnitude above optimal in any of the cold shot fractions at the inlet of first, second or third bed by 0.002, 0.003 or 0.003 respectively resulted in quenching of the reactor. The computation results for optimal cold shot distribution further showed that the reaction rate values at the exit of a bed and at the inlet of next bed differ significantly. For the base case, the reaction rate values at the outlet of first, inlet of second, outlet of second and inlet of third bed were 22.6, 13.8, 15.3 and 10.5 mol NH<sub>3</sub> /s m<sup>3</sup> respectively. However, Kramer and Westerterp (1963a) report that at the optimal cold shot addition the reaction rate values at outlet of a bed should be equal to the rate value at the inlet of the next bed. This could not be substantiated from the present investigations. As discussed in section 7.3.3, the ratio of actual to equilibrium conversion at the outlet of the three beds vary between 0.947 to 0.983 with an average value of 0.962. This

is found to substantiate the observations of Gaines (1977) that at optimal condition this ratio should be near about 0.935.

From the computation results of optimization it may be summarised that at the optimal condition the reactor performance improved substantially resulting in considerable increase in rate of ammonia production, decrease in bed temperature and consequent increase in catalyst life. It is also observed from Table A.1 that the total pressure drop across the reactor also decreased substantially. From a value of 2.77 atm for base case (set 0) to 2.26 atm in case of optimal condition, set 1. This is about 18.4 percent reduction and it will result in considerable saving in electrical energy required by the gas recirculation/ booster system.

### 7.3.5. Reactor Stability.

Figure 7.3 shows the three possible steady-state operating points of the reactor along with S (sigmoid) shaped heat generation curve and a near straight line heat removal curve. The intersections of heat removal line with heat generation curve give the three possible operating points for the reactor. The S-shaped curve for heat generation was obtained by plotting ammonia exit concentrations, % NH<sub>3</sub>, (in mol percent) and corresponding grid values of internal preheating section exit temperature, T<sub>SHE</sub>. The ammonia concentration, % NH<sub>3</sub>, and T<sub>SHE</sub> values were generated during the grid search. For grid search, the range for T<sub>SHE</sub> was chosen from 600 to 725 K with an interval of 25 K. The grid search is used for converging on actual feed temperature value for a given set of conditions with one set of trial value

of cold shot fractions. The procedure is discussed in section 5.1. It may be noted that for any chosen value of  $T_{SHE}$ , a corresponding exit ammonia concentration,  $\% NH_3$ , is obtained by continuing computation up to step 10 (section 5.1). The computed value of  $\% NH_3$  is proportional to the heat generation term. The plot of grid points ( $T_{SHE}$ ,  $\% NH_3$ ) is S-shaped similar to that reported by several other workers (Gaines, 1977; Kramer and Westerterp, 1963b; Reddy and Husain, 1978; Shah, 1967; van Heerden, 1953). The points for heat generation curve ( $T_{SHE}$ ,  $\% NH_3$ ) for set 0 are (600.0, 4.81), (625.0, 14.20), (650.0, 13.75), (675.0, 13.02), (700.0, 12.31) and (725.0, 11.61), and the corresponding points for set 1 are (600.0, 2.19), (625.0, 2.96), (650.0, 5.07), (675.0, 13.88), (700.0, 14.83), and (725.0, 14.46) respectively. It may be noted that for any assumed value of  $T_{SHE}$ , at the end of computation step 10 (section 5.1), the computed temperature of feed entering the external heat exchanger on shell side,  $T_{SHI}$ , is obtained. The value of  $T_{SHI}$  shall be equal to (within the limit of convergence) the actual feed temperature,  $T_F$ , only if  $T_{SHE}$  corresponds to one of the possible operating points of the reactor. For establishing all the possible reactor operating points computations had to be continued up to step 13 (section 5.1). As shown in Figure 7.3, the three possible operating points for base case (set 0) are (414.0, 1.61), (618.9, 11.47) and (658.3, 13.50) whereas the corresponding points for set 1 are (414.0, 1.61), (674.9, 13.84) and (695.1, 14.88). The heat removal curve is obtained by joining the three possible operating points by a straight line (since

they were found to lie on a straight line) for each set of conditions. The three operating points will also lie on the S-shaped curve as well as heat removal curve. As discussed in section 2.1 and also reported by van Heerden (1953), Shah (1967), Gaines (1977) and others (Kramer and Westerterp, 1963b; Reddy and Husain, 1978), the highest operating point is the desirable and stable operating point for each set of conditions. In case of set 0 and set 1 these are (658.3, 13.50) and (695.1, 14.88), respectively. The two S-shaped curves and heat removal curves are different obviously because of the different reaction paths followed for the two sets 0 and 1 having two different sets of cold shot fractions.

It is observed from Figure 7.3 that the optimal allocation of cold shot results in higher operating point being located nearer to the blowout point on the optimal S-shaped curve as compared to the corresponding locations for non-optimal set 0. This is very much to be expected as the maxima of the S-shaped curve is always nearer the blowout point. It may be further noted that even a small increase in the optimal cold shot fraction at the inlet of any bed (say, two percent) for set 1 will result in quenching. Whereas even large changes in the cold shot fraction at the inlet of any bed (say, fifty percent) for set 0 may still not result in quenching. This further clarifies the relatively poorer stability at optimal cold shot fractions. In the present investigations for optimal cold shot fractions the maxima of the S-shaped curve could not be achieved because it required a further fine tuning of cold shot fractions to such small

fractional values that are not feasible to be implemented in the actual plant operation. Therefore, in the present investigations during the search, the cold shot fraction values were rounded off to the third decimal place. This also provides for better reactor stability by moving somewhat away from the blow out point.

It may be, therefore, summarized that operation near optimal will always be at some sacrifice of reactor stability as observed from Figure 7.3 for the two cases of set 0 and set 1. However, this sacrifice pays richly in the form of quite substantial increase in the rate of ammonia production, decrease in bed temperatures with consequent increase in catalyst life and decrease in electrical energy requirements for the gas booster/recirculation system due to decrease in reactor pressure drop.

#### 7.4. Effect of Variations in Design and Operating Parameters on Reactor Performance.

The values chosen for the operation and design parameters for a three bed quench type reactor for ammonia synthesis are given in Table 7.2.1. For studying the effect of variations in the six operating and design parameters, it was considered desirable to vary only one parameter at a time in the range specified in Table 7.2.1, while keeping all the other parameters corresponding to the base condition values. As discussed earlier, it may be noted here that cold shot fraction to each bed inlet is not taken as a pre-specified parameter but is considered as an independent variable for the optimization for any chosen set of conditions. The two additional values of the varying parameter (except for  $H / N$  ratio and activity factor), namely, at the minimum and the maximum of the range, were used for obtaining simulation results. For  $H / N$  ratio and activity factor one more value within the range (other than the base value) was chosen in addition to minimum and maximum values of the range. These two (or three) computed results along with those obtained for the base conditions form a set for each parameter variation. Each of



the six parameters, that were permitted to vary, were treated as an independently varying parameter in order to study the effect of the same. The results of this sensitivity analysis can be very useful in the evolution of optimal conditions for design and operation of the multibed quench-type reactors for ammonia synthesis. The detailed computed results are given in Appendix-A, Tables A.1 to A.7. The summary of the computed results of simulation are given in Tables 7.3.1.1 and 7.3.1.2.

The general trends for changes in bed temperature and conversion in the reactor were similar to those obtained for the base conditions. Thus, further discussion on the same is not considered essential. The effect of the variations in the design and operating parameters can be discussed properly with the help of tabulated results as given in Tables 7.3.1.1, 7.3.1.2, and Appendix-Tables A.1 to A.7, and Figures 7.4 through 7.15.

#### 7.4.1. Feed Gas Flow Rate.

It is observed from Figure 7.4, Tables 7.3.1.1, 7.3.1.2 and A.2 that the decrease in feed gas flow rate by about 10 percent from the base condition value of  $0.74 \times 10^6$  (in cubic meter per hour at N.T.P. conditions) to  $0.667 \times 10^6$  results in an increase in conversion and decrease in bed temperature. The exit ammonia concentration (mol percent) increases to 15.188 (2.07 percent increase from base value). The behaviour is to be expected due to increase in residence time with decrease in flow rate. But the rate of ammonia production decreased by about 8 percent because increase in conversion was not commensurate with the decrease in flow rate. The total pressure drop is found to be 1.83 atm, a

reduction of about 20 percent from set 1. As observed from Figure 7.5, there was no noticeable change in reactor stability and it remained nearly the same (slightly better). The effect of increase in flow rate to  $0.82 \times 10^6 \text{ Nm}^3/\text{h}$  (11 percent increase from base value) results in decrease in the conversion and, in general, increase in bed temperature except in the third bed where bed temperature is slightly higher. The rate of ammonia production increases by 9.0 percent due to the combined effect of increase in flow rate and decrease in conversion (1.67 percent decrease from base value). The pressure drop increases by 23 percent to 2.78 atm due to higher flow rate. It is also observed from Figure 7.5 that the stability is nearly the same (slightly poorer). From Figure 7.4 and Table A.2, it may be observed that the ratios of actual to equilibrium ammonia concentration at the first, second and third bed outlets are 0.994, 0.932 and 0.947, respectively with an average value of 0.958. Similar effect of change in feed gas flow rate on reactor performance is reported by Shah (1967), Gaines (1977), Reddy and Husain (1978) and others. About 35 iterations including some quenched ones (no operating point except the trivial low conversion) were required to locate the optimal cold shot distribution in each case. The total cold shot fraction values ranged between 0.313 to 0.614. It is further observed from Table A.2 that the optimal allocation of cold shot fractions to each of the first, second and the third bed showed a declining trend with increase in flow rate. The values of cold shot fractions to each of the bed inlet and the total cold shot fraction for feed gas flow rates of  $0.667 \times 10^6$ ,

$0.740 \times 10^6$  and  $0.820 \times 10^6$  Nm<sup>3</sup>/h are (0.123, 0.253, 0.234, 0.610), (0.110, 0.233, 0.232, 0.575) and (0.098, 0.230, 0.219, 0.547) respectively. Therefore, the reactor operation at the cold shot values corresponding to optimum conditions of set 1 will result in non-optimal performance in case of decrease in flow rate whereas it will quench the reactor in case of significant increase in flow rate. This emphasises the need for establishing the new optimal cold shot distribution with the help of simulation model if change in feed gas flow rate becomes essential.

#### 7.4.2. H<sub>2</sub>/N<sub>2</sub> Ratio in Feed Gas.

It is observed from Figure 7.6, Table 7.3.1.1, 7.3.1.2 and A.3 that the decrease in H<sub>2</sub>/N<sub>2</sub> ratio from the base value of 3.0 results in a slight improvement in the third bed outlet ammonia concentration as well as the rate of ammonia production. For H<sub>2</sub>/N<sub>2</sub> ratio of 2.5, 2.8, 3.0 (base value) and 3.2 the rate of ammonia production in t/d are 1421.7 (+0.2 percent increase), 1422.4 (+0.23), 1419.2 (0.00) and 1416.2 (-0.20), respectively. The reactor stability as observed from Figure 7.7 also remains essentially the same as the plots nearly overlap each other. The best condition is at a value of H<sub>2</sub>/N<sub>2</sub> ratio of 2.8. Similar observations are also reported by other authors including Shah (1967), Gaines (1977) and Reddy and Husain (1978). However, Reddy and Husain found the best value at H<sub>2</sub>/N<sub>2</sub> ratio of 2.5 for a single bed reactor with high internal heat exchange capacity that may be due to non-optimal cold shot conditions at the bed inlet.

The optimal cold shot fractions for four  $H_2/N_2$  ratios are also nearly the same. The first, second, third bed and the total cold shot fractions for the  $H_2/N_2$  ratio of 2.5, 2.8, 3.0 and 3.2 are: (0.109, 0.237, 0.236, 0.582); (0.108, 0.240, 0.234, 0.582); (0.110, 0.233, 0.232, 0.575) and (0.108, 0.237, 0.226, 0.571), respectively. Only slight decrease in total cold shots requirement is observed as the  $H_2/N_2$  is increased from 2.8 to 3.2. There is no definite trend in the individual cold shot fraction values because of the reasons already discussed earlier that the region near optimal is flat and there could be other combination of individual cold shot fractions that will be nearly optimal. Therefore it may be summarized that optimal performance is not quite sensitive to changes in  $H_2/N_2$  ratio in the vicinity of 3.0 and plant operation at a value of 3.0 would be desirable from operational point of view. This will then not require continuous adjustments of make up feed gas  $H_2/N_2$  ratio.

#### 7.4.3. Inerts Concentration in Feed Gas.

It is observed from Figure 7.8 and Tables 7.3.1.1, 7.3.1.2 and A.4 that the effect of increase in concentration of mol percent inerts (consisting of methane and argon) from 10.68 to 13.95 with the base value of 12.84 was to decrease the conversion and increase the first bed temperature. However, the second and the third bed temperatures are lower compared to base case. The rate of production were found to be 1467.0, 1419.2 and 1397.1 t/d, respectively, for the three values of the inerts concentration, that is, 10.68, 12.84, and 13.95 mole percent. The increase in inerts lowers the partial pressures of hydrogen and

nitrogen and decreases the rate of reaction unless equilibrium inhibition is observed due to high temperature. In such a case, the inerts acting as heat carriers will shift the equilibrium favorably. Similar observations about the effect of change in inerts content on the reactor performance is also reported by Shah (1967), Gaines (1977), Reddy and Husain (1978) and Mansson and Andresen (1986).

The first, second, and the third bed and total cold shot fractions for the inerts concentration of 10.68, 12.84 and 13.95 mol percent are (0.145, 0.250, 0.234, 0.629), (0.110, 0.233, 0.232, 0.575) and (0.089, 0.249, 0.220, 0.558) respectively. Except in the case of second bed cold shot fractions other cold shot fractions do show a trend and the values decrease with increase in inerts. It is observed from Figure 7.9 that the reactor stability somewhat deteriorates with decrease in inerts concentration. However, the increase in pressure drop with the increase in inerts concentration is only marginal.

#### 7.4.4. Catalyst Activity Factor.

It is observed from Figure 7.10 and Tables 7.3.1.1, 7.3.1.2 and A.5 that at the catalyst activity factor values of 0.7, 0.8, 0.9, and 1.0 the rate of ammonia production in t/d was found to be 1312.5, 1366.2, 1395.6 and 1419.2, respectively. The corresponding optimal values of the first, second, third and total cold shot fractions are (0.030, 0.193, 0.192, 0.415); (0.080, 0.232, 0.203, 0.515); (0.096, 0.237, 0.220, 0.553) and (0.110, 0.233, 0.232, 0.575) for the activity factors of 0.7,

0.8, 0.9 and 1.0, respectively. The above also indicates a trend in the variation of the individual and total cold shot fractions. As the activity factor declines the cold shot fraction values also decline, but the decline in total cold shot fractions is not proportional to the decline in activity. This emphasises the fact that with a decline in the catalyst activity a new set of optimal cold shot fraction has to be found and used for getting the maximum advantage (production); otherwise, the reaction will quench or operation may be non-optimal. It is further observed that the total pressure drop increases at optimal cold shot fractions with the decrease in catalyst activity. This increase ranges from 2.0 to 14.0 percent of the base value of 2.26 atm.

The highest bed temperatures are found to be nearly the same with operation at changed activity factors. The stability of the reactor is found to deteriorate with decline in catalyst activity as observed from Figure 7.11.

It may, therefore, be summarised that the reactor may be operated with some loss of production even with used catalyst having lower activity factor. However, the cold shot distributions have to be readjusted to an appropriate lower value found by optimization. It was observed from computations for catalyst activity factor of 0.6 and lower that except for trivial operating point of low conversion no other operating point exists for activity factor of 0.6 and less. It is worthwhile to observe that the readjustment of cold shot distribution at lower optimal values helps in maintaining ammonia production rate close to fresh catalyst conditions even when the decline in catalyst

activity factor may be quite significant (for 30 percent decline in catalyst activity factor, the decline in ammonia production rate is only 7.5 percent of the base condition). It may be further observed that after a certain decline in activity factor, say, below 0.7, the catalyst may have to be replaced as economical operation will not be possible. Similar observations about the effect of decline in catalyst activity factor have also been reported by Gaines (1977) and van Heerden (1953).

#### 7.4.5. Total Volume of Catalyst.

It was observed from Figure 7.12 and Tables 7.3.1.1, 7.3.1.2 and A.6 that at the total catalyst volumes of 61.0, 67.6 and 75.0 m<sup>3</sup>, the exit ammonia concentration in mol percent were 14.646, 14.880 and 15.184, respectively. This increase in ammonia mole percent is obvious because increase in catalyst volume at constant feed gas flow rate at base value increases the residence time and is analogous to the effect of decrease in feed gas flow rate at constant catalyst volume. The effect of the decrease in feed gas flow rate for a constant total catalyst volume at base value is already discussed in section 7.4.1. The optimal values of the first, second, third bed and the total cold shot fractions are (0.096, 0.239, 0.214, 0.549); (0.110, 0.233, 0.232, 0.575) and (0.120, 0.253, 0.235, 0.608) for the total catalyst volumes of 61.0, 67.6 and 75.0 m<sup>3</sup>, respectively. Except for the second bed, the cold shot fractions show an increasing trend with the increase in catalyst volume at constant flow rate. The highest bed temperatures are virtually unchanged. Similar observations have been reported by Mansson and Andresen (1986) about the

effect of change in catalyst volume on reactor performance. Figure 7.13 indicates that the stability of the reactor increases slightly with the increase in total catalyst volume.

#### 7.4.6. Feed Gas Pressure (Operating Pressure).

It may be observed from Figure 7.14 and Tables 7.3.1.1, 7.3.1.2 and A.7 that at feed gas pressures (operating pressures) of 170.0, 190.0 and 210.0 atm the respective rates of production of ammonia are 1351.3, 1419.2 and 1495.4 tpd. The highest bed temperature at 170.0 atm is found to be about 20 K lower than that observed at the base value of pressure (190atm), set 1.

The optimal values of the first, second, third and the total cold shot fractions at operating pressures of 170.0, 190.0 and 210.0 atm are (0.089, 0.235, 0.199, 0.523); (0.110, 0.233, 0.232, 0.575) and (0.146, 0.253, 0.231, 0.630), respectively. The first bed and the total cold shot fraction values show an increasing trend with an increase in the operating pressure. It may be emphasised here that the increase in pressure greatly favours ammonia formation, but readjustment of cold shot fraction to a new set of optimal values is essential to keep the reaction away from quenching and also to maximize ammonia production rate. Stability of the reactor is found to improve significantly with increase in operating pressure. Similar observations are reported by Shah (1967), Gaines (1977), and Mansson and Andresen (1986) about the effect of change in operating pressure on reactor performance.



#### 7.4.7. Sensitivity Analysis.

It was observed from the discussions in previous sections that the reactor performance, in particular, conversion to ammonia, is quite sensitive to changes in the parameters of feed gas flow rate, inerts content of feed gas, catalyst activity factor, total volume of the catalyst and operating pressure. The increase in the flow rate or inerts concentration, decrease in the catalyst activity factor, catalyst volume or operating pressure result in significant decrease in exit conversion. The excessive increase in flow rate or inerts will result in quenching effect and the rate of reaction will become so small that the reactor will quench. Similarly a decrease in catalyst activity, catalyst volume or operating pressure will result in quenching of the reactor. The effect of changes in  $H^2/N^2$  ratio studied in the present investigation is found to be quite small and insignificant in nature. A slightly better performance is obtained at the  $H^2/N^2$  ratio of 2.8. However this will require continuous readjustment of make up feed gas  $H^2/N^2$  ratio. This may, therefore, be undesirable from the point of view of plant operation.

For a complex multidimensional problem, sensitivity analysis is a powerful tool to identify the dominant variables. Table 7.4.7 summarizes the effects of various design and operation parameters on ammonia production rate following the procedure discussed by Rudd and Watson (1968).

Table 7.4.7.

Comparison of Parameter Sensitivity.

Parameter	Unit	Base Value	Range of Variation	Sensitivity*	
				Absolute	Relative
Flow Rate	Nm <sup>3</sup> / h	0.740 *	0.667 * 10 <sup>6</sup> to 0.820 * 10 <sup>6</sup>	0.170	1.00
H / N Ratio	--	3.0	2.5 to 3.2	0.006	0.04
Inerts	mol	12.84	10.68 to 13.95	0.048	0.28
Concentration	%				
Catalyst Activity	--	1.0	0.7 to 1.0	0.060	0.35
Catalyst Volume	m <sup>3</sup>	67.6	61.0 to 75.0	0.036	0.21
Operating Pressure	atm	190	170 to 210	0.102	0.60

\* Absolute Sensitivity = (fractional change in maximum ammonia production rate at optimal cold shot distribution) / (change in parameter as a fraction of expected range of variation)

Relative Sensitivity = (Absolute sensitivity of parameter) / (Maximum of absolute sensitivities)

It may be observed from the relative sensitivity values given in the last column of the Table 7.4.7 that the maximum ammonia production rate at optimal cold shot distribution is highly sensitive to flow rate and operating pressure with relative sensitivity values as 1.00 and 0.60, respectively. Whereas ammonia production rate is moderately sensitive to catalyst activity factor, inerts concentration and catalyst volume with relative sensitivity values as 0.35, 0.28 and 0.21, respectively. However, ammonia production rate is almost insensitive to  $\frac{H}{N}$  ratio in the feed and shows a relative sensitivity value of 0.04 only.

#### 7.4.8. General Considerations.

It was observed from the computation results of optimization investigations that the value of individual cold shot fractions was very sensitive to the variations in operating parameters value and there existed, for each bed, an absolute maximum value beyond which the reactor quenched irrespective of the decrease in the cold shot to other beds. This limit for the first bed cold shot fraction is found to vary between 0.03 to 0.16 depending on the parameter varied and its value. For the second and the third bed cold shot fractions this limit was in the range from 0.19 to 0.35.

It was further observed that in general it is best to operate ammonia synthesis reactor near its blowout point to maximize conversion to ammonia as to obtain low bed temperatures and reduced pressure drop. However, this means sacrificing in terms of reactor stability. Some compromise,

therefore, may be desirable to operate the reactor at cold shot fraction values somewhat lower than the optimal in order to achieve good stability for small unintended perturbations in parameter values. It must be noted here that this compromise is at the cost of reduced rate of ammonia production. Therefore, the cold shot values can not be set much below the optimal to take care of even higher magnitude of disturbances in the parameters taking place in the plant. Rather, it will be more desirable to find the new set of optimal cold shot values for the new parameter values which may now exist as a consequence of higher disturbances, and operate the plant at some what lower cold shot values than the new set of optimal values. As discussed earlier, the region near optimal values of the cold shot fraction is rather flat, therefore a slight lowering of the values of the cold shot fraction from optimal, in order to achieve better reactor stability will result in only a slight decrease in the rate of the ammonia production.

#### 7.5. Conditions for Optimal Design and Operation.

Based on the results of optimization and the discussions presented in the foregoing sections it is observed that the operation of reactor should be maintained at near optimal cold shot distribution corresponding to a given set of values of the parameters. The concentration of inerts should be maintained as low as possible for high ammonia production rate.  $H_2/N_2$  ratio should be kept at 3.0 as reduction to 2.8 gives only a marginal advantage in production rate compared to inconvenience in

operation. The feed gas pressure (operating pressure) should be kept as high as permissible by reactor design (mechanical strength) considerations. The catalyst should be discarded after a period of time (about a few years depending upon the catalyst used and its condition) when the activity factor declines by about 20 to 30 percent. The reactor operation at the above conditions will certainly result in significant improvements in ammonia productivity.



8. CONCLUSIONS AND RECOMMENDATIONS

## 8.1. Conclusions.

8.1.1. A realistic, accurate and stable simulation model for a modern multibed quench reactor for ammonia synthesis was developed. The simulation model was tested over a wide range of variations in the design and the operating variables and the model seems to give reliable information on reactor performance. The model is capable of simulating the external and internal heat exchange as well as the addition of cold shot at the inlet of each bed.

8.1.2. A reliable and efficient optimization algorithm was developed for the maximization of ammonia production rate using cold shot distribution as an optimization variable.

8.1.3. The simulation model was validated using plant data of a large capacity three-bed quench reactor. The kinetic and heat exchange rate parameters of the reactor were established. These are:

(i) Frequency factor for the reverse reaction rate constant  

$$= 4.11482 * 10^{16} \text{ mol NH}_3 / \text{s/m catalyst}$$

(ii) Activation energy for the reverse reaction rate constant  

$$= 97622.4 \text{ kJ/kmol}$$

(iii) Correction for fugacity coefficient term in the rate equation  

$$= 1.379$$

(iv) External heat exchange capacity,  $(UA)_{H_2}$ , at feed gas flow rate of  $0.74 \times 10^6 \text{ Nm}^3/\text{h}$

$$= 316000 \text{ W/K}$$

8.1.4. The cold shot distribution as practiced at the time of plant data collection was found to be nonoptimal resulting in an ammonia production rate of 1286.9 t/d. Merely by using an optimal cold shot distribution without any other change gave an ammonia production rate of 1419.2 t/d - an increase of 10.28 percent over the prevalent ammonia production rate of the plant.

8.1.5. For an existing ammonia plant, the adjustment of cold shot distribution to an optimal value appears to be the most practical and powerful choice for the maximization of ammonia production rate. The simulation model developed in the course of this investigation can play a vital role for achieving the above objective.

8.1.6. The effect of variation of six design or operating parameters, namely, feed gas pressure, feed gas flow rate,  $H_2/N_2$  ratio in feed gas, inerts concentration in feed gas, catalyst activity factor and catalyst volume, was studied. The simulated results showing the effect of these parameters on optimal cold shot distribution and ammonia production rate are summarized in Table 7.3.1.1. Variations in  $H_2/N_2$  ratio appears to have insignificant effect on reactor performance and, therefore, use of  $H_2/N_2$  ratio of 3 is recommended.

8.1.7. The simulated results in Table 7.3.1.1. clearly indicate that the undesirable effect of adverse variation in parameter values can be greatly minimized by the adjustment of cold shot distribution to a new optimal value for any change in parameter values. It is significant to note that loss in ammonia production rate is restricted to about 7.52, 1.56 and 4.78 percent for a decrease in catalyst activity, catalyst volume and operating pressure by 30, 9.76 and 10.52 percent of the base values, respectively.

8.1.8. Conditions of steady-state stability were established for the first time for a three-bed quench-type ammonia synthesis reactor at optimal cold shot distribution corresponding to maximum ammonia production rate for wide variation in parameter values. In all the cases, it was found that the highest ammonia production rate could be achieved at conditions close to blowout point.

8.1.9. For optimal operation close to blowout point even pressure drop and catalyst bed temperatures were found to be lower with consequent decrease in energy requirement for gas booster/recirculation system and increase in catalyst life.

8.1.10. Stability consideration dictate that the reactor be operated slightly away from the blowout point in order to ensure good stability even when some unintended small perturbations in parameter values occur. Reduction in ammonia production rate for such an operation is likely to be insignificant (probably less



than 0.5 percent) because the optimal conditions are not very sharp and region around them appears to be flat in nature.

## 8.2. Recommendations.

8.2.1. It is recommended that the results of this study must be implemented on the plant for which the simulation model was developed.

8.2.2. Similar studies must be carried out for other industrial reactors including radial flow reactors for ammonia synthesis.

8.2.3. All ammonia synthesis reactors should have facilities for precise measurement and control of cold shot fraction at the inlet of each bed in addition to the facilities for the precise temperature and possibly ammonia concentration measurements at the inlet and the outlet of each bed.

REFERENCES

- Adelman, A., and W. F. Stevens, "Process Optimization by the Complex Method," *AIChE J*, **18**, 20(1972).
- Annable, D., "Application of the Temkin Kinetic Equation to Ammonia Synthesis in Large Scale Reactors," *Chem. Eng. Sci.*, **1**, 145(1952).
- Babuska, I., *Numerical Processes in Differential Equations*, Wiley, New York, 69(1966).
- Baddour, R. F., P. L. T. Brian, B. A. Logeais, and J. P. Eymery, "Steady-State Simulation of an Ammonia Synthesis Converter," *Chem. Eng. Sci.*, **20**, 281(1965).
- Beveridge, G. S. G., and R. S. Schechter, *Optimization Theory and Practice*, McGraw-Hill, New York (1970).
- Box, M. J., "A New Method of Constrained Optimization and a Comparison with Other Methods," *Computer J.*, **8**, 42(1965).
- Campbell, J. R., and J. L. Gaddy, "Methodology for Simultaneous Optimization with Reliability: Nuclear PWR Example," *AIChE J*, **22**, 1050(1976).
- Catalyst HandBook, Wolfe Scientific Books, London, 156(1970).
- Denbigh, K. G., *The Principles of Chemical Equilibrium*, 4th ed., Cambridge University Press, London, 152(1981).

Dodge, B. F., Chemical Engineering Thermodynamics, McGraw-Hill, New York, 495(1944).

Dyson, D. C., and J. M. Simon, "A Kinetic Expression with Diffusion Correction for Ammonia Synthesis on Industrial Catalyst," Ind. Eng. Chem. Fund., 7, 605(1968).

Eymery, J. P., Sc. D. Thesis, M. I. T. Cambridge, Ma, (1964)

Froment, G. F., and K. B. Bischoff, Chemical Reactor Analysis and Design, Wiley, New York, 506(1979a).

-----, 477(1979b).

Gaines, L. D., "Optimal Temperatures for Ammonia Synthesis Converters," Ind. Eng. Chem. Process Des. Dev., 16, 381(1977).

Gangiah, K., "A Constrained Polyhedron Search Method for Process Optimization," Indian Chemical Engineer, 22, 50(1980).

Gangiah, K., "Direct Search Methods for Constrained Optimization," Proceedings of the Computer Society of India, Division IV: Business Applications, CSI-78, 275(1978).

Heuckroth, M. W., J. L. Gaddy, and L. D. Gaines, "An Examination of the Adaptive Random Search Technique," AIChE J, 22(4), 744 (1976).

Hay, I., and G. D. Honti, "Ammonia" in The Nitrogen Industry, Ed. G. D. Honti, Part I, Akademiai Kiado, Budapest, 106(1976a).

-----, 110(1976b).

Hougen, O. A., and K. M. Watson, Chemical Process Principles, Part III, Wiley, New York, 886(1962).

International Critical Tables, 5, 178(1929).

-----, 7, 244(1930a).

-----, 7, 231(1930b).

-----, 7, 239(1930c).

-----, 7, 244(1930d).

Khayan, M. T., and F. F. Pironti, Ind. Eng. Chem. Process Des. Dev., 21, 470(1982).

Kirk-Othmer's Encyclopedia of Chemical Technology, Eds. H. F. Mark, D. F. Othmer, C. G. Overberger, and G. T. Seaborg, 3rd ed., Wiley, New York, 2, 471(1978).

Kjaer, J., Measurements and Calculation of Temperature and Conversion in Fixed-Bed Catalytic Reactors, Jul. Gjollierups Forlag, Copenhagen, Chapters 6 and 11, (1958).

Kramer, H., and K. R. Westerterp, Elements of Chemical Reactor Design and Operation, Academic Press, New York, 202(1963a).

-----, 128(1963b).

Lambert, J. P., Computational Methods in Ordinary Differential Equations, Wiley, New York, (1974).

Lutschutenkow, S., G. Reinig, G. Brack, and D. Balzer, "Simulating Steady-State Behavior of a Bed Reactor for Ammonia Synthesis," Intern. Chem. Eng., 18, 567(1978).

Luus, R., and T. H. I. Jaakola, "Optimization by Direct Search and Systematic Reduction of the Size of Search Region," AIChE J, 19, 760(1973).

Mansson, B., and B. Andresen, "Optimal Temperature Profile for an Ammonia Reactor," Ind. Eng. Chem. Process Des. Dev., 25, 59 (1986).

McAdams, W. H., Heat Transmission, McGraw-Hill, New York, 219(1954).

Milne, W. E., Numerical Solutions of Differential Equations, Wiley, New York, 49(1953).

Nelder, J. A., and R. Mead, "A Simplex Method for Function Minimization," Computer J., 7, 308(1965).

Nielsen, A., An Investigation on Promoted Iron Catalyst for the Synthesis of  $\text{NH}_3$ , 3rd ed., Jul. Gjolierups Forlag, Copenhagen, 3 (1968).

Pachaiyapan, V., Chemical Economy and Engineering Review, 16, 15 (1984).

Perry's Chemical Engineer's Handbook, 3rd ed., McGraw-Hill, New York, 347(1950).

Ramkumar, "Stability Analysis of Ammonia Synthesis Reactor," M. E. Dissertation, Department of Chemical Engineering, University of Roorkee, Roorkee, India, (1978).

Rase, H. F., Chemical Reactor Design for Process Plants, Wiley, New York, 2, 61(1977).

Reddy, K. V., and Asgar Husain, Proceedings of 1976 Summer Computer Conference, New Port Beach, CA, 286(1978).

Reddy, K. V., and Asghar Husain, "Modelling and Simulation of an Ammonia Synthesis Loop," Ind. Eng. Chem. Process Des. Dev., 21, 359(1982).

Rudd, D. F., and C. C. Watson, Strategy of Process Engineering, Wiley, New York, 252(1968).

Saraf, S. K., Winter School Lecture Notes, IIT Kanpur, India

Shah, M. J., "Control Simulation in Ammonia Production," Ind. Eng. Chem., 59, 72(1967).

Shipman, L. M., and J. B. Hickman, "Optimum Design of Ammonia Quench Converters," Chem. Eng. Prog., 64(5), 59(1968).

Singh, C. P. P., and D. N. Saraf, "Simulation of Ammonia Synthesis Reactors," Ind. Eng. Chem. Process Des. Dev., 18, 364 (1979).

Sinha, S. N., "Analysis and Simulation of ammonia synthesis reactor," M. E. Dissertation, Department of Chemical Engineering, University of Roorkee, Roorkee, India, (1977).

Sinha, S. N., S. K. Saraf, Surendra Kumar, and I. M. Mishra, "Analysis and Simulation of Ammonia Synthesis Reactor - Adiabatic Operation with Cold Shot Cooling," Proceedings of 34th Annual Conference of Indian Institute of Chemical Engineers, 3, 59(1981).

Slack, A. V., H. Y. Allgood, and H. E. Maune, "Operating Problems in Ammonia Synthesis," Chem. Eng. Prog., 49, 393(1953).

Temkin, M. I., and V. Pyzhev, Acta. Physicochem., 12, 327(1940).

Vancini, C. A., Synthesis of Ammonia, The McMillan Press, London, (1971).

Van Heerden, C., "Autothermic Process Properties and Reactors Design", Ind. Eng. Chem., 45, 1242(1953).

Vek, V., "Optimization of Large Reactors with Extremely Active Catalysts," Ind. Eng. Chem. Process Des. Dev., 412(1977).

Walas, S. M., Reaction Kinetics for Chemical Engineers, McGraw-Hill, New York, 282(1959).

Zardi, U., "Review these Developments in Ammonia and Methanol Reactors," Hydrocarbon Processing, August, 129(1982).

Zayarni, N. S., Intern. Chem. Eng., 2, 378(1963).

TABLE NO.A .1.

COMPUTED PROFILES OF AMMONIA MOLE PERCENT AND TEMPERATURE IN THE BED FOR DIFFERENT COLD SHOT DISTRIBUTIONS

Set No. 0, Base condition						Set No.1, Base condition with optimal cold shots				
Bed Pt. No.	% Of Total Catalyst Volume	Bed Temp. (K)	NH3 Mole % Actual	At. Max. Rate	% At. Equilibrium	Bed Temp. (K)	NH3 Mole % Actual	At. Max. Rate	At. Equilibrium	
1	2	3	4	5	6	7	8	9	10	
1	0.0	658.3	1.613	23.765	28.519	640.1	1.613	27.320	32.121	
11	2.3	673.2	2.543	21.096	25.750	652.4	2.377	24.903	29.683	
21	4.5	689.0	3.542	18.510	23.002	665.5	3.200	22.482	27.197	
31	6.8	706.3	4.666	15.942	20.201	679.9	4.126	19.989	24.576	
41	9.1	725.6	5.941	13.434	17.399	696.3	5.193	17.409	21.810	
51	11.4	746.1	7.333	11.147	14.755	714.8	6.428	14.805	18.943	
56	12.5	756.1	8.024	10.162	13.592	724.9	7.107	13.543	17.514	
61	13.6	765.3	8.662	9.336	12.606	735.1	7.814	12.335	16.141	
66	14.8	772.9	9.203	8.695	11.827	745.4	8.523	11.240	14.860	
71	15.9	778.7	9.619	8.235	11.261	754.9	9.195	10.290	13.744	
76	17.0	782.8	9.908	7.930	10.887	763.2	9.782	9.532	12.842	
81	18.2	785.3	10.092	7.739	10.655	769.6	10.246	8.980	12.170	
86	19.3	786.9	10.203	7.632	10.516	774.2	10.574	8.606	11.717	
91	20.5	787.7	10.266	7.568	10.439	777.1	10.785	8.378	11.439	
95	21.4	788.1	10.296	7.539	10.403	778.5	10.891	8.265	11.298	
98	22.0	788.4	10.311	7.525	10.382	779.3	10.945	8.205	11.225	
101	22.7	788.5	10.321	7.515	10.372	779.8	10.983	8.166	11.178	
1	22.7	692.9	7.806	17.887	22.324	675.4	7.963	20.739	25.371	
11	25.9	702.6	8.474	16.454	20.764	683.4	8.519	19.398	23.952	
21	29.1	712.9	9.190	15.033	19.194	692.2	9.125	18.022	22.476	
31	32.3	723.4	9.937	13.684	17.677	701.5	9.781	16.631	20.960	
41	35.5	733.7	10.675	12.468	16.283	711.3	10.477	15.267	19.458	
51	38.6	743.0	11.348	11.454	15.111	721.1	11.189	13.984	18.022	
56	40.2	747.0	11.640	11.038	14.627	725.9	11.538	13.396	17.351	
61	41.8	750.4	11.895	10.691	14.220	730.5	11.873	12.852	16.728	
66	43.4	753.3	12.110	10.408	13.880	734.8	12.187	12.361	16.169	
71	45.0	755.7	12.285	10.183	13.613	738.6	12.474	11.932	15.671	
76	46.6	757.6	12.422	10.009	13.407	742.0	12.727	11.570	15.245	
81	48.2	759.0	12.530	9.872	13.245	744.9	12.943	11.266	14.894	
86	49.8	760.1	12.610	9.775	13.126	747.3	13.122	11.017	14.605	
91	51.4	760.9	12.669	9.699	13.040	749.2	13.267	10.825	14.379	
95	52.6	761.3	12.705	9.659	12.986	750.5	13.359	10.701	14.231	
98	53.6	761.6	12.726	9.634	12.960	751.2	13.417	10.629	14.143	
101	54.5	761.9	12.744	9.608	12.933	751.9	13.466	10.562	14.066	
1	54.5	729.6	11.522	12.917	16.809	678.3	10.476	20.214	24.818	
11	59.1	739.2	12.226	11.837	15.559	685.0	10.954	19.110	23.649	
21	63.6	746.4	12.764	11.074	14.666	692.1	11.463	18.004	22.450	
31	68.2	751.1	13.115	10.603	14.110	699.4	11.996	16.901	21.257	
41	72.7	753.8	13.314	10.341	13.804	706.8	12.544	15.835	20.086	
51	77.3	755.1	13.416	10.208	13.646	714.1	13.086	14.844	18.985	
56	79.5	755.5	13.445	10.173	13.602	717.6	13.347	14.390	18.469	
61	81.8	755.8	13.466	10.147	13.570	721.0	13.596	13.962	17.992	
66	84.1	755.9	13.478	10.127	13.548	724.1	13.831	13.581	17.554	
71	86.4	756.1	13.488	10.111	13.532	726.9	14.047	13.234	17.166	
76	88.6	756.1	13.493	10.106	13.521	729.5	14.241	12.927	16.814	
81	90.9	756.2	13.498	10.096	13.510	731.7	14.414	12.665	16.511	
86	93.2	756.2	13.499	10.096	13.510	733.7	14.562	12.441	16.254	
91	95.5	756.2	13.501	10.091	13.505	735.3	14.689	12.250	16.038	
95	97.3	756.2	13.502*	10.086	13.499	736.4	14.775	12.128	15.891	
98	98.6	756.2	13.500*	10.086	13.499	737.2	14.830	12.043	15.801	
101	100.0	756.2	13.502*	10.086	13.499	737.8	14.880	11.975	15.716	
Total Pressure Drop, atm					2.77	2.26				
Cold Shot Distribution:										
First Bed					0.000	0.110				
Second Bed					0.245	0.233				
Third Bed					0.100	0.232				
Total					0.345	0.575				

\* These values should be read as 13.499, that is equal to equilibrium value.



TABLE NO. A.2

COMPUTED PROFILES OF AMMONIA MOLE PERCENT AND TEMPERATURE IN THE BED FOR DIFFERENT FEED FLOW RATES

Set No. 2(A), Flow rate = 0.667						Set No. 2(B), Flow rate=0.820				
Bed Pt. No.	% of Total Catalyst Volume	Bed Temp. (K)	NH3 Actual	NH3 Mole % At Equilibrium	NH3 Mole % At Equilibrium	Bed Temp. (K)	NH3 Actual	NH3 Mole % At Equilibrium	NH3 Mole % At Equilibrium	NH3 Mole % At Equilibrium
1	2	3	4	5	6	7	8	9	10	10
1	0.0	636.4	1.604	28.075	32.875	641.4	1.607	27.055	31.850	31.850
11	2.3	649.6	2.419	25.458	30.245	652.5	2.296	24.877	29.655	29.655
21	4.5	663.7	3.309	22.811	27.539	664.2	3.028	22.710	27.429	27.429
31	6.8	679.5	4.329	20.056	24.648	676.8	3.835	20.500	25.121	25.121
41	9.1	697.9	5.530	17.177	21.561	690.9	4.747	18.221	22.691	22.691
51	11.4	719.0	6.944	14.280	18.351	706.6	5.785	15.908	20.165	20.165
56	12.5	730.3	7.721	12.895	16.780	715.1	6.355	14.760	18.890	18.890
61	13.6	741.7	8.513	11.622	15.312	724.0	6.957	13.635	17.618	17.618
66	14.8	752.5	9.273	10.526	14.022	733.2	7.582	12.553	16.391	16.391
71	15.9	761.8	9.933	9.659	12.992	742.3	8.214	11.549	15.228	15.228
76	17.0	768.8	10.440	9.050	12.255	751.1	8.830	10.650	14.170	14.170
81	18.2	773.5	10.780	8.661	11.785	759.1	9.396	9.892	13.267	13.267
86	19.3	776.3	10.983	8.437	11.512	765.9	9.880	9.286	12.542	12.542
91	20.5	777.8	11.095	8.319	11.366	771.2	10.261	8.840	12.001	12.001
95	21.4	778.5	11.145	8.265	11.303	774.4	10.489	8.586	11.690	11.690
98	22.0	778.8	11.168	8.240	11.272	776.2	10.619	8.442	11.517	11.517
101	22.7	779.0	11.184	8.225	11.251	777.5	10.721	8.334	11.381	11.381
1	22.7	665.4	7.826	22.501	27.211	676.8	7.871	20.482	25.101	25.101
11	25.9	672.8	8.338	21.182	25.836	684.3	8.382	19.254	23.797	23.797
21	29.1	680.9	8.900	19.813	24.393	692.2	8.935	17.998	22.450	22.450
31	32.3	689.8	9.517	18.398	22.881	700.7	9.529	16.734	21.071	21.071
41	35.5	699.2	10.187	16.964	21.325	709.6	10.158	15.486	19.699	19.699
51	38.6	709.2	10.898	15.559	19.783	718.6	10.807	14.291	18.363	18.363
56	40.2	714.2	11.624	14.822	19.027	723.1	11.130	13.727	17.729	17.729
61	41.8	719.2	11.624	14.236	18.304	727.5	11.447	13.202	17.125	17.125
66	43.4	724.0	11.979	13.635	17.624	731.6	11.751	12.713	16.568	16.568
71	45.0	728.9	12.318	13.078	16.993	735.5	12.038	12.266	16.055	16.055
76	46.6	732.6	12.634	12.585	16.425	739.1	12.302	11.874	15.604	15.604
81	48.2	736.7	12.918	12.154	15.931	742.3	12.539	11.533	15.206	15.206
86	49.8	740.0	13.166	11.790	15.508	745.1	12.745	11.240	14.866	14.866
91	51.4	742.8	13.376	11.496	15.161	747.4	12.920	11.001	14.583	14.583
95	52.6	744.6	13.515	11.303	14.938	749.0	13.039	10.841	14.396	14.396
98	53.6	745.8	13.603	11.183	14.794	750.0	13.117	10.737	14.269	14.269
101	54.5	746.8	13.681	11.074	14.672	750.9	13.184	10.650	14.165	14.165
1	54.5	673.7	10.604	21.016	25.663	681.7	10.428	19.638	24.205	24.205
11	59.1	680.4	11.085	19.880	24.465	688.2	10.888	18.599	23.098	23.098
21	63.6	687.5	11.599	18.724	23.232	694.9	11.373	17.554	21.973	21.973
31	68.2	695.0	12.144	17.566	21.985	701.8	11.878	16.528	20.850	20.850
41	72.7	702.7	12.709	16.437	20.751	708.8	12.393	15.542	19.759	19.759
51	77.3	710.3	13.275	15.373	19.572	715.7	12.900	14.622	18.735	18.735
56	79.5	713.9	13.551	14.882	19.027	719.0	13.145	14.198	18.257	18.257
61	81.8	717.5	13.815	14.423	18.510	722.1	13.380	13.804	17.811	17.811
66	84.1	720.8	14.066	14.000	18.033	725.0	13.601	13.440	17.398	17.398
71	86.4	723.8	14.297	13.624	17.607	727.8	13.806	13.110	17.027	17.027
76	88.6	726.6	14.506	13.288	17.230	730.2	13.993	12.820	16.688	16.688
81	90.9	729.0	14.691	12.997	16.901	732.4	14.160	12.563	16.397	16.397
86	93.2	731.1	14.851	12.756	16.620	734.4	14.307	12.340	16.141	16.141
91	95.5	732.8	14.986	12.553	16.385	736.0	14.434	12.154	15.925	15.925
95	97.3	734.0	15.077	12.414	16.226	737.2	14.521	12.027	15.778	15.778
98	98.6	734.8	15.136	12.329	16.129	737.9	14.580	11.943	15.677	15.677
101	100.0	735.4	15.188	12.250	16.038	738.6	14.631	11.869	15.592	15.592
Total Pressure Drop, atm					1.83	2.78				
Cold Shot Distribution:										
First Bed					0.123	0.098				
Second Bed					0.253	0.230				
Third Bed					0.234	0.219				
Total					0.610	0.547				

TABLE NO.A.3

COMPUTED PROFILES OF AMMONIA MOLE PERCENT AND TEMPERATURE IN THE BED FOR DIFFERENT H<sub>2</sub>/N<sub>2</sub> RATIOS

Set No.3 (A), H <sub>2</sub> /N <sub>2</sub> ratio =2.5						Set No.3 (B), H <sub>2</sub> /N <sub>2</sub> ratio=2.8				Set No.3 (C), H <sub>2</sub> /N <sub>2</sub> ratio=3.2					
Bed Pt. No.	Of Total Catalyst Volume	Bed Temp. (K)	NH <sub>3</sub> Actual	Mole % At Equilibrium	NH <sub>3</sub> At Equilibrium	Bed Temp. (K)	Actual	NH <sub>3</sub> At Equilibrium	Mole % At Equilibrium	Bed Temp. (K)	Actual	NH <sub>3</sub> At Equilibrium	Mole % At Equilibrium		
1	2	3	4	5	6	7	8	9	10	11	12	13	14		
1	0.0	640.0	1.614	25.056	29.477	640.6	1.614	26.363	31.019	640.9	1.613	27.953	32.883		
11	2.3	652.5	2.395	22.784	27.180	653.4	2.405	23.946	28.580	653.3	2.384	25.454	30.357		
21	4.5	665.8	3.234	20.518	24.850	666.9	3.258	21.523	26.086	666.5	3.214	22.948	27.785		
31	6.8	680.6	4.131	18.188	22.399	681.9	4.224	19.034	23.465	681.1	4.150	20.372	25.079		
41	9.1	697.3	5.277	15.774	19.806	699.0	5.343	16.460	20.692	697.6	5.226	17.718	22.228		
51	11.4	716.4	6.553	13.343	17.111	718.5	6.643	13.876	17.827	716.3	6.468	15.054	19.285		
56	12.5	726.8	7.256	12.161	15.779	728.9	7.355	12.629	16.415	726.3	7.147	13.766	17.831		
61	13.6	737.3	7.985	11.047	14.498	739.6	8.089	11.466	15.074	736.5	7.851	12.545	16.434		
66	14.8	747.7	8.709	10.043	13.328	749.9	8.810	10.428	13.860	746.6	8.552	11.440	15.150		
71	15.9	757.2	9.381	9.200	12.322	759.2	9.470	9.567	12.840	756.0	9.212	10.492	14.027		
76	17.0	765.1	9.947	8.544	11.539	766.9	10.017	8.911	12.050	764.1	9.785	9.740	13.128		
81	18.2	771.0	10.373	8.088	10.988	772.5	10.421	8.461	11.502	770.3	10.233	9.192	12.464		
86	19.3	775.0	10.658	7.728	10.629	776.1	10.688	8.175	11.154	774.7	10.550	8.821	12.017		
91	20.5	777.4	10.833	7.621	10.418	778.4	10.849	8.006	10.945	777.5	10.753	8.594	11.738		
95	21.4	778.5	10.917	7.542	10.320	779.4	10.926	7.928	10.848	778.9	10.856	8.483	11.600		
99	22.0	779.1	10.958	7.501	10.271	779.9	10.965	7.885	10.802	779.6	10.908	8.423	11.531		
101	22.7	779.5	10.947	7.473	10.232	780.3	10.990	7.861	10.772	780.1	10.945	8.387	11.483		
1	22.7	672.8	7.899	19.387	23.667	672.3	7.872	20.602	25.120	674.6	7.910	21.485	26.254		
11	25.9	680.8	8.419	16.149	22.363	680.1	8.408	19.322	23.769	682.4	8.447	20.143	24.832		
21	29.1	689.4	9.052	16.870	20.992	688.5	8.995	17.994	22.353	690.9	9.033	18.758	23.357		
31	32.3	698.7	9.708	15.570	19.582	697.6	9.633	16.651	20.897	699.9	9.665	17.363	21.846		
41	35.5	708.6	10.409	14.289	18.171	707.2	10.316	15.315	19.434	709.3	10.337	15.989	20.329		
51	38.6	718.6	11.132	13.071	16.810	717.1	11.025	14.032	18.006	719.0	11.030	14.681	18.867		
56	40.2	723.5	11.490	12.505	16.168	721.9	11.379	13.438	17.330	723.7	11.373	14.071	18.182		
61	41.8	728.2	11.835	11.985	15.576	726.7	11.724	12.877	16.696	728.3	11.707	13.507	17.534		
66	43.4	732.7	12.161	11.514	15.037	731.1	12.053	12.362	16.113	732.6	12.025	12.986	16.941		
71	45.0	736.7	12.459	11.097	14.556	735.3	12.359	11.910	15.586	736.6	12.319	12.523	16.405		
76	46.6	740.2	12.723	10.741	14.142	739.0	12.635	11.513	15.123	740.2	12.584	12.119	15.938		
81	48.2	743.2	12.949	10.447	13.798	742.2	12.876	11.174	14.735	743.3	12.815	11.781	15.542		
86	49.8	745.7	13.137	10.208	13.519	744.9	13.080	10.899	14.410	745.9	13.012	11.499	15.212		
91	51.4	747.7	13.288	10.023	13.302	747.2	13.247	10.675	14.150	748.0	13.173	11.276	14.952		
95	52.6	749.0	13.384	9.902	13.163	748.6	13.357	10.534	13.983	749.4	13.279	11.128	14.777		
99	53.6	749.8	13.445	9.830	13.076	749.5	13.426	10.443	13.876	750.3	13.346	11.038	14.670		
101	54.5	750.5	13.496	9.772	13.004	750.3	13.485	10.367	13.790	751.1	13.403	10.959	14.580		
1	54.5	676.0	10.448	18.858	23.112	676.5	10.465	19.878	24.361	679.6	10.505	20.583	25.307		
11	59.1	682.6	10.925	17.836	22.028	683.0	10.936	18.818	23.233	686.3	10.984	19.462	24.109		
21	63.6	689.7	11.433	16.804	20.921	690.0	11.437	17.736	22.075	693.4	11.491	18.331	22.890		
31	68.2	697.0	11.969	15.774	19.800	697.2	11.965	16.668	20.915	700.6	12.022	17.210	21.675		
41	72.7	704.5	12.521	14.772	18.705	704.7	12.509	15.624	19.771	708.0	12.565	16.134	20.490		
51	77.3	711.9	13.070	13.835	17.664	712.0	13.053	14.643	18.689	715.2	13.100	15.139	19.377		
56	79.5	715.5	13.336	13.405	17.183	715.5	13.317	14.193	18.179	718.7	13.356	14.681	18.867		
61	81.8	718.9	13.591	13.004	16.728	718.9	13.571	13.769	17.707	721.9	13.601	14.255	18.385		
66	84.1	722.0	13.831	12.632	16.314	722.1	13.811	13.379	17.267	725.0	13.830	13.871	17.949		
71	86.4	725.0	14.052	12.302	15.941	725.0	14.034	13.024	16.865	727.7	14.041	13.523	17.558		
76	88.6	727.6	14.253	12.015	15.608	727.7	14.237	12.713	16.510	730.2	14.230	13.221	17.210		
81	90.9	729.9	14.430	11.759	15.319	730.1	14.418	12.441	16.197	732.4	14.396	12.958	16.906		
86	93.2	731.9	14.585	11.544	15.069	732.1	14.576	12.206	15.929	734.3	14.540	12.740	16.655		
91	95.5	733.6	14.715	11.365	14.862	733.9	14.711	12.014	15.707	735.9	14.662	12.556	16.440		
95	97.3	734.8*	14.804*	11.245	14.725*	735.1	14.804	11.879	15.552	737.0	14.744	12.431	16.295		
99	98.6	735.6*	14.863*	11.166	14.630*	735.9	14.865	11.791	15.453	737.7	14.798	12.350	16.203		
101	100.0	736.2*	14.914*	11.097	14.551*	736.6	14.918	11.719	15.365	738.3	14.845	12.280	16.122		
Total Pressure Drop, atm					2.25	2.25					2.27				
Cold Shot Distribution:															
First Bed					0.109	0.108					0.108				
Second Bed					0.237	0.240					0.237				
Third Bed					0.236	0.234					0.226				
Total					0.582	0.582					0.571				

\* Values should correspond to equilibrium values.

APPENDIX-A

TABLE NO. A.4

COMPUTED PROFILES OF AMMONIA MOLE PERCENT AND TEMPERATURE IN THE BED FOR DIFFERENT INERTS CONCENTRATIONS

Set No.4(A), Inerts concentration=10.68 Set No.4(B), Inerts Conc. =13.95

Bed Pt. No.	% Of Total Catalyst Volume	Bed Temp. (K)	NH3 Mole % Actual	NH3 Mole % At Max. Rate	NH3 Mole % At Equilibrium	Bed Temp. (K)	NH3 Mole % Actual	NH3 Mole % At Max. Rate	NH3 Mole % At Equilibrium	
1	2	3	4	5	6	7	8	9	10	
1	0.0	629.9	1.613	30.779	35.775	645.6	1.613	25.620	30.306	
11	2.3	640.7	2.268	28.466	33.483	659.2	2.463	23.076	27.720	
21	4.5	652.2	2.974	26.109	31.104	673.6	3.380	20.548	25.097	
31	6.8	664.9	3.767	23.640	28.565	689.7	4.420	17.978	22.356	
41	9.1	679.4	4.683	21.018	25.822	707.9	5.619	15.365	19.507	
51	11.4	696.2	5.760	18.257	22.859	728.1	6.986	12.828	16.662	
56	12.5	705.5	6.370	16.838	21.309	738.7	7.710	11.661	15.315	
61	13.6	715.5	7.029	15.423	19.742	748.9	8.425	10.614	14.096	
66	14.8	726.0	7.734	14.037	18.179	758.3	9.086	9.736	13.051	
71	15.9	736.9	8.470	12.728	16.673	766.1	9.644	9.055	12.234	
76	17.0	747.6	9.204	11.539	15.291	771.9	10.066	8.573	11.651	
81	18.2	757.5	9.889	10.534	14.105	775.9	10.352	8.265	11.274	
86	19.3	765.7	10.467	9.764	13.179	778.3	10.530	8.076	11.043	
91	20.5	771.8	10.902	9.221	12.520	779.7	10.633	7.969	10.915	
95	21.4	775.2	11.143	8.933	12.171	780.4	10.682	7.921	10.853	
98	22.0	777.0	11.272	8.785	11.992	780.7	10.706	7.896	10.823	
101	22.7	778.3	11.365	8.678	11.863	780.9	10.722	7.882	10.802	
1	22.7	665.7	7.983	23.488	28.409	670.7	7.642	21.033	25.600	
11	25.9	673.0	8.471	22.147	27.015	678.0	8.139	19.822	24.328	
21	29.1	680.9	9.009	20.747	25.535	685.8	8.681	18.570	22.994	
31	32.3	689.5	9.600	19.298	23.990	694.1	9.266	17.293	21.627	
41	35.5	698.8	10.245	17.824	22.392	703.0	9.893	16.021	20.235	
51	38.6	708.7	10.937	16.357	20.778	712.1	10.549	14.787	18.863	
56	40.2	713.8	11.295	15.642	19.984	716.7	10.881	14.193	18.204	
61	41.8	718.8	11.655	14.954	19.212	721.3	11.210	13.633	17.568	
66	43.4	723.8	12.013	14.302	18.475	725.7	11.532	13.104	16.968	
71	45.0	728.7	12.361	13.690	17.782	729.8	11.839	12.617	16.414	
76	46.6	733.2	12.691	13.141	17.145	733.7	12.127	12.176	15.909	
81	48.2	737.4	12.994	12.651	16.585	737.3	12.390	11.791	15.464	
86	49.8	741.1	13.265	12.226	16.094	740.4	12.622	11.459	15.078	
91	51.4	744.3	13.499	11.879	15.683	743.1	12.823	11.181	14.754	
95	52.6	746.4	13.658	11.642	15.412	744.9	12.960	10.997	14.536	
98	53.6	747.8	13.761	11.497	15.240	746.1	13.050	10.874	14.394	
101	54.5	749.0	13.851	11.368	15.085	747.1	13.129	10.772	14.275	
1	54.5	675.1	10.730	21.743	26.585	678.4	10.377	19.715	24.213	
11	59.1	681.9	11.206	20.552	25.325	684.9	10.841	18.676	23.107	
21	63.6	689.1	11.717	19.341	24.030	691.7	11.331	17.632	21.984	
31	68.2	696.7	12.261	18.118	22.710	698.7	11.844	16.594	20.857	
41	72.7	704.6	12.829	16.920	21.398	705.8	12.368	15.592	19.756	
51	77.3	712.5	13.403	15.787	20.139	712.8	12.887	14.656	18.723	
56	79.5	716.3	13.684	15.257	19.550	716.2	13.137	14.226	18.238	
61	81.8	720.0	13.956	14.760	18.992	719.4	13.377	13.826	17.787	
66	84.1	723.5	14.214	14.307	18.481	722.3	13.604	13.456	17.373	
71	86.4	726.7	14.454	13.897	18.010	725.1	13.813	13.125	16.997	
76	88.6	729.6	14.672	13.534	17.597	727.6	14.004	12.828	16.657	
81	90.9	732.2	14.865	13.218	17.234	729.8	14.174	12.570	16.363	
86	93.2	734.4	15.033	12.948	16.932	731.8	14.323	12.349	16.105	
91	95.5	736.3	15.174	12.728	16.673	733.5	14.450	12.161	15.893	
95	97.3	737.6	15.270	12.580	16.503	734.6	14.537	12.035	15.748	
98	98.6	738.4	15.333	12.482	16.392	735.3	14.596	11.952	15.648	
101	100.0	739.1	15.387	12.400	16.292	736.0	14.647	11.879	15.564	
Total Pressure Drop, atm					2.19	2.29				
Cold Shot Distribution:										
First Bed					0.145	0.089				
Second Bed					0.250	0.249				
Third Bed					0.234	0.220				
Total					0.629	0.558				

TABLE NO.A.5

CENTRE PROFILES OF AMBODIA HOLE PERCENT AND TEMPERATURE IN THE BED FOR DIFFERENT CATALYST ACTIVITIES

Set No.5(A), Catalyst Activity = 0.7						Set No.5(B), Catalyst Activity=0.8					Set No.5(C), Catalyst Activity=0.9			
Bed Total Catal-1st Volume	Bed Temp. (K)	NH3 Actual	NH3 Mole At. Max. Rate	% At Equil-ibrium	Bed Temp. (K)	NH3 Actual	NH3 Mole At. Max. Rate	% At Equil-ibrium	Bed Temp. (K)	NH3 Actual	NH3 Mole At. Max. Rate	% At Equil-ibrium		
2	3	4	5	6	7	8	9	10	11	12	13	14		
0.0	656.5	1.613	24.107	28.867	647.2	1.613	25.910	30.704	643.9	1.613	26.567	31.369		
2.3	667.2	2.278	22.155	26.851	658.1	2.290	23.829	28.588	655.7	2.351	24.270	29.042		
4.5	678.2	2.970	20.256	24.864	669.4	3.003	21.779	26.459	668.2	3.137	21.991	26.689		
6.8	689.9	3.713	18.374	22.856	681.6	3.781	19.705	24.283	681.9	4.011	19.662	24.237		
9.1	702.4	4.528	16.494	20.813	695.0	4.648	17.601	22.016	697.1	5.003	17.282	21.673		
11.4	716.1	5.424	14.633	18.747	709.8	5.621	15.480	19.693	714.2	6.137	14.888	19.033		
13.6	730.7	6.401	12.836	16.711	717.7	6.150	14.434	18.522	723.4	7.757	13.717	17.718		
15.9	745.7	7.427	11.188	14.805	725.9	6.704	13.407	17.369	732.9	9.403	12.590	16.431		
18.2	760.1	8.511	9.685	12.940	734.3	7.277	12.425	16.243	742.4	11.060	11.543	15.222		
20.5	774.7	9.656	8.256	11.127	742.8	7.859	11.507	15.172	751.6	12.701	10.609	14.126		
22.7	789.9	10.868	6.986	9.299	751.0	8.430	10.665	14.192	760.0	14.292	9.821	13.186		
25.0	805.7	12.147	5.822	7.591	758.6	9.068	9.938	13.326	767.0	15.795	9.195	12.436		
27.3	822.1	13.494	4.756	6.024	765.4	9.746	9.336	12.601	772.5	17.186	8.740	11.885		
29.6	839.1	14.911	3.784	4.527	771.0	10.464	8.865	12.033	776.3	18.465	8.433	11.507		
31.9	856.6	16.401	2.917	3.156	774.5	11.221	8.576	11.680	778.4	19.617	8.269	11.303		
34.2	874.6	17.956	2.159	1.927	776.6	12.019	8.408	11.475	779.5	20.699	8.181	11.199		
36.5	893.1	19.579	1.519	1.134	778.3	12.847	8.274	11.313	780.4	21.761	8.117	11.121		
38.8	912.1	21.263	0.986	0.628	678.6	7.671	20.195	24.798	675.6	7.812	20.690	25.325		
41.1	931.6	23.009	0.538	0.334	685.4	8.140	19.075	23.610	683.0	8.314	19.476	24.036		
43.4	951.6	24.818	0.179	0.157	692.7	8.643	17.934	22.381	690.8	8.857	18.227	22.697		
45.7	972.1	26.694	0.000	0.000	699.4	9.181	16.780	21.127	699.2	9.443	16.964	21.331		
48.0	993.1	28.639	0.000	0.000	706.4	9.750	15.637	19.868	707.9	10.065	15.716	19.952		
50.3	1014.6	30.656	0.000	0.000	713.7	10.339	14.534	18.641	716.9	10.709	14.511	18.611		
52.6	1036.6	32.749	0.000	0.000	721.7	10.937	13.499	17.473	725.8	11.351	13.402	17.363		
54.9	1059.1	34.911	0.000	0.000	729.0	11.521	13.024	16.929	733.0	11.960	12.901	16.786		
57.2	1082.1	37.144	0.000	0.000	735.0	12.081	12.579	16.419	739.0	12.533	12.441	16.260		
59.5	1105.6	39.449	0.000	0.000	741.8	12.613	12.170	15.948	744.0	13.065	12.003	15.784		
61.8	1129.6	41.826	0.000	0.000	748.8	13.101	11.801	15.519	748.1	13.557	11.669	15.362		
64.1	1154.1	44.277	0.000	0.000	755.4	13.548	11.475	15.139	751.1	14.009	11.360	15.005		
66.4	1179.1	46.794	0.000	0.000	761.5	13.959	11.194	14.810	753.5	14.426	11.100	14.699		
68.7	1204.6	49.379	0.000	0.000	767.5	14.337	10.996	14.578	755.3	14.800	10.929	14.500		
71.0	1230.6	52.024	0.000	0.000	773.4	14.682	10.867	14.429	756.7	15.123	10.815	14.368		
73.3	1257.1	54.729	0.000	0.000	779.1	15.000	10.753	14.291	757.6	15.394	10.722	14.253		
75.6	1284.1	57.494	0.000	0.000	784.6	15.291	10.649	14.167	758.1	15.620	10.644	14.144		
77.9	1311.6	60.319	0.000	0.000	789.9	15.556	10.554	14.054	758.4	15.802	10.574	14.040		
80.2	1339.6	63.194	0.000	0.000	795.0	15.797	10.468	13.951	758.4	15.941	10.513	13.941		
82.5	1368.1	66.119	0.000	0.000	800.0	16.014	10.389	13.858	758.1	16.038	10.459	13.848		
84.8	1397.1	69.094	0.000	0.000	804.8	16.207	10.317	13.774	757.6	16.093	10.411	13.761		
87.1	1426.6	72.119	0.000	0.000	809.4	16.377	10.251	13.699	756.9	16.116	10.368	13.680		
89.4	1456.6	75.194	0.000	0.000	813.7	16.524	10.191	13.632	756.0	16.106	10.329	13.614		
91.7	1487.1	78.319	0.000	0.000	817.8	16.648	10.136	13.572	754.9	16.063	10.294	13.561		
94.0	1518.1	81.494	0.000	0.000	821.6	16.749	10.085	13.519	753.6	16.000	10.262	13.511		
96.3	1549.6	84.719	0.000	0.000	825.2	16.827	10.038	13.472	752.1	15.917	10.233	13.464		
98.6	1581.6	87.994	0.000	0.000	828.6	16.882	9.995	13.430	750.4	15.804	10.207	13.420		
100.0	1614.1	91.319	0.000	0.000	831.8	16.914	9.957	13.392	748.5	15.661	10.183	13.379		
Total Pressure Drop, atm					2.56					2.30				
1st Shot Distribution:														
1st Bed					0.030					0.080				
2nd Bed					0.193					0.232				
3rd Bed					0.192					0.203				
Total					0.415					0.515				

APPENDIX-A

TABLE NO. A.6

COMPUTED PROFILES OF AMMONIA MOLE PERCENT AND TEMPERATURE IN THE BED FOR DIFFERENT CATALYST VOLUMES

Set No. 6(A), Catalyst volume = 61.0						Set No. 6(B), Catalyst volume=75.0				
Bed Pt. No.	% of Total Catalyst Volume	Bed Temp. (K)	NH3 Mole % Actual	At Max. Rate	% At Equilibrium	Bed Temp. (K)	NH3 Mole % Actual	At Max. Rate	% At Equilibrium	
1	2	3	4	5	6	7	8	9	10	
1	0.0	644.3	1.613	26.473	31.274	636.1	1.613	28.130	32.934	
11	2.3	656.3	2.355	24.166	28.930	649.1	2.422	25.537	30.324	
21	4.5	668.8	3.146	21.879	26.567	663.1	3.304	22.907	27.635	
31	6.8	682.6	4.026	19.548	24.114	678.9	4.316	20.159	24.759	
41	9.1	697.9	5.025	17.160	21.542	697.1	5.506	17.293	21.685	
51	11.4	715.1	6.166	14.766	18.902	718.0	6.908	14.401	18.487	
56	12.5	724.3	6.788	13.602	17.583	729.3	7.680	13.013	16.912	
61	13.6	733.8	7.436	12.484	16.305	740.7	8.471	11.732	15.435	
66	14.8	743.4	8.094	11.444	15.105	751.5	9.233	10.619	14.132	
71	15.9	752.5	8.733	10.521	14.017	760.9	9.903	9.735	13.083	
76	17.0	760.8	9.317	9.745	13.094	768.1	10.422	9.105	12.324	
81	18.2	767.7	9.812	9.135	12.361	773.0	10.774	8.700	11.832	
86	19.3	773.0	10.193	8.695	11.827	775.9	10.988	8.467	11.549	
91	20.5	776.8	10.464	8.398	11.465	777.5	11.105	8.339	11.392	
95	21.4	778.8	10.611	8.240	11.266	778.3	11.158	8.284	11.324	
98	22.0	779.9	10.690	8.156	11.168	778.6	11.183	8.255	11.293	
101	22.7	780.7	10.749	8.092	11.090	778.8	11.199	8.240	11.272	
1	22.7	675.8	7.802	20.672	25.299	665.0	7.835	22.552	27.266	
11	25.9	683.1	8.303	19.452	24.010	672.5	8.343	21.238	25.896	
21	29.1	690.9	8.846	18.210	22.678	680.5	8.902	19.874	24.458	
31	32.3	699.3	9.431	16.953	21.312	689.3	9.515	18.463	22.951	
41	35.5	708.0	10.052	15.705	19.940	698.7	10.180	17.033	21.405	
51	38.6	717.0	10.695	14.500	18.599	708.6	10.887	15.632	19.862	
56	40.2	721.5	11.018	13.935	17.963	713.6	11.249	14.955	19.110	
61	41.8	725.9	11.336	13.396	17.351	718.5	11.611	14.308	18.380	
66	43.4	730.1	11.644	12.895	16.780	723.4	11.965	13.700	17.700	
71	45.0	734.1	11.937	12.436	16.254	728.0	12.305	13.142	17.062	
76	46.6	737.8	12.209	12.022	15.778	732.3	12.622	12.644	16.494	
81	48.2	741.1	12.456	11.664	15.357	736.1	12.909	12.207	15.987	
86	49.8	744.1	12.673	11.355	14.999	739.5	13.160	11.837	15.564	
91	51.4	746.6	12.861	11.095	14.694	742.3	13.373	11.538	15.211	
95	52.6	748.3	12.988	10.924	14.489	744.2	13.515	11.340	14.977	
98	53.6	749.4	13.071	10.810	14.357	745.4	13.606	11.214	14.832	
101	54.5	750.4	13.145	10.712	14.242	746.4	13.684	11.105	14.705	
1	54.5	682.9	10.463	19.464	24.017	673.1	10.597	21.108	25.756	
11	59.1	689.4	10.931	18.416	22.900	679.7	11.072	19.983	24.569	
21	63.6	696.3	11.424	17.369	21.766	686.7	11.580	18.830	23.347	
31	68.2	703.3	11.937	16.334	20.641	694.1	12.119	17.683	22.104	
41	72.7	710.4	12.457	15.351	19.548	701.7	12.679	16.551	20.874	
51	77.3	717.3	12.967	14.440	18.528	709.3	13.242	15.486	19.699	
56	79.5	720.5	13.211	14.022	18.063	713.0	13.517	14.988	19.146	
61	81.8	723.6	13.443	13.635	17.624	716.5	13.782	14.522	18.623	
66	84.1	726.5	13.661	13.283	17.224	719.8	14.034	14.099	18.145	
71	86.4	729.2	13.861	12.970	16.860	722.9	14.268	13.711	17.706	
76	88.6	731.6	14.042	12.686	16.539	725.7	14.480	13.369	17.316	
81	90.9	733.7	14.203	12.446	16.260	728.2	14.669	13.072	16.981	
86	93.2	735.5	14.343	12.239	16.021	730.3	14.833	12.820	16.688	
91	95.5	737.1	14.462	12.064	15.818	732.1	14.973	12.606	16.448	
95	97.3	738.1	14.544	11.943	15.682	733.4	15.068	12.462	16.283	
98	98.6	738.9	14.599	11.864	15.592	734.2	15.129	12.372	16.180	
101	100.0	739.5	14.646	11.795	15.514	734.9	15.184	12.292	16.084	

Total Pressure Drop, atm	2.17	2.37
Cold Shot Distribution:		
First Bed	0.096	0.120
Second Bed	0.239	0.253
Third Bed	0.214	0.235
Total	0.549	0.608

TABLE NO. A.7

COMPUTED PROFILES OF AMMONIA MOLE PERCENT AND TEMPERATURE IN THE BED  
FOR DIFFERENT OPERATING PRESSURES

set No. 7 (A), Operating pressure = 170.0 set No. 7 (B), Pressure = 210.0

Bed Pt. No.	% Of Total Catalyst Volume	Bed Temp. (K)	NH3 Mole % Actual	NH3 Mole % At Max. Rate	NH3 Mole % At Equilibrium	Bed Temp. (K)	NH3 Mole % Actual	NH3 Mole % At Max. Rate	NH3 Mole % At Equilibrium	
1	2	3	4	5	6	7	8	9	10	
1	0.0	639.7	1.613	25.810	30.574	629.8	1.613	30.934	35.722	
11	2.3	650.2	2.268	23.771	28.491	640.6	2.280	28.693	33.517	
21	4.5	661.1	2.960	21.754	26.399	652.1	2.996	26.412	31.238	
31	6.8	673.0	3.720	19.699	24.237	664.7	3.799	24.004	28.797	
41	9.1	686.1	4.570	17.601	21.985	679.1	4.723	21.455	26.157	
51	11.4	700.6	5.531	15.480	19.656	695.6	5.806	18.747	23.296	
56	12.5	708.5	6.056	14.423	18.475	704.8	6.418	17.357	21.791	
61	13.6	716.7	6.608	13.385	17.305	714.7	7.080	15.965	20.262	
66	14.8	725.1	7.183	12.388	16.158	725.1	7.788	14.589	18.735	
71	15.9	733.6	7.769	11.449	15.072	735.8	8.528	13.272	17.247	
76	17.0	741.9	8.347	10.593	14.066	746.5	9.275	12.064	15.863	
81	18.2	749.7	8.892	9.846	13.180	756.4	9.983	11.027	14.650	
86	19.3	756.5	9.376	9.235	12.446	765.0	10.596	10.203	13.678	
91	20.5	762.0	9.775	8.760	11.869	771.5	11.072	9.608	12.965	
95	21.4	765.5	10.026	8.477	11.522	775.3	11.347	9.286	12.574	
96	22.0	767.6	10.176	8.309	11.319	777.4	11.497	9.110	12.366	
101	22.7	769.3	10.295	8.181	11.162	778.9	11.607	8.985	12.213	
1	22.7	671.1	7.598	20.013	24.569	665.7	8.109	23.823	28.609	
11	25.9	677.7	8.055	18.908	23.392	672.9	8.600	22.533	27.279	
21	29.1	684.8	8.548	17.782	22.180	680.7	9.139	21.176	25.863	
31	32.3	692.4	9.076	16.637	20.936	689.1	9.731	19.771	24.380	
41	35.5	700.3	9.635	15.502	19.681	698.3	10.375	18.333	22.843	
51	38.6	708.5	10.218	14.401	18.451	707.9	11.067	16.895	21.288	
56	40.2	712.6	10.513	13.875	17.859	712.9	11.426	16.186	20.512	
61	41.8	716.7	10.806	13.369	17.282	717.9	11.789	15.502	19.759	
66	43.4	720.6	11.094	12.890	16.734	722.9	12.152	14.849	19.027	
71	45.0	724.4	11.372	12.446	16.226	727.7	12.506	14.236	18.339	
76	46.6	728.0	11.637	12.033	15.750	732.3	12.846	13.673	17.700	
81	48.2	731.4	11.883	11.664	15.323	736.6	13.164	13.164	17.125	
86	49.8	734.4	12.107	11.340	14.944	740.4	13.451	12.718	16.614	
91	51.4	737.1	12.307	11.058	14.611	743.7	13.703	12.345	16.180	
95	52.6	739.0	12.448	10.861	14.385	746.1	13.878	12.091	15.891	
98	53.6	740.3	12.542	10.732	14.231	747.6	13.992	11.927	15.699	
101	54.5	741.4	12.628	10.619	14.093	748.9	14.093	11.785	15.536	
1	54.5	680.3	10.250	18.469	22.919	676.3	10.946	21.904	26.621	
11	59.1	686.6	10.698	17.485	21.854	683.1	11.434	20.733	25.398	
21	63.6	693.1	11.168	16.511	20.788	690.4	11.958	19.542	24.140	
31	68.2	699.7	11.652	15.553	19.735	698.0	12.514	18.339	22.856	
41	72.7	706.4	12.140	14.650	18.724	705.9	13.093	17.166	21.579	
51	77.3	712.8	12.615	13.815	17.788	713.7	13.677	16.050	20.354	
56	79.5	715.8	12.840	13.434	17.357	717.5	13.963	15.525	19.777	
61	81.8	718.6	13.054	13.083	16.958	721.2	14.239	15.038	19.236	
66	84.1	721.3	13.255	12.767	16.591	724.6	14.500	14.594	18.735	
71	86.4	723.8	13.439	12.478	16.260	727.8	14.743	14.187	18.280	
76	88.6	726.0	13.606	12.223	15.970	730.7	14.964	13.831	17.875	
81	90.9	727.9	13.754	12.001	15.711	733.2	15.160	13.516	17.525	
86	93.2	729.6	13.883	11.811	15.491	735.4	15.330	13.256	17.224	
91	95.5	731.1	13.994	11.648	15.301	737.3	15.474	13.035	16.976	
95	97.3	732.1	14.071	11.538	15.172	738.6	15.572	12.884	16.803	
98	98.6	732.7	14.121	11.465	15.088	739.4	15.635	12.793	16.694	
101	100.0	733.3	14.167	11.402	15.016	740.1	15.691	12.708	16.602	
Total Pressure Drop, atm					2.34	2.21				
Cold Shot Distribution:										
First Bed					0.089	0.146				
Second Bed					0.235	0.253				
Third Bed					0.199	0.231				
Total					0.523	0.630				

## RS APPENDIX-B

```

00100 C  OM START      PART 1 OF THE MAIN PROGRAM FOR SUMULATION OF AMMONIA SYNT
00200 C      MULTIBED QUENCH TYPE HIGH CAPACITY REACTOR
00300 C      INPUT STATEMENT PROGRAM
00400      DIMENSION PF(50),TF(50),F11(50),F22(50),F33(50),F44(50),
00500      1F55(50),FD22(50),FD33(50),FD44(50),Z11(50),Z22(50),Z33(50),
00600      2AZ(210,4),AP(210,4),AX(210,4),AT(210,4),AXRMNL(210,4),APATDL(100),
00700      2AZPL(210,4),APL(210,4),ATL(210,4),ANXL(210,4),ATHL(210,4),
00800      2AXENL(210,4),AXEL(210,4),ACXL(210,4),ACTL(210,4),ACTHL(210,4),
00900      3ATH(210,4),ACX(210,4),ACT(210,4),ACTH(210,4),ATH12(800)
01000      4,ATEM(100),ADEL(100),ATEP(100),ATEMP(100),ADET(100),FAIPL(17,20)
01100      5,ANX(210,4),AZP(210,4),M12(20),XLH(8),YLH(8),ADELT(800),APATD(100)
01200      6,VFT(50),FC1(50),FC2(50),FC3(50),FC4(50),FC5(50),FC5N(50),
01300      7VCAT(50),DBED2(50),DBED3(50),HLL(50),UAR(50),UAH(50),FF1(50),
01400      8PFN(20),TFN(20),VFTN(20),FC1N(20),FC2N(20),FC3N(20),FC4N(20),
01500      8AXMAX(8),ATMAX(8),ATHMAX(8),ALPS8(8),SINTL(210,4),XLPX(20,20),
01600      8QR1AV(210,4),WRXN(210,4),WRXNS(210,4),RINTL(210,4),OBLPF(20),
01700      9FD22N(20),DBED3N(20),HLLN(20),UARN(20),UAHN(20),RATIGN(50),
01800      AFF1N(20),RATIO(50),AGXLP(2,50),LPAQX(50),
01900      CFD33N(20),FD44N(20),VCATN(20),DBED2N(20),EFZIB(210,4)
02000      1,QR1B(210,4),EFZIA(8),ALZP(210,4),
02100      DAXEN(210,4),AXRMN(210,4),XEN(80,20),XRMN(80,20),AXE(210,4),
02200      EAXRM(210,4),PDRPF(8),
02300      FOBJLPN(50),OBJF(50),AQX(50,20),AQX1(20,20),NLEV(20)
02400      1,TA(15,4,5),AMMD(12),OBLPN(12),NBPTS(4,5),MLPD(15,4,5),
02500      1ATPL2(20,50),OBJF2(50),ANH3L(50),NOBJLP(20),
02600      1OBJF82(50),OBJF8(50),OBJF92(50),OBJF9(50),
02700      1AQX8(50,20),AGX9(50,20),
02800      1AZ7PL(8,50),AZ8PL(3,50),AZ9PL(7,50)
02900      1,STLP(11,50),SALP(11,50),STLP2(3,50),SALP2(3,50),
03000      1AZ11PL(30,50),AZ12PL(30,50),AZ14PL(17,50),AZ15PL(7,50),
03100      1AZ2PL(11,50),AZ3PL(11,50),AZ4PL(8,50),AZ5PL(8,50),
03200      1AZ6PL(8,50),FD55N(20),FD55(50),
03300      1OBJF3(50),OBJF4(50),OBJF5(50),
03400      1XLPX1(20,20),XLPX2(20,20),OBLPF1(20),OBLPF2(20),
03500      1N1DLPT(12),LPCBJN(12),APDRPL(12),APDRLP(50)
03600 C      8AXE2(4,310,4),AXRM2(4,310,4),
03700      COMMON/CB1/F1,F2,F3,F4,F5,LQQ,ITYPE,PARA1,PARA2,PARA3

```

RS

## APPENDIX-B

03800 1, PARA4, IOP26, IOP29, FF  
 03900 1/CB2/AZ, AP, AX, AT, ATH, AXMAX  
 04000 1, ATMAX, ATHMAX, ALPS8, W11L2, QR1AV, AXE2, AXRM2  
 04100 1, WRXN, WRXNS, RINTL, SINTL, EFZI8, QR1B, EFZIA, PDROP, IOL1/CB3/  
 04200 1AFD1, AFD2, AFD3, AFD4, Z1, Z2, Z3, HL, XW, UV, C4, RUA, HUA, C5, C61, C62, M15, K7  
 04300 2, FI11, FI12, FI13, FI21, FI22, FI23, FI31, FI32, FI33, FI41, FI42, FI43, M01,  
 04400 3FI51, FI52, FI53, PH1, PH2, PB11, S2, S11, S12, FTF1, S112, S122, AR1, AR2,  
 04500 4AR3, AR4, AR5, Q11, Q21, Q31, Q41, Q51, Q12, Q22, Q32, Q42, Q52,  
 04600 4IEL2P, UARLP, K5, KL51, IOPT3, AFD0,  
 04700 5Q13, Q23, Q33, Q43, Q53, HA11, HA21, HA31, HA41, HA51, HA61, HA71, HA12, M16,  
 04800 6HA22, HA32, HA42, HA52, HA62, HA72, HA13, HA23, HA33, HA43, HA53, HA63, K8,  
 04900 7HA73, HA14, HA24, HA34, HA44, HA54, HA64, HA74, NZ1, NZ2, NZ3, NZ4, MZ1, MZ2,  
 05000 8MZ3, MZ4, HAA21, HAA22, HAA23, HAA24, AHA21, AHA22, AHA23, AHA24, BHA21,  
 05100 9BHA22, BHA23, BHA24, HAB21, HAB22, HAB23, HAB24, AHA31, AHA32, AHA33, AHA34  
 05200 A/CB4/ANX, ZTI, PAN, AZP/CB20/ACX, ACT, ACTH  
 05300 B/CB7/ICSIZE, IOPT1, EFFAH, EFFAL  
 05400 1/CB9/FFL, RHNL, XINCL, XINCL2, TOL81, PHYL, PNIL, PAML, DELE, DELM  
 05500 1, IOL8, M88, IOP11, IOL81  
 05600 1/CB6/AXE, AXRM, AXEN, AXRMN, M12/CB71/NVARI, FAIPL, ND7PL, IOL8P  
 05700 1/CB74/AQXLP, G1, G2, G3, G4, G5, G6, G7, G8, G9, G10, G11, G12, G13, G14,  
 05800 1G15, G16, G17, G18, G19, G20, G21, G22, G23, G24, G25, G26, G27,  
 05900 1G28, G29, G30, G31, G32, G33, G34, G35, G36, G37, FDLIM  
 06000 OPEN(UNIT=3, DEVICE='DSK', FILE='DAA8.OUT')  
 06100 OPEN(UNIT=1, DEVICE='DSK', FILE='DAA2.DAT')  
 06200 OPEN(UNIT=2, DEVICE='DSK', FILE='DA17.DAT')  
 06300 OPEN(UNIT=4, DEVICE='DSK', FILE='ADAA8.OUT')  
 06400 OPEN(UNIT=8, DEVICE='DSK', FILE='D17.DAT')  
 06500 OPEN(UNIT=11, DEVICE='DSK', FILE='LP3.DAT')  
 06600 OPEN(UNIT=12, DEVICE='DSK', FILE='LPMANS.OUT')  
 06700 READ (1, \*)UARLP, IEL2P, IOL8P, ITYP11, NOBLP1, ITYPE, ITYPE8, WTFN,  
 06800 1W11, W11LI, W11LP, W11HL, PARA1, PARA2  
 06900 1, PARA3, PARA4, IOP26, IOP29, IOP201,  
 07000 1CSP11, CSP12, CSP1F, CSP22, IOPL8,  
 07100 1XINCL, XINCL2, TOL81, IOL8, IOL81, IOLP8, M88,  
 07200 1IOL1, IOL2, CSP33, C3, C2, C4, C51, C611, C621, EFFAH, EFFAL,  
 07300 1VW, IHH1, IHH2, IHH3, IHH4, C71, C72, C73, C74, KJ81,  
 07400 2M5, M81, M82, IJ1, IJ2, IJ3, IJ4, J5,



RS

## APPENDIX-B

```

07500      2K5L,M15,M16,M161,M162,K7,K8,FLPF,IOP11,
07600      3IOP12,ICSIZE,IOPT1,IOPT2,NDPTS,ND2PL,ND3PL,ND4PL,NDLPS,
07700      3NLPCSD,FACT,IOPT3,NVARI
07800      3,AC2,AIP5,TOL8,IOPT4,FDLIM,
07900      4IOPT5,IOPT8,XV,TV,THV,NXAXIS,NYAXIS,SPY1,SPX1,SPX2,HGT,ANGL,NUM
08000      5,(PFN(I),TFN(I),VFTN(I),RATION(I),FC3N(I),FC4N(I),FC5N(I),FD22N(I)
08100      6,FD33N(I),FD44N(I),FD55N(I),VCATN(I),DBED2N(I),DBED3N(I),HLLN(I)
08200      7,UARN(I),UAHN(I),FF1N(I),OBJLPN(I),NOBJLP(I)
08300      7,N1DLPT(I),LPCBJN(I),OBLPN(I),I=1,M5),
08400      8(XLH(I),I=1,NXAXIS),(YLH(I),I=1,NYAXIS),(NLEV(J),J=1,17)
08500      8,((FAIPL(I,J),J=1,NVARI),I=1,12),((AQXLP(I,J),I=1,2),J=1,NVARI)
08600      READ(2,*)((AQX1(I,J),I=1,NLEV(J)),J=1,17)
08700      KL511=K5L-1;KL51=KL511;K5=K5L
08800      READ(11,*)((NBPTS(K1,J),(TA(I,K1,J),NLPD(I,K1,J),I=1,NBPTS(K1,J)
08900      1,K1=1,K5),AMMD(J),APDRPL(J),J=1,M5)
09000      PRINT 8902
09100      IF(ITYPE.NE.2)GO TO 8903
09200      TYPE 8902
09300 8902   FORMAT(2X,'((NBPTS(K1,J),(TA(I,K1,J),NLPD(I,K1,J),I=1,NBPTS(K1,J)
09400      1,K1=1,K5),AMMD(J),APDRPL(J),J=1,M5)')
09500 8903   PRINT *,((NBPTS(K1,J),(TA(I,K1,J),NLPD(I,K1,J),I=1,NBPTS(K1,J))
09600      1,K1=1,K5),AMMD(J),APDRPL(J),J=1,M5)
09700      IF(ITYPE.NE.2)GO TO 8900
09800      TYPE *,((NBPTS(K1,J),(TA(I,K1,J),NLPD(I,K1,J),I=1,NBPTS(K1,J))
09900      1,K1=1,K5),AMMD(J),APDRPL(J),J=1,M5)
10000 8900   CONTINUE
10100      PRINT 791
10200      IF(ITYPE.NE.2)GO TO 650
10300      TYPE 791
10400 791    FORMAT(2X,'DATA REQUIRED: '//2X,'UARLP,IEL2P,IOL8P,ITYP11,
10500      1NOBLP1,ITYPE,ITYPE8,
10600      1WTFN,W11,W11LI,W11LP,W11HL
10700      1,PARA1,PARA2,PARA3,PARA4,IOP26,IOP29,IOP201,
10800      1CSP11,CSP12,CSP1F,CSP22,IOPL8,
10900      1XINCL,XINCL2,TOL81,IOL8,IOL81,IOLP8,M88,
11000      1IOL1,IOL2,CSP33,C3,C2,C4,C51,C611,C621,EFFAH,EFFAL,
11100      1VW,IHH1,IHH2,IHH3,IHH4,C71,C72,C73,C74,KJ81,

```

RS

## APPENDIX-B

```

11200 2M5,M81,M82,IJ1,IJ2,IJ3,IJ4,J5,
11300 2K5L,M15,M16,M161,M162,K7,K8,FLPF,IOP11,
11400 3IOP12,ICSIZE,IOPT1,IOPT2,NDPTS,ND2PL,ND3PL,ND4PL,NDLPS,
11500 3NLPCSD,FACT,IOPT3,NVARI
11600 3,AC2,AIP5,TOL8,IOPT4,FDLIM,
11700 4IOPT5,IOPT8,XV,TV,THV,NXAXIS,NYAXIS,SPY1,
11800 1SPX1,SPX2,HGT,ANGL,NUMBP
11900 5,(PFN(I),TFN(I),VFTN(I),RATION(I),FC3N(I),FC4N(I),FC5N(I),FD22N(I)
12000 6,FD33N(I),FD44N(I),FD55N(I),VCATN(I),DBED2N(I),DBED3N(I),HLLN(I)
12100 7,UARN(I),UAHN(I),FF1N(I),OBJLPN(I),NOBJLP(I)
12200 1,N1DLPT(I),LPCBJN(I),OBLPN(I),I=1,M5),
12300 8(XLH(I),I=1,NXAXIS),(YLH(I),I=1,NYAXIS),(NLEV(J),J=1,17)
12400 8,((FAIPL(I,J),J=1,NVARI),I=1,12),((AQXLP(I,J),I=1,2),J=1,NVARI)
12500 8,((AQX1(I,J),I=1,NLEV(J)),J=1,17)
12600 8,PARA1,PARA2,PARA3,PARA4,IOP26,IOP29,IOP201
12700 8,IHH1,IHH2,IHH3,IHH4,W11,W11L,W11H,J5,M81,M15,M16,M161,
12800 8K7,K8,C71,C72,C73,C74,FF,
12900 2UV,C2,IOPT2,ICSIZE,IOPT3,IOPT8,IOPT1,IOPT4,NUMBP'//
13000 22X,'DATA SUPPLIED: '/')
13100 650 PRINT *,UARLP,IEL2P,IOL8P,ITYP11,NOBLP1,ITYPE,ITYPE8,
13200 1WTFN,W11,W11LI,
13300 1W11LP,W11HL,PARA1,PARA2,PARA3,PARA4,ICP26,IOP29,IOP201
13400 1,CSP11,CSP12,CSP1F,CSP22,IOPL8,
13500 1XINCL,XINCL2,TOL81,IOL8,IOL81,IOLP8,M88,
13600 1IOL1,IOL2,CSP33,C3,C2,C4,C51,C611,C621,EFFAH,EFFAL,
13700 1VW,IHH1,IHH2,IHH3,IHH4,C71,C72,C73,C74,KJ81,
13800 2M5,M81,M82,IJ1,IJ2,IJ3,IJ4,J5,
13900 2K5L,M15,M16,M161,M162,K7,K8,FLPF,IOP11,
14000 3IOP12,ICSIZE,IOPT1,IOPT2,NDPTS,ND2PL,ND3PL,ND4PL,NDLPS,
14100 3NLPCSD,FACT,IOPT3,NVARI
14200 3,AC2,AIP5,TOL8,IOPT4,FDLIM,
14300 4IOPT5,IOPT8,XV,TV,THV,NXAXIS,NYAXIS,SPY1,SPX1,SPX2,HGT,ANGL,NUM
14400 5,(PFN(I),TFN(I),VFTN(I),RATION(I),FC3N(I),FC4N(I),FC5N(I),FD22N(I)
14500 6,FD33N(I),FD44N(I),FD55N(I),VCATN(I),DBED2N(I),DBED3N(I),HLLN(I)
14600 7,UARN(I),UAHN(I),FF1N(I),OBJLPN(I),NOBJLP(I)
14700 7,N1DLPT(I),LPCBJN(I),OBLPN(I),I=1,M5),
14800 8(XLH(I),I=1,NXAXIS),(YLH(I),I=1,NYAXIS),(NLEV(J),J=1,17)

```

RS

## APPENDIX-B

```

14900      8,((FAIPL(I,J),J=1,NVARI),I=1,12),((AQXLP(I,J),I=1,2),J=1,NVARI)
15000      8,((AQX1(I,J),I=1,NLEV(J)),J=1,17)
15100      IF(ITYPE.NE.2)GO TO 656
15200      TYPE *,UARLP,IEL2P,ICL8P,ITYP11,NOBLP1,ITYPE,ITYPE8,WTFN,W11,
15300      1W11LI,W11LP,W11HL,PARA1,PARA2,PARA3,PARA4,IOP26,IOP29,IOP201
15400      1,CSP11,CSP12,CSP1F,CSP22,IOPL8,
15500      1XINCL,XINCL2,TOL81,IOL8,IOL81,IOLP8,M88,
15600      1IOL1,IOL2,CSP33,C3,C2,C4,C51,C611,C621,EFFAH,EFFAL,
15700      1VW,IHH1,IHH2,IHH3,IHH4,C71,C72,C73,C74,KJ81,
15800      2M5,M81,M82,IJ1,IJ2,IJ3,IJ4,J5,
15900      2K5L,M15,M16,M161,M162,K7,K8,FLPF,IOP11,
16000      3IOP12,ICSIZE,IOPT1,IOPT2,NDPTS,ND2PL,ND3PL,ND4PL,NDLPS,
16100      3NLPCSD,FACT,IOPT3,NVARI
16200      3,AC2,AIP5,TOL8,IOPT4,FDLIM,
16300      4IOPT5,IOPT8,XV,TV,THV,NXAXIS,NYAXIS,SPY1,SPX1,SPX2,HGT,ANGL,NUM
16400      5,(PFN(I),TFN(I),VFTN(I),RATION(I),FC3N(I),FC4N(I),FC5N(I),FD22N(I)
16500      6,FD33N(I),FD44N(I),FD55N(I),VCATN(I),DBED2N(I),DBED3N(I),HLLN(I)
16600      7,UARN(I),UAHN(I),FF1N(I),OBJLPN(I),NOBJLP(I)
16700      7,M1DLPT(I),LPBJN(I),OBLPN(I),I=1,M5),
16800      8(XLH(I),I=1,NXAXIS),(YLH(I),I=1,NYAXIS),(NLEV(J),J=1,17)
16900      8,((FAIPL(I,J),J=1,NVARI),I=1,12),((AQXLP(I,J),I=1,2),J=1,NVARI)
17000      8,((AQX1(I,J),I=1,NLEV(J)),J=1,17)
17100 656      CONTINUE
17200 C      SEE READ STATEMENT FOR DATA BEFORE OUTPUT STATEMENTS PROGRAM AFTER
17300 C      STATEMENT NO.701 IN THE MAIN PROGRAM
17400 C      PART 2 OF THE MAIN PROGRAM FOR SIMULATION OF AMMONIA SYNTHESIS REA
17500 C      : INTERNAL PREHEATER OUTLET STREAM TEMPERATURES PREDICTION USING T
17600 C      AND ERROR TECHNIQUE BY MATCHING CALCULATED FEED TEMPERATURES WITH
17700 C      FEED TEMPERATURE
17800      GO TO 404
17900 405 MJK1=1;LPS=1;XVI=1.0/XV;TVI=1.0/TV;THVI=1.0/THV
18000      ISIGPL=1;ISIPL1=1;ISIPL2=1;ND7PL=1
18100      ILPS2=1;MLPK1=0;M1LP=1;M8LP=1;NOBLP=0;NV1LP=0;NV2LP=0
18200      ISM=1 ; MM1=1 ; IM=1 ; IOPT5=1;M=1;LQQ=1;NVLP1=0;KL51=K5-1
18300      G2=VFTN(1);G4=RATION(1);G6=FC3N(1);G8=FC4N(1);G10=FC5N(1)
18400      G12=FD22N(1);G14=FD33N(1);G16=FD44N(1);G18=PFN(1);G20=TFN(1)
18500      G22=VCATN(1);G24=DBED2N(1);G26=DBED3N(1);G28=HLLN(1);G30=UARN(1)

```

RS

## APPENDIX-B

```

18600      G32=UAHN(1);G34=FD55N(1);G35=PARA1;G36=PARA2;G37=PARA3
18700      SSE=0.0;SSE1=0.0;SSE2=0.0;SSE3=0.0;SSE4=0.0;SSE5=0.0
18800      SSE6=0.0;SSE7=0.0;SSE8=0.0;NDPTS=NLPCSD;ABCD2=-100.0
18900      IF(IOL2.EQ.1)NDPTS=N1DLPT(MJK1)
19000      DO 872 J=1,4
19100      DO 872 I=1,310
19200      AZ(I,J)=0.0;AP(I,J)=0.0;AX(I,J)=0.0;ANX(I,J)=0.0
19300      AT(I,J)=0.0;ATH(I,J)=0.0;AZP(I,J)=0.0
19400 872   CONTINUE
19500      IF(IOL2.NE.1)GO TO 205
19600      IOPT2=1;ITYP11=1
19700      GO TO 7224
19800      205 CONTINUE
19900      IF(IOL2.EQ.1)GO TO 7224
20000      IF(NOBJLP(MJK1)-1)7210,7224,7227
20100 7227  ITYPE8=2;IOPT2=2
20200      IF(M1LP.EQ.1)GO TO 7224
20300      IF(NOBJLP(MJK1).EQ.11)GO TO 7212
20400      M1LP=M1LP-1
20500      GO TO 7211
20600 7210  CONTINUE
20700      GO TO 7224
20800 7211  NDPT1S=N1DLPT(MJK1)
20900      IF(M1LP.GE.ND3PL)GO TO 8712
21000      CALL PNEXT(NV1LP,NCBJLP(MJK1),M1LP,AQX8,ISIPL1)
21100      IF(NV1LP.GT.NVARI)GO TO 8755
21200      M3LP=2
21300      CALL PCONV(M1LP,M3LP,AQX8)
21400      IF(M1LP.LE.NDPT1S)GO TO 147
21500      CALL ACOMP(LPIK,AQX8,M1LP,NVARI)
21600      IF(LPIK.EQ.0)GO TO 147
21700      OBJF82(M1LP)=OBJF82(LPIK);OBJF5(M1LP)=OBJF5(LPIK)
21800      OBJF8(M1LP)=OBJF8(LPIK);LPIK=0
21900 C     CALL FUNOBJ(OBJF8,M1LP,LPOBJN(MJK1),PATD,SSE,SSE1,SSE2,SSE3,
22000 C     1SSE4,SSE5,SSE6,SSE7,SSE8)
22100 8755  CALL OPTIMA(OBJF8,M1LP,AQX8,AQX1,IOPT8,NVARI,AC2,NLEV,
22200      1NOPTM1,TOL8,NMAX11,NDPT1S,XLPX1,

```

RS

## APPENDIX-B

```
22300      1OBLPF1,NLN81,ALPC11,YLPN1,IOL8P)
22400      IF(NOPTM1.EQ.0)GO TO 8621
22500      GO TO 8714
22600 8712      NMAX11=M
22700 8711      CONTINUE
22800      NOPTM1=NMAX11;M1LP=1;ISIPL1=1;ND7PL=1
22900 8714      CONTINUE
23000      IF(NOBLP.NE.11)GO TO 701
23100 C      DO 8712 L=1,NVARI
23200 C      AQX9(M8LP,L)=AQX8(NOPTM1,L)
23300 C8712      CONTINUE
23400      OBJF9(M8LP)=OBJF5(NOPTM1);NV1LP=0
23500      IF(OBJF33.EQ.0.0)GO TO 694
23600      OBJF92(M8LP)=OBJF5(NOPTM1)*OBJF33
23700      GO TO 7226
23800 694      OBJF92(M8LP)=OBJF5(NOPTM1)
23900      GO TO 7226
24000 8621      NPT1S2=NDPT1S*NDLPS
24100      IF(M1LP.GE.ND3PL)GO TO 8711
24200      M3LP=2
24300      CALL PCONV(M1LP,M3LP,AQX8)
24400      CALL ACOMP(LPIK,AQX8,M1LP,NVARI)
24500      IF(LPIK.EQ.0)GO TO 147
24600      OBJF82(M1LP)=OBJF82(LPIK);OBJF5(M1LP)=OBJF5(LPIK)
24700      OBJF8(M1LP)=OBJF8(LPIK);LPIK=0
24800      GO TO 8755
24900 7212      CONTINUE
25000      NOBLP=NOBJLP(MJK1);M1LP=M1LP-1;NOBJLP(MJK1)=10
25100      GO TO 7211
25200 7226      NDP1S=3
25300      IF(IOL8P.EQ.1)NDP1S=2
25400      IF(M8LP.GE.ND4PL)GO TO 701
25500      CALL PNEXT(NV2LP,NOBLP,M8LP,AQX9,ISIPL2)
25600      DO 8422 L=1,NVARI
25700      AQX8(1,L)=AQX9(M8LP,L)
25800 8422      CONTINUE
25900      IF(NV2LP.GT.NVARI)GO TO 8255
```

## RS APPENDIX-B

```

26000      M3LP=2
26100      CALL PCONV(M8LP,M3LP,AQX9)
26200      CALL ACOMP(LPIK,AQX9,M8LP,NVARI)
26300      IF(LPIK.EQ.0)GO TO 147
26400      OBJF92(M8LP)=OBJF92(LPIK)
26500      OBJF9(M8LP)=OBJF9(LPIK);LPIK=0
26600 C     CALL FUNOBJ(OBJF9,M8LP,LPOBJN(MJK1),PATD,SSE,SSE1,SSE2,SSE3,
26700 C     1SSE4,SSE5,SSE6,SSE7,SSE8)
26800 8255  CALL OPTIMA(OBJF9,M8LP,AQX9,AQX1,IOPT8,NVARI,AC2,NLEV,
26900      1NOPTM2,TOL8,NMAX12,NDP1S,XLPX2,
27000      1OBLPF2,NLN82,ALPC12,YLFN2,IOL8P)
27100      IF(NOPTM2.NE.0)GO TO 701
27200      NPT1S2=NDP1S*NDLPS
27300      IF(M8LP.GE.ND4PL)GO TO 701
27400      DO 8423 L=1,NVARI
27500      AQX8(1,L)=AQX9(M8LP,L)
27600 8423  CONTINUE
27700      M3LP=2
27800      CALL PCONV(M8LP,M3LP,AQX9)
27900      CALL ACOMP(LPIK,AQX9,M8LP,NVARI)
28000      IF(LPIK.EQ.0)GO TO 147
28100      OBJF92(M8LP)=OBJF92(LPIK)
28200      OBJF9(M8LP)=OBJF9(LPIK);LPIK=0
28300      GO TO 8255
28400 7224  CONTINUE
28500      IF(OBJLPN(M).EQ.0.0)GO TO 575
28600      PATD=OBJLPN(M);APATD(MJK1)=PATD;PATD1=PATD;IM8=1
28700      MLPK1=MLPK1+1;OBJF(M)=PATD
28800      FC12=100.0-(FC3N(MJK1)+FC4N(MJK1)+FC5N(MJK1))
28900      LFC1N=100*FC12*RATION(MJK1)/(1+RATION(MJK1))+0.5
29000      FC1N(MJK1)=LFC1N*0.01;FC2N(MJK1)=FC12-FC1N(MJK1)
29100      GO TO 719
29200 575   CONTINUE
29300      IF(ITYPE8.NE.1)GO TO 890
29400      IF(ICSIZE.EQ.2)GO TO 170
29500      PRINT 173
29600      IF(ITYPE.NE.2)GO TO 196

```

```
29700      TYPE 173
29800 173   FORMAT(2X,'ACTUAL VALUE OF EFFECTIVENESS FACTOR CALCULATED AND I
29900      INCLUDED IN REACTION RATE CALCULATION '/')
30000      GO TO 196
30100 170   PRINT 182
30200      IF(ITYPE.NE.2)GO TO 196
30300      TYPE 182
30400 182   FORMAT(2X,'FOR THIS DATA SET CALCULATION IS BASED ON EFFECTIVENE
30500      1 FACTOR OF UNITY '/')
30600 196   IF(IOPT3.NE.1)GO TO 197
30700      PRINT 80
30800      IF(ITYPE.NE.2)GO TO 83
30900      TYPE 80
31000 80    FORMAT(2X,'RUNGE-KUTTA FOURTH ORDER NUMERICAL INTEGRATION TECHNI
31100      1 IS BEING USED '/')
31200      GO TO 83
31300 197   PRINT 84
31400      IF(ITYPE.NE.2)GO TO 83
31500      TYPE 84
31600 84    FORMAT(2X,'MILNE PREDICTOR-CORRECTOR NUMERICAL INTEGRATION TECHN
31700      1UE IS BEING USED '/')
31800 83    IF(IOPT2.EQ.1)GO TO 890
31900      IF(IOPT8-2)893,894,767
32000 893   PRINT 768
32100      IF(ITYPE.NE.2)GO TO 890
32200      TYPE 768
32300 768   FORMAT(2X,'FOR OPTIMISATION SEARCH IS AT ACTUAL VALUES OF VARIAB
32400      1S THAT ARE SLIGHTLY ROUNDED OFF '/')
32500      GO TO 890
32600 894   PRINT 773
32700      IF(ITYPE.NE.2)GO TO 890
32800      TYPE 773
32900 773   FORMAT(2X,'FOR OPTIMISATION SEARCH IS AT ROUNDED OFF VALUE OF TH
33000      1VARIABLES '/')
33100      GO TO 890
33200 767   PRINT 776
33300      IF(ITYPE.NE.2)GO TO 890
```

RS

## APPENDIX-B

```

33400      TYPE 776
33500 776   FORMAT(2X,'FOR OPTIMISATION SEARCH IS AT CERTAIN SPECIFIED VALUE
33600      1OF THE VARIABLES'/)
33700 890   CONTINUE
33800      IF(IOL2.EQ.1)GO TO 143
33900      IF(M1LP.NE.1)GO TO 147
34000      IF(M8LP.NE.1)GO TO 147
34100      IF(M.EQ.1) GO TO 143
34200      IF(IOPT2.EQ.2) GO TO 147
34300      IF(M.GT.NDPTS) GO TO 147
34400 143   F=FF1N(MJK1);PARA1=G35;PARA2=G36;PARA3=G37;FF=VFTN(MJK1)/FLPF
34500      FC12=100.0-(FC3N(MJK1)+FC4N(MJK1)+FC5N(MJK1))
34600      LFC1N=100*FC12*RATION(MJK1)/(1+RATION(MJK1))+0.5
34700      FC1N(MJK1)=LFC1N*0.01;FC2N(MJK1)=FC12-FC1N(MJK1)
34800      CALL FLOWR(F11(MJK1),F22(MJK1),F33(MJK1),F44(MJK1),F55(MJK1),
34900 1VFTN(MJK1),FC1N(MJK1),FC2N(MJK1),FC3N(MJK1),FC4N(MJK1),IOPT5)
35000      PHY=FC1N(MJK1);PNI=FC2N(MJK1);PAM=FC3N(MJK1)
35100      PME=FC4N(MJK1);PAR=FC5N(MJK1);RHN=RATION(MJK1)
35200      VCAT1=VCATN(MJK1)*1.0E6
35300      Z11(MJK1)=VCAT1/(1+DBED2N(MJK1)+DBED3N(MJK1))
35400      Z22(MJK1)=Z11(MJK1)*DBED2N(MJK1)
35500      Z33(MJK1)=VCAT1-(Z11(MJK1)+Z22(MJK1))
35600      H1=Z11(MJK1)/IHH1;H2=Z22(MJK1)/IHH2;H3=Z33(MJK1)/IHH3
35700      H4=HLLN(MJK1)*1.0E6/IHH4
35800      GO TO 146
35900 147   VET(M)=G1;RATIO(M)=G3;FC3(M)=G5;FC4(M)=G7;FC5(M)=G9
36000      FD22(M)=G11;FD33(M)=G13;FD44(M)=G15;PF(M)=G17
36100      TF(M)=G19;VCAT(M)=G21;DBED2(M)=G23;DBED3(M)=G25;HLL(M)=G27
36200      UAR(M)=G29;UAH(M)=G31;FD55(M)=G33;PARA1=G35;PARA2=G36
36300      PARA3=G37;FF1(M)=FF1N(MJK1)
36400      FC12=100.0-(FC3(M)+FC4(M)+FC5(M))
36500      LFC1=100*FC12*RATIO(M)/(1+RATIO(M))
36600      FC1(M)=LFC1*0.01;FC2(M)=FC12-FC1(M)
36700      CALL FLOWR(F11(M),F22(M),F33(M),F44(M),F55(M),VET(M),FC1(M),
36800 1FC2(M),FC3(M),FC4(M),IOPT5)
36900      PHY=FC1(M);PNI=FC2(M);PAM=FC3(M);PME=FC4(M)
37000      PAR=FC5(M);RHN=RATIO(M)

```



```
37100 VCAT1=VCAT(M)*1.0E6
37200 Z11(M)=VCAT1/(1+DBED2(M)+DBED3(M))
37300 Z22(M)=Z11(M)*DBED2(M)
37400 Z33(M)=VCAT1-(Z11(M)+Z22(M))
37500 H1=Z11(M)/IHH1;H2=Z22(M)/IHH2;H3=Z33(M)/IHH3
37600 H4=HLL(M)*1.0E6/IHH4
37700 146 IF(IOPT3.EQ.1) GO TO 215
37800 HA11=0.5*H1 ; HA21=0.0833333*H1 ; HA31=0.5*HA21 ; HA41=4.0*H1
37900 HA51=2.666667*H1 ; HA61=2.0*H1 ; HA71=0.333333*H1 ; HA12=0.5*H2
38000 HA13=0.5*H3 ; HA14=0.5*H4 ; HA22=0.0833333*H2
38100 HA23=0.0833333*H3 ; HA24=0.0833333*H4 ; HA32=0.5*HA22
38200 HA33=0.5*HA23;HA34=0.5*HA24 ;HA42=4.0*H2 ;HA43=4.0*H3
38300 HA44=4.0*H4;HA52=2.666667*H2;HA53=2.666667*H3;HA54=2.666667*H4
38400 HA62=2.0*H2;HA63=2.0*H3;HA64=2.0*H4;HA72=0.333333*H2
38500 HA73=0.333333*H3;HA74=0.333333*H4;HAA21=5.0*HA21
38600 HAA22=5.0*HA22;HAA23=5.0*HA23;HAA24=5.0*HA24
38700 AHA21=23.0*HA21;AHA22=23.0*HA22;AHA23=23.0*HA23
38800 BHA24=16.0*HA24;HAB21=8.0*HA21;HAB22=8.0*HA22;HAB23=8.0*HA23
38900 AHA24=23.0*HA24;BHA21=16.0*HA21;BHA22=16.0*HA22;BHA23=16.0*HA23
39000 HAB24=8.0*HA24;AHA31=9.0*HA31;AHA32=9.0*HA32;AHA33=9.0*HA33
39100 AHA34=9.0*HA34;BHA31=19.0*HA31;BHA32=19.0*HA32
39200 BHA33=19.0*HA33;BHA34=19.0*HA34;CHA31=5.0*HA31
39300 CHA32=5.0*HA32;CHA33=5.0*HA33;CHA34=5.0*HA34
39400 215 CONTINUE
39500 IF(IOL2.EQ.1)GO TO 2780
39600 IF(M1LP.NE.1)GO TO 584
39700 IF(M8LP.NE.1)GO TO 584
39800 IF(M.EQ.1)GO TO 2780
39900 IF(IOPT2.EQ.2)GO TO 584
40000 IF(M.LE.NDPTS)GO TO 2780
40100 584 CONTINUE
40200 UV=TF(M);T=TF(M);Z1=Z11(M);Z2=Z22(M);XW=PF(M);F5=F55(M)
40300 Z3=Z33(M);HL=HLL(M)*1.0E6;F1=F11(M);F2=F22(M);F3=F33(M);F4=F44(M)
40400 RUA=UAR(M)*1.0E-6;HUA=UAH(M)*1.0E-6
40500 AFD2=FD22(M);AFD3=FD33(M);AFD4=FD44(M);AFD0=FD55(M)
40600 GO TO 2483
40700 2780 UV=TFN(MJK1);T=TFN(MJK1);Z1=Z11(MJK1)
```

40800 Z2=Z22(MJK1);XW=PFN(MJK1)  
 40900 Z3=Z33(MJK1);HL=HL LN(MJK1)\*1.0E6  
 41000 F1=F11(MJK1);F2=F22(MJK1);F3=F33(MJK1)  
 41100 F4=F44(MJK1);F5=F55(MJK1);RUA=UARN(MJK1)\*1.0E-6  
 41200 HUA=UAHN(MJK1)\*1.0E-6;AFD2=FD22N(MJK1);AFD3=FD33N(MJK1)  
 41300 AFD4=FD44N(MJK1);AFD0=FD55N(MJK1)  
 41400 2483 FT=F1+F2+F3+F4+F5;FTV=FT\*80.64;J=1  
 41500 FTT1=100./FT  
 41600 FFQ1=FF\*\*1.8;ZTI=100./(Z1+Z2+Z3+HL)  
 41700 C5=C51\*FFQ1;C61=C611\*FFQ1;C62=C621\*FFQ1  
 41800 ZC1=Z1\*0.000001  
 41900 ZC3=Z3\*0.000001;ZC2=Z2\*0.000001;HCL=HL\*0.000001  
 42000 RUAI=RUA\*1.0E+06;HUAH=HUA\*1.0E+06;CTVO=ZC1+ZC2+ZC3+HCL  
 42100 AFD1=1.0-AFD2-AFD3-AFD4;AFD01=AFD1-AFD0;CTVLP=CTVO/(ZC1+ZC2+ZC3)  
 42200 W1=W11;C21=C2;XWC5=C5\*XW\*AFD1\*\*1.8  
 42300 PH1=XW-0.75\*XWC5;PB11=XW-XWC5;S2=AFD1+AFD4;S11=S2+AFD2  
 42400 S12=S11+AFD3;PH2=XW-0.25\*XWC5  
 42500 FTF1=2.0\*F1/(3.0\*FT\*S2);S112=S11/S2;S122=S12/S2  
 42600 FI11=F1\*S2;FI21=F2\*S2;FI31=F3\*S2;FI41=F4\*S2;FI51=F5\*S2  
 42700 FI12=F1\*S11;FI22=F2\*S11;FI32=F3\*S11;FI42=F4\*S11;FI52=F5\*S11  
 42800 FI13=F1\*S12;FI23=F2\*S12;FI33=F3\*S12;FI43=F4\*S12;FI53=F5\*S12  
 42900 ZH1=IHH1;ZH2=IHH2;ZH3=IHH3;ZH4=IHH4;NZ1=IHH1-3  
 43000 IC71=C71;IC72=C72;IC73=C73;IC74=C74  
 43100 MZ1=IHH1/IC71;NZ2=IHH2-3;NZ3=IHH3-3  
 43200 NZ4=IHH4-3;MZ2=IHH2/IC72;MZ3=IHH3/IC73;MZ4=IHH4/IC74;AR1=F1\*AFD1  
 43300 AR2=F2\*AFD1;AR3=F3\*AFD1;AR4=F4\*AFD1;AR5=F5\*AFD1;Q11=FI11-AR1  
 43400 Q21=FI21-AR2;Q31=FI31-AR3;Q41=FI41-AR4;Q51=FI51-AR5  
 43500 Q12=F1\*AFD2;Q22=F2\*AFD2;Q32=F3\*AFD2;Q42=F4\*AFD2  
 43600 Q52=F5\*AFD2;Q13=F1\*AFD3;Q23=F2\*AFD3;Q33=F3\*AFD3  
 43700 Q43=F4\*AFD3;Q53=F5\*AFD3  
 43800 RFTI=0.01\*FTT1;AY3=F3\*RFTI  
 43900 FFL=F;RHNL=RHN;PHYL=PHY;PNIL=PNI;PAML=PAM  
 44000 UV20=UV+CSP11;LP8=1  
 44100 IF(W11L.LT.UV20)W11L=UV20  
 44200 W11L20=W11L+CSP11;W11L2=WV+W11LI;M106=0;M107=0  
 44300 C MODIFICATION TO MAIN PROGRAM  
 44400 ICONV=0;MMN=0;F1CON=F1\*0.9792;M7=0;IM17=1;IM8=1;IM80=2;IM83=2

```
44500      GO TO 407
44600 287    CSP1=CSP11;CSP2=CSF22;CSP3=CSP33*2
44700      IF(IOL2.EQ.1)GO TO 1192
44800      IF(J5.EQ.0)GO TO 1192
44900      IF(M81.EQ.1)GO TO 1192
45000      ISIG=1;W11H=W11HL;W1=W11H
45100 353    TH12=W1;ATH12(J)=W1
45200      IF(J.EQ.1)GO TO 371
45300      CALL COMPA(ADELT,ATH12,J,MMN)
45400      IF(MMN.NE.0)GO TO 368
45500 371    K5=K5L;KL51=K5-1
45600      CALL FEEDT(TF1,W1,F,H1,H2,H3,H4,VW,C71,C72,C73,C74,BHA31,BHA32,
45700 1BHA33,BHA34,CHA31,CHA32,CHA33,CHA34,J1,K11)
45800      M7=M7+1
45900      IF(LQQ.EQ.2)GO TO 362
46000      IF(AT(MQ1,K11)-W11L2)362,362,386
46100 386    DELT1=TF1-T;ADELT(J)=DELT1
46200      TPRD=XW-AP(M12(K5),K5)
46300      M106=M106+1;STLP(M106,M)=ATH(1,1)
46400      SALP(M106,M)=ANX(M12(KL51),KL51)
46500      IF(ITYPE8.NE.1)GO TO 291
46600      PRINT 423,M7,W1,DELT1,(K1,ANX(1,K1)
46700 1,AXEN(1,K1),AXRMN(1,K1),AX(1,K1),AT(1,K1),ATH(1,K1)
46800 1,EFZI8(1,K1)
46900 1,QR1B(1,K1),ALPS8(K1),AXMAX(K1),ATMAX(K1),ATHMAX(K1)
47000 1,ANX(M12(K1),K1),AXEN(M12(K1),K1),AXRMN(M12(K1),K1)
47100 1,AX(M12(K1),K1),AT(M12(K1),K1)
47200 1,ATH(M12(K1),K1),EFZI8(M12(K1),K1)
47300 1,QR1B(M12(K1),K1),EFZIA(K1),PDROP(K1)
47400 1,AP(M12(K1),K1),K1=1,KL51)
47500      IF(HL.EQ.0.0)GO TO 8425
47600      PRINT 707,AT(1,K5),ATH(1,K5),AT(M12(K5),K5),
47700 1ATH(M12(K5),K5),PDROP(K5),AP(M12(K5),K5),TPRD
47800 8425    CONTINUE
47900      IF(ITYPE.NE.2)GO TO 291
48000      TYPE 423,M7,W1,DELT1,(K1,ANX(1,K1)
48100 1,AXEN(1,K1),AXRMN(1,K1),AX(1,K1),AT(1,K1),ATH(1,K1)
```

```
48200      1,EFZI8(1,K1)
48300      1,QR1B(1,K1),ALPS8(K1),AXMAX(K1),ATMAX(K1),ATHMAX(K1)
48400      1,ANX(M12(K1),K1),AXEN(M12(K1),K1),AXRMN(M12(K1),K1)
48500      1,AX(M12(K1),K1),AT(M12(K1),K1)
48600      1,ATH(M12(K1),K1),EFZI8(M12(K1),K1)
48700      1,QR1B(M12(K1),K1),EFZIA(K1),PDR0P(K1)
48800      1,AP(M12(K1),K1),K1=1,KL51)
48900      IF(HL.EQ.0.0)GO TO 291
49000      TYPE 707,AT(1,K5),ATH(1,K5),AT(M12(K5),K5),
49100      1ATH(M12(K5),K5),PDR0P(K5),AP(M12(K5),K5),TPRD
49200 291    IF(ABS(DELT1).GT.C4)GO TO 281
49300      IF(ITYPE8.NE.1)GO TO 281
49400      IF(IOP11.EQ.1)GO TO 281
49500      PRINT 406,((AZP(M1,K1),AP(M1,K1),ANX(M1,K1),AT(M1,K1),
49600      1ATH(M1,K1),ACX(M1,K1),ACT(M1,K1),ACTH(M1,K1),M1=M15,M12(K11)
49700      1,M16),K1=K7,K5,K8)
49800      IF(ITYPE.NE.2)GO TO 281
49900      TYPE 406,((AZP(M1,K1),AP(M1,K1),ANX(M1,K1),AT(M1,K1),
50000      1ATH(M1,K1),ACX(M1,K1),ACT(M1,K1),ACTH(M1,K1),M1=M15,M12(K11)
50100      1,M16),K1=K7,K5,K8)
50200 281    CONTINUE
50300      IF(IOPL8.EQ.2)GO TO 516
50400      IF(W1.EQ.W11H)GO TO 398
50500      IF(W1.EQ.W11L)GO TO 398
50600 516    IF(J.EQ.1)GO TO 395
50700      IF(M7.GT.M8)GO TO 398
50800 317    IF(ABS(W2-W1).GT.CSP11)GO TO 395
50900 398    W11H8=ATH12(J);M7=0
51000      IF(ISIG.NE.1)GO TO 377
51100      ISIG=-1;W11H=W11H8;W11L=W11LP;W1=W11L;CSP3=CSP33*2;LP8=1;J=J+1
51200      GO TO 353
51300 395    IF(LP8.EQ.2)GO TO 290
51400      CSP3=CSP33*0.5;W1=W1+CSP3*ISIG
51500      GO TO 296
51600 290    CSP3=CSP3*0.5
51700      W1=W1+CSP3*ISIG
51800 296    J=J+1
```

```
51900      IF(W1.LT.W11L)W1=W11L
52000      GO TO 353
52100 362   CSP3=CSP3*0.5;W2=W1;W1=W1-CSP3*ISIG;LQG=1;LP8=2
52200      GO TO 353
52300 368   DELT1=ADEL(T(MMN));ADEL(T(J))=DELT1
52400      GO TO 317
52500 377   W11L=W11H8;IW11H=W11H*0.2;W11H=IW11H*5
52600      IW11L=W11L*0.2+0.50;W11L=IW11L*5
52700      IF(ITYPE8.NE.1)GO TO 120
52800      PRINT 278,W11H,W11L
52900      IF(ITYPE.NE.2)GO TO 120
53000      TYPE 278,W11H,W11L
53100 278   FORMAT(/2X,'FOR THIS DATA SET THE FEASIBLE REGION OF SEARCH FOR
53200      1D TEMPERATURE(K):',F7.1,2X,'TO',2X,F7.1/)
53300 120   DW11HL=W11H-W11L;W1=W11L;M7=0;CSP3=CSP33
53400      ICSP1=DW11HL*CSP1F;CSP1=ICSP1
53500      IF(CSP1.GT.CSP11)CSP1=CSP11
53600      IF(CSP1.LT.CSP12)CSP1=CSP12
53700      M8=DW11HL/CSP1+M82;W1=W11L;J=J+1
53800      IF(M8.LT.M81)M8=M81
53900      CSP2=CSP1*0.5+1.0
54000      IF(CSP2.GT.CSP22)CSP2=CSP22
54100      W11L20=W11L
54200      GO TO 305
54300 1192  CONTINUE
54400 305   TH12=W1;ATH12(J)=W1
54500      IF(M81.EQ.1)GO TO 53
54600      IF(J5.EQ.0)M8=M81
54700      IF(M7.GE.M8)GO TO 1503
54800      IF(J.EQ.1) GO TO 53
54900      CALL COMPA(ADEL(T),ATH12,J,MMN)
55000      IF(MMN.NE.0)GO TO 272
55100 53    K5=K5L;KL51=K5-1
55200      CALL FEEDT(TF1,W1,F,H1,H2,H3,H4,VW,C71,C72,C73,C74,BHA31,BHA32,
55300      1BHA33,BHA34,CHA31,CHA32,CHA33,CHA34,J1,K11)
55400      IF(M81.EQ.1)GO TO 62
55500      M7=M7+1
```

RS

## APPENDIX-B

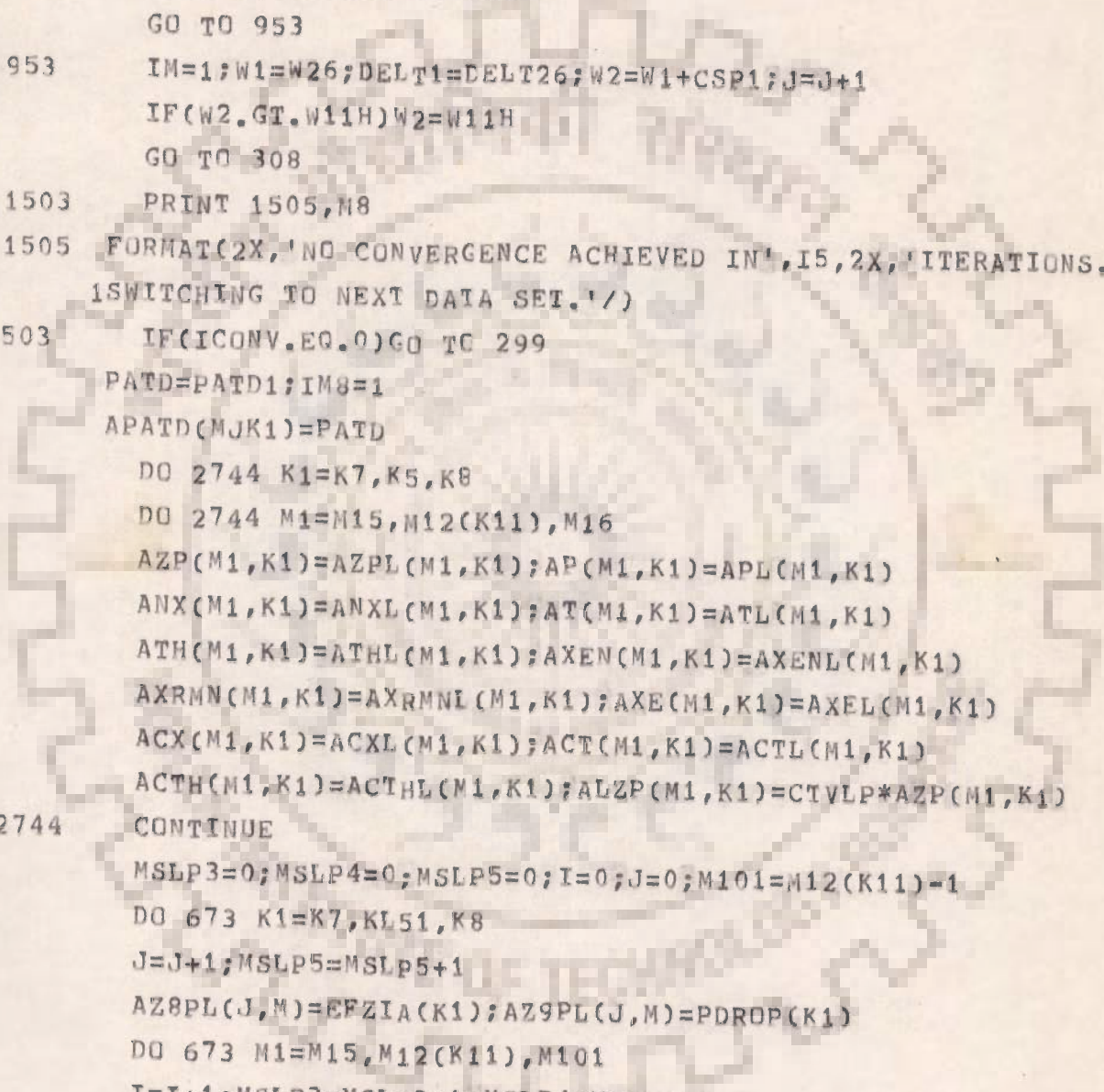
```
55600      IF(LQQ.EQ.2)GO TO 67
55700      IF(AT(MQ1,K11)-W11L2)71,71,62
55800 62    DELT1=TF1-T;ADELT(J)=DELT1
55900      W26=W1;DELT26=DELT1
56000      M106=M106+1;STLP(M106,M)=ATH(1,1)
56100      SALP(M106,M)=ANX(M12(KL51),KL51)
56200      GO TO 421
56300 67    CONTINUE
56400      IF(J5.EQ.0)GO TO 299
56500 2753  W1=W1+CSP1;LQQ=1
56600      GO TO 1192
56700 272  DELT1=ADELT(MMN)
56800 260    CONTINUE
56900      IF(M81.EQ.1)GO TO 401
57000      IF(J5.EQ.0)GO TO 321
57100      IF(ABS(DELT1)-C4)1170,1170,191
57200 191    CONTINUE
57300 152    IM=IM+1;W2=W1+CSP1;J=J+1
57400      IF(ICONV.EQ.0)GO TO 1152
57500 341    IF(W2.LT.W11H)GO TO 1152
57600      W2=W11H;IM8=2
57700 1152   CONTINUE
57800 308    TH12=W2;ATH12(J)=W2
57900      IF(M7.GE.M8)GO TO 1503
58000      IF(J.EQ.2)GO TO 1155
58100      CALL COMPA(ADELT,ATH12,J,MMN)
58200      IF(MMN.NE.0)GO TO 1272
58300 1155   K5=K5L;KL51=K5-1
58400      CALL FEEDT(TF2,W2,F,H1,H2,H3,H4,VW,C71,C72,C73,C74,BHA31,BHA32,
58500 1BHA33,BHA34,CHA31,CHA32,CHA33,CHA34,J1,K11)
58600      M7=M7+1
58700      IF(LQQ.EQ.2)GO TO 68
58800      IF(AT(MQ1,K11)-W11L2)72,72,64
58900 64    DELT2=TF2-T;ADELT(J)=DELT2
59000      IF(W2.GE.W11H)IM8=2
59100      W26=W2;DELT26=DELT2
59200      M106=M106+1;STLP(M106,M)=ATH(1,1)
```

```
59300      SALP(M106,M)=ANX(M12(KL51),KL51)
59400      GO TO 424
59500 68    W2=W2+CSP1;LQQ=1
59600      IF(IM8.EQ.2)GO TO 503
59700      IF(W2.LT.W11H)GO TO 308
59800      IM8=2;W2=W11H
59900      GO TO 1152
60000 1272 DELT2=ADEL(T(MMN)
60100      IF(W2.GE.W11H)IM8=2
60200 1260 IF(ABS(DELT2)-C4)1170,1170,153
60300 153 DW12=(W1-W2)*1.5
60400      IF(DELT1)1,503,5
60500 1 IF(DELT2)2,2,7
60600 5 IF(DELT2)7,7,2
60700 2     IM=1;W1=W2;DELT1=DELT2;W2=W1+CSP1;J=J+1
60800      IF(IM8.EQ.2)GO TO 503
60900      IF(W2.GT.W11H)W2=W11H
61000      GO TO 308
61100 7 J=J+1
61200      IF(M7.GE.M8)GO TO 1503
61300 116    W3=W2+(W1-W2)*ABS(DELT2)/(ABS(DELT2)+ABS(DELT1))
61400      IW3=W3
61500      TH12=W3;ATH12(J)=W3
61600      CALL COMPA(ADEL(T,ATH12,J,MMN)
61700      IF(MMN.NE.0) GO TO 1188
61800      K5=K5L;KL51=K5-1
61900      CALL FEEDT(TF3,W3,F,H1,H2,H3,H4,VW,C71,C72,C73,C74,BHA31,BHA32,
62000 1BHA33,BHA34,CHA31,CHA32,CHA33,CHA34,J1,K11)
62100      M7=M7+1
62200      IF(LQQ.EQ.2)GO TO 69
62300      IF(AT(MQ1,K11)-W11L2)73,73,66
62400 66    DELT3=TF3-T;ADEL(T(J)=DELT3
62500      GO TO 427
62600 69    W2=W3;LQQ=1
62700      GO TO 116
62800 1188 DELT3=ADEL(T(MMN)
62900 1520 IF(ABS(DELT3)-C4)1170,1170,188
```

```
63000 188 IF(DELT3)11,1170,35
63100 11 IF(DELT2)17,17,26
63200 35 IF(DELT2)26,26,17
63300 17 W2=W3;DELT2=DELT3
63400 GO TO 7
63500 26 W1=W3;DELT1=DELT3
63600 GO TO 7
63700 1170 IF(MMN,NE.0)GO TO 953
63800 M107=M107+1;STLP2(M107,M)=ATH(1,1)
63900 SALP2(M107,M)=ANX(M12(KL51),KL51)
64000 MM2=M106;M106=M106+1
64100 STLP(M106,M)=STLP(MM2,M);SALP(M106,M)=SALP(MM2,M)
64200 STLP(MM2,M)=ATH(1,1);SALP(MM2,M)=ANX(M12(KL51),KL51)
64300 GO TO 401
64400 321 ICONV=ICONV+1;M7=0
64500 PATD=AX(M12(K11),K5)*F1CON;APATD(MJK1)=PATD
64600 OBJF2(M)=PATD
64700 IF(ITYPE8,NE.1)GO TO 125
64800 PRINT 1718,PATD
64900 IF(ITYPE,NE.2)GO TO 125
65000 TYPE 1718,PATD
65100 1718 FORMAT(2X,'PRODUCTION RATE OF AMMONIA(TONS PER DAY)=' ,F7.1/)
65200 125 CONTINUE
65300 IF(IOL2.EQ.1)GO TO 1871
65400 IF(M81.EQ.1)GO TO 209
65500 1871 CONTINUE
65600 APATDL(ICONV)=PATD
65700 IF(ICONV.LE.1)GO TO 2717
65800 IF(APATDL(ICONV).LT.APATDL(ICONV-1))GO TO 2735
65900 2717 DO 2726 K1=K7,K5,K8
66000 DO 2726 M1=M15,M12(K11),M16
66100 AZPL(M1,K1)=AZP(M1,K1)
66200 APL(M1,K1)=AP(M1,K1)
66300 ANXL(M1,K1)=ANX(M1,K1)
66400 ATL(M1,K1)=AT(M1,K1)
66500 ATHL(M1,K1)=ATH(M1,K1)
66600 AXENL(M1,K1)=AXEN(M1,K1)
```



```
66700      AXRMNL(M1,K1)=AXRMN(M1,K1)
66800      AXEL(M1,K1)=AXE(M1,K1);ACXL(M1,K1)=ACX(M1,K1)
66900      ACTL(M1,K1)=ACT(M1,K1);ACTHL(M1,K1)=ACTH(M1,K1)
67000 2726  CONTINUE
67100      PATD1=APATDL(ICONV)
67200 2735  W1=W11L20;IM80=1
67300      IF(ICONV.GE.J5)GO TO 503
67400      IF(IM8.EQ.2)GO TO 503
67500      GO TO 953
67600 953   IM=1;W1=W26;DELT1=DELT26;W2=W1+CSP1;J=J+1
67700      IF(W2.GT.W11H)W2=W11H
67800      GO TO 308
67900 1503  PRINT 1505,M8
68000 1505  FORMAT(2X,'NO CONVERGENCE ACHIEVED IN',I5,2X,'ITERATIONS.THEREFORE
68100 1SWITCHING TO NEXT DATA SET.')
```



```
68200 503   IF(ICONV.EQ.0)GO TO 299
68300      PATD=PATD1;IM8=1
68400      APATD(MJK1)=PATD
68500      DO 2744 K1=K7,K5,K8
68600      DO 2744 M1=M15,M12(K11),M16
68700      AZP(M1,K1)=AZPL(M1,K1);AP(M1,K1)=APL(M1,K1)
68800      ANX(M1,K1)=ANXL(M1,K1);AT(M1,K1)=ATL(M1,K1)
68900      ATH(M1,K1)=ATHL(M1,K1);AXEN(M1,K1)=AXENL(M1,K1)
69000      AXRMN(M1,K1)=AXRMNL(M1,K1);AXE(M1,K1)=AXEL(M1,K1)
69100      ACX(M1,K1)=ACXL(M1,K1);ACT(M1,K1)=ACTL(M1,K1)
69200      ACTH(M1,K1)=ACTHL(M1,K1);ALZP(M1,K1)=CTVLP*AZP(M1,K1)
69300 2744  CONTINUE
69400      MSLP3=0;MSLP4=0;MSLP5=0;I=0;J=0;M101=M12(K11)-1
69500      DO 673 K1=K7,KL51,K8
69600      J=J+1;MSLP5=MSLP5+1
69700      AZ8PL(J,M)=EFZIA(K1);AZ9PL(J,M)=PDR0P(K1)
69800      DO 673 M1=M15,M12(K11),M101
69900      I=I+1;MSLP3=MSLP3+1;MSLP4=MSLP4+1
70000      AZ2PL(I,M)=AT(M1,K1);AZ3PL(I,M)=ATH(M1,K1)
70100      AZ4PL(I,M)=ANX(M1,K1);AZ5PL(I,M)=AXEN(M1,K1)
70200      AZ6PL(I,M)=AXRMN(M1,K1);AZ7PL(I,M)=QR1B(M1,K1)
70300 673   CONTINUE
```

```
70400 DO 674 M1=M15,M12(K11),M101
70500 I=I+1;MSLP3=MSLP3+1
70600 AZ2PL(I,M)=AT(M1,K5)
70700 AZ3PL(I,M)=ATH(M1,K5)
70800 674 CONTINUE
70900 MSLP6=MSLP5+2;AZ9PL((J+1),M)=PDRD(K5)
71000 AZ9PL((J+2),M)=TPRD
71100 I=0;MSLP=0
71200 IF(IOP201.NE.1)GO TO 677
71300 DO 675 K1=K7,KL51,K8
71400 DO 675 M1=5,M101,M16
71500 I=I+1;MSLP=MSLP+1
71600 AZ11PL(I,M)=AT(M1,K1);AZ12PL(I,M)=ANX(M1,K1)
71700 675 CONTINUE
71800 M167=2*M16;I=0;MSLP1=0
71900 DO 676 K1=K7,K5,K8
72000 DO 676 M1=7,M101,M167
72100 I=I+1;MSLP1=MSLP1+1
72200 AZ14PL(I,M)=ATH(M1,K1)
72300 676 CONTINUE
72400 I=0;MSLP2=0
72500 DO 677 M1=7,M101,M167
72600 I=I+1;MSLP2=MSLP2+1
72700 AZ15PL(I,M)=AT(M1,K5)
72800 677 CONTINUE
72900 J1=M;J11=1
73000 IF(IDP201.EQ.1)GO TO 7048
73100 WRITE(12,7049),(I,TPRD,PFN(I),TFN(I),VFTN(I),RATION(I)
73200 1,FC3N(I),FC4N(I),FC5N(I),FD44N(I),FD22N(I),FD33N(I)
73300 2,VCATN(I),OBJF2(I),
73400 2,DBED2N(I),DBED3N(I),HLLN(I),UARN(I),UAHN(I)
73500 2,FF1N(I),I=MJK1,MJK1)
73600 C PRINT 7049,(I,TPRD,PFN(I),TFN(I),VFTN(I),RATION(I)
73700 C 1,FC3N(I),FC4N(I),FC5N(I),FD44N(I),FD22N(I),FD33N(I)
73800 C 2,VCATN(I),OBJF2(I),
73900 C 2,DBED2N(I),DBED3N(I),HLLN(I),UARN(I),UAHN(I)
74000 C 2,FF1N(I),I=MJK1,MJK1)
```

```
74100 WRITE(3,7058),M106,M107,((STLP2(J,I),SALP2(J,I),J=1,M107),
74200 8(STLP(J,I),SALP(J,I),J=1,M106),I=M,M)
74300 C PRINT 7058,M106,M107,((STLP2(J,I),SALP2(J,I),J=1,M107),
74400 C 8(STLP(J,I),SALP(J,I),J=1,M106),I=M,M)
74500 7058 FORMAT(2I3,(6(F6.1,F7.3)/))
74600 WRITE(12,7050),((M1,ALZP(M1,K1),AT(M1,K1),ANX(M1,K1),
74700 2AXRMN(M1,K1),AXEN(M1,K1),M1=1,M12(K11)),K1=1,KL51)
74800 7050 FORMAT(2(I4,2F6.1,3F7.3)/)
74900 C PRINT 7050,((M1,AZP(M1,K1),AT(M1,K1),ANX(M1,K1),
75000 C 2AXRMN(M1,K1),AXEN(M1,K1),M1=1,M12(K11)),K1=1,KL51)
75100 IF(IOP201.NE.1)GO TO 7037
75200 7048 CONTINUE
75300 IF(IOPT2.NE.1)GO TO 7037
75400 WRITE(3,7049),(I,TFRD,PFN(I),TFN(I),VFTN(I),RATION(I)
75500 1,FC3N(I),FC4N(I),FC5N(I),FD44N(I),FD22N(I),FD33N(I)
75600 2,VCATN(I),OBJF2(I),
75700 2DBED2N(I),DBED3N(I),HLLN(I),UARN(I),UAHN(I)
75800 2,FF1N(I),I=M,M)
75900 C PRINT 7014,((STLP(J,I),SALP(J,I),J=1,M106),
76000 C 1(STLP2(J,I),SALP2(J,I),J=1,M107),I=M,M)
76100 7014 FORMAT(1X,10(F6.1,F7.3))
76200 7051 FORMAT(6(F6.1,F7.3)/)
76300 WRITE(3,7051),((STLP(J,I),SALP(J,I),J=1,M106),
76400 1(STLP2(J,I),SALP2(J,I),J=1,M107),I=M,M)
76500 IF(ITYPE.NE.2)GO TO 7030
76600 TYPE 7014,((STLP(J,I),SALP(J,I),J=1,M106),
76700 1(STLP2(J,I),SALP2(J,I),J=1,M107),I=M,M)
76800 7030 CONTINUE
76900 C PRINT 7016,((AZ11PL(J,I),J=1,MSLP),(AZ14PL(J,I),J=1,MSLP1)
77000 C 1,(AZ15PL(J,I),J=1,MSLP2),I=M,M)
77100 7016 FORMAT(1X,21(F6.1))
77200 7052 FORMAT(2X,12(F6.1))
77300 WRITE(3,7052),((AZ11PL(J,I),J=1,MSLP),(AZ14PL(J,I),J=1,MSLP1)
77400 1,(AZ15PL(J,I),J=1,MSLP2),I=M,M)
77500 IF(ITYPE.NE.2)GO TO 7031
77600 TYPE 7016,((AZ11PL(J,I),J=1,MSLP),(AZ14PL(J,I),J=1,MSLP1)
77700 1,(AZ15PL(J,I),J=1,MSLP2),I=M,M)
```

RS

## APPENDIX-B

```

77800 7031 CONTINUE
77900 C PRINT 7018,((AZ12PL(J,I),J=1,MSLP),I=M,M)
78000 7018 FORMAT(2X,18(F7.3))
78100 7053 FORMAT(2X,11(F7.3))
78200 WRITE(3,7053),((AZ12PL(J,I),J=1,MSLP),I=M,M)
78300 IF(ITYPE.NE.2)GO TO 7032
78400 TYPE 7018,((AZ12PL(J,I),J=1,MSLP),I=M,M)
78500 7032 CONTINUE
78600 C PRINT 7020,((AZ2PL(J,I),AZ3PL(J,I),J=1,MSLP3),I=M,M)
78700 7020 FORMAT(2X,21(F6.1))
78800 7054 FORMAT(2X,12(F6.1))
78900 WRITE(3,7054),((AZ2PL(J,I),AZ3PL(J,I),J=1,MSLP3),I=M,M)
79000 IF(ITYPE.NE.2)GO TO 7033
79100 TYPE 7020,((AZ2PL(J,I),AZ3PL(J,I),J=1,MSLP3),I=M,M)
79200 7033 CONTINUE
79300 C PRINT 7022,((AZ4PL(J,I),AZ5PL(J,I),AZ6PL(J,I),AZ7PL(J,I),
79400 C 1J=1,MSLP4),I=M,M)
79500 7022 FORMAT(2X,4(3F7.3,E11.3))
79600 7055 FORMAT(2X,2(3F7.3,E11.3))
79700 WRITE(3,7055),((AZ4PL(J,I),AZ5PL(J,I),AZ6PL(J,I),AZ7PL(J,I),
79800 1J=1,MSLP4),I=M,M)
79900 IF(ITYPE.NE.2)GO TO 7034
80000 TYPE 7022,((AZ4PL(J,I),AZ5PL(J,I),AZ6PL(J,I),AZ7PL(J,I),
80100 1J=1,MSLP4),I=M,M)
80200 7034 CONTINUE
80300 C PRINT 7024,((AZ8PL(J,I),J=1,MSLP5),I=M,M)
80400 7024 FORMAT(1X,18(F7.3))
80500 7056 FORMAT(2X,11(F7.3))
80600 WRITE(3,7056),((AZ8PL(J,I),J=1,MSLP5),I=M,M)
80700 IF(ITYPE.NE.2)GO TO 7035
80800 TYPE 7024,((AZ8PL(J,I),J=1,MSLP5),I=M,M)
80900 7035 CONTINUE
81000 C PRINT 7026,((AZ9PL(J,I),J=1,MSLP6),I=M,M)
81100 WRITE(3,7057),((AZ9PL(J,I),J=1,MSLP6),I=M,M)
81200 IF(ITYPE.NE.2)GO TO 7037
81300 TYPE 7026,((AZ9PL(J,I),J=1,MSLP6),I=M,M)
81400 7037 CONTINUE

```

```

      RS          APPENDIX-B
81500 7026      FORMAT(1X,18(F7.2))
81600          IF(IOL2.NE.1)GO TO 8256
81700 7057      FORMAT(2X,11(F7.2))
81800          J1=MJK1;J11=MJK1
81900 8256      CONTINUE
82000          ANH3L(J1)=ANX(M12(K11),K5);I1=0
82100          APDRLP(J1)=AP(M12(K11),K5)
82200          DO 8744 K1=K7,K5,KJ81
82300          DO 8744 I=1,NBPTS(K1,J11)
82400          I1=I1+I
82500          IF(NBPTS(K1,J11).EQ.1)GO TO 8745
82600          MN81=M15+NLPD(I,K1,J11)
82700          GO TO 8746
82800 8745      CONTINUE
82900          MN81=M12(K11)
83000 8746      ATPL2(I1,J1)=AT(MN81,K1)
83100          ERRT=TA(I,K1,J11)-ATPL2(I1,J1);SET=ERRT*ERRT;SSE1=SSE1+SET
83200          ERRT1=ATPL2(I1,J1)-ATPL2(I1,1);SET1=ERRT1*ERRT1;SSE2=SSE2+SET1
83300 8744      CONTINUE
83400          ERAM=AMMD(J11)-ANH3L(J1);ERAM1=ANH3L(J1)-ANH3L(1)
83500          APDL=APDRPL(J11)-APDRLP(J1);SEPD=APDL*APDL
83600          APDL1=APDRLP(J1)-APDRLP(1);SEPD1=APDL1*APDL1
83700          SSE3=SSE3+SEPD;SSE4=SSE4+SEPD1
83800          SEA=ERAM*ERAM*WTFN;SSE5=SSE5+SEA;SSE1=SSE1+SEA
83900          SEA1=ERAM1*ERAM1;SSE6=SSE6+SEA1;SSE7=SSE7+SSE1+SSE3+SSE5
84000          SSE8=SSE8+SSE2+SSE4+SSE6
84100          SSE=SSE+SSE1+SSE5
84200 C        PRINT 7039,SSE,SSE1,SSE2,SSE3,SSE4,SSE5,SSE6,SSE7,SSE8
84300 C        WRITE(3,7061),SSE,SSE1,SSE2,SSE3,SSE4,SSE5,SSE6,SSE7,SSE8
84400 7039      FORMAT(9E11.3)
84500 7061      FORMAT(7E11.3)
84600          IF(ITYPE.NE.2)GO TO 7041
84700          TYPE 7039,SSE,SSE1,SSE2,SSE3,SSE4,SSE5,SSE6,SSE7,SSE8
84800 7041      CONTINUE
84900          IF(IOL2.EQ.1)GO TO 209
85000          N2LEP=LPOBJN(MJK1)
85100          IF(ITYP11.NE.1)N2LEP=1

```

RS

## APPENDIX-B

```

85200      IF(M.NE.1)GO TO 7081
85300      SES=SSE;SES1=SSE1;SES2=SSE2;SES3=SSE3;SES4=SSE4;SES5=SSE5
85400      SES6=SSE6;SES7=SSE7;SES8=SSE8
85500 7081  CONTINUE
85600      CALL FUNOBJ(OBJF,M,N2LEP,PATD,OBLPN(ILPS2)
85700      1,SSE,SSE1,SSE2,SSE3,
85800      1SSE4,SSE5,SSE6,SSE7,SSE8,SES,SES1,SES2,SES3,SES4
85900      1,SES5,SES6,SES7,SES8,OBJF32)
86000      CALL FUNOBJ(OBJF3,M,LPOBJN(MJK1),PATD,OBLPN(ILPS2)
86100      1,SSE,SSE1,SSE2,SSE3,
86200      1SSE4,SSE5,SSE6,SSE7,SSE8,SES,SES1,SES2,SES3,SES4
86300      1,SES5,SES6,SES7,SES8,OBJF31)
86400      CALL FUNOBJ(OBJF4,M,NOBLP1,PATD,OBLPN(ILPS2)
86500      1,SSE,SSE1,SSE2,SSE3,
86600      1SSE4,SSE5,SSE6,SSE7,SSE8,SES,SES1,SES2,SES3,SES4
86700      1,SES5,SES6,SES7,SES8,OBJF33)
86800      GO TO 209
86900 299   APATD(MJK1)=0.0;PATD1=0.0;PATD=0.0;IM8=1;MLPK1=MLPK1+1
87000      M107=M107+1;SALP2(M107,M)=0.0;STLP2(M107,M)=0.0
87100      M107=M107+1;SALP2(M107,M)=0.0;STLP2(M107,M)=0.0
87200      IF(LPOBJN(MJK1).NE.1)GO TO 4441
87300      OBJF(M)=0.0
87400      GO TO 4442
87500 4441  OBJF(M)=ABCD2
87600 4442  CONTINUE
87700      IF(IOL2.EQ.1)GO TO 764
87800      IF(J5.EQ.0)GO TO 764
87900      GO TO 1703
88000 719  CONTINUE
88100      IF(OBJF(M).EQ.ABCD2)GO TO 761
88200 761   CONTINUE
88300      IF(OBJLPN(M).NE.0.0)IOPT2=3
88400      IF(IOPT2.EQ.3) GO TO 92
88500      IF(M.GT.1) GO TO 785
88600      IF(M1LP.GT.1)GO TO 4440
88700      IF(M8LP.GT.1)GO TO 4440
88800      92 VFT(M)=VFTN(MJK1)

```

RS

## APPENDIX-B

88900 RATIO(M)=RATION(MJK1)  
89000 FC1(M)=FC1N(MJK1);FC2(M)=FC2N(MJK1)  
89100 FC3(M)=FC3N(MJK1)  
89200 FC4(M)=FC4N(MJK1)  
89300 FC5(M)=FC5N(MJK1)  
89400 FD22(M)=FD22N(MJK1);FD33(M)=FD33N(MJK1)  
89500 FD44(M)=FD44N(MJK1);PF(M)=PFN(MJK1)  
89600 TF(M)=TFN(MJK1);VCAT(M)=VCATN(MJK1)  
89700 DBED2(M)=DBED2N(MJK1);DBED3(M)=DBED3N(MJK1)  
89800 HLL(M)=HLLN(MJK1);UAR(M)=UARN(MJK1);UAH(M)=UAHN(MJK1)  
89900 FF1(M)=FF1N(MJK1);FD55(M)=FD55N(MJK1)  
90000 G1=VFT(M);G3=RATIO(M);G5=FC3(M);G7=FC4(M);G9=FC5(M);G11=FD22(M)  
90100 G13=FD33(M);G15=FD44(M);G17=PF(M);G19=TF(M);G21=VCAT(M)  
90200 G23=DBED2(M);G25=DBED3(M);G27=HLL(M);G29=UAR(M);G31=UAH(M)



## APPENDIX-B

```

RS
00100      G33=FD55(M)
00200 4440  CONTINUE
00300      I26=M
00400      M3LP=1
00500      CALL PCONV(I26,M3LP,AQX)
00600 785   CONTINUE
00700      IF(M.LT.ND2PL)GO TO 98
00800      NOPTM=M
00900      GO TO 1709
01000      98 IF(IOPT2.EQ.3) GO TO 602
01100      NCOLD=12
01200      IF(IOL2.EQ.1)NCOLD=1
01300      CALL PNEXT(NVLPI,NCOLD,M,AQX,ISIGPL)
01400      IF(NVLPI.GT.NVARI)GO TO 755
01500      SSE=0.0;SSE1=0.0;SSE2=0.0;SSE3=0.0;SSE4=0.0;SSE5=0.0
01600      SSE6=0.0;SSE7=0.0;SSE8=0.0
01700      IF(IOPT8-2)1844,1808,1817
01800 1709  CONTINUE
01900      ISIGPL=1;ND7PL=1
02000      IF(IOL2.EQ.1)GO TO 7704
02100      DO 8701 I=1,M
02200      OBJF2(I)=OBJF(I)*OBJF32
02300 8701  CONTINUE
02400 C     IF(NOBJLP(MJK1).LT.2)GO TO 8761
02500 C     DO 8761 L=1,NVARI
02600 C     AQX8(MILP,L)=AQX(NOPTM,L)
02700 C8761 CONTINUE
02800      PRINT 866,OBJF31,OBJF33,(I,PF(I),TF(I),VFT(I),RATIO(I)
02900      1,FC3(I),FC4(I),FC5(I),FD44(I),FD22(I),FD33(I)
03000      2,VCAT(I),OBJF2(I),OBJF3(I),OBJF4(I),
03100      2,DBED2(I),DBED3(I),HLL(I),UAR(I),UAH(I)
03200      2,FD55(I),AQX(I,18),AQX(I,19),AQX(I,20),I=1,M)
03300      WRITE(3,7049),(I,TRPD,PF(I),TF(I),VFT(I),RATIO(I)
03400      1,FC3(I),FC4(I),FC5(I),FD44(I),FD22(I),FD33(I)
03500      2,VCAT(I),OBJF2(I),
03600      2,DBED2(I),DBED3(I),HLL(I),UAR(I),UAH(I)
03700      2,FF1(I),I=1,M)

```



RS

## APPENDIX-B

```
03800 7049  FORMAT(I3,F5.2,2F6.1,F9.1,F4.1,F5.2,F6.2,F5.2,3F6.3,F5.1
03900      1,F7.1/2F5.2,F6.2,F6.1,F7.1,F5.2)
04000      IF(IOP201.NE.1)GO TO 7027
04100      PRINT 7014,((STLP(J,I),SALP(J,I),J=1,M106),
04200      1(STLP2(J,I),SALP2(J,I),J=1,M107),I=1,M)
04300      WRITE(3,7051),((STLP(J,I),SALP(J,I),J=1,M106),
04400      1(STLP2(J,I),SALP2(J,I),J=1,M107),I=1,M)
04500      IF(ITYPE.NE.2)GO TO 7015
04600      TYPE 7014,((STLP(J,I),SALP(J,I),J=1,M106),
04700      1(STLP2(J,I),SALP2(J,I),J=1,M107),I=1,M)
04800 7015  CONTINUE
04900      PRINT 7016,((AZ11PL(J,I),J=1,MSLP),(AZ14PL(J,I),J=1,MSLP1)
05000      1,(AZ15PL(J,I),J=1,MSLP2),I=1,M)
05100      WRITE(3,7052),((AZ11PL(J,I),J=1,MSLP),(AZ14PL(J,I),J=1,MSLP1)
05200      1,(AZ15PL(J,I),J=1,MSLP2),I=1,M)
05300      IF(ITYPE.NE.2)GO TO 7017
05400      TYPE 7016,((AZ11PL(J,I),J=1,MSLP),(AZ14PL(J,I),J=1,MSLP1)
05500      1,(AZ15PL(J,I),J=1,MSLP2),I=1,M)
05600 7017  CONTINUE
05700      PRINT 7018,((AZ12PL(J,I),J=1,MSLP),I=1,M)
05800      WRITE(3,7053),((AZ12PL(J,I),J=1,MSLP),I=1,M)
05900      IF(ITYPE.NE.2)GO TO 7019
06000      TYPE 7018,((AZ12PL(J,I),J=1,MSLP),I=1,M)
06100 7019  CONTINUE
06200      PRINT 7020,((AZ2PL(J,I),AZ3PL(J,I),J=1,MSLP3),I=1,M)
06300      WRITE(3,7054),((AZ2PL(J,I),AZ3PL(J,I),J=1,MSLP3),I=1,M)
06400      IF(ITYPE.NE.2)GO TO 7021
06500      TYPE 7020,((AZ2PL(J,I),AZ3PL(J,I),J=1,MSLP3),I=1,M)
06600 7021  CONTINUE
06700      PRINT 7022,((AZ4PL(J,I),AZ5PL(J,I),AZ6PL(J,I),AZ7PL(J,I),
06800      1J=1,MSLP4),I=1,M)
06900      WRITE(3,7055),((AZ4PL(J,I),AZ5PL(J,I),AZ6PL(J,I),AZ7PL(J,I),
07000      1J=1,MSLP4),I=1,M)
07100      IF(ITYPE.NE.2)GO TO 7023
07200      TYPE 7022,((AZ4PL(J,I),AZ5PL(J,I),AZ6PL(J,I),AZ7PL(J,I),
07300      1J=1,MSLP4),I=1,M)
07400 7023  CONTINUE
```

RS

## APPENDIX-B

```

07500 PRINT 7024,((AZ8PL(J,I),J=1,MSLP5),I=1,M)
07600 WRITE(3,7056),((AZ8PL(J,I),J=1,MSLP5),I=1,M)
07700 IF(ITYPE.NE.2)GO TO 7025
07800 TYPE 7024,((AZ8PL(J,I),J=1,MSLP5),I=1,M)
07900 7025 CONTINUE
08000 PRINT 7026,((AZ9PL(J,I),J=1,MSLP6),I=1,M)
08100 WRITE(3,7057),((AZ9PL(J,I),J=1,MSLP6),I=1,M)
08200 IF(ITYPE.NE.2)GO TO 7027
08300 TYPE 7026,((AZ9PL(J,I),J=1,MSLP6),I=1,M)
08400 7027 CONTINUE
08500 IF(ITYPE.NE.2)GO TO 884
08600 TYPE 866,OBJF31,OBJF33,(I,PF(I),TF(I),VFT(I),RATIO(I)
08700 1,FC3(I),FC4(I),FC5(I),FD44(I),FD22(I),FD33(I)
08800 2,VCAT(I),OBJF2(I),OBJF3(I),OBJF4(I),
08900 2DBED2(I),DBED3(I),HLL(I),UAR(I),UAH(I)
09000 2,FD55(I),AQX(I,18),AQX(I,19),AQX(I,20),I=1,M)
09100 866 FORMAT(/2X,'OPTIMISATION RESULTS:'/2X
09200 1,'S.',29X,'DATA SET',29X,'MAXIMUM AMMONIA'/
09300 12X,'ND.',65X,'PRODUCTION RATE'/70X,'(TONS PER DAY)'/
09400 12X,F12.4,2X,F12.4/
09500 1(1X,I3,2X,2F6.1,F9.1,F4.1,F5.2,F6.2,F5.2,3F6.3,F5.1
09600 1,6X,F7.1,11X,F12.4,2X,F12.4/6X,2F5.2,F6.2,F6.1,F7.1,F6.3,F11.8,
09700 1F11.8,F8.4)/)
09800 884 ISM=1;M=NOPTM
09900 PRINT 1712,OBJF2(M),PF(M),TF(M),FF1(M),VFT(M),FC1(M)
10000 1,FC2(M),FC3(M),FC4(M),FC5(M),FD55(M),FD44(M),FD22(M),FD33(M)
10100 2,VCAT(M),DBED2(M),DBED3(M),HLL(M),UAR(M),UAH(M)
10200 IF(ITYPE.NE.2)GO TO 704
10300 TYPE 1712,OBJF2(M),PF(M),TF(M),FF1(M),VFT(M),FC1(M)
10400 1,FC2(M),FC3(M),FC4(M),FC5(M),FD55(M),FD44(M),FD22(M),FD33(M)
10500 2,VCAT(M),DBED2(M),DBED3(M),HLL(M),UAR(M),UAH(M)
10600 1712 FORMAT(/2X,'OPTIMUM PRODUCTION RATE OF AMMONIA(TONS PER DAY)='
10700 1,F10.2/2X,'OPTIMUM PARAMETERS:'/2X,'PRESSURE(ATM)='
10800 2,F8.2,8X,',FEED TEMPERATURE(K)='F8.2
10900 3,',CATALYST ACTIVITY FACTOR='F5.2/2X,
11000 4'FEED FLOW RATE(NORMAL CUBIC METER/HOUR)='F10.2/2X,
11100 5'FEED COMPOSITION(MOLE %):HYDROGEN='

```

RS

## APPENDIX-B

```

11200      6F8.2,' ,NITROGEN=' ,F8.2,' ,AMMONIA=' ,F8.2,' ,METHANE=' ,F8.2,
11300      7' ,ARGON=' ,F8.2/2X,' COLD SHOT DISTRIBUTION:' ,
11400      7'HEAT EXCHANGER EXIT(SHELL SIDE)=' ,F8.3,' ,FIRST BED='
11500      8,F8.3,' ,SECOND BED=' ,F8.3,' ,THIRD BED=' ,F8.3/2X,
11600      9'CATALYST VOLUME(CUBIC METER)=' ,F8.2,2X,
11700      A' ,CATALYST DISTRIBUTION:BED1:BED2:BED3=1.00:'
11800      B,F5.2,' :' ,F5.2/2X,' EXTERNAL PREHEATER VOLUME(CUBIC METER)='
11900      C,F8.2/2X,
12000      D'HEAT EXCHANGE CAPACITIES IN CAL/(SEC)(K)(CUBIC METER):INTERNAL=
12100      E' ,F8.2,' ,EXTERNAL=' ,F8.2/)
12200      GO TO 704
12300 7704   CONTINUE
12400      PRINT 7705,(AQX(NOPTM,J),J=18,20),OBJF2(NOPTM)
12500      PRINT 7706,(I,(AQX(I,J),J=18,20),OBJF2(I),I=1,M)
12600      PRINT 7707,(I,PFN(I),TFN(I),FF1N(I),VFTN(I),FC1N(I),
12700      1FC2N(I),FC3N(I),FC4N(I),FC5N(I),VCATN(I),HLLN(I),
12800      1UARN(I),UAHN(I),FD55N(I),FD44N(I),FD22N(I),FD33N(I),DBED2N(I),
12900      1DBED3N(I),I=1,M5)
13000      IF(ITYPE.NE.2)GO TO 5204
13100      TYPE 7707,(I,PFN(I),TFN(I),FF1N(I),VFTN(I),FC1N(I),
13200      1FC2N(I),FC3N(I),FC4N(I),FC5N(I),VCATN(I),HLLN(I),
13300      1UARN(I),UAHN(I),FD55N(I),FD44N(I),FD22N(I),FD33N(I),DBED2N(I),
13400      1DBED3N(I),I=1,M5)
13500      TYPE 7706,(I,(AQX(I,J),J=18,20),OBJF2(I),I=1,M)
13600      TYPE 7705,(AQX(NOPTM,J),J=18,20),OBJF2(NOPTM)
13700 7705   FORMAT(2X,'DATA VALIDATION RESULTS:OPTIMUM PARAMETERS OF REACTION
13800      1RATE:' /2X,' PARA1=' ,F8.4,' ,PARA2=' ,F11.8,' ,PARA3=' ,F8.4,' ,
13900      111X,' SUM OF SQUARES(AVG.)=' ,F12.4/)
14000 7706   FORMAT(2X,'S.' ,17X,' DATA SET' ,41X,' SUM OF SQUARES OF ERROR IN BED
14100      1/2X,' NO.' ,65X,' TEMP. AND AMMONIA EXIT MOLE(%) BETWEEN' /70X,
14200      1' COMPUTED RESULTS AND PLANT DATA(AVG.)' /((1X,I3,
14300      12X,F8.4,2X,F11.8,2X,F8.4,40X,F12.4/))
14400 7707   FORMAT(2X,'PLANT DATA SET:' /((2X,
14500      1' DATA SET NO.=' ,I3/2X,' FEED PRESS.(ATM)=' ,F8.2,2X,
14600      1' ,FEED TEMP.(K)=' ,F8.2,' ,CATALYST ACTIVITY FACTOR=' ,F5.2,
14700      12X,' ,FEED FLOW RATE(NM3/HR)=' ,F10.2/2X,
14800      1' FEED COMPOSITION(MOLE%):H2=' ,F8.2,' ,N2=' ,F8.2,' ,NH3=' ,F8.2,

```

RS

## APPENDIX-B

```

14900      1',CH4=',F8.2,',A=',F8.2/2X,'CATALYST VOL(M3)=',F7.2,2X,
15000      1',EXT.PREHEATER VOL(M3)=',F7.2,2X,',HEAT EXCHANGE CAPACITIES,CAI
15100      1 K M3:INTERNAL=',F8.1,',EXTERNAL=',F8.1/2X,
15200      1'COLD SHOT DISTRIBUTION:',
15300      7'HEAT EXCHANGER EXIT(SHELL SIDE)=',F8.3,',FIRST BED='
15400      1,F8.3,',SECOND BED=',F8.3,',THIRD BED=',F8.3/2X,
15500      1'CATALYST DISTRIBUTION:BED1:BED2:BED3:1.00:',F5.2,':',F5.2))
15600      GO TO 5204
15700 704    CONTINUE
15800      IF(NOBJLP(MJK1).GE.12)GO TO 701
15900 C     IF(M.GT.1)GO TO 8761
16000      IF(M1LP.GT.1)GO TO 8761
16100      IF(M8LP.GT.1)GO TO 8761
16200      DO 8761 L=1,NVARI
16300      AQX8(1,L)=AQX(1,L);AQX9(1,L)=AQX(1,L)
16400 8761    CONTINUE
16500      OBJF8(M1LP)=OBJF3(NOPTM)
16600      OBJF5(M1LP)=OBJF4(NOPTM)
16700      IF(OBJF31.EQ.0.0)GO TO 697
16800      OBJF82(M1LP)=OBJF3(NOPTM)*OBJF31
16900      GO TO 698
17000 697    OBJF82(M1LP)=OBJF3(NOPTM)
17100 698    CONTINUE
17200      M1LP=M1LP+1;M=1;NOPTM=0;NVLP1=0
17300      IF(NOBJLP(MJK1).GE.2)GO TO 205
17400 701    IF(MJK1.GE.M5)GO TO 204
17500      MM1=MM1+1;IM=IM+1;MJK1=MJK1+1;M1LP=1;NV1LP=0;NOPTM1=0
17600      ISIPL2=1;ND7PL=1;M8LP=1
17700      IF(IOL2.EQ.1)GO TO 205
17800      IF(NOBJLP(MJK1).GE.2)GO TO 205
17900      IF(IOP201.NE.1)GO TO 601
18000      READ(8,*)PARA1,PARA2,PARA3,PARA4,IOP26,IOP29,
18100      1IHH1,IHH2,IHH3,IHH4,W11,W11L,W11H,J5,M81,M15,M16,M161,
18200      1K7,K8,C71,C72,C73,C74,
18300      2UV,C2,IOPT2,ICSIZE,IOPT3,IOPT8,IOPT1,IOPT4,NUMBP
18400      PRINT 758
18500      IF(ITYPE.NE.2)GO TO 794

```

RS

## APPENDIX-B

```

18600      TYPE 758
18700 758  FORMAT(2X,'ADDITIONAL DATA FOR SUBSEQUENT SET: '/')
18800 794  PRINT *,PARA1,PARA2,PARA3,PARA4,IOP26,IOP29,
18900      1IHH1,IHH2,IHH3,IHH4,W11,W11L,W11H,J5,M81,M15,M16,M161,
19000      1K7,K8,C71,C72,C73,C74,FF,
19100      2UV,C2,IOPT2,ICSIZE,IOPT3,IOPT8,IOPT1,IOPT4,NUMBP
19200      IF(ITYPE.NE.2)GO TO 601
19300      TYPE *,PARA1,PARA2,PARA3,PARA4,IOP26,IOP29,
19400      1IHH1,IHH2,IHH3,IHH4,W11,W11L,W11H,J5,M81,M15,M16,M161,
19500      1K7,K8,C71,C72,C73,C74,FF,
19600      2UV,C2,IOPT2,ICSIZE,IOPT3,IOPT8,IOPT1,IOPT4,NUMBP
19700 601  IF(IOPT2.EQ.1)GO TO 205
19800      IF(M.GT.1)IOPT2=3
19900      GO TO 205
20000 602  IF(M.EQ.NDPTS)GO TO 755
20100      M=M+1
20200      IF(OBJLPN(M).EQ.0.0)GO TO 701
20300      PATD=OBJLPN(M);MJK1=MJK1+1;APATD(MJK1)=PATD;PATD1=PATD
20400      IM8=1;MLPK1=MLPK1+1;OBJF(M)=PATD
20500      GO TO 719
20600      M3LP=1;I26=0
20700 1835 I26=I26+1
20800      CALL PCONV(I26,M3LP,AQX)
20900      IF(I26.LT.M)GO TO 1835
21000 2600 CONTINUE
21100      GO TO 755
21200 209  GO TO 800
21300 764  IF(MJK1-M5)206,728,204
21400 728  IF(IOPT2-2)204,1907,719
21500 204  IF(IOL2.NE.1)GO TO 5204
21600      IF(MLPK1.EQ.M5)GO TO 5214
21700      OBJF2(M)=SSE/(M5-MLPK1);MJK1=1
21800      IF(OBJF2(1).EQ.0.0)GO TO 692
21900      OBJF(M)=-OBJF2(M)/OBJF2(1)
22000      GO TO 693

```

```

RS          APPENDIX-B
00100 692   OBJF(M)=-OBJF2(M)
00200 693   CONTINUE
00300       ML1KP=M5=MLPK1
00400       SSE=SSE/ML1KP;SSE1=SSE1/ML1KP;SSE2=SSE2/ML1KP;SSE3=SSE3/ML1KP
00500       SSE4=SSE4/ML1KP;SSE5=SSE5/ML1KP;SSE6=SSE6/ML1KP;SSE7=SSE7/ML1KP
00600       SSE8=SSE8/ML1KP
00700       IF(M.NE.1)GO TO 92
00800       SES=SSE;SES1=SSE1;SES2=SSE2;SES3=SSE3;SES4=SSE4;SES5=SSE5
00900       SES6=SSE6;SES7=SSE7;SES8=SSE8
01000       GO TO 92
01100 5214  MJK1=1;OBJF2(M)=100*OBJF2(1);OBJF(M)=-100.0
01200       GO TO 92
01300 1907  GO TO 719
01400 710   CONTINUE
01500       IF(IOL2.EQ.1)GO TO 701
01600       M=1
01700       GO TO 701
01800 206   IF(IOPT2-2)710,1907,719
01900 800   IF(IOPT4.EQ.2)GO TO 1703
02000       M1K1=1
02100       IF(IOPT2.NE.1) GO TO 605
02200       GO TO 614
02300 605   CONTINUE
02400 614   IF(IOPT2.NE.1)GO TO 620
02500       GO TO 1703
02600 620   CONTINUE
02700 1703  IF(ISM.EQ.1)GO TO 764
02800       IF(IOL2.EQ.1)GO TO 764
02900 755   CONTINUE
03000 854   CONTINUE
03100       N2LEP=LPOBJN(MJK1)
03200       IF(ITYP11.NE.1)N2LEP=1
03300       CALL FUNOBJ(OBJF,M,N2LEP,PATD,OBLPN(ILPS2)
03400       1,SSE,SSE1,SSE2,SSE3,
03500       1SSE4,SSE5,SSE6,SSE7,SSE8,SES,SES1,SES2,SES3,SES4
03600       1,SES5,SES6,SES7,SES8,OBJF32)
03700       CALL FUNOBJ(OBJF3,M,LPOBJN(MJK1),PATD,OBLPN(ILPS2)

```

RS

## APPENDIX-B

```

03800      1,SSE,SSE1,SSE2,SSE3,
03900      1SSE4,SSE5,SSE6,SSE7,SSE8,SES,SES1,SES2,SES3,SES4
04000      1,SES5,SES6,SES7,SES8,OBJF31)
04100      CALL FUNOBJ(OBJF4,M,NOBLP1,PATD,OBLPN(ILPS2)
04200      1,SSE,SSE1,SSE2,SSE3,
04300      1SSE4,SSE5,SSE6,SSE7,SSE8,SES,SES1,SES2,SES3,SES4
04400      1,SES5,SES6,SES7,SES8,OBJF33)
04500  857 CALL OPTIMA(OBJF,M,AGX,AQX1,IOPT8,NVARI,AC2,NLEV,
04600      1NOPTM,TOL8,NMAX1,NDPTS,XLPX,
04700      1OBLPF,NLN8,ALPC1,YLPN,IOL8P)
04800      SSE=0.0;SSE1=0.0;SSE2=0.0;SSE3=0.0;SSE4=0.0;SSE5=0.0
04900      SSE6=0.0;SSE7=0.0;SSE8=0.0
05000      IF(NOPTM.NE.0)GO TO 1709
05100      NDPTS2=NDPTS*NDLPS
05200      IF(M.GE.ND2PL)GO TO 881
05300      ISM=ISM+1 ; IM=1
05400      IF(IOPT8-2)1844,1808,1817
05500  881    NOPTM=NMAX1;M=M-1
05600      GO TO 1709
05700  1808 CALL INTEGR(AQX,NVARI,M)
05800      GO TO 862
05900  1817 CALL MLEVEL(AQX,NVARI,AQX1,M,NLEV)
06000      GO TO 862
06100  1844    CONTINUE
06200  862    CONTINUE
06300      I26=M
06400      M3LP=2
06500      CALL PCONV(I26,M3LP,AQX)
06600      IF(M.LE.NDPTS)GO TO 7224
06700      CALL ACOMP(LPIK,AQX,M,NVARI)
06800      IF(LPIK.EQ.0)GO TO 7224
06900      OBJF3(M)=OBJF3(LPIK);OBJF4(M)=OBJF4(LPIK)
07000      OBJF(M)=OBJF(LPIK);PATD=OBJF(LPIK)*OBLPN(ILPS2);LPIK=0
07100      IF(ISM.EQ.1)GO TO 764
07200      GO TO 857
07300  C      OUTPUT STATEMENTS PROGRAM
07400  404 PRINT 403,IJ1,IJ2,IJ3,IJ4

```

RS

## APPENDIX-B

```

07500     IF(ITYPE.NE.2)GO TO 405
07600     TYPE 403,IJ1,IJ2,IJ3,IJ4
07700 403 FORMAT(/1X,57X,6HSTART // 44X,6HDATE: ,I3,2H.,,I3,2H.,,I5,9H) R
07800 1UN.NO. ,I3 // 2X, 62HNAME OF THE STUDENT(PART TIME):SUDHINDRA
07900 2NATH SINHA,LECTURER // 2X,81HDEPARTMENT OF CHEMICAL ENGINEERI
08000 3NG,UNIVERSITY OF ROORKEE,ROORKEE(U.P.),PIN 247667 //2X,'PHD THE
08100 4SIS PROBLEM : STABILITY ANALYSIS AND OPTIMIZATION OF A MULTIBED
08200 8QUENCH REACTOR FOR AMMONIA SYNTHESIS' /
08300 5 /2X,'PHD.THESIS SUPERVISOR: DR.SHANT KUMAR SARAF,SC.D.(M.I
08400 6.T.,U.S.A.),PROFESSOR,DEPTT.OF CHEM.ENGG.,UNIVERSITY OF ROORKEE'
08500 7//)
08600     GO TO 405
08700 407 CONTINUE
08800     IF(ITYPE8.NE.1)GO TO 287
08900     IF(M.EQ.1) GO TO 632
09000     IF(IDPT2-2)632,638,647
09100 647 IF(M.GT.NDPTS) GO TO 638
09200 632 PRINT 408,XW,UV,VFTN(MJK1),FC1N(MJK1),FC2N(MJK1),FC3N(MJK1),
09300 1FC4N(MJK1),FC5N(MJK1),AFD4,AFD2,AFD3,AFD01,ZC1,ZC2,ZC3,HCL,RUAI
09400     IF(ITYPE.NE.2)GO TO 806
09500     TYPE 408,XW,UV,VFTN(MJK1),FC1N(MJK1),FC2N(MJK1),FC3N(MJK1),
09600 1FC4N(MJK1),FC5N(MJK1),AFD4,AFD2,AFD3,AFD01,ZC1,ZC2,ZC3,HCL,RUAI
09700     GO TO 806
09800 638 PRINT408,XW,UV,VFT(M),FC1(M),FC2(M),FC3(M),FC4(M)
09900 1,FC5(M),AFD4,AFD2,AFD3,AFD01,ZC1,ZC2,ZC3,
10000 2HCL, RUAI
10100     IF(ITYPE.NE.2)GO TO 806
10200     TYPE 408,XW,UV,VFT(M),FC1(M),FC2(M),FC3(M),FC4(M)
10300 1,FC5(M),AFD4,AFD2,AFD3,AFD01,ZC1,ZC2,ZC3,
10400 2HCL, RUAI
10500 408 FORMAT( 2X,'FEED : PRESSURE(ATM)=' ,F7.1, ' ;TEMP.(K)=' ,F7.1
10600 1//2X,'VOLUMETRIC FLOW RATE OF TOTAL FEED(NORMAL CUBIC METER/HOUR)=
10700 2',F10.1//2X,'FEED COMPOSITION(MOLE%):'//2X,'HYDROGEN',
10800 35X,F8.2/2X,'NITROGEN',5X,F8.2/2X,'AMMONIA',6X,F8.2/2X,'METHANE',
10900 46X,F8.2/2X,'ARGON',8X,F8.2//2X,'COLD SHOT DISTRIBUTION:FIRST BED='
11000 5,F6.3,' ,SECOND BED=' ,F6.3,' ,THIRD BED=' ,F6.3,' :EXTERNAL PREHEATER
11100 6FEED=' ,F6.3// 2X,

```



## RS APPENDIX-B

```

11200 7'CATALYST SPLIT IN CUBIC METER: FIRST BED=',
11300 8F7.1,12H,SECOND BED=,F7.1,11H,THIRD BED=,F7.1 / 2X,40HHEAT EXCH
11400 9ANGER TUBE SIDE VOLUME(CU.MR.)=,F7.1/2X,52HRAE OF HEAT TRANSFER/(
11500 ATEMP,DIFFERENCE)FOR REACTOR= , F7.1 )
11600 806 PRINT807,HUAI ,F
11700 IF(ITYPE.NE.2)GO TO 287
11800 TYPE 807,HUAI ,F
11900 807 FORMAT(2X,42HHEAT TRANSFER CAPACITY FOR HEAT EXCHANGER=,
12000 1F8.1,42H CAL./(SEC)(K)(CU.MR.OF TUBE SIDE VOLUME) /2X,
12100 225HCATALYST ACTIVITY FACTOR= ,F5.2/)
12200 GO TO 287
12300 401 IF(IOL2.EQ.1)GO TO 1874
12400 IF(M81.EQ.1)GO TO 875
12500 1874 CONTINUE
12600 IF(IOP12.EQ.1)GO TO 566
12700 JJ1=J1-1;JJ2=J1-2
12800 PRINT 560,((I,QR1AV(I,K1),WRXN(I,K1),WRXNS(I,K1),RINTL(I,K1),
12900 1SINTL(I,K1),I=1,JJ2,M162),JJ1,QR1AV(JJ1,K1),WRXN(JJ1,K1),
13000 1WRXNS(JJ1,K1),RINTL(JJ1,K1),SINTL(JJ1,K1),K1=1,3)
13100 IF(ITYPE.NE.2)GO TO 566
13200 TYPE 560,((I,QR1AV(I,K1),WRXN(I,K1),WRXNS(I,K1),RINTL(I,K1),
13300 1SINTL(I,K1),I=1,JJ2,M162),JJ1,QR1AV(JJ1,K1),WRXN(JJ1,K1),
13400 1WRXNS(JJ1,K1),RINTL(JJ1,K1),SINTL(JJ1,K1),K1=1,3)
13500 560 FORMAT(3X,'I',3X,'RATEAV',5X,'DRT',2X,'SUM DRT',1X,'INTEGRAL',
13600 11X,'SUM INTGL'/(I5,5E9.2,I4,5E9.2))
13700 566 IF(IOP11.EQ.1)GO TO 321
13800 IF(ITYPE8.NE.1)GO TO 321
13900 IF(IOPT3.EQ.1) GO TO 452
14000 875 PRINT 406,((AZP(M1,K1),AP(M1,K1),ANX(M1,K1),AT(M1,K1),ATH(M1,K1),
14100 1ACX(M1,K1),ACT(M1,K1),ACTH(M1,K1),M1=M15
14200 2,M12(K11),M16),K1=K7,K5,K8)
14300 IF(ITYPE.NE.2)GO TO 416
14400 TYPE 406,((AZP(M1,K1),AP(M1,K1),ANX(M1,K1),AT(M1,K1),ATH(M1,K1),
14500 1ACX(M1,K1),ACT(M1,K1),ACTH(M1,K1),M1=M15
14600 2,M12(K11),M16),K1=K7,K5,K8)
14700 406 FORMAT( 1X,24X,44HREACTOR CONVERSION AND TEMPERATURE PROFILES //
14800 1 11X,'REACTOR ',5X,8HPRESSURE,4X,' AMMONIA ' ,5X,

```

RS

## APPENDIX-B

```

14900      29HBED TEMP.,2X,9HPREHEATER,3X,42HDIFF.IN VALUE OBTAINED AND LAST I
15000      3TERATION      /      3X,'BED VOLUME(PERCENT)',3X,5H(ATM),5X,'      (MOL
15100      4E )' ,5X,10H(DEGREE K),2X,8HTEMP.(K),3X,10HCONVERSION,5X,9HBED TEM
15200      5P. ,5X,15HPREHEATER TEMP.      //(4X,F10.2,10X,F8.2,3X,F10.3,5X,
15300      6F8.1,3X,F8.1,4X,F10.6,4X,F10.6,8X,F10.6      /  ))
15400 416      IF(IOPT1.EQ.2)GO TO 321
15500      PRINT 1701,((AZP(M1,K1),AXE(M1,K1),AXEN(M1,K1),AXRM(M1,K1),AXRMN
15600      1(M1,K1),M1=M15,M12(K11),M16),K1=K7,KL51,K8)
15700      IF(IOLP8.EQ.2)GO TO 587
15800 C      PRINT 593,(((AXE2(MLPK,M1,K1),AXRM2(MLPK,M1,K1),MLPK=1,4),
15900 C      1M1=M15,M12(K11),M16),K1=K7,KL51,K8)
16000 C593      FORMAT(2X,7X,'XE1',7X,'XRM1',7X,'DXE1',7X,'DXRM1',
16100 C      16X,'XE2',8X,'XRM2',6X,'DXE2',7X,'DXRM2'/(2X,8F11.4))
16200 587      IF(ITYPE.NE.2)GO TO 321
16300      TYPE 1701,((AZP(M1,K1),AXE(M1,K1),AXEN(M1,K1),AXRM(M1,K1),AXRMN
16400      1(M1,K1),M1=M15,M12(K11),M16),K1=K7,KL51,K8)
16500      IF(IOLP8.EQ.2)GO TO 321
16600 C      TYPE 593,(((AXE2(MLPK,M1,K1),AXRM2(MLPK,M1,K1),MLPK=1,4),
16700 C      1M1=M15,M12(K11),M16),K1=K7,KL51,K8)
16800      GO TO 321
16900 452      PRINT 458,((AZP(M1,K1),AP(M1,K1),ANX(M1,K1),AT(M1,K1),ATH(M1,K1),
17000      1 M1=M15,M12(K11),M161), (AZP(M1,K1),AP(M1,K1),ANX(M1,K1),AT(M1,K1),
17100      2 ATH(M1,K1),M1=M12(K11),M12(K11)),K1=K7,K5,K8)
17200      IF(ITYPE.NE.2)GO TO 461
17300      TYPE 458,((AZP(M1,K1),AP(M1,K1),ANX(M1,K1),AT(M1,K1),ATH(M1,K1),
17400      1 M1=M15,M12(K11),M161), (AZP(M1,K1),AP(M1,K1),ANX(M1,K1),AT(M1,K1),
17500      2 ATH(M1,K1),M1=M12(K11),M12(K11)),K1=K7,K5,K8)
17600 458      FORMAT(1X,24X,'REACTOR CONVERSION AND TEMPERATURE PROFILES:'
17700      1//3X,'REACTOR CATALYST',5X,'PRESSURE',4X,'      AMMONIA',5X,
17800      2'BED TEMP.',2X,'PREHEATER'/3X,'BED VOLUME(PERCENT)',3X
17900      3,'(ATM)',5X,'      (MOLE )',5X,'(DEGREE K)',2X,'TEMP.(K)')//
18000      4(4X,F10.2,10X,F8.2,3X,F10.3,5X,F8.1,3X,F8.1//))
18100 461      IF(IOPT1.EQ.2)GO TO 321
18200 1727      PRINT 1701 ,((AZP(M1,K1),AXE(M1,K1),AXEN(M1,K1),AXRM(M1,K1),
18300      1AXRMN(M1,K1),M1=M15,M12(K11),M161),K1=K7,KL51,K8)
18400      IF(IOLP8.EQ.2)GO TO 596
18500 C      PRINT 593,(((AXE2(MLPK,M1,K1),AXRM2(MLPK,M1,K1),MLPK=1,4),

```

## APPENDIX-B

RS

```

18600 C      1M1=M15,M12(K11),M16),K1=K7,KL51,K8)
18700 596    IF(ITYPE.NE.2)GO TO 321
18800      TYPE 1701 ,((AZP(M1,K1),AXE(M1,K1),AXEN(M1,K1),AXRM(M1,K1),
18900      1AXRMN(M1,K1),M1=M15,M12(K11),M161),K1=K7,KL51,K8)
19000      IF(IOLP8.EQ.2)GO TO 321
19100 C      TYPE 593,((AXE2(MLPK,M1,K1),AXRM2(MLPK,M1,K1),MLPK=1,4),
19200 C      1M1=M15,M12(K11),M16),K1=K7,KL51,K8)
19300 1701   FORMAT(4X,'BED VOL.', 16X,'EQUILIBRIUM', 20X,'CONVERSION'
19400      13X,'(PERCENT)', 16X,'CONVERSION', 21X,'AT MAXIMUM RATE' / 23X,
19500      2'HYDROGEN', 3X,'MOLE % AMMONIA', 9X,'HYDROGEN', 4X,'MOLE % AMMO
19600      3NIA'//(2X,F10.2, 9X,F10.3, 5X,F10.3, 6X,F10.3, 5X,F10.3//))
19700      GO TO 321
19800 138    CONTINUE
19900      IF(IOP12.EQ.1)GO TO 565
20000      JJ1=J1-1;JJ2=J1-2
20100      PRINT 560,((I,GR1AV(I,K1),WRXN(I,K1),WRXNS(I,K1),RINTL(I,K1),
20200      1SINTL(I,K1),I=1,JJ2,M162),JJ1,GR1AV(JJ1,K1),WRXN(JJ1,K1),
20300      1WRXNS(JJ1,K1),RINTL(JJ1,K1),SINTL(JJ1,K1),K1=1,3)
20400      IF(ITYPE.NE.2)GO TO 565
20500      TYPE 560,((I,GR1AV(I,K1),WRXN(I,K1),WRXNS(I,K1),RINTL(I,K1),
20600      1SINTL(I,K1),I=1,JJ2,M162),JJ1,GR1AV(JJ1,K1),WRXN(JJ1,K1),
20700      1WRXNS(JJ1,K1),RINTL(JJ1,K1),SINTL(JJ1,K1),K1=1,3)
20800 565    IF(IOP11.EQ.1)GO TO 209
20900      IF(ITYPE8.NE.1)GO TO 209
21000      IF(IOPT3.EQ.1)GO TO 139
21100      PRINT 406,((AZP(M1,K1),AP(M1,K1),ANX(M1,K1),
21200      1AT(M1,K1),ATH(M1,K1),ACX(M1,K1),ACT(M1,K1),ACTH(M1,K1), M1=M15,
21300      2M12(K11),M16),K1=K7,K5,K8)
21400      IF(ITYPE.NE.2)GO TO 209
21500      TYPE 406,((AZP(M1,K1),AP(M1,K1),ANX(M1,K1),
21600      1AT(M1,K1),ATH(M1,K1),ACX(M1,K1),ACT(M1,K1),ACTH(M1,K1), M1=M15,
21700      2M12(K11),M16),K1=K7,K5,K8)
21800      GO TO 209
21900 139    PRINT 458,((AZP(M1,K1),AP(M1,K1),ANX(M1,K1),AT(M1,K1),ATH(M1,K1),
22000      1 M1=M15,M12(K11),M161),AZP(M1,K1),AP(M1,K1),ANX(M1,K1),AT(M1,K1),
22100      2 ATH(M1,K1),M1=M12(K11),M12(K11)),K1=K7,K5,K8)
22200      IF(ITYPE.NE.2)GO TO 209

```

RS

## APPENDIX-B

```

22300      TYPE 458,((AZP(M1,K1),AP(M1,K1),ANX(M1,K1),AT(M1,K1),ATH(M1,K1),
22400      1 M1=M15,M12(K11),M161),(AZP(M1,K1),AP(M1,K1),ANX(M1,K1),AT(M1,K1),
22500      2 ATH(M1,K1),M1=M12(K11),M12(K11)),K1=K7,K5,K8)
22600      GO TO 209
22700 421    TPRD=XW-AP(M12(K5),K5)
22800      IF(ITYPE8.NE.1)GO TO 260
22900      PRINT 423,M7,W1,DELT1,(K1,ANX(1,K1)
23000      1,AXEN(1,K1),AXRMN(1,K1),AX(1,K1),AT(1,K1),ATH(1,K1)
23100      1,EFZI8(1,K1)
23200      1,QR1B(1,K1),ALPS8(K1),AXMAX(K1),ATMAX(K1),ATHMAX(K1)
23300      1,ANX(M12(K1),K1),AXEN(M12(K1),K1),AXRMN(M12(K1),K1)
23400      1,AX(M12(K1),K1),AT(M12(K1),K1)
23500      1,ATH(M12(K1),K1),EFZI8(M12(K1),K1)
23600      1,QR1B(M12(K1),K1),EFZIA(K1),PDR0P(K1)
23700      1,AP(M12(K1),K1),K1=1,KL51)
23800      IF(HL.EQ.0.0)GO TO 8427
23900      PRINT 707,AT(1,K5),ATH(1,K5),AT(M12(K5),K5),
24000      1ATH(M12(K5),K5),PDR0P(K5),AP(M12(K5),K5),TPRD
24100 8427    CONTINUE
24200      IF(ITYPE.NE.2)GO TO 260
24300      TYPE 423,M7,W1,DELT1,(K1,ANX(1,K1)
24400      1,AXEN(1,K1),AXRMN(1,K1),AX(1,K1),AT(1,K1),ATH(1,K1)
24500      1,EFZI8(1,K1)
24600      1,QR1B(1,K1),ALPS8(K1),AXMAX(K1),ATMAX(K1),ATHMAX(K1)
24700      1,ANX(M12(K1),K1),AXEN(M12(K1),K1),AXRMN(M12(K1),K1)
24800      1,AX(M12(K1),K1),AT(M12(K1),K1)
24900      1,ATH(M12(K1),K1),EFZI8(M12(K1),K1)
25000      1,QR1B(M12(K1),K1),EFZIA(K1),PDR0P(K1)
25100      1,AP(M12(K1),K1),K1=1,KL51)
25200      IF(HL.EQ.0.0)GO TO 260
25300      TYPE 707,AT(1,K5),ATH(1,K5),AT(M12(K5),K5),
25400      1ATH(M12(K5),K5),PDR0P(K5),AP(M12(K5),K5),TPRD
25500 423  FORMAT(1X,14HITERATION NO.=,I2,52H,ASSUMED INTERNAL PREHEATER OUTL
25600      1ET STREAM TEMP.(K)= ,F6.1,1X,',CAL.AND GIVEN FEED TEMP.DIFF.(K)=
25700      2,F7.1/16X,'NH3 MOLE ',7X,'H2 FR.',1X,'BED',
25800      25X,'SHELL',3X,'EFF.',8X,'RATE',8X,'MAXIMA IN BED' /
25900      211X,'ACTUAL EQU. MAX.RATE',1X,'CONV.'

```

RS

## APPENDIX-B

```

26000 2,2X,'TEMP,K',2X,'TEMP,K',2X,'FACTOR'
26100 2,12X,'VOL.',2X,'H2 FR.CONV.',2X,'BED T(K)'
26200 2,2X,'SHELL T(K)'/C
26300 22X,'BED NO.=' ,I3 /2X,'INLET',3X,F6,3
26400 2,1X,F6.3,1X,F6.3,1X,F6.3,1X,F7.1,1X,F7.1
26500 2,1X,F7.3,1X,E10.3,1X,F6.2,3X,F8.3,5X,F7.1,2X,F7.1/2X,'EXIT'
26600 2,4X,F6.3,1X,F6.3,1X,F6.3,1X,F6.3
26700 2,1X,F7.1,1X,F7.1,1X,F7.3,1X,E10.3
26800 2/2X,'AVERAGE EFFECTIVENESS FACTOR=' ,F8,3
26900 2,2X,'BED PRESSURE DROP(ATM)=' ,F8,2,2X,
27000 2,'EXIT PRESSURE(ATM)=' ,F8,2))
27100 707 FORMAT(2X,'HEAT EXCHANGER:' /2X,
27200 2'INLET',31X,F7.1,1X,F7.1/2X,'EXIT',32X,F7.1,1X,F7.1/
27300 22X,'TUBE SIDE PRESSURE DROP(ATM)=' ,F8,2,2X,'EXIT PRESSURE(ATM)=
27400 2,F8,2,' ,TOTAL PRESSURE DROP(ATM)=' ,F8,2)
27500 GO TO 260
27600 424 TPRD=XW-AP(M12(K5),K5)
27700 IF(ITYPE8.NE.1)GO TO 1260
27800 PRINT 423,M7,W2,DELT2,(K1,ANX(1,K1)
27900 1,AXEN(1,K1),AXRMN(1,K1),AX(1,K1),AT(1,K1),ATH(1,K1)
28000 1,EFZI8(1,K1)
28100 1,QR1B(1,K1),ALPS8(K1),AXMAX(K1),ATMAX(K1),ATHMAX(K1)
28200 1,ANX(M12(K1),K1),AXEN(M12(K1),K1),AXRMN(M12(K1),K1)
28300 1,AX(M12(K1),K1),AT(M12(K1),K1)
28400 1,ATH(M12(K1),K1),EFZI8(M12(K1),K1)
28500 1,QR1B(M12(K1),K1),EFZIA(K1),PDRDP(K1)
28600 1,AP(M12(K1),K1),K1=1,KL51)
28700 IF(HL.EQ.0.0)GO TO 8429
28800 PRINT 707,AT(1,K5),ATH(1,K5),AT(M12(K5),K5),
28900 1ATH(M12(K5),K5),PDRDP(K5),AP(M12(K5),K5),TPRD
29000 8429 CONTINUE
29100 IF(ITYPE.NE.2)GO TO 1260
29200 TYPE 423,M7,W2,DELT2,(K1,ANX(1,K1)
29300 1,AXEN(1,K1),AXRMN(1,K1),AX(1,K1),AT(1,K1),ATH(1,K1)
29400 1,EFZI8(1,K1)
29500 1,QR1B(1,K1),ALPS8(K1),AXMAX(K1),ATMAX(K1),ATHMAX(K1)
29600 1,ANX(M12(K1),K1),AXEN(M12(K1),K1),AXRMN(M12(K1),K1)

```

RS

## APPENDIX-B

```

29700      1,AX(M12(K1),K1),AT(M12(K1),K1)
29800      1,ATH(M12(K1),K1),EFZI8(M12(K1),K1)
29900      1,QR1B(M12(K1),K1),EFZIA(K1),PDRDP(K1)
30000      1,AP(M12(K1),K1),K1=1,KL51)
30100      IF(HL.EQ.0.0)GO TO 1260
30200      TYPE 707,AT(1,K5),ATH(1,K5),AT(M12(K5),K5),
30300      1ATH(M12(K5),K5),PDRDP(K5),AP(M12(K5),K5),TPRD
30400      GO TO 1260
30500 427    TPRD=XW-AP(M12(K5),K5)
30600      IF(ITYPE8.NE.1)GO TO 1520
30700      PRINT 423,M7,W3,DELT3,(K1,ANX(1,K1)
30800      1,AXEN(1,K1),AXRMN(1,K1),AX(1,K1),AT(1,K1),ATH(1,K1)
30900      1,EFZI8(1,K1)
31000      1,QR1B(1,K1),ALPS8(K1),AXMAX(K1),ATMAX(K1),ATHMAX(K1)
31100      1,ANX(M12(K1),K1),AXEN(M12(K1),K1),AXRMN(M12(K1),K1)
31200      1,AX(M12(K1),K1),AT(M12(K1),K1)
31300      1,ATH(M12(K1),K1),EFZI8(M12(K1),K1)
31400      1,QR1B(M12(K1),K1),EFZIA(K1),PDRDP(K1)
31500      1,AP(M12(K1),K1),K1=1,KL51)
31600      IF(HL.EQ.0.0)GO TO 8430
31700      PRINT 707,AT(1,K5),ATH(1,K5),AT(M12(K5),K5),
31800      1ATH(M12(K5),K5),PDRDP(K5),AP(M12(K5),K5),TPRD
31900 8430    CONTINUE
32000      IF(ITYPE.NE.2)GO TO 1520
32100      TYPE 423,M7,W3,DELT3,(K1,ANX(1,K1)
32200      1,AXEN(1,K1),AXRMN(1,K1),AX(1,K1),AT(1,K1),ATH(1,K1)
32300      1,EFZI8(1,K1)
32400      1,QR1B(1,K1),ALPS8(K1),AXMAX(K1),ATMAX(K1),ATHMAX(K1)
32500      1,ANX(M12(K1),K1),AXEN(M12(K1),K1),AXRMN(M12(K1),K1)
32600      1,AX(M12(K1),K1),AT(M12(K1),K1)
32700      1,ATH(M12(K1),K1),EFZI8(M12(K1),K1)
32800      1,QR1B(M12(K1),K1),EFZIA(K1),PDRDP(K1)
32900      1,AP(M12(K1),K1),K1=1,KL51)
33000      IF(HL.EQ.0.0)GO TO 1520
33100      TYPE 707,AT(1,K5),ATH(1,K5),AT(M12(K5),K5),
33200      1ATH(M12(K5),K5),PDRDP(K5),AP(M12(K5),K5),TPRD
33300      GO TO 1520

```

RS

## APPENDIX-B

```

33400 71 PRINT 74,M7,K11,J1,AT(MQ1,K11),AX(MQ1,K11),ATH(MQ1,K11)
33500     IF(ITYPE.NE.2)GO TO 67
33600     TYPE 74,M7,K11,J1,AT(MQ1,K11),AX(MQ1,K11),ATH(MQ1,K11)
33700 74 FORMAT(1X,14HITERATION NO.= ,I3,21H,CATALYST BED NUMBER= ,I3,
33800     115H,BED POINT NO.= ,I5,
33900     2',BED TEMP.AT THIS POINT IS BELOW MINIMUM DESIRED(K)=',
34000     3F8.1//2X,'AT THIS PT.FR. CONVERSION OF HYDROGEN= ',F8.3,
34100     4'SHELL SIDE TEMP.(K)=' ,F8.1/2X,'THEREFORE SWITCHING TO NEXT ITERA
34200     5TION BY ASSUMING ANOTHER TEMPERATURE'/)
34300     GO TO 67
34400 72 PRINT 74,M7,K11,J1,AT(MQ1,K11),AX(MQ1,K11),ATH(MQ1,K11)
34500     IF(ITYPE.NE.2)GO TO 68
34600     TYPE 74,M7,K11,J1,AT(MQ1,K11),AX(MQ1,K11),ATH(MQ1,K11)
34700     GO TO 68
34800 73 PRINT 74,M7,K11,J1,AT(MQ1,K11),AX(MQ1,K11),ATH(MQ1,K11)
34900     IF(ITYPE.NE.2)GO TO 69
35000     TYPE 74,M7,K11,J1,AT(MQ1,K11),AX(MQ1,K11),ATH(MQ1,K11)
35100     GO TO 69
35200 231 FORMAT( 1X,56X,7HTHE END )
35300 5204 PRINT 231
35400     TYPE 231
35500     STOP
35600     END
35700     SUBROUTINE FEEDT(TF,W1,F,H1,H2,H3,H4,VW,C71,C72,C73,C74,BHA31,
35800     1BHA32,BHA33,BHA34,CHA31,CHA32,CHA33,CHA34,J,K1 )
35900 C     SUBROUTINE NO. 1 FOR CALCULATION OF FEED TEMPERATURE TO AMMONIA SYN
36000 C     REACTOR
36100     DIMENSION AZ(210,4),AP(210,4),AX(210,4),AT(210,4),ATH(210,4),
36200     1ACX(210,4),ACT(210,4)
36300     1,ACTH(210,4),EFZI8(210,4),EFZIA(8),QR1B(210,4)
36400     1,QR1AV(210,4),WRXN(210,4),WRXNS(210,4),RINTL(210,4),SINTL(210,4)
36500     2,ANX(210,4),AZP(210,4),AXMAX(8),ATMAX(8),ATHMAX(8),ALPS8(8)
36600     3,AXE(210,4),AXRM(210,4),AXEN(210,4),AXRMN(210,4),M12(20),PDROP(8)
36700 C     2,AXE2(4,310,4),AXRM2(4,310,4)
36800     COMMON/CB1/F1,F2,F3,F4,F5,LQQ,ITYPE,PARA1,PARA2,PARA3
36900     1,PARA4,IOP26,IOP29,FLPF
37000     1/CB2/AZ,AP,AX,AT,ATH,AXMAX

```

```

37100      1,ATMAX,ATHMAX,ALPS8,W11L,QR1AV,AXE2,AXRM2
37200      1,WRXN,WRXNS,RINTL,SINTL,EFZI8,QR1B,EFZIA,PDROP,IOL1/CB3/
37300      1AFD1,AFD2,AFD3,AFD4,Z1,Z2,Z3,HL,XW,UV,C4,RUA,HUA,C5,C61,C62,M15,K7
37400      2,FI11,FI12,FI13,FI21,FI22,FI23,FI31,FI32,FI33,FI41,FI42,FI43,M1,
37500      3FI51,FI52,FI53,PH1,PH2,PB11,S2,S11,S12,FTF1,S112,S122,AR1,AR2,
37600      4AR3,AR4,AR5,Q11,Q21,Q31,Q41,Q51,Q12,Q22,Q32,Q42,Q52,
37700      5IEL2P,UARLP,K5,KL51,IOPT3,AFD0,
37800      5Q13,Q23,Q33,Q43,Q53,HA11,HA21,HA31,HA41,HA51,HA61,HA71,HA12,M16,
37900      6HA22,HA32,HA42,HA52,HA62,HA72,HA13,HA23,HA33,HA43,HA53,HA63,K8,
38000      7HA73,HA14,HA24,HA34,HA44,HA54,HA64,HA74,NZ1,NZ2,NZ3,NZ4,MZ1,MZ2,
38100      8MZ3,MZ4,HAA21,HAA22,HAA23,HAA24,AHA21,AHA22,AHA23,AHA24,BHA21,
38200      9BHA22,BHA23,BHA24,HAB21,HAB22,HAB23,HAB24,AHA31,AHA32,AHA33,AHA34
38300      A/CB4/ANX,ZTI,PAM,AZP/CB5/LK,AN3T1,ZCTV/CB20/ACX,ACT,ACTH
38400      B/CB6/AXE,AXRM,AXEN,AXRMN,M12/CB7/ICSIZE,IOPT1,EFFAH,EFFAL
38500      1/CB9/FEL,RHNL,XINCL,XINCL2,TOL81,PHYL,PNIL,PAML,DELE
38600      1,DELM,IOL8,M88,IOP11,IOL81
38700      M1=1
38800      K1=1
38900      K3=1
39000      LK=1
39100 C    CALCULATION OF FIRST REACTOR BED CONVERSION AND TEMPRATURE PROFILES
39200      ZCTV=0.
39300      UA1=RUA
39400      AX(M1,K1)=0.0
39500      ATH(M1,K1)=W1
39600      TB1=ATH(M1,K1)
39700 C    CALCULATION FOR MIXTURE TEMPERATURE ENTERING FIRST BED
39800      XB12=0.0
39900      IF(AFD4)21,22,21
40000      22 TB=ATH(M1,K1)
40100      GO TO 23
40200      21 CALL MTEMP(TB,W1,F1,AR1,AR2,AR3,AR4,AR5,Q11,Q21,Q31,Q41,Q51,
40300      1XB12,PB11,UV,C4,IOP26)
40400      23 AP(M1,K1)=PB11
40500      C6=C61*(AFD1+AFD4)**1.8
40600 C    CALCULATION FOR REACTOR PROFILES BY MILNE PREDICTOR CORRECTOR METH
40700 C    NUMERICAL INTEGRATION

```



## RS APPENDIX-B

```

40800      IF(IOPT3.NE.1) GO TO 110
40900 110   CALL RNUMI(M1,K1,K3,TB,AFD1,NZ1,MZ1,HA11,HA21,HAA21,AHA21,BHA21,
41000      1HA31,HA41,HA51,HA61,HA71,FI11,FI21,FI31,FI41,FI51,Z1,HL,H1,C6,
41100      2VW,C71,UA1,F,PH1,HAB21,AHA31,BHA31,CHA31,J,TB1  )
41200 107   IF(LQQ.EQ.2)GO TO 800
41300      IF(AT(M1,K1)-W11L)11,11,12
41400 C     CALCULATION FOR SECOND BED PROFILES
41500      12 IF(K5.LE.1)GO TO 800
41600 440   IF(Z2.NE.0.0)GO TO 431
41700      K5=K5-1;KL51=KL51-1
41800      GO TO 14
41900 431   IF(IEL2P.NE.1)GO TO 452
42000      LK=2;UA1=RUA*UARLP
42100 452   TH12=AT(M1,K1)
42200      PB1=AP(M1,K1)
42300      XB12=AX(M1,K1)
42400      IF(AFD2)24,25,24
42500      25 TB=AT(M1,K1)
42600      GO TO 26
42700      24 CALL MTEMP(TB,TH12,F1,FI11,FI21,FI31,FI41,FI51,Q12,Q22,Q32,
42800      1Q42,Q52,XB12,PB1,UV,C4,IOP26)
42900      26 C6=((S112-FTF1*XB12)*(AFD1+AFD4))**1.8*C61
43000      ZCTV=Z1;TB1=ATH(M1,K1)
43100      IF(IOPT3.NE.1) GO TO 119
43200 119   CALL RNUMI(M1,K1,K3,TB,AFD1,NZ2,MZ2,HA12,HA22,HAA22,AHA22,
43300      1BHA22,HA32,HA42,HA52,HA62,HA72,FI12,FI22,FI32,FI42,FI52,Z2,
43400      2HL,H2,C6,VW,C72,UA1,F,PH1,HAB22,AHA32,BHA32,CHA32,J,TB1  )
43500 116   IF(LQQ.EQ.2)GO TO 800
43600      IF(AT(M1,K1)-W11L)11,11,14
43700 C     CALCULATION OF THIRD BED REACTOR PROFILES
43800      14 IF(K5-2)800,461,462
43900 461   IF(Z2.NE.0.0)GO TO 800
44000 462   CONTINUE
44100      IF(Z3.NE.0.0)GO TO 404
44200      K5=K5-1;KL51=KL51-1
44300      GO TO 15
44400 404   XB12=AX(M1,K1)

```

## APPENDIX-B

RS

```

44500      PB1=AP(M1,K1)
44600      TH12=AT(M1,K1)
44700      IF(AFD3)27,28,27
44800  28  TB=AT(M1,K1)
44900      GO TO 29
45000  27  CALL MTEMP(TB,TH12,F1,FI12,FI22,FI32,FI42,FI52,Q13,Q23,Q33,Q43,
45100      1Q53,XB12,PB1,UV,C4,ICP26)
45200  29  C6=((S122-FTF1*XB12)*(AFD1+AFD4))**1.8*C61
45300      ZCTV=Z2+Z1;TB1=ATH(M1,K1)
45400      IF(IOPT3.NE.1)GO TO 128
45500  128  CALL RNUMI(M1,K1,K3,TB,AFD1,NZ3,MZ3,HA13,HA23,HAA23,AHA23,BHA23,
45600      1HA33,HA43,HA53,HA63,HA73,FI13,FI23,FI33,FI43,FI53,Z3,HL,H3,C6,
45700      2VW,C73,UA1,F,PH1,HAB23,AHA33,BHA33,CHA33,J,TB1 )
45800  125  IF(LQQ.EQ.2)GO TO 800
45900      IF(AT(M1,K1)-W11L)11,11,15
46000  C    CALCULATION OF HEAT EXCHANGER PROFILES
46100  15  IF(K5-2)800,470,471
46200  470  IF(Z2.NE.0.0)GO TO 800
46300      IF(Z3.NE.0.0)GO TO 800
46400      GO TO 468
46500  467  IF(Z3.EQ.0.0)GO TO 468
46600      IF(Z2.EQ.0.0)GO TO 468
46700      GO TO 800
46800  471  IF(K5.LE.3)GO TO 467
46900  468  IF(HL.NE.0.0)GO TO 425
47000      K5=K5-1
47100      GO TO 800
47200  425  UA11=HUA
47300      FI10=F1*AFD1;FI20=F2*AFD1;FI30=F3*AFD1;FI40=F4*AFD1
47400      FI50=F5*AFD1;Q101=-F1*AFD0;Q201=-F2*AFD0;Q301=-F3*AFD0
47500      Q401=-F4*AFD0;Q501=-F5*AFD0;PB12=PH2;AFD11=AFD1-AFD0
47600      XB12=0.0;TH12=ATH(M1,K1)
47700      IF(AFD0)200,201,200
47800  201  TB1=ATH(M1,K1)
47900      GO TO 202
48000  200  CALL MTEMP(TB1,TH12,F1,FI10,FI20,FI30,FI40,FI50,
48100      1Q101,Q201,Q301,Q401,Q501,

```

## RS APPENDIX=B

```

48200      1XB12,PB12,UV,C4,IOP26)
48300 202      CONTINUE
48400      TB=AT(M1,K1)
48500      C6=C62
48600      LK=2
48700      ZCTV=Z1+Z2+Z3
48800      IF(IOPT3.NE.1) GO TO 137
48900 137      CALL RNUMI(M1,K1,K3,TB,AFD11,NZ4,MZ4,HA14,HA24,HAA24,AHA24,BHA24,
49000      1HA34,HA44,HA54,HA64,HA74,FI13,FI23,FI33,FI43,FI53,HL,HL,H4,C6,
49100      2VW,C74,UA11,F,PH2,HAB24,AHA34,BHA34,CHA34,J,TB1  )
49200      11 TF=ATH(M1,K1)
49300 C        PRINT *,IOPT3,LQQ,UA1,UA11
49400 800      RETURN
49500      END
49600      SUBROUTINE RNUMI (M1,K1,K3,TB,FD1,NL,M2,HA1,HA2,HAA2,AHA2,BHA2,
49700      1HA3,HA4,HA5,HA6,HA7,FI1,FI2,FI3,FI4,FI5,Z1,HL,H,C6,VW,C7,UA1,F,
49800      2PH,HAB2,AHA3,BHA3,CHA3,J,TB1  )
49900 C        SUBROUTINE NO.2 FOR NUMERICAL INTEGRATION OF AMMONIA SYNTHESIS REAC
50000 C        DIFFERENTIAL EQUATIONS BY MILNE PREDICTOR AND CORRECTOR METHOD
50100      DIMENSION WX(310),WT(310),WTH(310),P(310),T(310),TH(310),
50200      1AZ(210,4),AP(210,4),AX(210,4),AT(210,4),ATH(210,4),ACX(210,4),
50300      2ACT(210,4),ACTH(210,4),XN(310),TN(310),THN(310),Z(310),X(310),
50400      3CX(310),CT(310),CTH(310),AXMAX(8),ATMAX(8),ATHMAX(8)
50500      4,ANX(210,4),AZP(210,4),ALPS8(8),SINTL(210,4),RINTL(210,4)
50600      4,QR1AV(210,4),WRXN(210,4),PDROP(8),AELP2(4,2),
50700      4WRXNS(210,4),EFZI8(210,4),QR1B(210,4),EFZIA(8),EFFZI(310)
50800      5,XE(310),XRM(310),AXE(210,4),AXRM(210,4),AXEN(210,4)
50900      6,AXRMN(210,4),M12(20),QR1(310),QHR3(310),QAK(310),QAKF(310),
51000      7QAKR(310),QAN1(310),QAN2(310),QAN3(310),QAN4(310),QAN5(310)
51100 C        4AXE2(4,310,4),AXRM2(4,310,4)
51200      COMMON/CB1/F1,F2,F3,F4,F5,LQQ,ITYPE,PARA1,PARA2,PARA3
51300      1,PARA4,IOP26,IOP29,FLPF
51400      1/CB2/AZ,AP,AX,AT,ATH,AXMAX
51500      1,ATMAX,ATHMAX,ALPS8,W11L,QR1AV,AXE2,AXRM2
51600      1,WRXN,WRXNS,RINTL,SINTL,EFZI8,QR1B,EFZIA,PDROP,IOL1
51700      1/CB4/ANX,ZTI,PAM,AZP/CB5/LK,AN3T,ZCTV
51800      2/CB20/ACX,ACT,ACTH

```

```
51900      2/CB9/FFL,RHNL,XINCL,XINCL2,TOL81,PHYL,PNIL,PAML,DELE,DELM
52000      3,IOL8,M88,IOP11,IOL81/CB7/ICSIZE,IOPT1,EFFAH,EFFAL
52100      3/CB8/AKR,AK,AKF,AELP8,ITYP,ZIF/CB6/AXE,AXRM,AXEN,AXRMN,M12
52200      4/CB35/QR1,QHR3,QAK,QAKF,QAKR,QAN1,QAN2,QAN3,QAN4,QAN5,EFFZI
52300      AB11=0.666667*FI1 ; FIT=FI1+FI2+FI3+FI4+FI5
52400      AZ1=Z1;WRXS=0.0;SINT=0.0;SEFZI=0.0
52500      I=1;LP17=1;ITYP=ITYPE
52600      Z(I)=0.0
52700      P(I)=AP(M1,K1)
52800      X(I)=AX(M1,K1);ABLPS=FI2-FI*0.3333333*AX(M1,K1)
52900      T(I)=TB
53000      TH(I)=TB1
53100      IF(K3=1)302,301,302
53200 302 K1=K1+1
53300 301 M1=1
53400      J=I
53500      AZ(M1,K1)=Z(I)
53600      AZP(M1,K1)=(Z(I)+ZCTV)*ZTI
53700      AP(M1,K1)=P(I)
53800      AX(M1,K1)=X(I)
53900      AT(M1,K1)=T(I)
54000      ACX(M1,K1)=0.0
54100      ACT(M1,K1)=0.0
54200      ACTH(M1,K1)=0.0
54300      ANX(M1,K1)=PAM
54400      IF(T(J)=W11L)304,304,303
54500 303 ATH(M1,K1)=TH(I)
54600      CALL DEV(I,WX,WT,WTH,P,T,TH,X,FD1,
54700      1FI1,FI2,FI3,FI4,FI5,F,AZ1,HL,UA1,PH)
54800      IF(LQG.EQ.2)GO TO 800
54900      IF(LK.EQ.2)GO TO 206
55000      IF(IOPT1.NE.1)GO TO 206
55100      CALL CONV(X,XE,XRM,P,T,J,AELP2)
55200      AXE(M1,K1)=XE(J)
55300      AXRM(M1,K1)=XRM(J)
55400      CALL AMMC(AN3E,AN3MR,AB11,FI3,FIT,XE,XRM,J)
55500      AXEN(M1,K1)=AN3E
```

## RS APPENDIX-B

```

55600      AXRMN(M1,K1)=AN3MR
55700 C      DO 704 LQ2P=1,4
55800 C      AXE2(LQ2P,M1,K1)=AELP2(LQ2P,1)
55900 C      AXRM2(LQ2P,M1,K1)=AELP2(LQ2P,2)
56000 704      CONTINUE
56100 206      ANX(M1,K1)=AN3T
56200      HC6=C6*H
56300      Z(I+1)=H
56400      P(I+1)=P(I)-HC6
56500      X(I+1)=X(I)+H*WX(I)
56600      T(I+1)=T(I)+H*WT(I)
56700      TH(I+1)=TH(I)+H*WTH(I)
56800      4 J=I+1
56900      IF(T(J)-W11L)304,304,305
57000 305 CALL DEV(J,WX,WT,WTH,P,T,TH,X,FD1,
57100      1FI1,FI2,FI3,FI4,FI5,F,AZ1,HL,UA1,PH      )
57200      IF(X(J).LT.0.0)LQ2=2
57300      IF(LQ2.EQ.2)GO TO 800
57400      TN(I+1)=T(I)+HA1*(WT(J)+WT(I))
57500      XN(I+1)=X(I)+HA1*(WX(J)+WX(I))
57600      THN(I+1)=TH(I)+HA1*(WTH(J)+WTH(I))
57700      CX(I+1)=(XN(I+1)-X(I+1))
57800      CT(I+1)=(TN(I+1)-T(I+1))
57900      CTH(I+1)=(THN(I+1)-TH(I+1))
58000      X(I+1)=XN(I+1)
58100      T(I+1)=TN(I+1)
58200      TH(I+1)=THN(I+1)
58300      IF(ABS(CX(I+1))-VW*0.01)1,1,4
58400      1 IF(ABS(CT(I+1))-VW)5,5,4
58500      5 IF(ABS(CTH(I+1))-VW)3,3,4
58600      3 M1=M1+1
58700      IF(LK.EQ.2)GO TO 8
58800      IF(LP17.EQ.2)GO TO 422
58900      IF(X(J).GT.X(J-1))GO TO 431
59000      AXMAX(K1)=X(J-1);ATMAX(K1)=T(J-1);ATHMAX(K1)=TH(J-1)
59100      ALPS8(K1)=(Z(J-1)+ZCTV)*ZTI;LP17=2
59200      GO TO 431

```

## APPENDIX-B

RS

```

59300 422      IF(AXMAX(K1).GE.X(J))GO TO 431
59400          AXMAX(K1)=X(J);ATMAX(K1)=T(J);ATHMAX(K1)=TH(J)
59500          ALPS8(K1)=(Z(J)+ZCTV)*ZTI
59600 431      IF(IOPT1,NE.1)GO TO 8
59700          IF(IOP11.EQ.1)GO TO 8
59800          CALL CONV(X,XE,XRM,P,T,J,AELP2)
59900          AXE(M1,K1)=XE(J)
60000          AXRM(M1,K1)=XRM(J)
60100          CALL AMNC(AN3E,AN3MR,AB11,FI3,FIT,XE,XRM,J)
60200          AXEN(M1,K1)=AN3E
60300          AXRMN(M1,K1)=AN3MR
60400 C        DO 710 LQ2P=1,4
60500 C          AXE2(LQ2P,M1,K1)=AELP2(LQ2P,1)
60600 C          AXRM2(LQ2P,M1,K1)=AELP2(LQ2P,2)
60700 710      CONTINUE
60800      8 CONTINUE
60900          AX(M1,K1)=X(I+1)
61000          AT(M1,K1)=T(I+1)
61100          ATH(M1,K1)=TH(I+1)
61200          ACT(M1,K1)=CT(I+1)
61300          ACX(M1,K1)=CX(I+1)
61400          ACTH(M1,K1)=CTH(I+1)
61500          AZ(M1,K1)=Z(I+1)*0.000001
61600          AZP(M1,K1)=(Z(I+1)+ZCTV) *ZTI
61700          ANX(M1,K1)=AN3T
61800          AP(M1,K1)=P(I+1)
61900          X(I+2)=X(I+1)+HA1*(3.0*WX(J)-WX(I))
62000          T(I+2)=T(I+1)+HA1*(3.0*WT(J)-WT(I))
62100          TH(I+2)=TH(I+1)+HA1*(3.0*WTH(J)-WTH(I))
62200          Z(I+2)=Z(I+1)+H
62300          P(I+2)=P(I+1)-HC6
62400          WXI1=HAB2*WX(I+1)
62500          WXI2=HA2*WX(I)
62600          WTI1=HAB2*WT(I+1)
62700          WTI2=HA2*WT(I)
62800          WTHI1=HAB2*WTH(I+1)
62900          WTHI2=HA2*WTH(I)

```

RS APPENDIX-B

```

63000 12 J=I+2
63100 IF(T(J)-W11L)304,304,306
63200 306 CALL DEV(J,WX,WT,WTH,P,T,TH,X,FD1,
63300 1FI1,FI2,FI3,FI4,FI5,F,AZ1,HL,UA1,PH )
63400 IF(X(J).LT.0.0)LOQ=2
63500 IF(LOQ.EQ.2)GO TO 800
63600 XN(I+2)=X(I+1)+HAA2*WX(J)+WXI1-WXI2
63700 TN(I+2)=T(I+1)+HAA2*WT(J)+WTI1-WTI2
63800 THN(I+2)=TH(I+1)+HAA2*WTH(J)+WTHI1-WTHI2
63900 CX(I+2)=(XN(I+2)-X(I+2))
64000 CT(I+2)=(TN(I+2)-T(I+2))
64100 X(I+2)=XN(I+2)
64200 CTH(I+2)=(THN(I+2)-TH(I+2))
64300 T(I+2)=TN(I+2)
64400 TH(I+2)=THN(I+2)
64500 IF(ABS(CX(I+2))-VW*0.01)11,11,12
64600 11 IF(ABS(CT(I+2))-VW)14,14,12
64700 14 IF(ABS(CTH(I+2))-VW)15,15,12
64800 15 M1=M1+1
64900 IF(LK.EQ.2)GO TO 17
65000 IF(LP17.EQ.2)GO TO 425
65100 IF(X(J).GT.X(J-1))GO TO 434
65200 AXMAX(K1)=X(J-1);ATMAX(K1)=T(J-1);ATHMAX(K1)=TH(J-1)
65300 ALPS8(K1)=(Z(J-1)+ZCTV)*ZTI;LP17=2
65400 GO TO 434
65500 425 IF(AXMAX(K1).GE.X(J))GO TO 434
65600 AXMAX(K1)=X(J);ATMAX(K1)=T(J);ATHMAX(K1)=TH(J)
65700 ALPS8(K1)=(Z(J)+ZCTV)*ZTI
65800 434 IF(IOPT1.NE.1)GO TO 17
65900 IF(IOP11.EQ.1)GO TO 17
66000 CALL CONV(X,XE,XRM,P,T,J,AELP2)
66100 AXE(M1,K1)=XE(J)
66200 AXRM(M1,K1)=XRM(J)
66300 CALL AMMC(AN3E,AN3MR,AB11,FI3,FIT,XE,XRM,J)
66400 AXEN(M1,K1)=AN3E
66500 AXRMN(M1,K1)=AN3MR
66600 C DO 713 LO2P=1,4

```

RS

APPENDIX-B

```

66700 C      AXE2(LQ2P,M1,K1)=AELP2(LQ2P,1)
66800 C      AXRM2(LQ2P,M1,K1)=AELP2(LQ2P,2)
66900 713    CONTINUE
67000 17     AX(M1,K1)=X(J)
67100       AT(M1,K1)=T(J)
67200       ATH(M1,K1)=TH(J)
67300       ACT(M1,K1)=CT(J)
67400       ACTH(M1,K1)=CTH(J)
67500       ACX(M1,K1)=CX(J)
67600       AZ(M1,K1)=Z(J)*0.000001
67700       AZP(M1,K1)=(Z(J)+ZCTV)*ZTI
67800       ANX(M1,K1)=AN3T
67900       AP(M1,K1)=P(J)
68000       X(I+3)=X(I+2)+AHA2*WX(I+2)-BHA2*WX(I+1)+HAA2*WX(I)
68100       T(I+3)=T(I+2)+AHA2*WT(I+2)-BHA2*WT(I+1)+HAA2*WT(I)
68200       TH(I+3)=TH(I+2)+AHA2*WTH(I+2)-BHA2*WTH(I+1)+HAA2*WTH(I)
68300       Z(I+3)=Z(I+2)+H
68400       P(I+3)=P(I+2)-HC6
68500       WXN1=BHA3*WX(I+2)
68600       WXN2=CHA3*WX(I+1)
68700       WXN3=HA3*WX(I)
68800       WTN1=BHA3*WT(I+2)
68900       WTN2=CHA3*WT(I+1)
69000       WTHN1=BHA3*WTH(I+2)
69100       WTN3=HA3*WT(I)
69200       WTHN2=CHA3*WTH(I+1)
69300       WTHN3=HA3*WTH(I)
69400 22     J=I+3
69500       IF(T(J)-W11L)304,304,307
69600 307    CALL DEV(J,WX,WT,WTH,P,T,TH,X,FD1,
69700       1FI1,FI2,FI3,FI4,FI5,F,AZ1,HL,UA1,PH)
69800       IF(X(J).LT.0.0)LQQ=2
69900       IF(LQQ.EQ.2)GO TO 800
70000       XN(I+3)=X(I+2)+AHA3*WX(I+3)+WXN1-WXN2+WXN3
70100       TN(I+3)=T(I+2)+AHA3*WT(I+3)+WTN1-WTN2+WTN3
70200       THN(I+3)=TH(I+2)+AHA3*WTH(I+3)+WTHN1-WTHN2+WTHN3
70300       CX(I+3)=(XN(I+3)-X(I+3))

```



RS

## APPENDIX-B

```

70400      CT(I+3)=(TN(I+3)-T(I+3))
70500      CTH(I+3)=(THN(I+3)-TH(I+3))
70600      X(I+3)=XN(I+3)
70700      T(I+3)=TN(I+3)
70800      TH(I+3)=THN(I+3)
70900      IF(ABS(CX(I+3))-VW*0.01)21,21,22
71000  21  IF(ABS(CT(I+3))-VW)23,23,22
71100  23  IF(ABS(CTH(I+3))-VW)24,24,22
71200  24  M1=M1+1
71300      IF(LK.EQ.2)GO TO 26
71400      IF(LP17.EQ.2)GO TO 416
71500      IF(X(J).GT.X(J-1))GO TO 440
71600      AXMAX(K1)=X(J-1);ATMAX(K1)=T(J-1);ATHMAX(K1)=TH(J-1)
71700      ALPS8(K1)=(Z(J-1)+ZCTV)*ZTI;LP17=2
71800      GO TO 440
71900  416  IF(AXMAX(K1).GE.X(J))GO TO 440
72000      AXMAX(K1)=X(J);ATMAX(K1)=T(J);ATHMAX(K1)=TH(J)
72100      ALPS8(K1)=(Z(J)+ZCTV)*ZTI
72200  440  IF(IOP11.NE.1)GO TO 26
72300      IF(IOP11.EQ.1)GO TO 26
72400      CALL CONV(X,XE,XRM,P,T,J,AELP2)
72500      AXE(M1,K1)=XE(J)
72600      AXRM(M1,K1)=XRM(J)
72700      CALL AMMC(AN3E,AN3MR,AB11,F13,FIT,XE,XRM,J)
72800      AXEN(M1,K1)=AN3E
72900      AXRMN(M1,K1)=AN3MR
73000  C    DO 719 LG2P=1,4
73100  C    AXE2(LG2P,M1,K1)=AELP2(LG2P,1)
73200  C    AXRM2(LG2P,M1,K1)=AELP2(LG2P,2)
73300  719  CONTINUE
73400  26  CONTINUE
73500      AX(M1,K1)=X(J)
73600      AT(M1,K1)=T(J)
73700      ATH(M1,K1)=TH(J)
73800      ACT(M1,K1)=CT(J)
73900      ACTH(M1,K1)=CTH(J)
74000      ACX(M1,K1)=CX(J)

```

## RS APPENDIX-B

```

74100      AZ(M1,K1)=Z(J)*0.000001
74200      AZP(M1,K1)=(Z(J)+ZCTV)*ZTI
74300      ANX(M1,K1)=AN3T
74400      AP(M1,K1)=P(J)
74500      L11=1
74600      K=1
74700  101  X(K+4)=X(K)+HA4*WX(K+2)+HA5*(WX(K+3)-2.0*WX(K+2)+WX(K+1))
74800      T(K+4)=T(K)+HA4*WT(K+2)+HA5*(WT(K+3)-2.0*WT(K+2)+WT(K+1))
74900      TH(K+4)=TH(K)+HA4*WTH(K+2)+HA5*(WTH(K+3)-2.0*WTH(K+2)+WTH(K+1))
75000      Z(K+4)=Z(K+3)+H
75100      P(K+4)=P(K+3)-HC6
75200      IF(L11-1) 25,89,25
75300  25  X(K+4)=X(K+4)+CX(K+3)
75400      T(K+4)=T(K+4)+CT(K+3)
75500      TH(K+4)=TH(K+4)+CTH(K+3)
75600  89  L11=2
75700      WXK1=HA6*WX(K+3)
75800      WTK1=HA6*WT(K+3)
75900      WTHK1=HA6*WTH(K+3)
76000      WXK2=WXK1/3.0
76100      WXK3=HA7*WX(K+2)
76200      WTK2=WTK1/3.0
76300      WTK3=HA7*WT(K+2)
76400      WTHK2=WTHK1/3.0
76500      WTHK3=HA7*WTH(K+2)
76600  29  J=K+4
76700      IF(T(J)-W11L)304,304,308
76800  308  CALL DEV(J,WX,WT,WTH,P,T,TH,X,FD1,
76900      1FI1,FI2,FI3,FI4,FI5,E,AZ1,HL,UA1,PH)
77000      IF(X(J).LT.0.0)LQ0=2
77100      IF(LQ0.EQ.2)GO TO 800
77200      XN(K+4)=X(K+2)+WXK1+HA7*WX(K+4)-WXK2+W XK3
77300      TN(K+4)=T(K+2)+WTK1+HA7*WT(K+4)-WTK2+WTK3
77400      THN(K+4)=TH(K+2)+WTHK1+HA7*WTH(K+4)-WTHK2+WTHK3
77500      CX(K+4)=(XN(K+4)-X(K+4))
77600      CT(K+4)=(TN(K+4)-T(K+4))
77700      X(K+4)=XN(K+4)

```

## RS APPENDIX-B

```

77800      CTH(K+4)=(THN(K+4)-TH(K+4))
77900      T(K+4)=TN(K+4)
78000      TH(K+4)=THN(K+4)
78100      IF(ABS(CX(K+4))-VW*0.01)31,31,29
78200  31  IF(ABS (CT(K+4))-VW)32,32,29
78300  32  IF(ABS(CTH(K+4))-VW)33,33,29
78400  33  IF(LK.EQ.2)GO TO 38
78500      IF(LP17.EQ.2)GO TO 407
78600      IF(X(K+4).GT.X(K+3))GO TO 542
78700      AXMAX(K1)=X(K+3);ATMAX(K1)=T(K+3);ATHMAX(K1)=TH(K+3)
78800      ALPS8(K1)=(Z(K+3)+ZCTV)*ZTI;LP17=2
78900      GO TO 542
79000  407  IF(AXMAX(K1).GE.X(J))GO TO 542
79100      AXMAX(K1)=X(J);ATMAX(K1)=T(J);ATHMAX(K1)=TH(J)
79200      ALPS8(K1)=(Z(J)+ZCTV)*ZTI
79300  542  IF(IOPT1.NE.1)GO TO 38
79400      IF(IOP11.EQ.1)GO TO 38
79500      CALL CONV(X,XE,XRM,P,T,J,AELP2)
79600      AXE((M1+1),K1)=XE(J)
79700      AXRM((M1+1),K1)=XRM(J)
79800      CALL AMNC(AN3E,AN3MR,AB11,FI3,FIT,XE,XRM,J)
79900      AXEN((M1+1),K1)=AN3E
80000      AXRMN((M1+1),K1)=AN3MR
80100  C    DO 722 LQ2P=1,4
80200  C    AXE2(LQ2P,(M1+1),K1)=AELP2(LQ2P,1)
80300  C    AXRM2(LQ2P,(M1+1),K1)=AELP2(LQ2P,2)
80400  722  CONTINUE
80500  38  M3=K+4
80600      M4=M2*(M1-3)
80700      IF(M3-M4)34,34,35
80800  35  M1=M1+1
80900      AZ(M1,K1)=Z(M3) *0.000001
81000      AP(M1,K1)=P(M3)
81100      AX(M1,K1)=X(M3)
81200      AT(M1,K1)=T(M3)
81300      ATH(M1,K1)=TH(M3)
81400      ACX(M1,K1)=CX(M3)

```

```
81500      ACT(M1,K1)=CT(M3)
81600      ACTH(M1,K1)=CTH(M3)
81700      AZP(M1,K1)=(Z(J)+ZCTV)*ZTI
81800      ANX(M1,K1)=AN3T
81900      34 IF(K-NL)191,192,192
82000      191 K=K+1
82100      GO TO 101
82200      192 K3=K3+1
82300      IF(LK.EQ.2)GO TO 309
82400      IF(LP17.EQ.2)GO TO 309
82500      ALPS8(K1)=(Z(K+4)+ZCTV)*ZTI;AXMAX(K1)=X(K+4)
82600      ATMAX(K1)=T(K+4);ATHMAX(K1)=TH(K+4);LP17=1
82700 C      PRINT *,IOPT1,LQQ,((AZP(I,J),AT(I,J),ATH(I,J),I=1,M1),J=1,K1)
82800      GO TO 309
82900 304      M1=M1+1
83000      AT(M1,K1)=T(J)
83100      AX(M1,K1)=X(J)
83200      ATH(M1,K1)=TH(J)
83300      IF(IOL1.NE.2)GO TO 309
83400      PRINT 935,F1,F2,F3,F4,F5,(N,X(N),T(N),TH(N),P(N),QAN1(N),QAN2(N)
83500      1QAN3(N),QAN4(N),QAN5(N),QR1(N),QHR3(N),QAK(N),QAKF(N),QAKR(N),
83600      2WX(N),WT(N),WTH(N),N=1,J)
83700      IF(ITYPE.NE.2)GO TO 309
```

RS

APPENDIX-B

```

00100      TYPE 935,F1,F2,F3,F4,F5,(N,X(N),T(N),TH(N),P(N),QAN1(N),QAN2(N),
00200      1QAN3(N),QAN4(N),QAN5(N),QR1(N),QHR3(N),QAK(N),QAKF(N),QAKR(N),
00300      2WX(N),WT(N),WTH(N),N=1,J)
00400 935      FORMAT(2X,5F10.1/(2X,I5,F10.3,8F10.1/2X,8E10.3/))
00500 309      M12(K1)=M1;JJ1=J-1;LP17=1
00600          PDROP(K1)=P(1)-P(J)
00700          IF(IOP11.NE.1)GO TO 701
00800          CALL CONV(X,XE,XRM,P,T,J,AELP2)
00900          AXE(M1,K1)=XE(J)
01000          AXRM(M1,K1)=XRM(J)
01100          CALL AMMC(AN3E,AN3MR,AB11,FI3,FIT,XE,XRM,J)
01200          AXEN(M1,K1)=AN3E
01300          AXRMN(M1,K1)=AN3MR
01400 C          DO 728 LQ2P=1,4
01500 C          AXE2(LQ2P,M1,K1)=AELP2(LQ2P,1)
01600 C          AXRM2(LQ2P,M1,K1)=AELP2(LQ2P,2)
01700 728      CONTINUE
01800 701      IF(LK.EQ.2)GO TO 800
01900          DO 830 I=1,JJ1
02000          EFZI8(I,K1)=EFFZI(I)
02100          QR1B(I,K1)=QR1(I);SEFZI=EFFZI(I)+SEFZI
02200          WRXN(I,K1)=(QR1(I+1)-QR1(I))*2.016/(T(I+1)-T(I))
02300          WRXNS(I,K1)=WRXN(I,K1)+WRXS;WRXS=WRXNS(I,K1)
02400          QR1AV(I,K1)=(QR1(I+1)+QR1(I))*1.008
02500          IF(QR1AV(I,K1).NE.0.0)GO TO 557
02600          RINTL(I,K1)=1.0E8
02700          GO TO 566
02800 557      RINTL(I,K1)=WRXN(I,K1)*(X(I+1)-X(I))/(QR1AV(I,K1)*QR1AV(I,K1))
02900 566      SINTL(I,K1)=RINTL(I,K1)+SINT;SINT=SINTL(I,K1)
03000 830      CONTINUE
03100          EFZI8(J,K1)=EFFZI(J);EFZIA(K1)=(SEFZI+EFFZI(J))/J
03200 800      RETURN
03300          END
03400          SUBROUTINE DEV(I,WX,WT,WTH,P,T,TH,X,FD1,
03500          1FI1,FI2,FI3,FI4,FI5,F,AZ1,HL,UA1,PH)
03600 C          SUBROUTINE NO.3 FOR CALCULATION OF DERIVATIVE VALUES FROM AMMONIA
03700 C          SYNTHESIS REACTOR

```

```
03800 C EQUATIONS FOR NUMERICAL INTEGRATION
03900 DIMENSION WX(310),WT(310),WTH(310),P(310),T(310),TH(310),X(310)
04000 1,QR1(310),QHR3(310),QAK(310),QAKF(310),QAKR(310),QAN1(310),
04100 2QAN2(310),QAN3(310),QAN4(310),QAN5(310),EFFZI(310)
04200 COMMON/CB1/F1,F2,F3,F4,F5,LQQ,ITYPE,PARA1,PARA2,PARA3
04300 1,PARA4,IOP26,IOP29,FLPF
04400 1/CB5/LK,AN3T,ZCTV
04500 2/CB7/ICSIZE,IOPT1,EFFAH,EFFAL/CB8/AKR,AK,AKF,ABLP8,ITYP,EFFAC
04600 3/CB35/QR1,QHR3,QAK,QAKF,QAKR,QAN1,QAN2,QAN3,QAN4,QAN5,EFFZI
04700 PP=P(I);ITYP=ITYPE
04800 TT=T(I)
04900 THH=TH(I)
05000 AB=F1*X(I)
05100 AN1=FI1-AB
05200 AB1=0.33333*AB
05300 AN2=FI2-AB1
05400 AN3=FI3+0.66667*AB
05500 C EFFECTIVENESS FACTOR EFFECT
05600 IF(LK.EQ.2)GO TO 314
05700 IF(ICSIZE.EQ.2)GO TO 305
05800 ETA=AN3/(AN3+2.0*AN2)
05900 CALL ZIFA(EFFAC,PP,TT,ETA,BLP1,BLP2,BLP3,BLP4,BLP5,BLP6)
06000 EFFZI(I)=EFFAC
06100 IF(EFFAC.GE.EFFAH)GO TO 107
06200 IF(EFFAC.LE.EFFAL)EFFAC=EFFAL
06300 GO TO 314
06400 107 EFFAC=EFFAH
06500 GO TO 314
06600 305 EFFAC=1.0
06700 314 CONTINUE
06800 AN4=FI4
06900 AN5=FI5
07000 ANT=AN1+AN2+AN3+AN4+AN5
07100 ANTI=1/ANT;Y1=AN1*ANTI;Y2=AN2*ANTI;Y3=AN3*ANTI;Y13=Y1/Y3
07200 Y13S=Y13*Y13;ALPHA=PARA3*0.5;Y13P=Y1*Y13S*PP;Y13PA=Y13P**ALPHA
07300 AN3T=100.*Y3
07400 IF(LK.EQ.2) GO TO 202
```

```
07500      TT11=TT-273.0
07600 201   IF(IOP29-2)404,407,408
07700 407   HR3=-10906.0-(5.293-(3.429E-3-2.01E-6*TT11)*TT11)*TT11
07800      GO TO 422
07900 408   HR3=- (0.54526+(840.609+459.734E6/(TT*TT))/TT)*PP-
08000      1(5.34685+(.2525E-3-1.69167E-6*TT)*TT)*TT-9157.09
08100      GO TO 422
08200 404   HR3=-15564.51+(7.0646-(14.8399E-03-(3.3563E-07-1.1625E-10*TT)*
08300 1TT)*TT)*TT-PP*(3.01975-(4.4552E-03-1.928E-06*TT)*TT)
08400      AK=EXP (0.50327*(9184.0/TT-7.2949*ALOG (TT)+(3.4966E-03+
08500 1(1.6781E-07-3.875E-11*TT)*TT)*TT+23.05))
08600      GO TO 416
08700 422   AK17=(2250.322/TT-C.8534-0.656*ALOG(TT)-(2.58987E-4-
08800 11.48961E-7*TT)*TT)
08900      AK=10**AK17
09000 416   CONTINUE
09100      AKF=(1.7343-8.143E-04*PP+
09200 1(5.714E-07*PP-2.6714E-03+2.0E-06*TT)*TT)*PARA4
09300      AKKF=AK/AKF;AKSQ=AKKF*AKKF
09400      PANT=PP*Y1
09500      IF(PP)11,11,15
09600 15 IF(PANT)11,11,12
09700 11 PRINT 14,PANT,PP
09800      IF(ITYPE.NE.2)GO TO 35
09900      TYPE 14,PANT,PP
10000 14 FORMAT(1X,5HPANT= ,E15.6,10H,PRESSURE= ,F10.4 /)
10100 35     LQQ=2
10200      GO TO 800
10300 12 SPANT=SQRT(PANT)
10400      AKR=((300.0/PP)**0.63)*EXP (-24092.2*(PARA2/TT)+(33.5566/PARA1))
10500      R11=29.4204*(AKSQ*PP*Y2-1/Y13P)*Y13PA*F*AKR*1.0E-06
10600      R1=R11*EFFAC
10700      B7=-0.666667*HR3*R1
10800      GO TO 203
10900 202 R1=0.0
11000      B7=0.0
11100 203 WX(I)=R1/F1;UALP1=UA1*FLPF**0.8
```

## RS APPENDIX-B

```

11200      B4=-UALP1*(TT-THH)
11300      B1=B7+B4
11400      CALL HEATC (CP1,CP2,CP3,CP4,CP5,PP,TT,IOP26      )
11500      B2=AN1*CP1+AN2*CP2+AN3*CP3+AN4*CP4+AN5*CP5
11600      WT(I)=B1/B2
11700      CALL HEATC (CP1,CP2,CP3,CP4,CP5,PH,THH,IOP26)
11800      B3=FD1*(F1*CP1+F2*CP2+F3*CP3+F4*CP4+F5*CP5      )
11900      WTH(I)=B4/B3
12000      QR1(I)=R1;QHR3(I)=HR3;QAK(I)=AK;QAKF(I)=AKF;QAKR(I)=AKR
12100      QAN1(I)=AN1;QAN2(I)=AN2;QAN3(I)=AN3;QAN4(I)=AN4;QAN5(I)=AN5
12200 800  RETURN
12300      END
12400 C      SUBROUTINE NO.4 FOR CALCULATION OF MIXTURE STREAM TEMPERATURE BY TR
12500 C      AND ERROR TECHNIQUE
12600      SUBROUTINE MTEMP(TB21,TB12,F1,R11,R22,R33,R44,R55,Q1,Q2,Q3,Q4,Q5,
12700      1XB12,PB1,UV,C4,IOP26)
12800      I=1;C41=0.5
12900      RT=R11+R22+R33+R44+R55-0.666667*F1*XB12
13000      QT=Q1+Q2+Q3+Q4+Q5
13100      W1=(RT*TB12+QT*UV)/(RT+QT)
13200      192 TB21=W1
13300      CALL TEMP(AT1,F1,R11,R22,R33,R44,R55,Q1,Q2,Q3,Q4,Q5,XB12,PB1,
13400      1TB12,TB21,UV,IOP26)
13500      DELT1=AT1-W1
13600      IF(ABS(DELT1)-C41) 151,151,191
13700      191 IF(I-1)153,152,153
13800      152 W2=AT1
13900 134      TB21=W2
14000      CALL TEMP(AT2,F1,R11,R22,R33,R44,R55,Q1,Q2,Q3,Q4,Q5,XB12,PB1,
14100      1TB12,TB21,UV,IOP26)
14200      DELT2=AT2-W2
14300      IF(ABS(DELT2)-C41)154,154,153
14400      153 DW12=(W1-W2)
14500      I=I+1
14600      IF(DELT1)1,151,5
14700      1 IF(DELT2)2,154,7
14800      5 IF(DELT2)7,154,2

```



## RS APPENDIX-B

```
14900 2 IF(ABS(DELT1)-ABS(DELT2))161,161,162
15000 161 W2=W1+DW12
15100 GO TO 134
15200 162 W1=W2-DW12
15300 GO TO 192
15400 7 W3=W2+(W1-W2)*ABS(DELT2)/(ABS(DELT2)+ABS(DELT1))
15500 IW3=W3*100.0+0.5;W3=IW3*0.01
15600 TB21=W3
15700 CALL TEMP(AT3,F1,R11,R22,R33,R44,R55,Q1,Q2,Q3,Q4,Q5,XB12,PB1,
15800 1TB12,TB21,UV,IOP26)
15900 DELT3=AT3-W3
16000 IF(ABS(DELT3)-C41)170,170,188
16100 170 TB21=AT3
16200 GO TO 155
16300 188 IF(DELT3)11,170,35
16400 11 IF(DELT2)17,154,26
16500 35 IF(DELT2)26,154,17
16600 17 W2=W3
16700 DELT2=DELT3
16800 GO TO 7
16900 26 W1=W3
17000 DELT1=DELT3
17100 GO TO 7
17200 154 TB21=AT2
17300 GO TO 155
17400 151 TB21=AT1
17500 155 RETURN
17600 END
17700 SUBROUTINE TEMP(T,F1,R11,R22,R33,R44,R55,Q1,Q2,Q3,Q4,Q5,XB12,
17800 1PB1,TB12,TB21,UV,IOP26)
17900 C SUBROUTINE NO. 5 FOR CALCULATION OF MIXTURE TEMPERATURE FROM ENTHAL
18000 C BALANCE
18100 XBF1=F1*XB12
18200 R1=R11-XBF1
18300 R2=R22-0.33333*XBF1
18400 R3=R33+0.66667*XBF1
18500 R4=R44
```

RS

## APPENDIX-B

```

18600      R5=R55
18700      CALL HEATC(CP1,CP2,CP3,CP4,CP5,PB1,TB12,IOP26  )
18800      C1=TB12*(R1*CP1+R2*CP2+R3*CP3+R4*CP4+R5*CP5  )
18900      CALL HEATC(CP1,CP2,CP3,CP4,CP5,PB1,UV,IOP26  )
19000      C2=UV*(Q1*CP1+Q2*CP2+Q3*CP3+Q4*CP4+Q5*CP5  )
19100      CALL HEATC(CP1,CP2,CP3,CP4,CP5,PB1,TB21,IOP26  )
19200      C3=(R1+Q1)*CP1+(R2+Q2)*CP2+(R3+Q3)*CP3+(R4+Q4)*CP4+(R5+Q5)*CP5
19300      T=(C1+C2)/C3
19400      RETURN
19500      END
19600      SUBROUTINE HEATC(CP1,CP2,CP3,CP4,CP5,P,T,IOP)
19700 C      SUBROUTINE NO. 6 FOR CALCULATION OF HEAT CAPACITY AT GIVEN TEMPERAT
19800 C      AND PRESSURE
19900          T11=T-273.0
20000          IF(IOP-2)2,3,8
20100 3          CP3=8.497+(8.001E-3-1.764E-6*T11)*T11
20200          GO TO 17
20300 2          CP3=102.7524-(21.63767E-02-(13.12707E-05-1.5981E-09*T)*T)*T-
20400          1P*(6.7571E-02-(1.6847E-04-1.009514E-07*T)*T)
20500 17          CP1=6.952-(4.576E-04-(9.563E-07-2.079E-10*T)* T)*T
20600          CP2=6.903-(3.753E-04-(1.93E-06-6.861E-10*T)*T)*T
20700          CP4=4.750+(1.2E-02+(3.03E-06-2.63E-09*T)*T)*T
20800          GO TO 11
20900 8          CP3=8.497+(8.001E-3-1.764E-6*T11)*T11
21000 C          CPNH2=8.62+(0.002+7.2E-9*TT11)*TT11
21100          CP2=6.822+(1.631E-3-0.345E-6*TT11)*TT11
21200 C          CPN2=6.815+(317E-4+5.3E-8*TT11)*TT11
21300          CP1=6.919+(0.218E-3+0.279E-6*TT11)*TT11
21400 C          CPH2=6.5+0.0009*TT11
21500          CP4=3.00+(0.0228-4.8E-6*T)*T
21600 11          CP5=4.9675
21700      RETURN
21800      END
21900 C      SUBROUTINE NO. 21
22000 C      RUNGE KUTTA FOURTH ORDER NUMERICAL INTEGRATION
22100 C      METHOD. ERROR IS APPROXIMATELY FIFTH POWER OF H.
22200 C      SUBROUTINE NO.7 FOR CALCULATION OF EFFECTIVE

```

RS

## APPENDIX-B

22300 C      MASS FACTOR OF LARGER SIZE CATALYST  
22400 C      PARTICLES OF 6MM AND 10 MM  
22500      SUBROUTINE ZIFA(ZIF,P,T,ETA,B1,B2,B3,B4,B5,B6)



RS

## APPENDIX-B

```

00100      IF(P=150.0)20,26,35
00200      35 IF(P=225.0)20,26,47
00300      47 IF(P=300.0)71,26,71
00400      26 CB0=1 ; CB1=1 ; CB2=1 ; CB3=1 ; CB4=1 ; CB5=1 ; CB6=1
00500      IF(P=225)44,56,80
00600      44 B0=-17.539096*CB0 ; E1=0.07697849*CB1
00700      B2=6.900548*CB2 ; B3=-1.08279E-4*CB3
00800      B4=-26.42469*CB4 ; B5=4.927648E-8*CB5
00900      B6=38.93727*CB6
01000      GO TO 200
01100      56 B0=-8.2125534*CB0 ; E1=0.03774149*CB1
01200      B2=6.190112*CB2 ; B3=-0.5354571E-4*CB3
01300      B4=-20.86963*CB4 ; B5=2.379142E-8*CB5
01400      B6=27.88403*CB6
01500      GO TO 200
01600      80 B0=-4.6757259*CB0 ; E1=0.02354872*CB1
01700      B2=4.687353*CB2 ; B3=-0.3463308E-4*CB3
01800      B4=-11.28031*CB4 ; B5=1.540881E-8*CB5
01900      B6=10.46627*CB6
02000      GO TO 200
02100      20 CB0=2.06351463-0.007090097*P ; CB1=2.019427635-0.006796184*P
02200      CB2=1.205907125-0.001372714*P ; CB3=2.010967778-0.006739785*P
02300      CB4=1.420444667-0.002802964*P ; CB5=2.03437015-0.0068958*P
02400      CB6=1.567746018-0.003784973*P
02500      GO TO 44
02600      71 CB0=4.025692759-0.010085642*P;CB1=3.410792604-0.008035975*P
02700      CB2=2.282394563-0.004274648*P;CB3=3.184342831-0.007281142*P
02800      CB4=4.400374635-0.011334582*P;CB5=3.176056425-0.007253521*P
02900      CB6=7.656721067-0.02218907*P
03000      GO TO 80
03100      200 ZIF=B0+(B1+(B3+B5*T)*T)*T+(B2+(B4+B6*ETA)*ETA)*ETA
03200      RETURN
03300      END
03400 C      SUBROUTINE NO. 8 FOR CALCULATION OF
03500 C      CONVERSION AT EQUILIBRIUM AND MAXIMUM
03600 C      REACTION RATE AT CONVERGED VALUES IN THE
03700 C      CATALYST BED

```

## APPENDIX-B

RS

```

03800 SUBROUTINE CONV(XACT,XE,XRM,P,T,I,AELP2)
03900 DIMENSION XACT(310),XE(310),XRM(310),XY(310),P(310),
04000 1T(310),ADELP(4),AELP2(4,2),RATE(800)
04100 COMMON/CB8/AKR,AK,AKF,ABLP8,ITYPE,ZIF
04200 1/CB9/FF,RATIO,XINCL,XINCL2,TOL8,FC1,FC2,FC3,DELE,DELM
04300 1,IOL8,M88,IOP11,ICL81
04400 1/CB26/CONSL7,CONSL8,SCONL8,TWTH,PP,TT,DAKR,DAK,DAKF,RAKKE
04500 REAL KC1,KC2,KC3
04600 J=1;PP=P(I) ; TT=T(I)
04700 RAKKE=AK/AKF ; SRAE=RAKKE*RAKKE
04800 CONP=1.29904*PP ; MC=1 ; KC1=CONP*RAKKE
04900 CONSL7=29.4204*AKR*FF/PP**0.5;CONSL8=PP*RAKKE
05000 SCONL8=CONSL8*CONSL8;TWTH=2/3
05100 Y3F=1.5*(100-FC3)/FC1;Y1F=225*FC3/(FC1*FC1)
05200 278 IF(MC.EQ.1) GO TO 287
05300 KC1=KC3
05400 287 AKC1=KC1+1
05500 BKC1=2*KC1+Y3F
05600 CKC1=KC1-Y1F
05700 AKCK=4*AKC1*CKC1
05800 BKSQ=BKC1*BKC1
05900 IF(AKCK.GT.BKSQ) GO TO 305
06000 ROOT=(BKSQ-AKCK)**0.5
06100 AKC2=2*AKC1;ROOT2=ROOT/AKC2
06200 BKC2=BKC1/AKC2;BKROOT=BKC2+ROOT2
06300 C IF(BKROOT.LT.1.0)GO TO 35
06400 IF(BKC2.LE.ROOT2)GO TO 35
06500 LXY=(BKC2-ROOT2)*10000+0.5;XY(I)=LXY*0.0001
06600 IF(IOL81.NE.1)GO TO 1109
06700 PRINT 1101,XY(I)
06800 TYPE 1101,XY(I)
06900 1109 CONTINUE
07000 1101 FORMAT(F7.3)
07100 GO TO 26
07200 35 LXY=(BKC2+ROOT2)*10000+0.5;XY(I)=LXY*0.0001
07300 IF(IOL81.NE.1)GO TO 1118
07400 PRINT 1101,XY(I)

```

## RS APPENDIX-B

```
07500          TYPE 1101,XY(I)
07600 1118     CONTINUE
07700          IF(XY(I).GT.1.0)GO TO 305
07800 26       IF(MC.EQ.2)GO TO 350
07900          XE(I)=XY(I)
08000          GO TO 332
08100 350     XRM(I)=XY(I)
08200          IF(RATIO.NE.3.0)GO TO 443
08300 C        IF(ZIF.NE.1.0)GO TO 443
08400          GO TO 377
08500 443     CONTINUE
08600          GO TO 458
08700 305     PRINT 308,PP,TT
08800          IF(ITYPE.NE.2)GO TO 107
08900          TYPE 308,PP,TT
09000 308     FORMAT(2X,'PRESSURE(ATM)=' ,F10.3,8X,' ,TEMPERATURE(K)=' ,F10.3/)
09100 107     IF(MC.EQ.2) GO TO 800
09200          PRINT 809
09300          IF(ITYPE.NE.2)GO TO 116
09400          TYPE 809
09500 809     FORMAT(2X,'CONVERSION AT EQUILIBRIUM IS COMING COMPLEX/NEGATIVE OR
09600          1ZERO.'/)
09700 116     XE(I)=0.0
09800          GO TO 332
09900 800     PRINT 818
10000          IF(ITYPE.NE.2)GO TO 125
10100          TYPE 818
10200 818     FORMAT(2X,'CONVERSION AT MAXIMUM RATE IS COMING COMPLEX/NEGATIVE O
10300          1R ZERO.'/)
10400 125     XRM(I)=0.0
10500          GO TO 377
10600 332     CONTINUE
10700          IF(RATIO.EQ.3.0)GO TO 431
10800 458     ABC=1;XLPE=XY(I)
10900          IF(MC.EQ.2)GO TO 1100
11000 C        XLPE=XACT(I);ABC=-1
11100 1100     XEL=(1-ABC*XINCL2)*XLPE
```

## APPENDIX-B

```

RS
11200 C      XINCL2=(XE(I)-XRM(I))*0.2
11300      CALL LMINP(XEL,MC,ADELP,RATE,LMP)
11400      IF(MC.EQ.2)GO TO 440
11500      XE(I)=XEL
11600      DO 530 LP=1,4
11700 530    AELP2(LP,1)=ADELP(LP)
11800      GO TO 431
11900 440    XRM(I)=XEL
12000      DO 533 LP=1,4
12100 533    AELP2(LP,2)=ADELP(LP)
12200      GO TO 377
12300 431 MC=2
12400      TINV=1/TT
12500      DAKR=24092.2*AKR*TINV*TINV
12600      DAK=AK*0.50327*(3.4966E-3-TINV*(9184.0*TINV+7.2949)+
12700      1TT*(3.3562E-7-TT*11.625E-11))
12800      DAKF=5.714E-7*PP+4.0E-6*TT-2.6714E-3
12900      KC2=2.0*AKR*RAKKF*(DAK-RAKKF*DAKF)/(AKF*DAKR)+SRAF
13000      KC3=CONP*KC2**0.5
13100      GO TO 278
13200 377 CONTINUE
13300      IF(IOL81.NE.1)GO TO 1105
13400      PRINT 1106,((AELP2(LP,LP1),LP=1,4),LP1=1,2),
13500      2(RATE(LP),LP=1,LMP)
13600      TYPE 1106,((AELP2(LP,LP1),LP=1,4),LP1=1,2),
13700      2(RATE(LP),LP=1,LMP)
13800 1106    FORMAT(8F7.3,6E11.3/)
13900 1105    CONTINUE
14000      RETURN
14100      END
14200 C SUBROUTINE NO.9
14300 C      SUBROUTINE NO. 10
14400      SUBROUTINE COMPA(DELT,T,J,J1)
14500      DIMENSION DELT(800),T(800)
14600      I=1;J1=0
14700 26 IF(ABS(T(J)-T(I)).EQ.0.0)GO TO 35
14800      I=I+1

```

## RS APPENDIX-B

```

14900      IF(I.EQ.J) GO TO 44
15000      GO TO 26
15100      35 T(J)=T(I)
15200      DELT(J)=DELT(I)
15300      J1=I
15400      GO TO 53
15500      44 DELT(J)=8.0
15600      53 RETURN
15700      END
15800      SUBROUTINE OPTIMA(OBJF,M,X,X1,IOP,NV,
15900      1AC2,NLEV,NOPTM,TOL8,NMAX1,NDPTS,X8,
16000      2OBJ,NN8,AC1,YN,ILP)
16100 C      SUBROUTINE NO.11 FOR COMPLEX SEARCH TECHNIQUE
16200      DIMENSION OBJF(50),X(50,20),X1(20,20),
16300      1OBJ(20),X8(20,20),NLEV(20),X8N(20)
16400      CALL MAXMIL(OBJF,M,OBMAX1,
16500      1OBMAX2,OBMIN,NMAX1,NMAX2,NMIN,NDPTS,ILP)
16600      IF(M.GT.NDPTS) GO TO 251
16700 32      IN=0;IK=0;NN8=1;AC1=AC2;LP=0;NDPT1=NDPTS-1
16800 260      DO 17 L=1,NDPTS
16900      IF(L.EQ.NMIN)GO TO 17
17000      LP=LP+1
17100      OBJ(LP)=OBJF(L)
17200      DO 17 K=1,NV
17300      X8(LP,K)=X(L,K)
17400 17      CONTINUE
17500      OBJ(NDPTS)=OBJF(NMIN)
17600      DO 116 K=1,NV
17700 116      X8(NDPTS,K)=X(NMIN,K)
17800 125      CONTINUE
17900      278 CALL NPOINT(IN,OBMIN,OBJ,X8,NV,NN8,AC1
18000      1,NOPTM,TOL8,OBMAX1,OBMAX2,NMAX1,NMIN,NDPTS)
18100      IF(NN8.NE.1)GO TO 440
18200      YN=OBJ(NDPTS)
18300 440      CONTINUE
18400      IF(NOPTM.NE.0)GO TO 71
18500      M=M+1

```



## RS APPENDIX-B

```

18600      DO 74 K=1,NV
18700      74 X(M,K)=X8(NDPTS,K)
18800          GO TO 80
18900      251 CONTINUE
19000      206 OBJ(NDPTS)=OBJF(M)
19100          DO 233 K=1,NV
19200      233 X8(NDPTS,K)=X(M,K)
19300          IF(OBJ(NDPTS).LE.YN)GO TO 125
19400          NNS=1;AC1=AC2;LP=0;NDPT1=NDPTS-1
19500          CALL MIN(OBJ,NDPTS,OBMIN,NMIN)
19600          DO 143 K=1,NV
19700      143  X8N(K)=X8(NMIN,K)
19800          DO 134 L=1,NDPTS
19900          IF(L.EQ.NMIN)GO TO 134
20000          LP=LP+1
20100          IF(L.EQ.LP)GO TO 134
20200          OBJ(LP)=OBJ(L)
20300          DO 134 K=1,NV
20400          X8(LP,K)=X8(L,K)
20500      134  CONTINUE
20600          OBJ(NDPTS)=OBMIN
20700          DO 890 K=1,NV
20800      890  X8(NDPTS,K)=X8N(K)
20900          GO TO 125
21000      80  OBJF(M)=0.0
21100      71  RETURN
21200          END
21300          SUBROUTINE NPOINT(IN,YN,Y,X,N,N1,AC
21400              1,NOPTM,TOLB,YMAX1,YMAX2,NMAX1,NMIN,NDPTS)
21500          DIMENSION Y(20),X(20,20)
21600      C    SUBROUTINE NO.12 FOR NEXT OPTIMISATION POINT
21700          I=0;NOPTM=0;NDPT1=NDPTS-1;XMEAN=0.0
21800      227  CONTINUE
21900          IF(N1-2)38,47,56
22000      38  CONTINUE
22100      65  I=I+1;XMEAN=0.0
22200          DO 332 L=1,NDPT1

```

## APPENDIX-B

```

RS
22300 332 XMEAN=X(L,I)+XMEAN
22400 XMEAN=XMEAN/NDPT1
22500 X(NDPTS,I)=XMEAN+(XMEAN-X(NDPTS,I))*AC
22600 IF(I.LT.N) GO TO 65
22700 N1=N1+1
22800 IN=3
22900 GO TO 80
23000 47 AC=-0.5*AC
23100 GO TO 38
23200 56 AC=0.5*AC
23300 GO TO 38
23400 80 CONTINUE
23500 IF((YMAX1-YMAX2).GT.TOL8)GO TO 233
23600 NOPTM=NMAX1
23700 233 CONTINUE
23800 RETURN
23900 END
24000 SUBROUTINE INTEGR(X,N,M)
24100 DIMENSION X(50,20),IX(20)
24200 C SUBROUTINE NO.13 FOR MAKING REAL VARIABLES
24300 C TO ITS NEAREST ROUNDED OFF VALUE
24400 DO 8 K=1,17
24500 IX(K)=X(M,K)*100+0.5;X(M,K)=IX(K)*0.01
24600 8 CONTINUE
24700 RETURN
24800 END
24900 SUBROUTINE MLEVEL(X,N,X1,M,N1)
25000 DIMENSION X(50,20),X1(20,20),N1(20)
25100 C SUBROUTINE NO.14 FOR MAKING VARIABLES TO
25200 C THEIR NEAREST SPECIFIED LEVEL
25300 C FEED DATA THROUGH DATA FILE'DA17.DAT'
25400 C IN DESCENDING ORDER,SAY 20,15,10,SO ON.
25500 J=1;K=1;LP1=1
25600 80 IF(X(M,J)-X1(K,J))26,29,29
25700 26 IF(K.GE.N1(J))GO TO 11
25800 K=K+1;LP1=2
25900 GO TO 80

```

## RS APPENDIX-B

```
26000 29      IF(LP1,EG.1)GO TO 11
26100          LP1=1
26200          IF(ABS(X(M,J)-X1((K-1),J)),GE.
26300 1ABS(X(M,J)-X1(K,J)))GO TO 11
26400          X(M,J)=X1((K-1),J)
26500          GO TO 74
26600 11      X(M,J)=X1(K,J)
26700 74      IF(J.GE.N)GO TO 53
26800          J=J+1;K=1;LP1=1
26900          GO TO 80
27000 53      RETURN
27100          END
27200 C      SUBROUTINE NO. 15
27300          SUBROUTINE ACOMP(IK,X,M,N)
27400          DIMENSION X(50,20)
27500          J=1
27600 35 I=1
27700 17 IF(X(M,I).EQ.X(J,I)) GO TO 8
27800          J=J+1
27900          IF(J.GE.M) GO TO 71
28000          GO TO 35
28100 8 I=I+1
28200          IF(I.GT.N) GO TO 80
28300          GO TO 17
28400 71 IK=0
28500          GO TO 89
28600 80 IK=J
28700 89 RETURN
28800          END
28900 C      SUBROUTINE NO. 16
29000          SUBROUTINE MINMAX(X,N,XMAX,XMIN,NDIM)
29100          DIMENSION X(NDIM)
29200          J=1 ; A=X(1)
29300          DO 26 J=2,N
29400          IF(A.GE.X(J)) GO TO 26
29500          A=X(J)
29600 26 CONTINUE
```

```
29700      XMAX=A
29800      I=1
29900      A1=X(1)
30000      DO 80 J=2,N
30100      IF(A1.LE.X(J))GO TO 80
30200      A1=X(J)
30300      80 CONTINUE
30400      XMIN=A1
30500      RETURN
30600      END
30700 C     SUBROUTINE NO. 17
30800      SUBROUTINE AMMC(AN3E,AN3MR,AB1,FI3,FIT,XE,XRM,I)
30900      DIMENSION XE(310),XRM(310)
31000      COMMON/CB9/FF,RATIO,XINCL,XINCL2,TOL8,FC1,FC2,FC3,DELE,DELM
31100      1,IOL8,M88,IOP11
31200      J=1 ; X=XE(I)
31300      17 AB2=2*FC1*X/3
31400      AN3T1=100*(FC3+AB2)/(100-AB2)
31500      IF(J.GE.2)GO TO 26
31600      AN3E=AN3T1
31700      X=XRM(I)
31800      J=2
31900      GO TO 17
32000      26 AN3MR=AN3T1
32100      RETURN
32200      END
32300 C     SUBROUTINE NO.18
32400      SUBROUTINE FLOWR(F1,F2,F3,F4,F5,VFT,FC1,FC2,FC3,FC4,I)
32500      C1=1.1355E-4
32600      C2=1.1135E-4
32700      C3=1.1349E-4
32800      C4=1.1351E-4
32900      C5=1.136E-4
33000      IF(I.EQ.2)GO TO 26
33100      17 CONTINUE
33200      FC5=100.0-(FC1+FC2+FC3+FC4)
33300      FCLP=FC1/C1+FC2/C2+FC3/C3+FC4/C4+FC5/C5
```

RS

## APPENDIX-B

```
33400      FTC=100*VFT/FCLP
33500      IF1=FTC*FC1+0.5
33600      F1=IF1
33700      IF2=FTC*FC2+0.5
33800      F2=IF2
33900      IF3=FTC*FC3+0.5
34000      F3=IF3
34100      IF4=FTC*FC4+0.5
34200      F4=IF4
34300      IF5=FTC*FC5+0.5
34400      F5=IF5
34500      GO TO 80
34600 26  IVFT=0.01*((F1/C1)+(F2/C2)+(F3/C3)+(F4/C4)+(F5/C5))+0.5
34700      VFT=IVFT
34800      FTC=0.01*(F1+F2+F3+F4+F5)
34900 35  IFC1=100*F1/FTC+0.5
35000      FC1=IFC1/100
35100      IFC2=100*F2/FTC+0.5
35200      FC2=IFC2/100
35300      IFC3=100*F3/FTC+0.5 ; FC3=IFC3/100
35400      IFC4=100*F4/FTC+0.5 ; FC4=IFC4/100
35500      FC5=100.0-(FC1+FC2+FC3+FC4)
35600 80  RETURN
35700      END
35800 C    SUBROUTINE NO. 19
35900
36000 C    SUBROUTINE NO. 20
36100      SUBROUTINE FUNCBJ(X,M,N1,P,P1,S,S1,S2,S3,S4,S5,S6,S7,S8
36200      1,S20,S21,S22,S23,S24,S25,S26,S27,S28,G)
36300      DIMENSION X(50)
36400      IF(N1-2)2,3,7
36500 7     IF(N1-4)8,11,12
36600 12    IF(N1-6)17,80,21
36700 21    IF(N1-8)26,29,30
36800 30    IF(N1-10)35,38,38
36900 2     G=P1
37000      IF(P1.EQ.0.0)GO TO 44
```

```
37100      X(M)=P/P1
37200      GO TO 20
37300 44    X(M)=P
37400      GO TO 20
37500 3     G=S21
37600      IF(S21.EQ.0.0)GO TO 45
37700      X(M)=-S1/S21
37800      GO TO 20
37900 45    X(M)=-S1
38000      GO TO 20
38100 8     G=S22
38200      IF(S22.EQ.0.0)GO TO 46
38300      X(M)=-S2/S22
38400      GO TO 20
38500 46    X(M)=-S2
38600      GO TO 20
38700 11    G=S23
38800      IF(S23.EQ.0.0)GO TO 47
38900      X(M)=-S3/S23
39000      GO TO 20
39100 47    X(M)=-S3
39200      GO TO 20
39300 17    G=S24
39400      IF(S24.EQ.0.0)GO TO 48
39500      X(M)=-S4/S24
39600      GO TO 20
39700 48    X(M)=-S4
39800      GO TO 20
39900 80    G=S25
40000      IF(S25.EQ.0.0)GO TO 50
40100      X(M)=-S5/S25
40200      GO TO 20
40300 50    X(M)=-S5
40400      GO TO 20
40500 26    G=S26
40600      IF(S26.EQ.0.0)GO TO 51
40700      X(M)=-S6/S26
```

```
40800      GO TO 20
40900 51    X(M)=-S6
41000      GO TO 20
41100 29    G=S27
41200      IF(S27.EQ.0.0)GO TO 53
41300      X(M)=-S7/S27
41400      GO TO 20
41500 53    X(M)=-S7
41600      GO TO 20
41700 35    G=S28
41800      IF(S28.EQ.0.0)GO TO 52
41900      X(M)=-S8/S28
42000      GO TO 20
42100 52    X(M)=-S8
42200      GO TO 20
42300 38    G=S20
42400      IF(S20.EQ.0.0)GO TO 56
42500      X(M)=-S/S20
42600      GO TO 20
42700 56    X(M)=-S
42800 20    RETURN
42900      END
43000 C    SUBROUTINE NO. 21
43100      SUBROUTINE MIN(X,N,XMIN,NMIN)
43200      DIMENSION X(20)
43300      I=1;NMIN=1
43400      A1=X(1)
43500      DO 80 J=2,N
43600      IF(A1.LE.X(J))GO TO 80
43700      A1=X(J)
43800      NMIN=J
43900 80 CONTINUE
44000      XMIN=A1
44100      RETURN
44200      END
44300 C    SUBROUTINE NO. 22
44400      SUBROUTINE MAXMIL(X,N,XMAX1,XMAX2,
```

RS

## APPENDIX-B

```

44500      1XMIN,NMAX1,NMAX2,NMIN,NDPTS,ILP)
44600      DIMENSION X(50)
44700      NMAX=1;LP=1;NMAX1=1;NDLP=NDPTS+2
44800 53      I=1
44900      IF(LP.EQ.1)GO TO 56
45000      IF(NMAX.EQ.1)I=I+1
45100 56      A=X(I);II1=I+1
45200      DO 26 J=II1,N
45300          IF(J.EQ.NMAX1)GO TO 26
45400          IF(A.GE.X(J)) GO TO 26
45500          A=X(J);NMAX=J
45600 26 CONTINUE
45700          IF(LP.NE.1)GO TO 35
45800      XMAX1=A;NMAX1=NMAX;LP=2
45900      GO TO 53
46000 35      XMAX2=A;NMAX2=NMAX
46100      I=1;NMIN=1
46200      IF(ILP.EQ.1)GO TO 101
46300      IF(N.LE.NDLP)I=I+1
46400 101     CONTINUE
46500      A1=X(I);II1=I+1;NMIN=I
46600      DO 80 J=II1,N
46700          IF(A1.LE.X(J))GO TO 80
46800          A1=X(J);NMIN=J
46900 80 CONTINUE
47000      XMIN=A1
47100      RETURN
47200      END
47300 C  SUBROUTINE NO.23
47400      SUBROUTINE LMIMP(TB21,MC,DELP2,R11,LMP)
47500      DIMENSION ADELTA(800),ATH12(800),DELP2(4),R11(800)
47600      COMMON/CB9/FF,RATIO,XINCL,XINCL2,C4,FC1,FC2,FC3,DELE,DELM
47700      1,IOL8,M88,IOP11,ICL81
47800      1/CB8/AKR,AK,AKF,ABLP8,ITYPE,ZIF/CB26/CONSL7,CONSL8
47900      1,SCONL8,TWTH,F,T,DAKR,DAK,DAKF,RAKFF
48000      LMP=1;I=0;ATLP=1.0;C41=0.0008
48100      W1=TB21

```



```
48200 192      I=I+1
48300          IF(W1.GT.ATLP)W1=2.0*ATLP-W1
48400          IF(W1.LT.0.0)W1=-W1
48500          ATH12(I)=W1
48600          IF(I.EQ.1)GO TO 224
48700          CALL COMPA(ADELTA,ATH12,I,LP)
48800          IF(LP.NE.0)GO TO 227
48900 224      CALL DELTAP(DELT1,W1,MC,R11(LMP),LMP)
49000          GO TO 233
49100 227      DELT1=ADELTA(LP)
49200 233      ADELTA(I)=DELT1
49300 C        IF(IOL81.NE.1)GO TO 323
49400          IF(I.GE.M88)GO TO 151
49500 323      IF(ABS(DELT1)-C41) 151,151,191
49600 191      IF(I-1)153,152,153
49700 152      W2=W1*XINCL
49800 134      TB21=W2
49900          I=I+1
50000          IF(W2.GT.ATLP)W2=2*ATLP-W2
50100          IF(W2.LT.0.0)W2=-W2
50200          ATH12(I)=W2
50300          CALL COMPA(ADELTA,ATH12,I,LP)
50400          IF(LP.NE.0)GO TO 236
50500 200      CALL DELTAP(DELT2,W2,MC,R11(LMP),LMP)
50600          GO TO 242
50700 236      DELT2=ADELTA(LP)
50800 242      ADELTA(I)=DELT2
50900 C        IF(IOL81.NE.1)GO TO 314
51000          IF(I.GE.M88)GO TO 154
51100 314      IF(ABS(DELT2)-C41)154,154,153
51200 153      DW12=(W1-W2)*2.0
51300 209      IF(DELT1)1,151,5
51400 1        IF(DELT2)2,154,7
51500 5        IF(DELT2)7,154,2
51600 2        IF(ABS(DELT1)-ABS(DELT2))161,161,162
51700 161      W2=W1+DW12
51800          GO TO 134
```

## RS APPENDIX-B

```
51900 162 W1=W2-DW12
52000 GO TO 192
52100 7 W3=W2+(W1-W2)*ABS(DELT2)/(ABS(DELT2)+ABS(DELT1))
52200 TB21=W3
52300 I=I+1;ATH12(I)=W3
52400 CALL COMPA(ADELT,ATH12,I,LP)
52500 IF(LP.NE.0)GO TO 245
52600 CALL DELTAP(DELT3,W3,MC,R11(LMP),LMP)
52700 GO TO 251
52800 245 DELT3=ADELT(LP)
52900 251 ADELT(I)=DELT3
53000 C IF(IOL8.NE.1)GO TO 206
53100 IF(I.GE.M88)GO TO 305
53200 206 IF(ABS(DELT3)-C41)170,170,188
53300 170 TB21=W3
53400 GO TO 155
53500 188 IF(DELT3)11,170,35
53600 11 IF(DELT2)17,154,26
53700 35 IF(DELT2)26,154,17
53800 17 W2=W3
53900 DELT2=DELT3
54000 GO TO 7
54100 26 W1=W3
54200 DELT1=DELT3
54300 GO TO 7
54400 305 TB21=W3
54500 GO TO 155
54600 154 TB21=W2
54700 GO TO 155
54800 151 TB21=W1
54900 155 CONTINUE
55000 DELP2(1)=ATH12(I);DELP2(2)=ADELT(I);DELP2(3)=ATH12(I-1)
55100 DELP2(4)=ADELT(I-1)
55200 RETURN
55300 END
55400 C SUBROUTINE NO.24
55500 SUBROUTINE DELTAP(Delta,XEL,MC,R1,LMP)
```

```
55600 COMMON/CB9/FF,RATIO,XINCL,XINCL2,TOL8,FC1,FC2,FC3,DELE,DELM
55700 1,IOL8,M88,IOP11,ICL81
55800 1/CB8/AKR,AK,AKF,ABLP8,ITYPE,ZIF/CB26/CONSL7,CONSL8
55900 1,SCONL8,TWTH,P,T,DAKR,DAK,DAKF,RAKKE
56000 FC1XE=FC1*XEL;FLPC=100-TWTH*FC1XE;FLPCI=1/FLPC
56100 FC1LP=FC1*FLPCI*FLFCI;Y1=FLPCI*(FC1-FC1XE)
56200 Y2=FLPCI*(FC2-FC1XE/3);Y3L=FC3+TWTH*FC1XE
56300 Y3=Y3L*FLPCI;Y15P=Y1**1.5;Y1BY3=Y15P/Y3
56400 IF(MC.EQ.2)GO TO 17
56500 DELTA=1-1/(CONSL8*Y1BY3*(Y2**0.5))
56600 DELE=DELTA
56700 GO TO 260
56800 17 CONTINUE
56900 C GO TO 44
57000 260 ETA=Y3/(Y3+2*Y2)
57100 CALL ZIFA(ZIF,P,T,ETA,B1,B2,B3,B4,B5,B6)
57200 DZIT=B1+(2*B3+3*B5*T)*T
57300 44 SCONLP=SCONL8*Y1BY3*Y2;R1=CONSL7*(SCONLP-1/Y1BY3)*ZIF
57400 LMP=LMP+1
57500 IF(MC.NE.2)GO TO 26
57600 DRT=R1*DAKR/AKR+2*CONSL7*SCONLP*(DAK-RAKKE*DAKF)/AK
57700 C GO TO 47
57800 DELTA=1+R1*DZIT/(ZIF*DRT);DELM=DELTA
57900 GO TO 26
58000 47 DELTA=DRT;DELM=DELTA
58100 26 CONTINUE
58200 C TYPE 11,XEL,DELTA
58300 C PRINT 11,XEL,DELTA
58400 C11 FORMAT(2F8.3)
58500 RETURN
58600 END
58700 C SUBROUTINE NO.25
58800 SUBROUTINE PCONV(I26,N,AQX)
58900 DIMENSION AQX(50,20),LPAQX(50),AQXLP(2,50),A(20),A1(20)
59000 COMMON/CB74/AQXLP,A2,A22,A3,A23,A4,A24,A5,A25,A6,A26,A7,A27,
59100 1A8,A28,A9,A29,A10,A30,A11,A31,A12,A32,A13,A33,A14,A34,A15,
59200 1A35,A16,A36,A17,A37,A18,A38,A19,A20,A21,FDLIM
```

```
59300 A(1)=A2;A(2)=A3;A(3)=A4;A(4)=A5;A(5)=A6;A(6)=A7;A(7)=A8
59400 A(8)=A9;A(9)=A10;A(10)=A11;A(11)=A12;A(12)=A13;A(13)=A14
59500 A(14)=A15;A(15)=A16;A(16)=A17;A(17)=A18;A(18)=A19;A(19)=A20
59600 A(20)=A21;A1(1)=A22;A1(2)=A23;A1(3)=A24;A1(4)=A25;A1(5)=A26
59700 A1(6)=A27;A1(7)=A28;A1(8)=A29;A1(9)=A30;A1(10)=A31;A1(11)=A32
59800 A1(12)=A33;A1(13)=A34;A1(14)=A35;A1(15)=A36
59900 A1(16)=A37;A1(17)=A38
60000 M=I26;A1(18)=1.0;A1(19)=1.0;A1(20)=1.0
60100 IF(N,NE.1)GO TO 200
60200 DO 53 I=1,20
60300 IF(A1(I).EQ.0.0)GO TO 152
60400 AQX(I26,I)=A(I)/A1(I)
60500 GO TO 53
60600 152 AQX(I26,I)=A(I)
60700 53 CONTINUE
60800 GO TO 80
60900 200 CONTINUE
61000 862 DO 515 L=1,17
61100 LPAQX(L)=AQX(M,L)*1000+0.5;AQX(M,L)=LPAQX(L)*0.001
61200 IF(AQX(M,L).LT.AQXLP(1,L))GO TO 521
61300 AQX(M,L)=AQXLP(1,L)
61400 GO TO 515
61500 521 IF(AQX(M,L).GT.AQXLP(2,L))GO TO 515
61600 AQX(M,L)=AQXLP(2,L)
61700 515 CONTINUE
61800 LPAQX(18)=AQX(M,18)*10000+0.5;AQX(M,18)=LPAQX(18)*0.0001
61900 LPAQX(19)=AQX(M,19)*1000000+0.5;AQX(M,19)=LPAQX(19)*0.000001
62000 LPAQX(20)=AQX(M,20)*10000+0.5;AQX(M,20)=LPAQX(20)*0.0001
62100 DO 62 I=1,20
62200 IF(A1(I).EQ.0.0)GO TO 155
62300 A(I)=AQX(I26,I)*A1(I)
62400 GO TO 62
62500 155 A(I)=AQX(I26,I)
62600 62 CONTINUE
62700 FD24=A(6)+A(7)+A(8)+A(17)
62800 IF(FD24.LE.FDLIM)GO TO 92
62900 FD24I=100.0*FDLIM/FD24
```

```
63000      IFD11=A(17)*FD24I;A(17)=IFD11*0.01
63100      IF(A1(17).EQ.0.0)GO TO 161
63200      AQX(I26,17)=A(17)/A1(17)
63300      GO TO 164
63400 161   AQX(I26,17)=A(17)
63500 164   CONTINUE
63600      IFD22=A(6)*FD24I
63700      A(6)=IFD22*0.01
63800      IFD33=A(7)*FD24I
63900      A(7)=IFD33*.01
64000      A(8)=FDLIM-A(6)-A(7)-A(17)
64100      DO 170 I=6,8
64200
64300      IF(A1(I).EQ.0.0)GO TO 165
64400      AQX(M,I)=A(I)/A1(I)
64500      GO TO 170
64600 165   AQX(M,I)=A(I)
64700 170   CONTINUE
64800 92    CONTINUE
64900      A2=A(1);A3=A(2);A4=A(3);A5=A(4);A6=A(5);A7=A(6);A8=A(7)
65000      A9=A(8);A10=A(9);A11=A(10);A12=A(11)
65100      A13=A(12);A14=A(13);A15=A(14)
65200      A16=A(15);A17=A(16);A18=A(17);A19=A(18);A20=A(19);A21=A(20)
65300 80    RETURN
65400      END
65500 C    SUBROUTINE NO.26
65600      SUBROUTINE PNEXT(N1,N3,N4,X,ISIG)
65700      DIMENSION F(17,20),X(50,20)
65800      COMMON/CB71/N2,F,M1,ILP
65900      IF(ISIG.NE.1)M1=2
66000
66100 2      N1=N1+1
66200      IF(N1.GT.N2)GO TO 8
66300      IF(F(N3,N1).EQ.0.0)GO TO 2
66400      N4=N4+1
66500      DO 3 L=1,N2
66600      IF(L.NE.N1)GO TO 7
```

RS

## APPENDIX-B

```
66700      X(N4,L)=X(1,L)+F(N3,N1)*ISIG
66800      IF(ILP.NE.1)ISIG=-ISIG
66900      GO TO 3
67000 7     X(N4,L)=X(1,L)
67100 3     CONTINUE
67200      IF(ILP.EQ.1)GO TO 8
67300      IF(M1.NE.2)N1=N1-1
67400      M1=1
67500 8     RETURN
67600      END
67700 C     THE END QM
```

